Listeriolysin S, a contact-dependent bacteriocin from Listeria monocytogenes hyper-virulent strains

Jazmin Meza Torres

Université de Paris

École doctorale Bio SPC - ED 562

Unité Yersinia, Département de Microbiologie, Institut Pasteur

Listeriolysin S, a contact-dependent bacteriocin from *Listeria monocytogenes* hyper-virulent strains

Par Jazmín Meza Torres

Thèse de doctorat de Microbiologie

Dirigée par Javier Pizarro-Cerdá

Présentée et soutenue publiquement à Paris le 20 novembre 2020

Devant un jury composé de :

Président du jury :
Hélène Bierne, Directrice de recherche, INRA (MICALIS)

Rapporteurs :
Ina Atrée, Directrice de recherche CNRS, CEA Grenoble
Laurent Dortet, Co-directeur CNR de la Résistance aux antibiotiques, CHU Bicêtre

Examinateurs :
Olivier Dussurget, Professeur Université de Paris et Institut Pasteur
Alain Filloux, Professeur Imperial College of London

Directeur de thèse :
Javier Pizarro-Cerdá, Directeur de Recherche Unité Yersinia, Institut Pasteur

Membre invitée :
Pascale Cossart, Professeur Émérite Institut Pasteur et Secrétaire perpétuelle Académie des Sciences

Titre : Listeriolysine S, une bactériocine dépendante d'un contact produite par des souches hyper-virulentes de *Listeria monocytogenes*

Résumé :

Listeria monocytogenes (*Lm*) est un pathogène bactérien responsable de la listériose, une maladie qui induit des gastroentérites, des avortements chez la femme enceinte et des méningites chez le nouveau-né. Les épisodes les plus sévères de listériose sont associés à des souches hyper-virulentes de *Lm* qui produisent la Listeriolysine S (LLS). La LLS est une microcine modifiée avec des thiazole/oxazoles (TOMM), qui inhibe la croissance de certaines bactéries Gram-positives, modifie la composition du microbiote intestinal et favorise la colonisation de l'intestin et l'invasion d'organes profonds comme le foie et la rate. Mes travaux de thèses ont pour objectifs d'étudier le rôle cytotoxique de la LLS, les mécanismes bactéricides de la LLS, les mécanismes régulateurs de l'expression de la LLS et la contribution de la LlsX, une protéine spécifique de *Lm*, dans l'activité biologique de la LLS. Nos résultats ont montré que la LLS cible exclusivement des cellules procaryotes et ne présente aucune activité cytotoxique pour les cellules eucaryotes *in vivo* au cours de l'infection par *Lm*. Nous avons identifié *in silico* de boîtes de régulation transcriptionnelle putatives et des ARNs régulateurs putatifs qui pourraient être impliqués dans le contrôle de l'expression de la LLS. Par microscopie électronique et fractionnement subcellulaire des bactéries productrices de la LLS, j'ai pu montrer que la LLS est localisée au niveau de la membrane de la bactérie productrice et n'est pas secrétée dans le surnageant. En utilisant un insert de culture cellulaire Transwell et une approche de microscopie micro-fluidique en temps réel, j'ai pu également montrer que la LLS inhibe la croissance bactérienne de manière dépendante d'un contact entre la bactérie productrice de LLS et la bactérie cible. Mes travaux ont montré également que la LLS induit la perméabilisation des membranes des bactéries cibles, produit l'arrêt de leur croissance et provoque leur lyse. Nos résultats indiquent qu'une augmentation des charges négatives de la surface bactérienne augmente la sensibilité à la LLS. De plus, nous avons montré une interaction directe entre la LLS et LlsX au niveau de la membrane cellulaire des bactéries productrices de LLS et que LlsX est nécessaire à l'expression et la stabilisation de la LLS. Dans l'ensemble, nos résultats démontrent que LLS est la première TOMM qui présente un mécanisme d'inhibition dépendant d'un contact, que la LLS altère l'intégrité de la membrane de la cellule cible et agit exclusivement contre les cellules procaryotes lors d'une infection *in vivo.*

Mots clefs : Listeriolysine S (LLS), bactériocine, *Listeria monocytogenes*, inhibition dépendante du contact, perméabilisation de la membrane cellulaire, microcine modifiée avec thiazole/oxazole.

Title: Listeriolysin S, a contact-dependent bacteriocin from *Listeria monocytogenes* hyper-virulent strains

Abstract:

Listeria monocytogenes (*Lm*) is a bacterial pathogen that causes listeriosis, a foodborne disease characterized by gastroenteritis, meningitis, bacteremia, and abortions in pregnant women. The most severe human listeriosis outbreaks are associated with a subset of *Lm* hyper-virulent strains that produce Listeriolysin S (LLS). LLS is a thiazole/oxazole modified microcin (TOMM) that targets specific Gram-positive bacteria, modifies the gut microbiota and allows efficient *Lm* gut colonization and invasion of deeper organs. The objectives of this work were to investigate the LLS cytotoxic role, the LLS bactericidal mechanism, the mechanism(s) regulating LLS expression, and the contribution of the *Lm*-specific LlsX protein to the LLS biological activity. We demonstrate that LLS is no cytotoxic for eukaryotic host cells, targeting exclusively prokaryotic cells during *in vivo* infections. We have identified *in silico* several putative transcriptional boxes and putative RNA-regulatory elements which could regulate LLS expression. Using subcellular fractionation assays and transmission electron microscopy, we identified that LLS remains associated to the bacterial cell membrane and cytoplasm of LLS-producer bacteria, and it is not secreted to the bacterial extracellular space. Applying trans-well co-culture systems and microfluidic-coupled microscopy, we determined that LLS requires direct contact between LLS-producer and LLS-target bacteria to display bactericidal activity, and it is thus a contact-dependent bacteriocin. We also demonstrate that contact-dependent exposure to LLS leads to permeabilization of the target bacterial cell membrane, promoting target-bacteria growth arrest and lysis. Our results indicate that a net increase in bacterial surface negative charges augments the susceptibility to LLS. Moreover, we revealed the direct interaction between LLS and LlsX at the cell membrane of LLS-producer bacteria, and we show that LlsX is required for expression and/or stabilization of LLS. Overall, our results demonstrate that LLS is the first TOMM that displays a contact-dependent inhibition mechanism, impairing the target cell membrane integrity and targeting exclusively prokaryotic cells during *in vivo* infections.

Keywords: Listeriolysin S (LLS), bacteriocin, *Listeria monocytogenes*, contact-dependent inhibition, cell membrane permeabilization, thiazole/oxazole-modified microcin.

RÉSUMÉ DE LA THÈSE

Les bactériocines sont définies comme : « des protéines ou peptides antimicrobiens d'origine ribosomale produites par une bactérie, actives contre d'autres bactéries et contre lesquels les bactéries productrices possèdent un mécanisme d'immunité spécifique » (15, 16). En général, elles ont un spectre étroit d'activité antibactérienne. Ils peuvent subir des modifications post-traductionnelles (PTM) qui leur permettent d'afficher des structures très diverses et des mécanismes d'action variés (6). Les bactériocines constituent un groupe de molécules très hétérogène. Un groupe spécifique de bactériocines produites à la fois par des bactéries Gram-positives et Gram-négatives sont les microcines modifiées par des thiazole/oxazoles (TOMM).

Les TOMMs sont produites à partir de clusters des gènes qui permettent la production de peptides présentant des modifications post-traditionnelles avec des hétérocycles thiazoles, oxazoles et/ou méthyl-oxazoles. Les TOMMs démontrent diverses activités, incluant par exemple l'inhibition de l'ADN gyrase ou induisant des dommages à la membrane des bactéries cibles, et peuvent également présenter une activité cytotoxique vis-à-vis des cellules eucaryotes. Cette famille comprend la Microcine B17 d'*Escherichia coli*, la Streptolysine S (SLS) de *Streptococcus pyogenes*, la Clostridiolysine S (CLS) de *Clostridium botulinum,* et d'autres molécules telles que la Listeriolysine S (LLS) de *Listeria monocytogenes* (*Lm*) (208–210).

Lm est un pathogène bactérien responsable de la listériose, une maladie d'origine alimentaire (254). Après l'ingestion d'aliments contaminés, des individus sains peuvent souffrir d'une gastro-entérite légère à sévère (255). Néanmoins, de niveaux faibles de contamination alimentaire peuvent entraîner une méningite chez le nouveau-né et chez les personnes immunodéprimées ou âgées, et des avortements chez la femme enceinte (256, 257). Lors du passage de la barrière épithéliale, *Lm* peut disséminer dans le sang, le foie, la rate, le cerveau et le placenta (254). Jusqu'à présent, les épisodes plus sévères de listériose ont été associés à des souches qui produisent la LLS (252, 253). La LLS est produite par des souches hyper-virulentes de *Lm* (253).

La LLS est une bactériocine présentant une faible activité hémolytique. Cette protéine inhibe *in vitro* la croissance de certaines souches de *Lm* ainsi que de certains

Firmicutes (i.e. *Lactococcus lactis* et *Staphylococcus aureus*). La LLS est exprimée majoritairement dans l'intestin des souris infectées par voie orale. Cette bactériocine modifie notamment le microbiote intestinal et est associée à la disparition d'espèces protectrices du microbiote (i.e. *Alloprevotella* et *Allobaculum*). Ainsi, la LLS favorise la colonisation de l'intestin par *Lm* et sa translocation à travers la barrière intestinale, produisant une infection plus sévère (308).

La découverte de l'association entre l'hyper-virulence de certaines souches de *Lm* et la modulation de la composition du microbiote intestinal de l'hôte par la LLS ouvre de nouvelles perspectives dans la compréhension de la listériose jusqu'ici rarement explorées. Elle ouvre également de nouveaux défis et questions autour du fonctionnement de cette molécule, notamment l'identification de son mécanisme d'action bactéricide, sa structure, son (ses) signal (signaux) d'activation, ainsi que la contribution spécifique de ses activités cytotoxiques et hémolytiques à la virulence de *Lm in vivo.*

Le premier objectif de mes travaux de thèse s'est inscrit dans l'étude du rôle cytotoxique de la LLS. J'ai étudié l'importance du rôle cytotoxique du LLS en évaluant sa contribution lors de l'infection des cellules eucaryotes par *Lm*, ainsi que ses effets sur les macrophages et les cellules épithéliales. Le deuxième objectif a été de comprendre les mécanismes d'activité bactéricide de la LLS. En utilisant une diversité d'approches (méthodes biochimiques, microscopie microfluidique, cytométrie en flux), mon travail a mis à jour le mécanisme utilisé par cette bactériocine pour tuer les bactéries cibles. Le troisième objectif de ce doctorat était d'étudier les mécanismes qui régulent l'expression de la LLS. Nous avons identifié *in silico* de boîtes putatives de régulation transcriptionnelle et des ARNs régulateurs putatifs qui pourraient être impliqués dans le contrôle de l'expression de la LLS. De plus, nous avons criblé des composés chimiques et des conditions physico/chimiques présentes dans l'intestin qui pourraient induire l'expression de LLS. Le quatrième objectif était de caractériser la contribution de la LlsX, une protéine spécifique de *Lm*, à la production, la maturation et l'export de LLS. Nous avons effectué des analyses *in silico* pour prédire sa localisation subcellulaire et sa fonction. De plus, des études d'interaction ont été réalisées pour étudier la localisation subcellulaire de la LlsX et son interaction avec la LLS.

Pour évaluer la cytotoxicité de la LLS, nous avons mesuré la libération de lactate déshydrogénase par des macrophages et des cellules épithéliales après 24 heures d'infection par une souche de *Lm* produisant LLS. Nos résultats ont montré que la LLS exprimée par *Lm* intracellulaire n'est pas cytotoxique pour les cellules hôtes eucaryotes. Nous avons étudié également la contribution de la LLS lors des infections cellulaires par *Lm in vitro*. Nous montrons que la LLS n'a aucun rôle lors d'une infection cellulaire par *Lm.*

Pour caractériser le mécanisme d'action de la LLS sur des bactéries cibles, la LLS a été fusionnée avec différents tags (en position C terminal) qui ne modifient pas son activité biologique. Par microscopie électronique et fractionnement subcellulaire des bactéries productrices de LLS, nos travaux ont montré que la LLS est localisée au niveau de la membrane de la bactérie productrice et n'est pas secrétée dans le surnageant de culture. En utilisant un insert de culture cellulaire Transwell et une approche de microscopie micro-fluidique en temps réel, nos résultats montrent que la LLS inhibe la croissance bactérienne de manière dépendante d'un contact entre la bactérie productrice de LLS et la bactérie cible. Nos travaux ont mis en évidence que la LLS induit la perméabilisation de la membrane des bactéries cibles, produit l'arrêt de leur croissance et provoque leur lyse. Nos résultats indiquent également qu'une augmentation des charges négatives de la surface bactérienne augmente la sensibilité à la LLS. De même, certaines souches de *Clostridium perfringens* ont été identifiées comme sensibles à l'activité de la LLS.

Nos travaux *in silico* ont permis de prédire des régions régulatrices putatives dans le cluster de gènes LLS. Concernant notre criblage *in vitro*, le signal activant l'expression de la LLS n'a été pas identifié. Nous avons effectué l'analyse de l'activation LLS en utilisant une faible concentration de composés. De ce fait, nous ne pouvons pas écarter la possibilité qu'une concentration plus élevée des composées utilisés ou une combinaison de plusieurs d'entre eux soient nécessaires pour activer de l'expression de la LLS. En raison de la complexité et richesse de l'environnement intestinal, les possibilités sont vastes.

Nous avons démontré une interaction directe entre la LLS et LlsX au niveau de la membrane cellulaire des bactéries productrices de LLS. Par ailleurs, nos résultats

indiquent que la LlsX est nécessaire à l'expression et à la stabilisation de la LLS. Ces données suggèrent que l'activité de la LlsX est essentielle à la maturation de la LLS, soutenant l'hypothèse que la LlsX pourrait agir comme un chaperon durant le processus de maturation de la LLS. Pour aller plus loin, nous nous sommes également intéressés à la fonction de la protéine putative d'immunité LlsP. Nos analyses *in silico* suggèrent que la LlsP est une protéine membranaire qui pourrait agir comme une métalloprotéase intramembranaire inactivant la LLS afin de conférer une immunité aux bactéries productrices. D'autre part, la LlsP pourrait également cliver le peptide signal de la LLS. L'expression hétérologue de la LlsP chez les bactéries cibles ne les protège pas contre la LLS. Cependant, un mutant delta-*llsP* généré chez une bactérie productrice de la LLS n'est pas viable. Ces résultats suggèrent que la LlsP est en effet une protéine d'immunité qui protège les bactéries productrices de l'activité LLS mais la LlsP ne protège pas les cellules cibles exposées à la LLS. Ce concept d'auto-immunité a été proposé pour la SLS, où l'immunité fournie par SagE est uniquement présente chez les bactéries productrices de SLS (215). D'autres études fonctionnelles sont nécessaires pour comprendre le mécanisme spécifique des protéines d'immunité putatives.

Nous proposons un modèle hypothétique concernant la maturation, l'export et le mécanisme d'activité de la LLS dans lequel LlsX agit comme un chaperon qui stabilise la LLS lors de sa modification post-traductionnelle. Puis la LLS modifiée est transféré à la métalloprotéase LlsP qui clive le peptide signal. Ce clivage protéolytique pourrait conduire à l'exportation de la LLS à travers le transporteur ABC LlsGH. Par la suite, la LLS mature pourrait être attachée à la membrane des bactéries productrices par des interactions avec l'acide lipotéichoïque (comme il a été proposé pour la SLS) (34). Lors d'un contact avec une bactérie cible, la LLS est alors transférée via des interactions avec des charges négatives de la surface bactérienne. Des études fonctionnelles et biochimiques supplémentaires sont nécessaires pour comprendre l'interaction moléculaire entre les produits géniques de l'opéron LLS.

Dans l'ensemble, nos résultats démontrent que LLS cible exclusivement les cellules procaryotes lors d'une infection *in vivo*. La LLS est la première TOMM qui présente un mécanisme d'inhibition dépendant d'un contact, inhibe la croissance et altère l'intégrité de la membrane, produisant la lyse la bactérie cible.

To our angel Mauricio, for being the greatest source of inspiration and force of motivation.

A nuestro ángel Mauricio por ser la mayor fuente de inspiración y fuerza de motivación.

ACKNOWLEDGMENTS

These 4 years of PhD experiences mold me into a more mature and stronger person. So full of amazing experiences, lessons and emotions: laughs, tears, stress, experiments, music, and coffee. But most of all so full of amazing scientists, friends and advisors.

I am grateful to Pr. Ina Atrée, Pr. Hélène Bierne, Pr. Laurent Dortet, Pr. Alain Filloux Pr. Pascale Cossart and Pr. Olivier Dussurget for their valuable time, for reading and evaluating my work.

I want to thank my supervisor Javier Pizarro for trusting me and supporting me. I am very grateful for his support, motivation, enthusiasm, rigorous and great scientific preparation through all the ups and downs of this project. I want to thank Pascale Cossart for welcoming me at her unit, giving me the opportunity to pursuit science, teaching me a great vision of science and inspiring me in so many ways. I want to thank Olivier Dussurget for sharing his scientific knowledge with me, for all the helpful discussions, for all his kindness and great advises.

I am grateful to all the **UIBC** members: Fabrizia Stavru, David Ribet, Edith Gouin, Marie-Anne Nahori, Matthew Eldridge, Julia Spano, Nam Tham, Julien Blonbou, Marie-Thérèse Vicente, Daryl David for all the amazing support, stimulating environment and shared science. I am especially grateful to JuanJo for his motivation, support, wisdom, advises and amazing friendship. Lilliana Radoshevich, Filipe Carvalho and Alessandro Pagliuso for all the scientific advises, kindness and support. Anna for your amazing friendship, for making me lovely birthday cakes and for wonderful times. Nathalie Rolhion and Sabrina Jabs for being cheerful and motivating me to liberate stress and run.

I am grateful to all members of the **Yersinia Unit** for your kindness, advises, support and for creating such a nice environment to work: Anne Derbise, Anne-Sophie Le Guern, Christian Demeure, Cyryl Savin, Pierre Goossens, Sylvie Bremont, Rémi Beau, Hebert Echenique Rivera, Julien Madej, Elisabeth Gutierrez, Guillem Mas Fiol, Nadira Frescaline, Mara Carloni, Clarisse Leseigneur, Pierre Le Bury, Oceane Blaise, and

Marion Lemarignier. Thank you all for make me feel at home during the last year of my thesis!!

I want to thank all the **collaborators** for your amazing help and support: Thibault Chaze, Marriette Matondo, Quentin Giai Gianetto, Dmitry Ershov, Jean Yves Tinevez, Alexandre Chenal, Fabrice Agou, Agnès Zettor, Sara Consalvi and Martin Sachse. I want to thank Pr. Emmanuel Lemichez for being a great tutor, being supportive and for having great science discussions with me. I am grateful Giulia Manina for all your helpful discussion, support and patience to teach me a hard technique.

To all **Dance your PhD** members!! A lovely experience that made me see the PhD in a different and crazy way full of life and movement! **Magda** thanks for all your energy and passion! **Jonathan Weitzman** thanks for giving PhD students the opportunity to combine and enjoy art and science at the same time.

À **mes amis pasteuriens** : **Cami** pour ton grand soutien, pour être à mon écoute, pour tous les déjeuners et pause-café. **Mélo** (ma guapita) pour ton soutien, avis sur la vie et scientifiques, pause-café, latino dancing, et pour toutes les folies que nous sommes vécues ensembles (tu me manques !!). **Annie** pour être quelqu'un d'exceptionnel et formidable (ma maman de Paris) pour m'apprendre le français, la culture française et pour ton soutien avec mes dossiers et papiers ! **Miliça** et **Sumith** pour m'adopter à Heidelberg et pour les cafés, soirées, danses et je vous aime (après tout nous sommes le trio amoureux) !!

À **Renaud** mi *guapito* et mon complice. Pour ton soutien avec tous mes rêves, pour ton guide, et tes mots de réconfort. Je suis très ravie de t'avoir parce que tu croire dans mes capacités et tu renfonce la confiance en moi. Pour ta patience pour m'apprendre le français, pour ton aide avec tous les papiers, avec la bureaucratie française et avec les dossiers en français.

A mi **familia** por su apoyo incondicional, por creer en mis sueños y confiar en mi. Por todos esos consejos, palabras de aliento y amor en los momentos mas importantes a pesar de la distancia. A mi **mamá** por ser una guía excepcional en mi vida, mejorar la confianza en mi, siempre estar ahí con consejos y palabras de aliento. A mi **papá** por

siempre apoyarme y guiarme para lograr mis sueños. A **Naza** por ser esa hermana increíble que siempre me calma y enseña a estar en paz conmigo misma. A mi hermana de corazón **Emily** por todo el apoyo a la distancia, por todos estos años de amistad, for cheering me up y por siempre creer en mi y motivarme.

A mis amigos de la **Universidad de Costa Rica**. A **Esteban** por creer en mis capacidades y por ser un amigo incondicional. A **Carlos Chacón** por todas las enseñanzas de vida, fuente de inspiración y motivación para seguir en la ciencia. A **las chicas del Master** Diana, Gaby, Tati, Pame y Fanny por el apoyo incondicional en esta aventura tan loca que emprendimos juntas, pero desde distintos lugares del mundo. En mi mente siempre estarán todos esos momentos que vivimos en el lab, los almuerzos, cafés, chismecillos, bailadas, calambres… ¡Las extraño a todas muchísimo y espero volverlas a ver en algún lugar del mundo! ¡Las amo!

A los de **Parissiempre**: a esa comunidad tica tan especial. Por todos esos momentos PURA VIDA, de alegría, karaoke en Le Royal, de salsa tequila y corazón ¡¡y baile latino!! ¡Por hacerme sentir mas cerca de Costa Rica y hacerme reír siempre! ¡Sin ustedes Paris no seria lo mismo!

TABLE OF CONTENTS

LIST OF ABBREVIATIONS

ABC	ATP-binding cassette
ACN	Acetonitrile
ADA	3-Azido D-alanine
ADP	Adenosine diphosphate
AIEC	Adherent-invasive *E. coli*
AmmAc	ammonium acetate
AMP	Adenosine monophosphate
ATP	Adenosine triphosphate
BAHD1	Bromo adjacent homology domain-containing 1 protein
BCA	Bicinchoninic acid
BCAA	Branched-chain amino acid
BHI	Brain heart infusion media
Blp	bacteriocin-like peptide
BrEA	2-bromoethylamine
c-di-GMP	Cyclic diguanylate
CB2	Carnobacteriocin B2
CC	Clonal complex
CDC	Cholesterol-dependent cytolysin
CDI	Contact-dependent inhibition
CDS	Contact-dependent signaling
CFU	Colony forming units
CHAPS	3-[(3-cholamidopropyl) diméthylammonio]-1-propanesulfonate
CIP	Collection Institut Pasteur
CLS	Clostridyolysin S
CO_2	Carbon dioxide
CoA	Coenzyme A
CPBP	CAAX proteases and bacteriocin-processing enzymes
Crp	cAMP receptor protein
CSP	Competence-stimulating peptide
CW	Cell wall
CY	Cytoplasm
DNA	Deoxyribonucleic acid
dNTP	Deoxyribonucleoside triphosphate
dsb	Double strand break
dTMP	Deoxythymidine monophosphate
dUMP	Deoxyuridine monophosphate
Em	Emmision
ER	Endoplasmic reticulum
Ex	Excitation
FA	Formic acid
FKBP	FK506-binding protein
FMN	Flavin mononucleotide
Fnr	Nitrate reductase regulator
fROI	Focus region of interest
GAP	Peptidoglycolipid Addressing Protein Family
GAS	Group A *Streptococcus pyogenes*
GFM	Germ-free mice
GFP	Green fluorescent protein
GIT	Gastrointestinal tract
GMP	Guanosine monophosphate
GTP	Guanosine triphosphate
H_2O_2	Hydrogen peroxide
H3K18	Lysine 18 from histone 3
HAD	Haloacid dehydrogenase
HCD	higher-energy collision dissociation
HEPES	4-(2-hydroxyethyl)-1-piperazineethanesulfonic acid
HMM	Hidden Markov Model
HTH	Helix-turn-helix
HTS	High-throughput screening
IB	Induction buffer
iBAQ	Intensity Based Absolute Quantification
IM	Inner membrane
IMP	Inosine monophosphate
InlA/B/C	Internalin A/B/C
IP	Immunoprecipitation

IPTG	Isopropyl-β-D-thiogalactopyranoside
ISGs	Interferon-stimulated genes
ITP	Inosine triphosphate
KLB	Klebsazolicin
LAB	Lactic acid bacteria
Lan	Lanthionine
LC-LMS/MS	Liquid chromatography-tandem mass spectrometry
LDH	Lactate dehydrogenase
LIPI-3	*Listeria* pathogenicity island 3
LLO	Listeriolysin O
LLS	Listeriolysin S
Lm	*Listeria monocytogenes*
LntA	Nuclear targeted protein A
LTA	Lipoteichoic acid
M	Membrane
Man-PTS	Mannose phosphotransferase system
MBP	Maltose binding protein
McC	Microcin C
Mcc	Microcin
MccB17	Microcin B17
MccJ25	Microcin J25
MCP	Modified core peptide
meLan	β-methyl lanthionine
MES	2-(N-morpholino) ethanesulfonic acid
MFP	Membrane fusion protein
MIC	Minimum inhibitory concentration
MICOS	Mitochondrial contact site and cristae organization system
min	minutes
MLST	Multilocus sequence typing
MOPS	3-(N-morpholino) propanesulfonic acid
MRE11	meiotic recombination 11
mRNA	Messenger RNA
MRSA	Methicillin-resistant *S. aureus*
ms	milliseconds
MS	Mass spectrometry
NBD	Nucleotide-binding domain
NCE	normalized collisional energy
NDk	Nucleoside diphosphate kinase
NDP	Nucleoside diphosphate
NMP	Nucleoside monophosphates
NMR	Nuclear Magnetic Resonance
NTP	Nucleoside triphosphate
NTPase	Nucleoside-triphosphatase
NTPase	Nucleoside-triphosphatase
OD	Optical density
OM	Outer membrane
OMP	Outer membrane protein
ORF	Open reading frames
P	Phosphate
PAGE	Polyacrylamide gel electrophoresis
PBS	Phosphate-buffered saline
PCR	Polymerase chain reaction
PEP	Peptidase domain
Pfam	Protein family database
PFGE	Pulse-field gel electrophoresis
PHZ	Phazolicin
PlcA	Phosphatidylinositol-specific phospholipase C
PlcB	Broad-range phospholipase C
PMNs	Human polymorphonuclear neutrophil granulocytes
PP_i	Pyrophosphate
PPIase	Peptidyl-prolyl cis/trans isomerase
PplA	Pheromone-encoding lipoprotein A
(p)ppGpp	guanosine pentaphosphate
PrfA	Positive regulatory factor A protein
PS	Phosphatidylserine
PTM	Post-translational modification
PTS	Phosphotransferase system

PVDF	Polyvinylidene fluoride
PZN	Plantazolicin
QS	Quorum Sensing
RiPP	Ribosomally-synthesized and post-translationally modified peptide
RMA	relative microcolony area
RNA	Ribonucleic acid
RNAC	RNA core
RNS	Reactive Nitrogen species
rNTP	ribo-Nucleoside monophosphate
ROI	Region of interest
ROS	Reactive Oxygen species
rRNA	Ribosomal RNA
rROI	Reference region of interest
RT	Room temperature
RTX	Repeats-in toxins
S2P	Site-2 protease
SD	Standard deviation
SDS	Sodium dodecyl sulfate
SEM	standards errors of the means
SIRT2	Sirtuin 2
SLAPs	Spacious *Listeria*-containing phagosomes
SLS	Streptolysin S
SN	Supernatant
SPI	Signal peptidase I
SPII	Signal peptidase II
sROI	Signal region of interest
ssDNA	Single strand DNA
ssRNA	Single strand RNA
ST	Sequence type
STS	Staphylysin S
SUMO	Small Ubiquitin-like Modifier
T1SS	Type 1 secretion system
T4SS	Type 4 secretion system
T5SS	Type 5 secretion system
T6SS	Type 6 secretion system
T7SS	Type 7 secretion system
TCA	Trichloroacetic acid
TCEP	tris(2-carboxyethyl) phosphine
TCS	Two-component system
TEM	Transmission electron microscopy
TERT	Telomerase reverse transcriptase
TFA	Trifluoroacetic acid
TIM-4	Mucin domain-containing protein 4
TMD	Transmembrane domain
TMPDB	Transmembrane Protein Database
TOMM	Thiazole/oxazole-modified microcin
TPS	Two-partner secretion system
tRNA	Transfer RNA
UCP	Unmodified core peptide
VOC	Vicinal oxygen chelate
VRE	Vancomycin-resistant enterococci
WT	Wild type
XMP	Xanthosine monophosphate
XTP	Xanthosine triphosphate

LIST OF FIGURES

LIST OF TABLES

INTRODUCTION

Part I: Generalities and classification of bacteriocins

1. 1 History and definition of bacteriocins

The production of antimicrobial compounds is ubiquitous and is present in the three domains of life (1–3). Eukaryotic cells synthetize antimicrobial peptides as defensive weapons to neutralize microbes. For example β-defensins, produced by epithelial cells in the skin as well as in the respiratory and gastrointestinal tract (GIT), allow to reinforce the mucosal barrier against microbial infection (3). The antimicrobial peptides produced by *Bacteria* and *Archaea* are designated as bacteriocins.

The first reference of bactericidal activity mediated by a bacteriocin dates from 1877, when Pasteur and Joubert reported the growth inhibition of *Bacillus anthracis* by bacteria isolated from urine samples (4, 5). The first described bacteriocin was produced by *Escherichia coli* and was discovered by André Gratia in 1925. This bacteriocin is called the colicin V and inhibits the growth of other *E. coli* strains (6, 7). The term bacteriocin was introduced by François Jacob in 1953 (8) and subsequently used by Tagg *et al*. (9) in 1976 and Klaenhammer (10) in 1988 to describe a variety of antagonistic factors, antibiotic-like substances and bactericidal proteins targeting closely related bacterial species (6).

It has been estimated that each species of *Bacteria* and *Archaea* produce at least one bacteriocin (11, 12), and their discovery may be hampered by the lack of detection of their antimicrobial activity (9). More recently, it has been shown that some bacteria are able to produce two or more bacteriocins (13), reflecting the importance of these molecules which provide competitive advantages in complex niches (14).

Bacteriocins are defined as: “ribosomally synthetized antimicrobial peptides or proteins produced by one bacterium and active against other bacteria and to which the producer has a specific immunity mechanism”(15, 16). In general, they have a narrow spectrum of antibacterial activity, which means that they act only against closely related bacterial strains. They can be decorated or not with post-translational modifications (PTMs) that enable them to display highly diverse structures and diverse mechanisms of action (6).

It is important to make the difference between bacteriocins and traditional antibiotics. Traditional antibiotics are non-ribosomally synthetized molecules produced by enzymes and usually active against a broad spectrum of bacteria. Secondly, traditional antibiotics require a higher dose to be effective compared to the dose required for bacteriocins to act against target bacteria, which is at nanomolar concentrations (2).

The family of bacteriocins comprise a huge diversity of proteins regarding size, structures, mechanism of action, export and secretion mechanisms, immunity mechanisms, and targets (13, 17). Their classification is complex due to its great diversity and several approaches have been proposed to classify bacteriocins. For practical reasons, they can be divided in two main groups: bacteriocins produced by Gram-positive and Gram-negative bacteria and further subdivided regarding its size and the presence or absence of post translational modifications (16). In the case of post-translationally-modified bacteriocins a comprehensive nomenclature for ribosomally-synthesized and post-translationally modified peptides (RiPPs) has recently been proposed (1).

1.2 Classification of bacteriocins

Bacteriocins are an extremely heterogeneous group of molecules, and its classification is complex and depends on several features: the origin of the bacteriocin (whether it is produced from a Gram-positive or Gram-negative bacteria), the absence or presence of post-translational modifications(16), its molecular mass (18) and other criteria that will be mentioned later.

The more general classification of bacteriocins considers their origin. Bacteriocins produced by Gram-negative bacteria are divided in two groups according to their size: higher molecular mass molecules displaying between 30 and 80 kDa are called colicins, and smaller molecules (<10 kDa) are named microcins. Bacteriocins produced by Gram-positive bacteria range between 1 and 10 kDa (18) and are divided into two major groups according to their modifications: the heat-stable highly-modified lantibiotics (Class I) and the heat-stable non-modified (or with potential minor modifications) bacteriocins (Class II) (2). Sub-classification of bacteriocins from Gram-positive bacteria mainly relies on their structural features, whereas sub-classification of bacteriocins from Gram-negative bacteria depends on functional criteria like

receptors and killing mechanisms in the case of colicins, and killing mechanisms, post-translational modifications and gene cluster organization in the case of microcins (6). A specific group of microcins produced by both Gram-negative and Gram-positive bacteria, the thiazole/oxazole-modified microcins (TOMMs), will be specifically discussed in Part III of the Introduction.

1.2.1 Bacteriocins from Gram-negative bacteria

Bacteriocins from Gram-negative bacteria have been mainly studied in *Enterobacteriaceae,* and have been particularly well described in *E. coli*. As mentioned above, there are two major families: colicins and microcins. Though colicins were initially reported in *E. coli*, a number of colicins have been described in other Gram-negative bacteria and are named colicin-like bacteriocins. By analogy with colicins, they carry the name of the producing species followed by the suffix *-cin* (4). As examples, bacteriocins from *Pseudomonas* and *Photorhabdus luminescens* which are highly similar to colicins in domain organization, are called pyocins and lumicins respectively. To mention other examples of colicins-like molecules, pesticins are produced by *Yersinia pestis*, klebicins by *Klebsiella pneumoniae* (6), cloacins by *Enterobacter cloacae*, and megacins by *Bacillus megaterium* (19). In general, the classification of bacteriocins from Gram-negative bacteria is clear enough for colicins, but for microcins it is more complex due to their high structural heterogeneity (6).

1.2.1.1 Colicins

The colicins are in general high molecular mass proteins from 30 to 80 kDa and their production is induced by the SOS response genes as a consequence of DNA damage (6). Colicins are produced by *E. coli* strains that harbor the colicinogenic plasmid. The typical colicin operon has 3 genes: *cxa* encodes for the colicin, *cxi* or *imx* encode for an immunity protein, and *brp* encodes for a lipoprotein that modifies the cell envelope and activates the phospholipase A, killing the producer cell and favoring the release of the colicin to the external medium (6, 20, 21). In general, colicins share a common modular structure which includes: a central receptor-binding domain (R) with high-affinity to surface receptors in target bacteria (which define their narrow spectrum of activity) (19), a N-terminal translocation domain (T) which transfers the colicin from its initial binding site in the outer membrane (OM) through the periplasmic regions, and

the C-terminal domain (catalytic, carboxy-terminal or channel forming) which possesses the cytotoxic or enzymatic activity that is inserted into or across the inner membrane (IM) (22, 23).

The colicins that use Tol proteins to be translocated are classified as group A colicins and the colicins that use the TonB proteins are classified as group B colicins (Table 1). Colicins and colicin-like bacteriocins can be further subdivided according to their mechanism of action. The three main mechanisms of action include: formation of voltage-dependent channels in the inner membrane, nuclease activity, or degradation of the peptidoglycan (Table 1) (6).Group A colicins are encoded by small plasmids and are released to the external medium while group B colicins are encoded by large plasmids, are not secreted and remain in the cytoplasm because are not co-expressed with a lysis protein (19).

Table 1. Main characteristics of group A and B colicins and colicin-like bacteriocins

Name of the bacteriocin *Producer*	**Number of residues and gene (active bacteriocin)**	**Receptor**	**Translocation system**	**Killing mechanism**
Group A				
Colicin A *Citrobacter freundii* *E. coli*	592, *caa*,	BtuB	OmpF TolA, B, Q, R	Pore-forming
Colicin K *E. coli*	548, *cka*	Tsx	OmpF, OmpA TolA, B, Q, R	Pore-forming
Colicin N *E. coli*	387, *cna*,	OmpF	OmpF TolA, Q, R	Pore-forming
Colicin U *E. coli*	618, *cua*	OmpA	OmpF, LPS TolA, B, Q, R	Pore-forming
Colicin S4 *E. coli*	499, *csa*	OmpW	OmpF,TolA, B, Q, R	Pore-forming
Colicin E1 *E. coli*	522, *cea*	BtuB	TolC TolA, Q, R	Pore-forming
Colicin E2 *E. coli*	581, *ceaB*	BtuB	OmpF, TolA, B, Q, R	DNase
Colicin E3 *E. coli*	551, *ceaC*,	BtuB	OmpF, TolA, B, Q, R	rRNase
Colicin E4 *E. coli*	177, *cea4*	BtuB	OmpF, TolA, B, Q, R	rRNase
Colicin E5 *E. coli*	unknown, *cea5*	BtuB	OmpF, TolA, B, Q, R	tRNase
Colicin E6 *E. coli*	551, *cea6*	BtuB	OmpF, TolA, B, Q, R	rRNase
Colicin E7 *E. coli*	576, *cea7*	BtuB	OmpF, TolA, B, Q, R	DNase
Colicin E8 *E. coli*	unknown, *cea8*	BtuB	OmpF, TolA, B, Q, R	DNase

Colicin E9 *E. coli*	582, *cea9*, 1FSJ	BtuB	OmpF, TolA, B, Q, R	DNase
Cloacin DF13 *E. cloacae*	561, *ccl*	IutA	TolA, Q, R	rRNase
Pyocin AP41 *Pseudomonas aeruginosa*	776	(?)	TolA, B, Q, R	DNase
Alveicins A *Hafnia alvei*	408, *aat*	(?)	TolA, B, Q, R	Pore-forming
Alveicin B *H. alvei*	358, *abt*	(?)	TolA, B, Q, R	Pore-forming
Marcescin 28b *Serratia marcescens*	–	Omp4e/ OmpAf	OmpF TolA, B, Q, R	Pore-forming
Group B				
Colicin B *E. coli*	510, *cba*	FepA	FepA (?) TonB, ExbB, D	Pore-forming
Colicin Ia *E. coli*	626, *cia*	Cir	Cir, TonB, ExbB, D	Pore-forming
Colicin Ib *E. coli*	626, *ciaB*	Cir	Cir (?) TonB, ExbB, D	Pore-forming
Colicin 5 *E. coli*	490, *cfa*	Tsx	TolC, TonB, ExbB, D	Pore-forming
Colicin 10 *E. coli*	490, *cta*	Tsx	TolC, TonB, ExbB, D	Pore-forming
Colicin D *E. coli*	697, *cda*	FepA	FepA (?) TonB, ExbB, D	tRNase (Arg tRNA)
Colicin M *E. coli*	271, *cma*	FhuA	FhuA (?) TonB, ExbB, D	Degradation of peptidoglycan
Pesticin *E. coli*	357, *pst*	FyuA	FhuA (?) TonB, ExbB, D	Muramidase
Pyocin S1 *P. aeruginosa*	618, *pyoS1A*	Ferripyoverdine receptor	(?) TonB, ExbB, D	DNase
Pyocin S2 *P. aeruginosa*	690, *pyoS2A*	Ferripyoverdine receptor	(?) TonB, ExbB, D	DNase
Pyocin S3 *P. aeruginosa*	768, *pyoS3A*	Ferripyoverdine receptor	TonB, ExbB, D	DNase
Undetermined group				
Klebicin C *K. pneumoniae* *K. oxytoca*	619, *kca*	(?)	non-TonB	rRNase
Klebicin D *K. pneumoniae*	716, *kda*	(?)	(?)	tRNase
Pyocin S4 *P. aeruginosa*	764	(?)	(?)	tRNase
Pyocin S5 *P. aeruginosa*	498	(?)	(?)	Pore-forming
Carocin S1 *Herwinia carotovora*	361, *caroS1K*	(?)	(?)	DNase (?)

Adapted from Rebuffat (2011)(6).

Colicins can use the same receptor and system to be translocated or colicins can use a receptor that is different from the system they use to be translocated. The most common receptors are OM proteins that allow the entry of essential nutrients such as

vitamins, sugars and metals (i.e. iron-bound siderophores) (19, 22). Receptors that are typically hijacked by colicins include siderophore receptors such as FhuA, FepA, Cir and Fiu (6), the vitamin B12 receptor BtuB (24), and the nucleoside receptor Tsx (6). The receptors could be used as translocators, but in some cases the receptor is different from the translocator. The translocators can be OM porins such as OmpF (25). The translocation of colicins through the OM relies on the Tol and Ton machineries. These machineries are anchored to the OM receptors and to the IM to provide energy by means of the proton motif force (6). The Ton machinery is composed of the IM proteins TonB, ExbB and ExbD while Tol contains more IM proteins such as TolA, TolQ and TolR, the periplasmic protein TolB and the OM lipoprotein Pal (19).

1.2.1.2 Microcins

The microcins are small hydrophobic, highly stable peptides that generally are produced under stress conditions (i.e. starvation). Peptides range from 1 to 10 kDa and are resistant to proteases, extreme pHs and high temperatures (6). They display bactericidal activities against closely related species. They can be encoded in the chromosome, or carried in a plasmid. In general, the gene clusters involved in the production of microcins encode a precursor of the microcin, secretion machineries, an immunity protein and in some cases post-transcriptional modifications enzymes. Microcins are potent molecules and their minimum inhibitory concentration (MIC) is in the nanomolar range (26). They have been less studied than colicins, and among the 14 microcins identified so far, only 7 have their structures fully characterized (6, 26).

The microcins represent a very diverse family regarding structures and mechanisms of action, which complicates its sub-classification. The most accepted sub-classification takes into account three criteria: posttranslational modifications, gene cluster organization and the sequences of the leader peptides (6). Class I microcins are peptides with a molecular mass below 5 kDa, subjected to extensive post-translational modifications (Table 2). Class II microcins includes higher molecular mass peptides (between 5-10 kDa) and is further subdivided into subclass IIa and IIb: subclass IIa does not display post-translational modifications (but some of them may present disulfide bonds), while subclass IIb are linear microcins that may carry a C-terminal post-translational modification (Table 2) (26).

Table 2. Main characteristics of class I and II microcins.

Name	Post-translational modification Name of the genes	Receptor	Translocation system	Killing mechanism
Class I				
B17	Thiazole and oxazole rings mcbB, mcbC, mcbD	OmpF	OmpF (?) SbmA	DNA gyrase inhibition
C7-C51	Modified nucleotide mccB, mccC, mccE	OmpF	OmpF (?) YejA, B, E, F	Cleavage in the target cell adenylate that inhibits Asp-tRNA synthetase
J25	Lasso structure mcjB, mcjC	FhuA	Fhua (?) TonB, ExbB, D, SbmA	RNA polymerase inhibition. Mitochondrial proteins and lipids damages
Class II				
Class IIa				
L	2 disulfide bonds	Cir	Cir, TonB, ExbB, D SdaC	Membrane permeability modification (?)
V	1 disulfide bond	Cir	Cir (?), TonB, ExbB, D	Membrane permeability modification
24	no disulfide bond	(?)	(?)	Mannose permease (ManYZ) targeting (?)
Class IIb				
E492	Siderophore anchored at the C-terminus mceC, mceD, mceI, mceJ	FepA, Cir, Fiu	FepA, Cir, Fiu (?) TonB, ExbB, D	Inner membrane channels. ManYZ targeting (mannose permease)
M	Siderophore anchored at the C-terminus mcmL, mcmK	FepA, Cir, Fiu	FepA, Cir, Fiu (?) TonB, ExbB, D	(?)
H47	Siderophore anchored at the C-terminus mchA, mchS1, mchD mchC	FepA, Cir, Fiu	FepA, Cir, Fiu (?) TonB, ExbB, D	F_0F_1 ATP synthetase
147 (predicted *in silico*)	Siderophore anchored at the C-terminus	FepA, Cir, Fiu	FepA, Cir, Fiu (?) TonB, ExbB, D	(?)
G492 (predicted *in silico*)	Siderophore anchored at the C-terminus	FepA, Cir, Fiu (?)	FepA, Cir, Fiu (?) TonB, ExbB, D	(?)

Adapted from Rebuffat (2011)(6).

1.2.2 Bacteriocins from Gram-positive bacteria

The continuous discovery and characterization of many diverse bacteriocins from Gram-positive bacteria reveals their high heterogeneity, complexifying their classification (5). Bacteriocins produced by lactic acid bacteria (LAB) have been of great interest because they can be potentially employed in food preservation, food safety and in human and veterinary medicine (15, 16, 27). The earliest classification of LAB bacteriocins divided them into 8 groups based on heat resistance, host range,

trypsin sensitivity and the degree of cross-reactivity between various bacteriocin and host combinations (5). This classification was subsequently modified by Klaenhammer in 1993, grouping LAB bacteriocins in 4 classes: Class I or lantibiotics, Class II, Class III and Class IV (Table 3) (28, 29).

Table 3. Original classification of bacteriocins from Gram-positive bacteria

Group	Description	Distinctive features
Class I	Post-translationally modified bacteriocins	Contain the unusual amino acids Lan, meLan and dehydrated residues
Class II	Unmodified peptides	Small (<10 kDa) heat-stable membrane-active peptides
Class III	Unmodified proteins	Large (>30 kDa) heat-labile proteins
Class IV	Complex proteins	Contain lipid or carbohydrate moieties

Adapted from Rea *et al.* (2011) (5).

1.2.2.1 Class I or post-translationally modified bacteriocins

Class I is subdivided into Class 1a lantibiotics, Class Ib the labyrinthopeptins and Class Ic sactibiotics. More recently identified, the thiopeptides and the bottromycins are also included in this group (Table 6) (16, 30).

1.2.2.1.1 Class Ia or lantibiotics

The term lantibiotic is derived from *lanthionine*-containing *antibiotics*. Lantibiotics are small membrane-active peptides (<5kDa) containing lanthionine (Lan) and/or β-methyl lanthionine (meLan), as well as dehydrated residues as dehydroalanine and dehydrobutyrine. These uncommon residues form covalent bridges between amino acids, resulting in internal rings that provide lantibiotics their specific structure. Lantibiotics can contain other uncommon amino acid residues that are the result of post-translational modification of D-alanines and L-serines (15). The genes responsible for the production of lantibiotics are organized in clusters in the chromosome, in a plasmid or in a transposon (31). Lantibiotics are further subdivided into 4 subclasses based on the pathway involved in the maturation of the peptide and the presence or absence of antibiotic activity (29, 32). When they display antimicrobial activity they are called lantibiotics, and in the absence of antimicrobial activity they are named lantipeptides (1).

-Subclass I lantibiotics

They are modified by two different enzymes: LanB which dehydrates threonine/serine residues, and LanC which mediates thioether cyclization (Figure 1) (33). The peptides are exported by LanT, an ABC transporter, and the leader peptides are cleaved by LanP, a serine protease (32). These peptides have a linear structure (29), are amphiphilic, and form of pores in membranes, leading to the loss of membrane potential (15). The prototype is nisin, which is probably the best characterized bacteriocin (5).

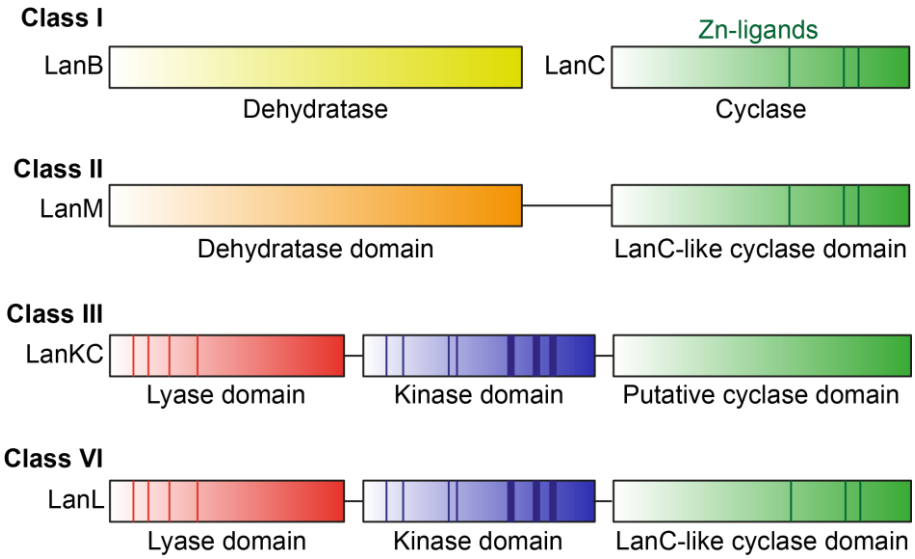

Figure 1. Classification of lantipeptides based on the biosynthetic enzymes that introduce the post-translational modifications. The dark areas show conserved regions responsible for the catalytic activity. Adapted from Arnison *et al.* (2013).

-Subclass II lantibiotics

They are modified by the bifunctional synthetase LanM, displaying a dehydratase domain at the N-terminus and a cyclase domain at the C-terminus (Figure 1) (33). Secretion and leader processing is also performed by the multifunctional protein LanT, displaying a conserved N-terminal cysteine protease domain (5, 32). They have a more globular structure than subclass I lantibiotics (29). Lactocin S and the two-component lantibiotic lacticin 3147 belong to this subclass (5).

-Subclass III lantipeptides

They are modified by the trifunctional synthetase LanKC which displays a lyase N-terminal domain, a central kinase domain and a putative C-terminal cyclase domain (Figure 1) (29). They lack antibiotic activity and function in aerial mycelium production

in *Streptomyces* (32). Three different subclass III lantipeptides have been described so far: SapB, AmfS and SapT (5).

-Subclass IV lantipeptides

This recently added subclass includes peptides modified by the Lan synthetase LanL, which generates dehydroamino acids via phosphorylation of serine or threonine residues by a central protein kinase N-terminal domain, and subsequently eliminates a phosphate by a lyase domain. LanL also contains a C-terminal cyclase domain (Figure 1). The modified peptides also lack antimicrobial activity as for subclass III (34).

Alternatively, lantibiotics can be divided into 12 groups (Table 4) based on the sequences of the unmodified pro-peptides (15, 27).

1.2.2.1.2 Class Ib or labyrinthopeptins

These are lantibiotics that contain labionin, a carbacyclic post-translationally modified amino acid. The first described compounds include labyrinthopeptins A1, A2 and A3 (A1 derivative) which have a globular structure that consists primarily of hydrophobic amino acids. The modifications are produced by the enzyme LabKC, with an N-terminal serine/threonine kinase function and a C-terminal Lan cyclase (35). These compounds have the motifs Ser-Xxx-Xxx-Ser-Xxx-Xxx-Xxx-Cys in the pro-peptides (35).

1.2.2.1.3 Class Ic or sactibiotics

They form cysteine sulphur to α-carbon bridges (5). The first described is Subtilosin A, produced by *Bacillus subtilis*. It is a cyclic peptide and is extensively posttranslationally modified, with cross-linkages between the sulphurs of three cysteine residues and the α-carbon of two phenylalanines and one threonine (5, 36). More recently, a second sactibiotic was identified, a two-peptide bacteriocin (Trnα and Trnβ) produced by *B. thuringiensis* 6431 and active against *Clostridium difficile,* named thuricin CD (37). It is characterized by the presence of cross-linkages as in Subtilosin A (5). Thuricin CD presents two S'-adenosylmethionines in each peptide and also possess unusual posttranslational modifications that generate catalytic radicals and an unusual iron sulphur cluster [4Fe–4S] (5, 37).

Table 4. Classification of lantibiotics

Subclass	Enzymes	Groups	Lantibiotic examples
I Type A (Linear)	Modification LanB/C Export LanT Leader cleavage LanP	Planosporicin	Planosporicin
		Nisin	Nisin A, Nisin Z, Nisin F, Nisin U, Nisin U2, Nisin Q, Subtilin and Ericin A
		Epidermin	Epidermin, Epidermin', Gallidermin, Staphylococcin T, NY266, Mutacin 1140, Clausin and Mutacin I
		Streptin	Streptin
		Pep 5	Pep5, Epicidin 280 and Epicidin K7
II Type B (Globular)	Modification LanM Export and cleavage LanT	Lacticin 481	Mecedocin, Lacticin 481, MukA1, MukA2, MukA3, MukA', Salivaricin B, Lacticin J46, Mutacin II, Butyrivibriocin, RumA, Streptococcin SA-F22, Nukacin ISK-1, Variacin, Salivaricin A and Bovicin HJ50
		Mersacidin	RumB, Plantaricin C, Mersacidin, Michiganin, Actagardine, C55a, Ltnα, SmbB, bhtA-alpha, Plwa, BhaA1 and BliA1
		LtnA2	Ltnβ, C55b, Plwb, SmbA/bhtA-beta, BhaA2 and BliA2
		Cytolysin	CylLl and CylLs
		Lactosin S	LasA
		Cinnamycin	Cinnamycin, Duramycin, Duramycin B, Duramycin C and Ancovenin
		Sublacin	Sublacin 168
III Type C	No antibiotic activity	-	RamS, AmpfS and SapT
IV Type D	Modification LanL No antibiotic activity	-	Venezuelin

Adapted from Rea *et al.* (2011) (5).

1.2.2.1.4 Thiopeptides or thiazolyl peptides

They are highly modified sulfur-containing peptides with a macrocycle that comprises thiazole, oxazole and indole rings, and often multiple dehydrated amino acid residues. The majority are produced by Actinobacteria but they have been isolated also from Firmicutes from the *Staphylococcus* and *Bacillus* genera. In general, they inhibit protein synthesis mostly in Gram-positive bacteria, but some thiopeptides have also demonstrated antimalarial, antifungal and anticancer activities (38). They are subclassified according to their central heterocyclic domain and their oxidation state into 5 series (Table 6): (a) piperidines, (b) pehydropiperidines, (c) dihydroimidazopiperidines, (d) trisubstituted pyridines, and (e) hydroxypyridine thiopeptides (1, 38).

1.2.2.1.5 Bottromycins

They have a macrocyclic amidine, a decarboxylated C-terminal thiazole and several rare β- methylated amino acid residues. Instead of a N-terminal leader peptide, they contain a C-terminal leader peptide (35-37 residues) and an 8-mer core peptide (Table 6) (1). The N-terminal methionine of the core peptide is first cleaved, and subsequently the peptides are post-translationally modified. The bottromycins have been isolated from *Streptomyces spp.* and have activity against methicillin-resistant *Staphylococcus aureus* (MRSA) and vancomycin-resistant enterococci (VRE).The most studied is Bottromycin A2, which inhibits protein synthesis by interacting with the bacterial 50S ribosomal subunit (30).

1.2.2.2 Class II or unmodified bacteriocins

This is an heterogenous group of small (<10 kDa) peptides, with standard amino acids that can be linked by disulfide bridges or cyclized at the N and C terminus with moderate-to-high heat stability (5). In general, they are non-Lan containing, membrane-active peptides that possess a Gly-Gly processing site at the bacteriocin's precursor (29, 36). They have amphiphilic helices with varying amounts of hydrophobicity and generally kill cells through membrane permeabilization (5, 39). They are cationic and their N-terminal half forms a β-sheet-like structure that binds to the target cell surface, while the hydrophobic C-terminal half penetrates into the target cell membrane, following a conformational change that promotes membrane-leakage (15, 39) (Table 6). They are divided into 4 subclasses: IIa, IIb, IIc and IId (see below) (28).

1.2.2.2.1 Subclass IIa pediocin-like bacteriocins

They are *Listeria*-active peptides that vary in length from 37 to 58 residues, with a hydrophilic N-terminal region that contains the consensus sequence Y-G-N-G-V-X_1-C-X_2-K/N-X_3-X_4-C (where X is any amino acid), often called as "pediocin box". The C-terminal region is variable, hydrophobic, and/or amphiphilic. The target specificity is determined by the C-terminal region that penetrates into the membrane of the target bacteria, and this region is also involved in the recognition of immunity proteins (15, 39, 40). They are produced by a wide range of Gram-positive bacteria and have a very narrow spectrum of activity (5). Since they have a high cysteine content, they possess

at least one disulfide bridge that contributes to their antibacterial activity. They resist to elevated temperatures and to extreme pHs (40).The cleavage of the leader peptide from its precursor generally occurs at a Gly-Gly motif and is performed by an ABC transporter and its accessory protein (5, 29). The pediocin-like bacteriocins kill target cells by disrupting the proton motif force (39).

The structure studies by Nuclear Magnetic Resonance (NMR) and circular dichroism have shown that in general the pediocin-like bacteriocins are unstructured in aqueous solutions, and upon contact with membranes they acquire a 3D structure. This structure consists of a conserved N-terminal region that forms three strands β-sheet-like structures, stabilized by a disulfide bridge, and the more hydrophobic C-terminal part forms (with a few exceptions) a hairpin-like structure that consists of an amphiphilic α-helix. There is a flexible hinge between these two regions at the conserved Asn17/Asp17 that is stabilized by a disulfide bridge or a conserved central tryptophan residue (5, 39). The prototype peptide from this family is the pediocin PA-1, produced by *Pediococcus acidilactici* and used commercially as an anti-*Listeria* food preservation product (Table 5) (29, 41).

1.2.2.2.2 Subclass IIb two-peptide unmodified bacteriocins

They consist of two different peptides, and optimal activity requires both peptides in about equal amounts (5, 39). The genes encoding the two peptides of the bacteriocin are next to each other in the same operon which includes the immunity protein, an ABC-transporter system, as well as an accessory protein of unknown function (42). The mechanism of action involves the dissipation of the membrane potential, the leakage of ions and/or decrease in intracellular ATP levels (15, 42). They are usually cationic, between 30 to 50 residues long, hydrophobic and/or amphiphilic and synthetized with a 15-30 residues N-terminal leader sequence (GG type) that is cleaved off by an ABC-transporter system (39). The production of some two-peptide bacteriocins is constitutive, whereas for others it is regulated through a three-component regulatory system that consist of a peptide pheromone, and a two-component system (a histidine kinase and a response regulator) (42). They can be subdivided into groups type E (enhanced) and type S (synergistic) (15). In E type, each peptide of the couple possess inhibitory activity but the combination of the two

components results in greatly enhanced killing activity. In the S type, the bacteriocin activity depends completely on the joint action of both peptides (29).

The amino acid sequences and structures of the two-peptide bacteriocins are diverse, but there is a GXXXG conserved motif that is present in both peptides (5). The structures of plantaricin EF, plantaricin JF and lactococcin G were elucidated and showed that these peptides form amphiphilic α-helixes when exposed to membranes (42). It has been proposed that the interaction of both peptides and the formation of the α-helices operates through the GxxxG conserved motif, essential for the antimicrobial activity as well (5, 43, 44). It has been also proposed that the α-helices interact with an integral membrane protein inducing a conformational change in the protein, which in turn causes membrane-leakage (42). However, the presence of a β-sheet in brochocin C rather than α-helices confirms the diversity of structures among this subclass of bacteriocins that might need further sub-classification in the future (5). The prototype and more characterized bacteriocin of this group is lactococcin G (Table 5) (39).

Table 5. Classification of Class II or unmodified peptides

Subclass	Motif	Distinctive feature	Examples
IIa	YGNGV (N is any amino acid)	Pediocin-like	Pediocin PA-1, Sakacin G, Sakacin P Coagulin, Divergicin M35, Enterocin A, Leucocin A, Leucocin C, Plantaricin 423.
IIb	GXXXG	Two unmodified peptides	ABP-118, Brochocin, Lacticin F, Lactocin 705, Mutacin IV, Plantaricin E/F, Plantaricin NC8, Plantaricin S, Salivaricin P, Thermophilin 13, Lactococcin G, Lactococcin Q and Enterocin 1071.
IIc	-	Covalent linkage of their N- and C-termini (circular)	Acidocin B, Butyrivibriocin AR10, Carnocyclin A, Circularin A, Enterocin AS-48, Gassericin A, Lactocyclicin Q, and Uberolysin.
IId	-	Unmodified, linear, non-pediocin-like	Lactococcin A, Lactococcin B, Aureocin A70 and Aureocin A53

Adapted from Rea *et al.* (2011) and Martin-Visscher *et al.* (2011) (5, 45).

1.2.2.2.3 Subclass IIc circular bacteriocins

These are thiol-activated peptides requiring reduced cysteine residues for activity. The precursor proteins undergo posttranslational modifications resulting in the covalent linkage of their N- and C-termini (head-to-tail) to create a circular backbone. Generally, they are heat-stable, protease-resistant and display anti-listerial activity (5, 45).

However, the structures of many of these bacteriocins have not been elucidated (15). For the 7 cyclic bacteriocins that have been characterized, they are all cationic and relatively hydrophobic, they range from 3.4 to 7.2 kDa and show a more heterogeneous structure than IIa and IIb bacteriocins. The mode of action of these characterized circular bacteriocins is similar to the IIa and IIb bacteriocins that induce cell membrane permeabilization by allowing the passage of small molecules, leading to the disruption of the proton motif force (Table 5) (39).

1.2.2.2.4 Subclass IId unmodified, linear, non-pediocin-like bacteriocins

They are placed in this category simply because they do not belong to any other subclass and they do not follow the previously described criteria (5). They do not have sequence similarity to other class II bacteriocins (46). As a consequence, they are a diverse group of around 30 bacteriocins that are principally produced by LAB but also by other bacteria like *Staphylococcus*, *Weissella* and *Propionibacterium sp*. (29, 37, 39). As examples, Lactococcin A, Lactococcin B, Aureocin A70 and Aureocin A53 (Table 5) (39). They can be subdivided in 3 groups: *sec*-dependent bacteriocins, leaderless bacteriocins (no N-terminal leader sequence) and non-subgrouped bacteriocins (46).

1.2.2.3 Class III or large bacteriocins

These are large (>10 kDa), generally heat-labile antimicrobial proteins, often with enzymatic activity (29). Some are produced by LAB including helveticin J from *Lactobacillus helveticus*, zoocin A from *Streptococcus zooepidermicus*, enterolysin A produced by *Enterococcus faecalis*, millericin B produced by *Streptococcus milleri* and *linocin M18* produced by a strain of *Brevibacterium linens.* They also include some that are not produced by LAB as lysostaphin (5).

1.2.2.3.1 Bacteriolysins

They can be further divided into: bacteriolysins (bacteriolytic enzymes) and non-lytic bacteriocins (Table 6) (29). The bacteriolysins present specific domains for receptor binding, translocation and lethal activity (15). Their mechanism of action is through cell-wall hydrolysis. They have a catalytic domain at the N-terminus that has homology to endopeptidases, and the C-terminus contains the target recognition site. In contrast

to conventional bacteriocins, they do not have immunity proteins and their mechanism of resistance relies on the modifications of the cell wall of the producer bacterium (15).

The prototype and most studied bacteriolysin is lysostaphin, a plasmid-encoded glycylglycine endopeptidase that kills target cells by specifically hydrolyzing the pentaglycine cross-bridges in the peptidoglycan. The plasmid encodes an immunity factor that makes producer cells resistant by adding serine residues, rather than glycine, to the cross-bridges in the peptidoglycan (29). For the non-lytic bacteriocins, their mechanism of action involves formation of pores. The first non-lytic bacteriocin described is helveticin J (29).

1.2.2.4 Class IV

These are proteins composed of one or more chemical moieties, either lipid or carbohydrate (29) (Table 6).

1.2.2.4.1 Glycocins

This group includes *O*- (attached to Ser or Thr residues) and *S*-linked (attached to Cys) glycosylated antimicrobial peptides. The best characterized glycocins are sublacin 168 produced by *B. subtilis* 168 and glycocin F produced by *L. plantarum* KW30. These two bacteriocins are glycosylated on Cys residues. In sublancin, a glucose is attached to a Cys residue (*S*-linked glycosylation) in the precursor peptide and the other four Cys form two disulfide bridges (47). In glycocin F, a *S*-linked glycosylation is located on a different Cys residue and a N-acetylglucosamine is conjugated to a Ser residue (*O*-linked glycosylation) (48). The two alpha-helices formed by the two disulfide bridges appear to be the recognition elements for the S-glycosyltransferase in sublancin (49).

1.2.2.4.2 Lipolanthines

These are lanthipeptide variants with an avionin moiety (triamino-dicarboxylic acid moiety) and an N-terminal guanidine fatty acid. The first elucidated is microvionin from *Microbacterium arborescens* 5913, active against MRSA and *S. pneumonia* (30). Genome-mining techniques revealed some lipolanthine gene clusters in *Nocardia terpenica, N. altamirensis* and *Tsukamurella sp.* 1543. Lipolanthine biosynthesis

requires the biosynthetic pathways of ribosomal peptides, and the fatty acid or polyketides biosynthetic pathways (50).

Table 6. Updated classification scheme for bacteriocins from Gram-positive bacteria

Class	Description	Subclasses	Key features	Further divisions
Class I	Modified peptides	Lantibiotics	MeLan residues	Four sub-classes (Table 4)
		Labyrinthopeptins	Contain labionin, a carbacyclic amino acid	-
		Sactibiotics	Cysteine sulfur to α-carbon bridges	Single- and two-peptide bacteriocins
		Thiopeptides	Heterocycles, azol(in)e rings, dehydro-residues	Series a-e
		Bottromycins	Macrocyclic amidine, decarboxylated C-terminal thiazole, β-methylated residues	-
Class II	Non-modified peptides (Table 5)	IIa	Pediocin-like (YGNGV motif)	Four subclasses I–IV
		IIb	Two-peptide bacteriocins	Two subclasses: A and B
		IIc	Circular bacteriocins	Two subclasses: I and II
		IId	Unmodified, linear, non-pediocin-like, single-peptide bacteriocins	-
Class III	Non-bacteriocin lytic proteins	Bacteriolysins	Large (>10 kDa), heat-labile antimicrobial proteins	Lytic and non-lytic enzymes
Class IV	Lipid or carbohydrate moieties	Glycocins	Glycosylated antimicrobial peptides	*O*-linked and *S*-linked
		Lipolanthines	N-terminal fatty acid, avionin moiety (aminovinylcysteine-labionin hybrid)	-

Adapted from Rea *et al.* (2011), Cotter *et al.* (2013) and Acedo *et al.* (2018) (5, 16, 30).

1.2.3 Other groups of bacteriocins

They cannot be classified in the previous groups because they are produced by both Gram-positive and Gram-negative bacteria (Table 7).

Table 7. Classification scheme for bacteriocins present in Gram-positive and Gram-negative bacteria.

Class	Description	Further divisions and examples
Linaridins	Have a linear structure and contain dehydrated amino acids	- Cypemicin
Proteusins	Contain multiple hydroxylations, epimerizations and methylations	- Polytheonamide A and B
TOMMs	Possess heterocycles but no other modifications	- Microcin B17, Goadsporin and Plantazolicin
Lasso peptides	Lasso structure	Two-disulfide bonds (siamycin I, siamycin II) No disulfide bonds (lariatin A, Microcin J25 One disulfide bond (BI-32169)
Cyanobactins	Macrocycles with heterocycles, prenylated or *N*-methylated	Patellamide-like (patellamide A) Anacyclamide-like (Anacyclamide A10)
Microviridins	Lactone and lactam structures with the central motif TXKXPSDX(E/D) (D/E)	- Microviridin A and marinostatin 1-12

Adapted from Cotter *et al.* (2013) and Acedo *et al.* (2018).

1.2.2.5.1 Linaridins

They have a linear structure and contain dehydrated amino acids (16). They are characterized by the presence of thioether crosslinks as the lantibiotics but they are generated by a different biosynthetic pathway. The first described bacteriocin of this family is cypemycin, produced by *Streptomyces sp.* OH-4156 (51). Its biosynthetic cluster does not include none of the four types of dehydratases that are present in the lanthipeptides clusters. Cypemicin does not contain Lan bridges but has dehydrated threonines and a C-terminal *S*-[(Z)-2-aminovinyl]-D-cysteine. Cypemycin also has two L-*allo*-isoleucine residues and an N-terminal *N*, *N*-dimethylalanine. Cypemycin-like gene clusters are present in Actinobacteria, Proteobacteria and Acidobacteria, and are also present in Archaea (52).

1.2.2.5.2 Proteusins

They contain multiple hydroxylations, epimerizations and methylations (16). They are complex 48-mer peptides that contain a N-acyl moiety and a high number of non-proteinogenic residues as *tert*-leucine and *C*-methylated amino acids. They have D-amino acids in alternation with L-amino acids (53). They form membrane pores by acquiring a β-helical secondary structure, and membrane insertion is favored by the

lipophilic *N*-acyl unit (54). Proteusins were found in the sponge *Theonella swinhoei* which harbors a great diversity of symbiotic bacteria that are responsible of producing these compounds. However, these symbionts are not yet cultivable (1, 55).

1.2.2.5.3 Thiazole/Oxazole-Modified Microcins (TOMMs)

Also called linear azol(ine)-containing peptides. They are decorated with thiazole, (methyl) oxazole heterocycles and can be sometimes reduced to azoline (1, 56). The first discovered TOMM was Streptolysin S (SLS) from *Streptococcus pyogenes* but due to its complex physicochemical properties, its chemical structure remains elusive (56, 57). However, the structure of microcin B17 (MccB17) produced by *E. coli* is known and the heterocycles derive from cysteine, serine and threonine residues of a ribosomal precursor peptide (58). The heterocycles are introduced to the precursor peptide by a heterotrimeric synthetase complex that includes a dehydrogenase and a cyclodehydratase heterodimer. The leader peptide is then removed and an ABC transporter system is dedicated to export the modified peptide out of the producer cell (56). This cluster of genes is widely distributed in different prokaryotic phyla as well as in the Archaea kingdom (59). A more detailed review of TOMMs can be found in Part III of the Introduction.

1.2.2.5.4 Lasso peptides

They are characterized by a knotted structure called the lasso fold. They consist of 16-21 amino acid residues, with an N-terminal macrolactam that results from the condensation of the N-terminal amino group with a carboxylate side chain of a glutamate or aspartate at position 8 or 9 (1). The N-terminal amino acid of lasso peptides is either a glycine or cysteine and the amino acid that closes the ring is aspartic acid or glutamic acid (60). They are highly resistant to proteases and denaturing agents (1). They are more frequently produced by Actinobacteria (*Streptomyces*, *Rhodococcus*), but some are produced by Proteobacteria (*Escherichia, Burkholderia*) (61–63). They are classified into three classes. The first class contain two disulfide bonds and the first residue is a Cys (siamycin I, siamycin II, aborycin and SSV-2083). The class II does not contain disulfide bonds and the first residue is a Gly (anantin, capistruin, lariatin A, Microcin J25 and others). The class III is a single peptide with one disulfide bond (BI-32169). They have a broad antibacterial

spectrum activity, several have antiviral activities, while other function as receptor antagonists (60).

1.2.2.5.5 Cyanobactins

They include peptides with N-to-C macrocyclization encoded on a precursor peptide with proteolytic cleavage. Macrocyclization is produced by two serine proteases. Some biosynthetic clusters encode for a cyclodehydratase and two conserved proteins of unknown function. Others also possess dehydrogenases that catalyze the heterocyclization to form thiazol(ine)e and oxazoline motifs, several are prenylated on Ser, Thr, or Tyr, while others are *N*-methylated on His (1, 64). They were isolated from an uncultivated symbiotic cyanobacterium of the tunicate *Lissoclinum patella* from the tropical coral reefs. The first two isolated peptides were ulicyclamide and ulithiacyclamide from *Prochloron didemni*. Today, more than 100 compounds have been isolated from cultivated cyanobacteria (65). They have been also isolated from *Streptomyces spp*., they are similarly cyclized from head-to-tail and contain heterocycles but some heterocycles derive from non-proteinogenic amino acids (66).

1.2.2.5.6 Microviridins

They are cyclic, *N*-acetylated with 13 or 14 amino acid residues that contain an intramolecular ω-ester and/or ω-amide bond (1). They have lactams formed between ω-carboxy groups of glutamate or aspartate and the ε-amino group of lysine. They also contain lactones generated by esterification of the ω-carboxy groups of glutamate or aspartate with the hydroxyl groups of serine and threonine. Lactone and lactam formation end up building an unparalleled tricyclic architecture. The central part has a conserved motif TXKXPSDX(E/D)(D/E) , while the N- and C-terminal parts are highly variable (67). They have been isolated from cyanobacteria of the genera *Microcystis* and *Planktothrix*. The prototype of the family is microviridin A produced by *Microcystis viridis* strain NIES 102. Bioinformatic analyses suggest that they are widespread in cyanobacteria, and in sphingobacteria and proteobacteria as well (68). They have been described as inhibitors of serine protease activity (1).

1.2.4 RiPPs

At present the nomenclature used to classify natural products of ribosomal origin is non-uniform, confusing, and in some cases contradictory. For this reason, a more recent classification and nomenclature was proposed by Arnison *et al* (2013) that includes all the ribosomally-synthetized and post-translationally-modified peptides (RiPPs) irrespectively of their biological functions or origin including bacteria, fungi, plants, and cone snails.

A size limit of 10 kDa is artificially imposed to exclude RiPPs from the post-translationally modified proteins (1). In general, all RiPPs are synthesized as a longer precursor peptide of around 20-110 amino acid residues. The unmodified precursor peptide is generally labelled with the letter “A” (encoded by *xxx*A gene). The modified precursor peptide prior to removal of the leader peptide is abbreviated mXxxA (Figure 1) (1). The peptide that will be modified is called core peptide or core region (69). In the core peptide we can distinguish between the unmodified core peptide (UCP) and the modified core peptide (MCP) after the post-translational modifications (Figure 2) (1).

At the N-terminus of the core peptide is located a leader peptide that includes the secretion signal and is usually important for recognition by many post-translational modification enzymes and for export (69). In rare occasions the leader peptide can be located at the C-terminus of the core peptide and is called follower peptide (1). The recognition mechanisms of the leader peptides by the biosynthetic enzymes are still mostly unknown but many leader peptides tend to form α-helices (65, 70–73) and they are thought to play an important role in post-translational modifications, export and immunity. Some studies suggest that different biosynthetic enzymes in a pathway recognize different segments of the leader peptides (65, 73–75).

The last residue of the leader peptide that is not incorporated in the final RiPP is numbered -1. Some peptides have C-terminal recognition sequences that allow its excision and cyclization (Figure 2). The C-terminal recognition sequences or follower peptides can be numbered with +1 from the site of final cleavage (Figure 2) (1).

For this work we decided not to use this classification system because it includes RiPPs produced by organisms from all domains of life. We wanted to focus on RiPPs produced exclusively by bacteria. Examples of RiPPs that were explained earlier include: microcins, lantibiotics, thiopeptides, bottromycins, glycocins, linaridins, proteusins, TOMMs, lasso peptides, cyanobactins, and microviridins (1).

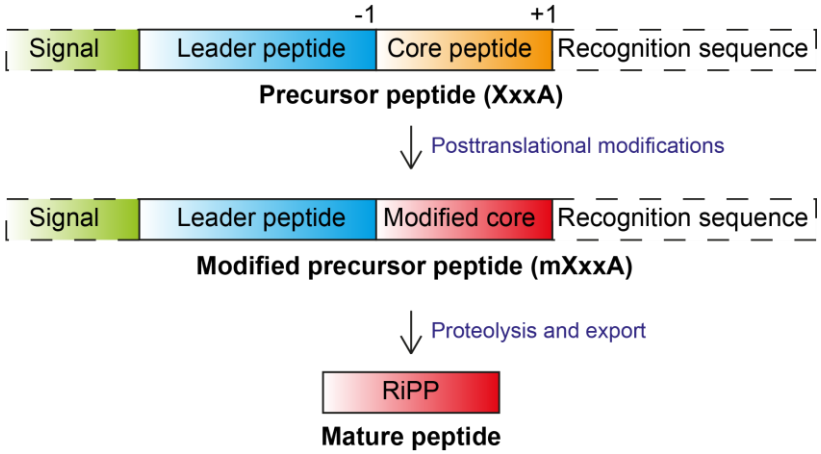

Figure 2. **Nomenclature and general biosynthetic pathway of RiPPs.** The precursor peptide contains a core region that is transformed into the mature product. Many of the post-translational modifications are guided by leader peptide and the recognition sequences. C-terminal recognition sequences are sometimes also present for peptide cyclization in cyanobactins. In some cases, the C-terminal is a leader-like peptide or follower peptide (bottromycins). The unmodified core peptide (UCP) is represented in orange and the modified core peptide (MCP) is represented in red. Adapted from Arnison *et al.* (2013).

Part II: Functional aspects of bacteriocins

2.1 Regulation of expression

The expression of most studied bacteriocins is tightly regulated, which is consistent with the significant energetic cost of production of these molecules (76). In general, the production of bacteriocins is associated to environmental stress, poor nutrient conditions, high cell-density, quorum sensing associated-mechanisms, temperature, and/or concentration of specific molecules such as inducer peptides or pheromones (18).

The expression of bacteriocins can be controlled at several levels: transcriptional, translational or post-translational, and also their release can be tightly regulated. Expression can be controlled simultaneously by different conditions such as in colicin K, where transcription is controlled synergistically by the SOS response and by (p)ppGpp (77, 78). The interaction between regulatory networks that monitor competitors in complex and changing environments, and which influence bacteriocin production, is still poorly understood (76, 79).

2.1.1 Colicins and the SOS response

In a population, only a few cells (from 0,1% in colicin E2 to 3% in colicin K) produce colicins under normal conditions. However, upon induction of the SOS response by mutagenic or carcinogenic agents (i.e. UV light or mitomycin C), up to 50% of the cell population produces colicins (21, 80). The transcription of the colicin operons is repressed by the LexA protein, the repressor of the SOS genes, whereas the immunity protein is under the control of a constitutive promoter to protect producer cells against exogenous colicin molecules (25, 81). The stress response activates RecA which stimulates LexA auto-cleavage and release from the LexA boxes, allowing the transcription of the colicin operon (19). LexA is the common repressor of colicin transcription but other repressors or activators may play a role to further modulate the expression of some colicin operons. For example, colicin synthesis can be stimulated by thymine starvation, stringent response, catabolite repression, stationary phase of growth, anaerobiosis, high temperatures or nutrient depletion (19).

The synthesis of group A colicins is lethal for the producer cells. Indeed, when colicin production exceeds a threshold, a lysis protein present in the colicin operon is also produced. The lysis proteins are small lipoproteins that modify the cell envelope and activate an outer membrane phospholipase A that kills the producer cell, allowing colicin release (21). The operons encoding colicins from group B may contain or not the lysis gene. Consequently, their synthesis can be lethal (or not) for producer cells (19). It is not known how group B colicins are released from their host cells in the absence of the lysis protein. A recent study suggest that prophages may provide a release mechanism for the group B colicin ColIb (82).

2.1.2 Quorum sensing regulation

Quorum sensing (QS) is a communication mechanism used by bacteria to coordinate a population response. Bacteria secreted molecules named pheromones are sensed by other bacteria in a concentration-dependent manner to elicit a response (83). The pheromones are commonly small molecules, such as acyl-homoserine lactone derivatives for Gram-negative bacteria, and small peptides for Gram-positive bacteria, which signal through two-component systems (84, 85). QS allows to activate bacteriocin production against related bacteria when the competition for nutrients is higher, ensures the synchronization of the bacteriocin production in a bacterial population, and the energy that is used to produce the bacteriocins is shared between the producers so the effort of fighting competitors is potentiated (86).

2.1.2.1 Peptide autoregulation

Nisin acts as a pheromone that regulates its own production and processing upon activation of the two-component system NisKR, encoded in the nisin biosynthetic gene cluster (87). Autophosphorylation of the conserved histidine domain in NisK and subsequent phosphor-transfer to the conserved aspartate residue within the N-terminal receiver domain of NisR induces a conformational change in its output domain, which leads to binding to specific target promoter regions (88). NisKR controls the expression of nisin from: the *nisA* promoter (encodes for the nisin peptide) and the *nisF* promoter (encodes for the ABC transporter) (89–91) (Figure 3). The *nisI* promoter is independent of the NisKR system and controls the production of the immunity protein, providing the cell with a basal level of immunity (92).

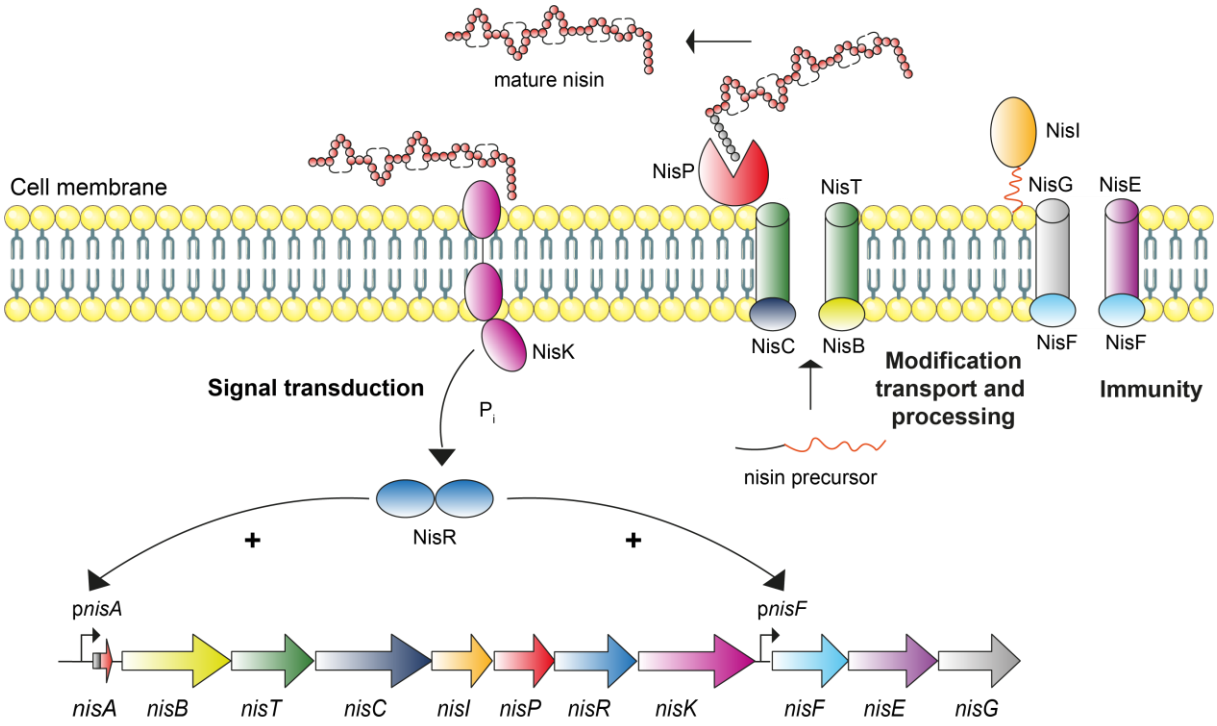

Figure 3. Representation of nisin biosynthesis and regulation in *Lactococcus lactis*. This model could also be applied to subtilin in *Bacillus subtilis.* Nisin and subtilin act as peptide pheromones involved in the activation of their own biosynthesis via two-component signal transduction machinery composed of NisK and NisR or SpaK and SpaR, respectively. Adapted from Kleerebezem and Quadri (2001).

2.1.2.2 Three component regulatory systems

In these systems, the pheromones are unmodified small cationic peptides without antimicrobial activity, that are synthetized as precursors displaying N-terminal extensions with double-glycine cleavage sites (87). The processing of the N-terminal extensions is accomplished by the same machinery that processes and exports the bacteriocins. The bacteriocin gene clusters encode the antimicrobial peptide and the cognate immunity protein, the processing and secretion machinery, the pheromone precursor, the sensor kinase and a response regulator of a two-component system that is subject to auto-regulation, called the three-component regulatory system (87).

The class II bacteriocins carnobacteriocins, plantaricin A, enterocin A, sakacin A and sakacin 674 are regulated by peptide pheromones without antimicrobial activity (87). The carnobacteriocin B2 (CB2) and BM1 display a double auto-induction mechanism in which the expression of the biosynthetic gene cluster required for bacteriocin

production and immunity is simultaneously controlled by a two-component system activated by the antimicrobial peptide, and by a second peptide pheromone without antimicrobial activity (Figure 4) (87, 93–96).

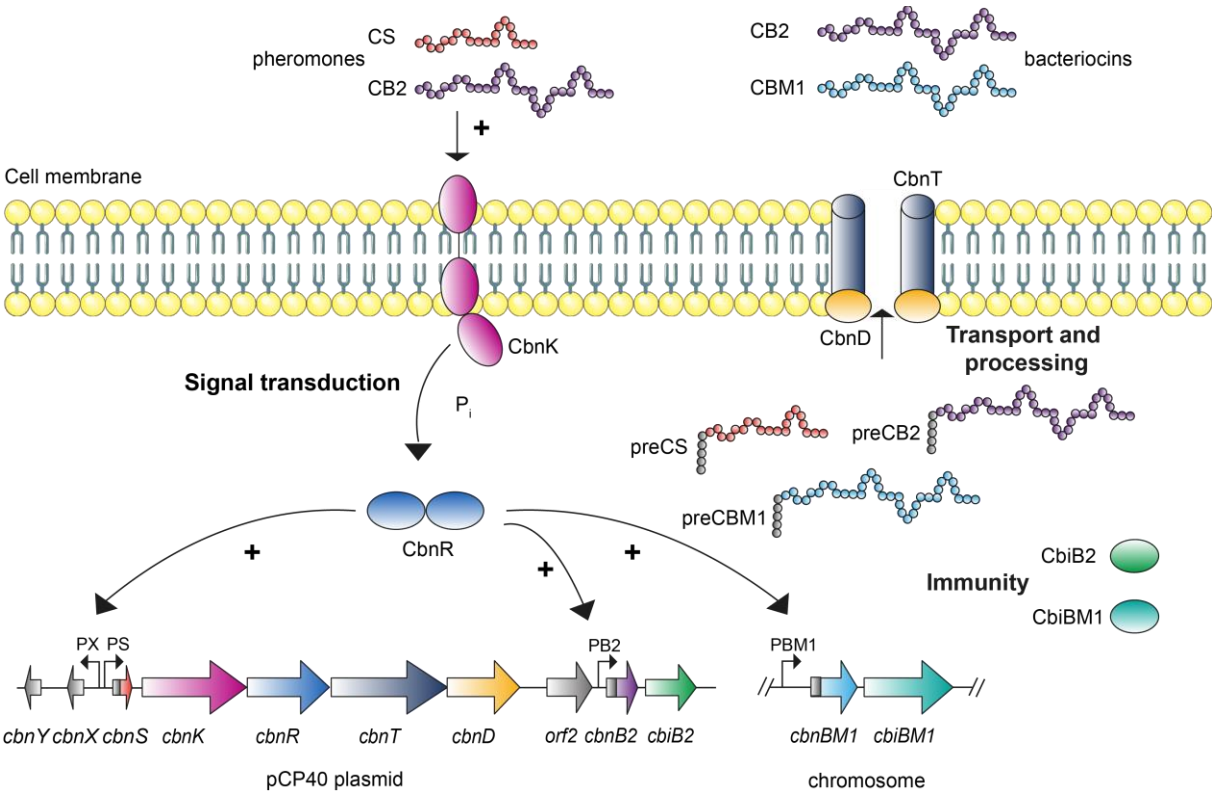

Figure 4. Representation of carnobacteriocin B2 and BM1 biosynthesis and regulation in *Carnobacterium piscicola*. Auto-induction regulation in class II bacteriocin production in gram-positive bacteria. This model represents the regulation of carnobacteriocin B2 and BM1 where not only the pheromone or synthetic peptide (CS) triggers the bacteriocin production, but also the bacteriocin (CB2) itself. Both act as peptide pheromones involved in induction of *cbn* gene transcription via a common two-component signal transduction cascade, involving CbnK and CbnR. The loci encoding for both bacteriocins pCP40 and *cbn* are represented. The promoters involved are shown with arrows. Adapted from Kleerebezem and Quadri (2001).

2.1.2.3 Precursor peptide processing regulated by quorum sensing

The Agr QS system in *S. epidermidis* is responsible for the regulation of surface proteins and virulence factors. The lantibiotic epidermin extracellular processing of the N-terminal leader peptide by the EpiP protease is controlled by the Agr system. Agr does not interfere with the transcription of the epidermin biosynthetic genes only with the precursor peptide processing (97).

2.1.3 Competence-regulated bacteriocins

Competence is the bacterial capacity to uptake extracellular DNA to repair a damaged genome, or to acquire new genes conferring antibiotic resistance or encoding new toxins (98). In *S. pneumoniae*, competence is regulated by a secreted pheromone called the competence-stimulating peptide (CSP). The CSP precursor is ComC (99), which is cleaved during export by ComAB (an ABC transporter/protease) to yield active CSP. Extracellular CSP binds and activates the cognate histidine kinase receptor ComD of the ComDE two-component signal-transduction system (Figure 5) (83).

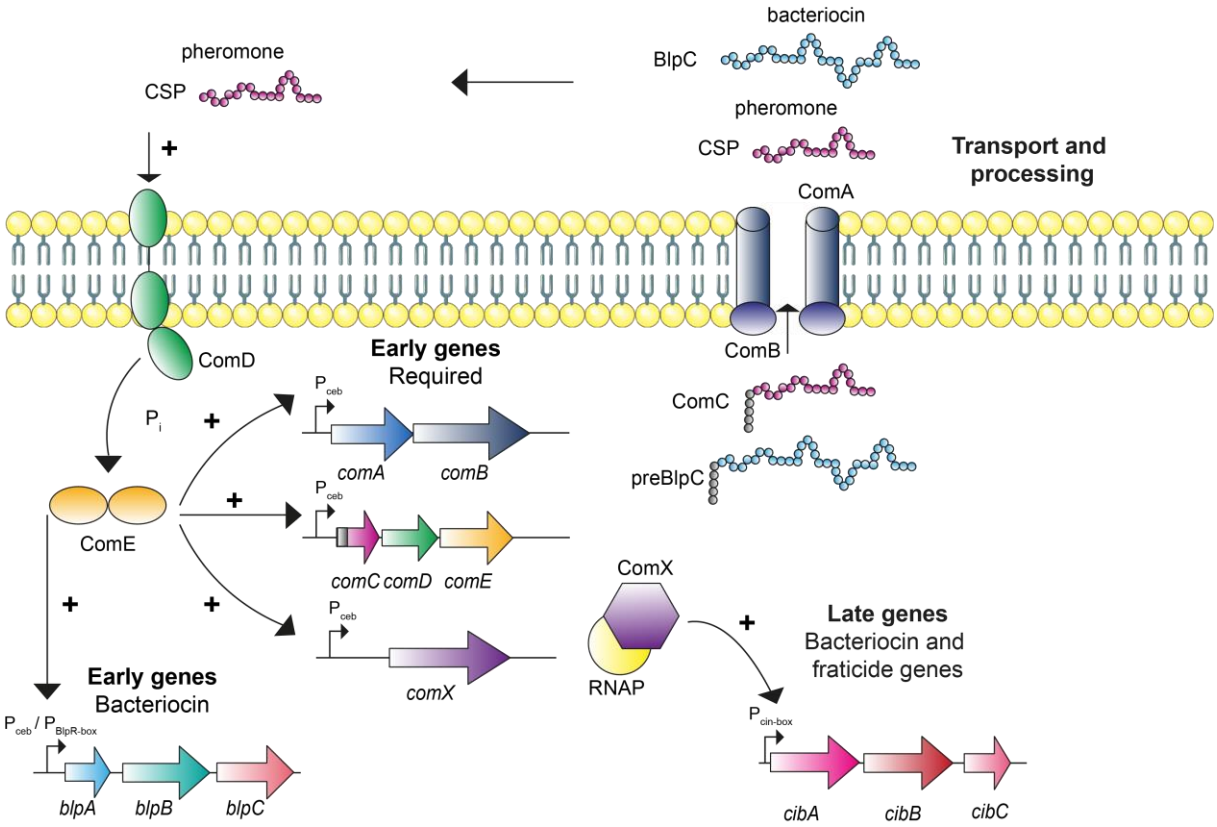

Figure 5. Bacteriocins regulated by the ComABCDE QS pathway of *Streptococcus pneumoniae*. The two phases of competence development are controlled by ComE, for induction of early genes, and by ComX, for induction of late genes. Phosphorylated ComE binds at PCeb, a promoter site containing a ComE binding site (Cbe). The bacteriocin operon *blpABC* is dually regulated either by ComE or BlpR. The late genes are directly regulated by the ComX/RNAP (RNA polymerase) complex and consist of genes required for DNA uptake, homologous recombination as well as the lytic genes encoding effectors of fratricide and the two-peptide bacteriocin CibAB. The ComAB complex exports and processes ComC into the mature peptide pheromone CSP and also process BlpC. Adapted from Shanker and Federle (2017).

In response to CSP stimulation some late genes are upregulated through the complex ComX/RNA polymerase, including the two-peptide bacteriocin CibAB (Figure 5). The bacteriocin CibAB is responsible for the lysis of cells lacking the immunity factor CibC (100). This fratricide mechanism is restricted to closely related strains and allows competent cells to acquire DNA sequences to maintain genome integrity or to acquire new genes from the pneumococcal meta-gene pool to provide phenotypic heterogeneity that could enhance fitness within the community (83). A second bacteriocin, regulated by CSP, is Blp (bacteriocin-like peptide). The transporter BlpAB and the immunity proteins BlpY and BlpZ are activated upon CSP induction. These genes are regulated by the BlpRH two-component system activated by the peptide pheromone BlpC (100, 101).

2.1.4 Growth conditions

The production of bacteriocins can be influenced by growth conditions including nutrient limitation, pH, oxygen, salt concentration or temperature (86). For example, the plasmid-encoded microcin J25 of *E. coli* is induced upon starvation during the stationary growth phase. The production of microcin J25 is independent of RpoS, the cyclic AMP-Crp complex, OmpR and H-NS (102). Colicin K is transcribed in response to (p)ppGpp, a molecule that is synthetized in response to carbon or nitrogen starvation or when micronutrients become scarce (78). Some bacteriocins as colicin V, produced by Enterobacteria and plant pathogens such as *Xylella fastidiosa*, and also some pyocins, are expressed when iron is limited (103–105).

The production of sakacin, which depends on a QS system, is also temperature dependent. The bacteriocin production is lost between 33 and 35°C and activated at 30°C (106). The enterocins production, which is also dependent on a QS system, varies with pH and salt concentration. At acidic pH and high salt concentration, enterocins are less produced or not produced at all. It is proposed that the salts or pH could affect the interaction of the pheromone and its receptor because it involves electrostatic interactions (86). Lacticin 481 is regulated at the transcriptional level by pH. During growth, *L. lactis* produces lactic acid, which in turn leads to a decrease in the pH of the growth medium from 7 to 5.8, increasing lacticin production through an unknown transcriptional regulator (107).

2.2 Export and Secretion mechanisms

Bacteriocins can be released to the external milieu via ABC transporters (108, 109) or through the Sec-dependent pathway (110). Bacteriocins can also reach their targets upon intimate physical contact between producer and target bacteria, through Type 5 (known as two-partner secretion system) (111–113) or Type VI secretion systems (114, 115) in Gram-negative bacteria, and Type VII secretion system in Gram-positive bacteria (116).

2.2.1 ABC transporters

The secretion of bacteriocins in Gram-positive and Gram-negative bacteria is usually achieved via ABC transporters, which use the energy from ATP hydrolysis as a source of energy to export their substrates (108).

2.2.1.1 Architecture of ABC transporters

ABC exporters have two cytoplasmic conserved nucleotide-binding domains (NBDs), which are the sites for ATP binding and hydrolysis, and two transmembrane domains (TMDs), which bind and transport substrates in (import) or out (export) (117). The TMDs are composed of hydrophobic α-helices that interact with NBDs. Together, they form a transmission interface that allows binding and hydrolysis of ATP coupled to the ligand transport (108). The NBDs contain conserved specific ATP binding and hydrolysis motifs (LSGGQ or C-motif, Walker A and Walker B motifs, A, H and Q-loops) (118, 119). In contrast, the TMDs have diverse sequences, sizes and structures to provide high (or low) specificity to the ABC transporter (120). ABC transporters experience conformational changes and switch between inward and outward-facing states, exposing the ligand binding site to the inside or the outside of the membrane. Initially, the NBDs dimerize upon ATP binding, subsequently other conformational changes occur at the TMDs and these changes trigger the transport of the ligand (108).

2.2.1.2 Types of ABC transporters

In general, bacteriocins are transported in a mature form. For this, they must undergo a proteolytic cleavage to remove the N-terminal leader sequence and in some cases the peptide must be post-translationally modified (121). However, some precursor peptides are transported before being processed, as it is the case for microcin C (122).

Some ABC transporters have also a dual activity because they are involved in self-immunity and/or in the maturation of the peptides by cleaving the leader sequence (121, 123, 124). Based on their structure and the signal sequence of their cognitive substrates, they are divided into three groups: McjD-, NisT- and SunT-types (109).

2.2.1.2.1 McjD-type ABC transporters in Gram-negative bacteria

The prototype of this class is the McjD ABC transporter, which transports the microcin J25 (MccJ25) and provides self-immunity to producer cells. McjD transports mature MccJ25 from the cytoplasm to the periplasm, and the outer membrane protein TolC exports the bacteriocin out of the producer cells (Figure 6B) (60). In absence of MccJ25, McjD exists in an occluded conformation, where the TMD remains shielded to both the cytoplasmic and periplasmic sides of the membrane. Once MccJ25 is produced, McjD changes to an inward-open conformation and its binding cavity becomes accessible to the peptide. MccJ25 and ATP-binding induce a transient outward-open conformation for the bacteriocin release to the periplasm, and subsequently the TMD adopts an occluded conformation. The ATP hydrolysis resets the transporter to its inward conformation. The specificity of McjD is extremely high, because it cannot transport other lasso peptides closely related to MccJ25; also, other related ABC transporters are not able to export MccJ25 (125).

2.2.1.2.2 NisT-type ABC transporters in Gram-positive bacteria

The NisT-type ABC exporters are named after the transporter involved in nisin export, and are used by many other lantibiotics. NisT forms an homodimer that displays high tolerance regarding the number of substrates that can be transported (121). The export of nisin through NisT brings the modified precursor peptide NisA (prenisin) outside the producer cells where it is cleaved by the subtilisin-like serine-protease NisP localized at the cell wall (LPXTG anchorage) (Figure 6A) (108, 121).

2.2.1.2.3 Bi-functional SunT-type ABC transporters

These transporters are present in both Gram-negative and Gram-positive bacteria (108). They have an additional N-terminal peptidase domain (PEP), which removes the leader peptide sequence of the transported substrates (Figure 6C) (121). They assure the processing and export of precursor peptides displaying a leader region with

a double-Gly type motif (108). The leader sequence is important to protect the precursor peptide from degradation and to guide the products through secretion (71). They are responsible for secretion and maturation of various bacteriocins, such as SunT for glycocin sublancin 168, NukT for lantibiotic nukacin ISK-1, PedD for class IIa pediocin PA-1. They are also involved in the transport of other peptides such as bacteriocin communication signal peptides (discussed in section 2.1.2.1) (121). They have shown to have broad tolerance to the length and amino acid sequence of the leader peptide, and the amphipathic α-helix is proposed to be critical in recognition (126).

2.2.2 Sec-dependent pathway

The Sec-pathway is present in both Gram-positive and Gram-negative bacteria. The transport complex in *E. coli* is formed by the channel SecYEG, the membrane complex SecDFyajC that stimulates preprotein translocation by an unknown mechanism, and the ATPAse motor SecA (Figure 6D) (127). In Gram-positive bacteria, the SecY and SecA proteins are well conserved and the genes that encode for SecE and SecG are shortened compared to *E. coli* homologues (121). The precursor peptides transported by the Sec-dependent pathway possess diverse N-terminal signal sequences that vary in length and amino acids sequences. The signal peptidase I (SPI) or II (SPII) remove the leader sequence (128). Some examples of bacteriocins that use the Sec-dependent pathway to be transported are the enterocin P and the lactococcin 972 (121).

2.2.3 Contact-dependent inhibition (CDI) systems

CDI was initially discovered in *E. coli*, which can inhibit the growth of target bacteria upon direct cell-to-cell contact (129). Several CDI systems have been now described in diverse Gram-negative and Gram-positive bacteria including *Burkholderia thailandensis, Neisseria meningitidis*, *P. aeruginosa, Acinetobacter baumannii* and *S. aureus* (112, 115, 116).

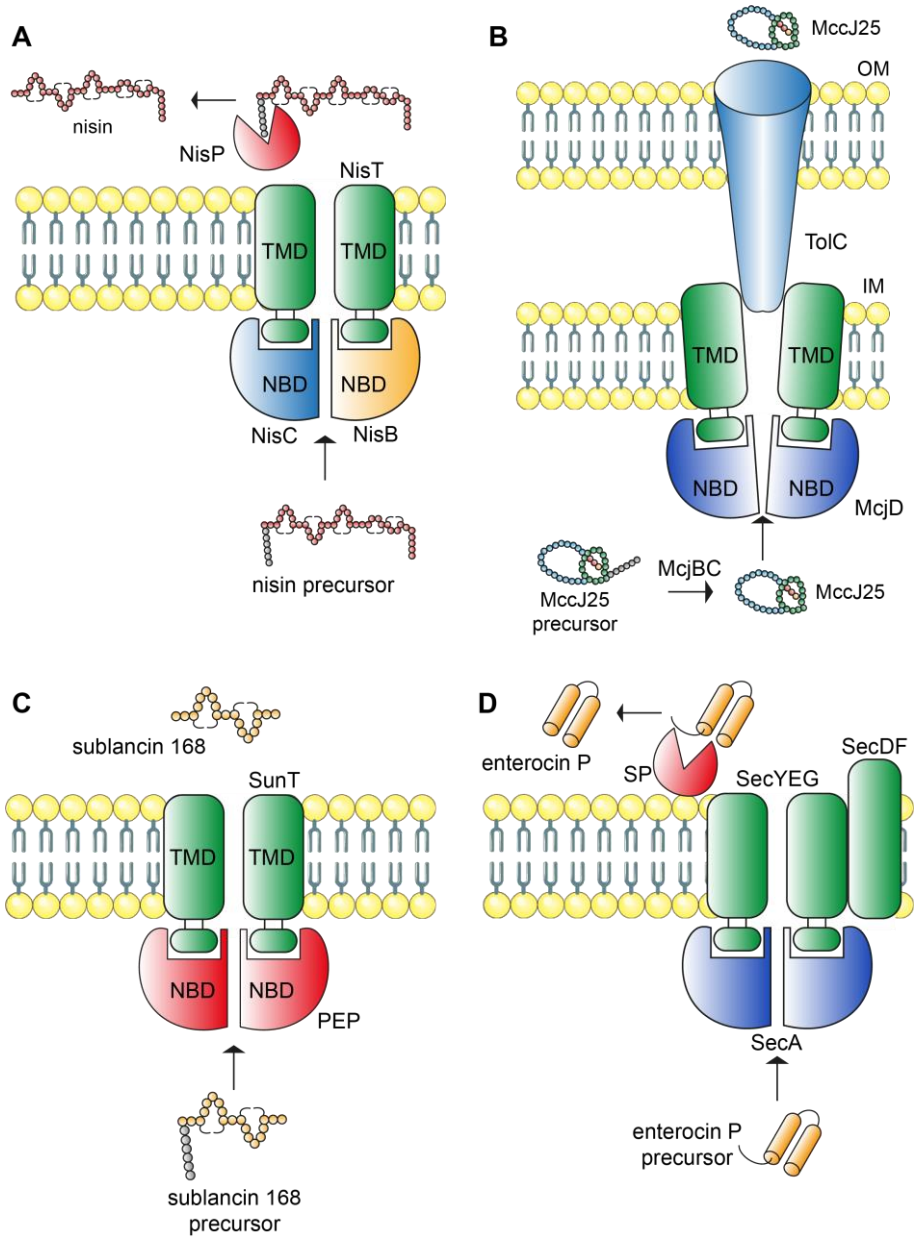

Figure 6. Models of different types of ABC-like transport pathways in bacteriocin production. Main components of three identified major pathways in bacteriocin production are displayed. **A**. NisT type of transporter and NisP peptidase. **B**. McjD-type ABC transporters **C**. SunT type of transporter. **D.** Sec-dependent pathway. TMD, transmembrane domain. NBD, nucleotide-binding domains. PEP N-terminal peptidase domain. SP, signal peptidase. Adapted from Zheng and Sonomoto (2018) and Vincent and Moreno (2009).

2.2.3.1 Type 1 secretion system (T1SS)

T1SS are present in Gram-negative bacteria. They belong to the RTX (repeats-in toxins) family, characterized by highly conserved Gly- and Asp-rich nona-peptide repeated motifs, with the consensus sequence GGXGXDXUX (where X and U are any

amino acid and a large hydrophobic one, respectively). T1SS are composed of three components: two-IM proteins, an ABC transporter and a membrane fusion protein (MFP) which work together and an OM protein that can be the TolC protein (130). Together, they form a tri-partite “channel-tunnel” from the cytoplasm to the extracellular space in presence of the substrate (Figure 7). Secretion is triggered by the C-terminal region of the substrate protein transported by the T1SS (131). A certain level of promiscuity is found in the T1SS (132).

The Gram-negative bacterium *Caulobacter crescentus* produces a two-protein bacteriocin called CdzC/CdzD, which forms insoluble aggregates that are retained on the outer membrane of producer cells and display a CDI mechanism against bacteria that lack the immunity protein CdzI. This bacteriocin uses a T1SS encoded elsewhere in the genome (133).

2.2.3.2 Type 5 secretion system (T5SS)

In *E. coli,* CDI is mediated by the CdiB/CdiA two-partner secretion system (TPS), also known as T5SS (129). CdiB is an outer β-barrel membrane protein that facilitates secretion of the CdiA exoprotein to the bacterial cell surface. The CdiA N-terminal region is conserved across species, and the variable C-terminal part (called CdiA-CT) is translocated into target bacteria, displaying in general nuclease or tRNase activity (Figure 8A). The immunity protein CdiI protects the producer cells from autoinhibition by binding and inactivating CdiA-CT toxins, or by occluding the toxin active site (112, 134). Additionally, interaction of the complex CdiA-CT/CdiI with nucleic acids and/or proteins induces the upregulation of genes encoding pili and the polysaccharide synthesis machinery in a process called contact-dependent signaling (CDS), allowing increase in biofilm formation and the response to stress in dense bacterial communities (115).

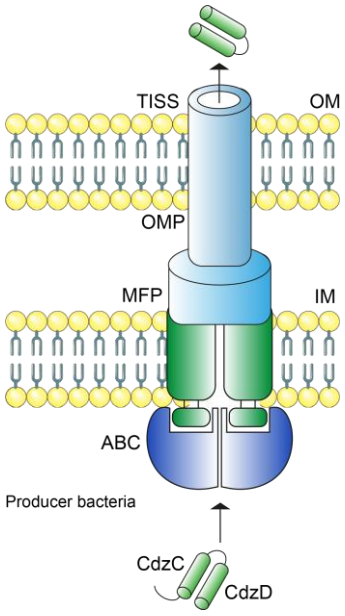

Figure 7. A model of bacterial T1SS. ABC transporter protein, membrane fusion protein (MFP), and outer membrane protein (OMP) form a transporter complex protruding through the inner and outer membranes of Gram-negative bacteria. Protein secretion occurs in a single step, bypassing the periplasmic space directly to the extracellular medium. ATP hydrolysis by the ATPase domain of ABC protein provides energy for protein transport. The putative C-terminal secretion signal is recognized by the ABC protein, stimulating conformational change of the transporter complex and ATP hydrolysis, which leads to secretion of the passenger protein. Adapted from Angkawidjaja and Kanaya (2006).

2.2.3.3 Type VI secretion systems (T6SS)

The T6SS is a contractile nanomachine that delivers toxins directly from the cytoplasm of Gram-negative bacteria to the cytoplasm of neighboring cells (135). The T6SS is a multi-protein complex that spans the IM and OM, and is formed of a cytoplasmic tube, a puncturing tip, and an outer sheath that surrounds the tube. Upon cell-cell contact, the outer sheath contracts, forcing the inner tube and puncturing device into the neighboring cell, where the effectors carried by the inner tube or the tip are released (Figure 8B) (115). They can deliver toxic effectors into eukaryotic cells and also antibacterial effectors into prokaryotic cells including nucleases, peptidoglycan-degrading amidases, and membrane targeting lipases (135–137). Bacteria protect from self-intoxication by producing specific immunity proteins to each effector. These systems can mediate intra- and inter-species competition (115, 138). An example of a T6SS effector from S. Thyphimurium is Tae4, an antibacterial amidase that kills *K. oxytoca* and is essential for *Salmonella* to establish the infection within the host gut

(139). A second example is *B. fragilis* T6SS effector-immunity pair Bte2 that is functional in the mammalian gut providing a competitive advantage by antagonizing non immune *B. fragilllis* and other gut commensals or gut pathogens (135, 140, 141).

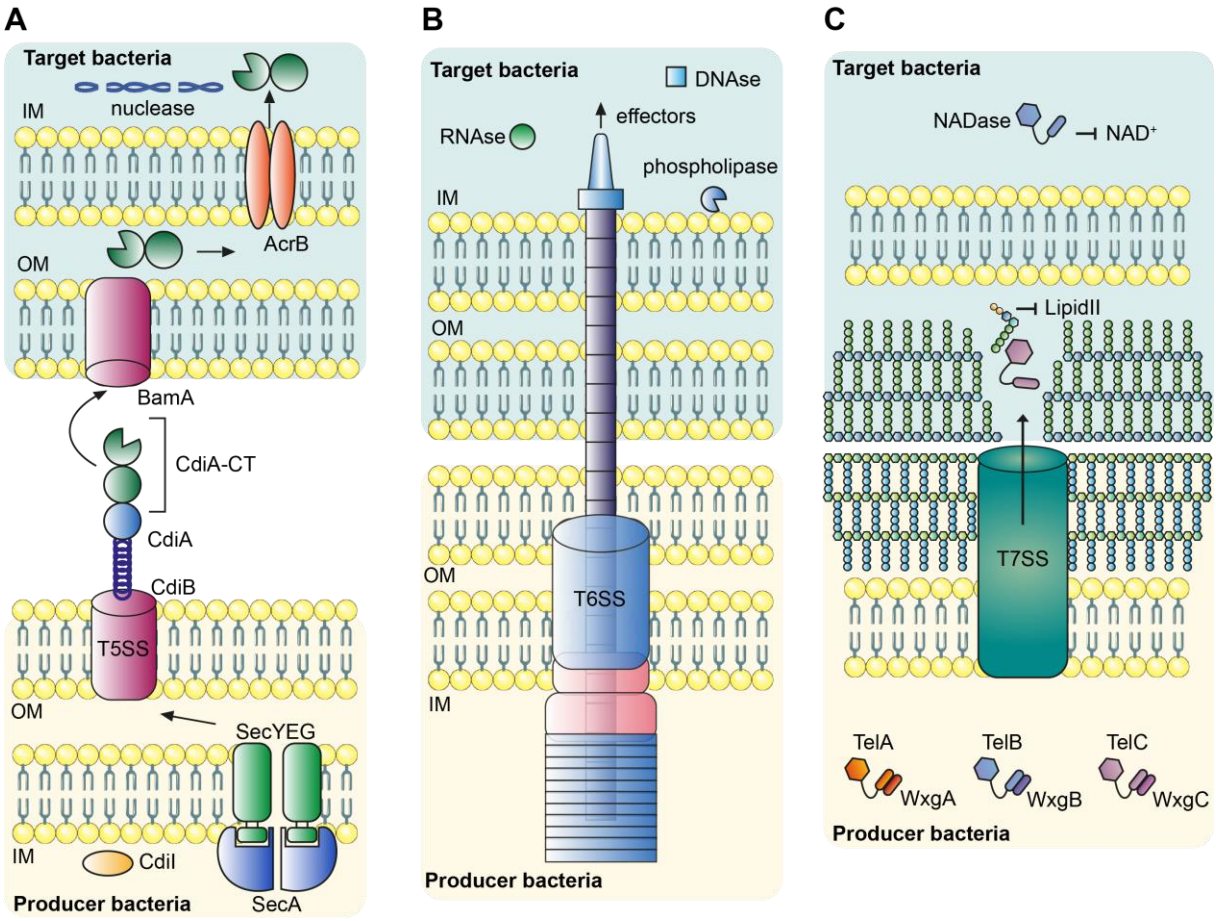

Figure 8. Model of contact dependent delivery by T5SS, T6SS and T7SS. **A.** The active portion of the protein CdiA-CT is translocated into target cells via specific outer and inner membrane receptors. Once in the cytoplasm, Cdia-CT degrades the cell DNA or tRNA, causing growth inhibition and cell death. The producer cell is protected from CdiA-CT by the CdiI immunity protein. **B**. The T6SS uses a contractile mechanism to propel an effector-loaded producer cell into the target cell. T6SS effectors include nucleases, peptidoglycan-degrading amidases, and membrane targeting lipases that are able to kill the target bacteria. **C**. T7SS-dependent cell-cell delivery of LXG toxins between bacteria. The producer cell contains cognate TelA-C (light shades) and WxgA-C (dark shades) pairs and intoxicate a susceptible target cell. Adapted from Garcia (2018); Chassaing and Cascales (2018); Whitney *et al*. (2017)

2.2.3.4 Type VII secretion system (T7SS)

In Gram-positive bacteria, the T7SS (or ESX-1 secretion system) was first identified in *Mycobacterium tuberculosis* and uses ATP to export one or more substrates that belong to the WXG100 protein family (142). In Firmicutes, the T7SS was first described in *S. aureus* and is able to export the DNAse EssD to kill other bacterial in a CDI manner. More recently, the CDI LXG polymorphic toxins have been also described in Firmicutes. These toxins consist of a conserved N-terminal domain (LXG), a middle domain of variable length, and a C-terminal variable toxin domain (116). The LXG proteins require their cognate WXG100-like partners for export through the T7SS. In *S. intermedius,* these toxins are able to degrade the cell wall by interfering the lipid II in a contact-dependent manner (Figure 8C) (116).

2.2.3.5 Other CDI systems

In *Xanthomonas,* the type IV secretion system (T4SS) deliver a peptidoglycan hydrolase upon cell-cell contact, this toxin bounds a specific immunity protein. Also, in Gram-positive bacteria the YD repeat containing protein WapA from *B. subtilis* mediates interbacterial antagonism in a CDI manner (115).

2.3 Mechanisms of action

Bacteriocins display diverse killing mechanisms (16). Bacterial cell envelope receptors might behave as bacteriocin final targets, or as docking molecules that allow bacteriocin internalization and targeting of cytoplasmic bacterial molecules. We can therefore divide the bacteriocins in two major categories: bacteriocins that function at the cell envelope, and bacteriocins that are active inside cells (Figure 9) (38).

2.3.1 Perturbation of the cell envelope integrity

The bacterial cell surface negative charge is commonly exploited by many cationic bacteriocins for initial membrane interaction (143–145). Perturbation of the cell envelope integrity might be achieved by inhibition of enzymatic activities or through pore formation (143, 146).

2.3.1.1 Lipid II targeting

In Gram-positive bacteria, lipid II is an important target for several bacteriocins. Nisin, mutacin, gallidermin, and epidermin possess two rings (A and B) that allow them to interact with lipid II as a docking molecule and to span through the membrane forming pores (31). Some lantibiotics can remove lipid II from the septum and block cell wall synthesis (147). In the case of mersacidin, binding to the lipid II precursor inhibits the trans-glycosylation of the peptidoglycan synthesis (148). Other mechanism has been described for plantaricin C, which forms complexes with both lipid I and lipid II, inhibiting the addition of the first glycine of the pentapeptide chain of lipid II (149).

2.3.1.2 Mannose phosphotransferase system targeting

The mannose phosphotransferase system (Man-PTS) is the specific receptor for many pediocin-like bacteriocins (150). Only members of the group I of the Man-PTS family serve as receptors for class IIa bacteriocins (151). The two models to explain their mechanism of action are: (a) the bacteriocin binds the receptor leading to an irreversible opening of an intrinsic channel; or (b) the bacteriocin employs the receptor as a docking molecule, allowing bacteriocin insertion in the target membrane and oligomerization to form a pore (152, 153).

The first model proposes that the N-terminal part of the bacteriocin binds to the extracellular loop of the IIC subunit from the Man-PTS and the C terminal part interacts with the transmembrane segments that entrap the bacteriocin within the receptor (151, 154). The most accepted model to explain the mechanism of action of pediocin-like bacteriocins is the second one; this model proposes that the Man-PTS is a docking molecule with a key function in binding and anchoring the bacteriocin to the membrane. The subsequent interaction of the bacteriocin with the membrane is independent of the man-PTS, and this step is responsible for the membrane disruption (152).

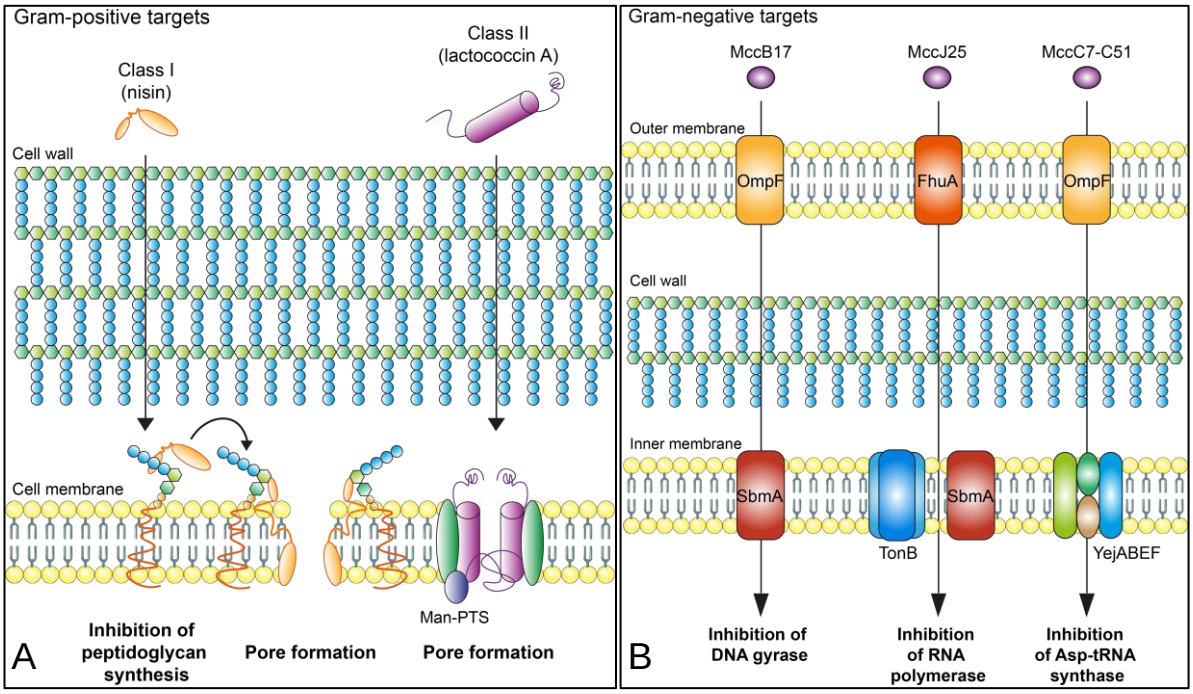

Figure 9. General mechanisms of action of bacteriocins. (A) In general, bacteriocins that inhibit Gram-positive bacteria target the cell envelope. Some class I bacteriocins inhibit the synthesis of peptidoglycan by blocking the lipid II precursor and could also induce pore formation. Other bacteriocins such as class II (lactococcin A) bind to the Man-PTS and induce the formation of pores. (B) Many bacteriocins that inhibit Gram-negative bacteria are transported through the outer and inner membrane before targeting bacteria. They can block the DNA, RNA or protein synthesis. For example, MccB17 inhibits DNA gyrase, MccJ25 inhibits RNA polymerase, and MccC7-C51 inhibits aspartyl-tRNA synthase. There are some exceptions for bacteriocins that target Gram-positive bacteria and inhibit translation such as thiopeptides and bottromycins and also for bacteriocins that target Gram-negative bacteria and form pore such as MccE492. Adapted from Cotter *et al.* (2013).

2.3.1.3 Membrane insertion and pore formation

The insertion of bacteriocins in the membrane depends on the composition of amino acids and is usually one part the is inserted in the case of nisin the amino terminal part is inserted into monolayers. Once the molecule is inserted into the membrane the lipid bilayer organization is disturbed (146).

Three models for membrane disruption by antimicrobial peptides have been proposed (143, 146). The first model is the wedge-like model or toroidal model where the orientation of the bacteriocin is parallel to the surface of the membrane. A water core

is formed in the center of the pore, with the bacteriocin and lipid head groups forming the wall of the pore (143). In the case of nisin, the pore formation is induced by the complete translocation of the C-terminal part across the membrane inducing an intermonolayer contact of phospholipids. Multiple nisin molecules can produce a large local disturbance of the bilayer organization causing formation of transient lipid-protein pores (146).

The second model is the barrel-stave, the antimicrobial peptides are inserted and diffuse laterally through the lipid bilayer, where peptides are arranged into helices and create a barrel/stave-like channels that span the membrane (143). This model is proposed for class II bacteriocins where a bundle of α-helical peptides is perpendicular to the surface of the membrane. The hydrophilic faces of a bundle of amphipathic α-helical peptides form the inner wall of the pore. The outer face of the bundles, the hydrophobic side will face the fatty acyl chains of the membrane lipids (146).

A third model has been proposed “carpet-like” where the single peptide molecules are oriented in a parallel manner across the membrane surface and interfere with the bilayer organization without forming peptides aggregates (146). At certain concentration of the peptide, the bilayers are disrupted and form micelles, destroying the membrane in a detergent like manner (143). The numerous peptides will cause the collapse of the membrane due to the movements of the phospholipoids leading to transient permeability (146).

More recently a model based on structural and functional studies was proposed for two-peptide bacteriocins, where the two peptides form a membrane-penetrating helix-helix structure that interacts with GXXXG-motifs. It is believed that the helix-helix is also capable of interacting with an integral membrane protein triggering a conformational alteration in the protein leading to membrane leakage (155).

2.3.1.4 Pore specificity

Lantibiotics form large non-specific pores, that mediate efflux of amino acids, ATP or ions, favoring dissipation of the transmembrane electrical potential and causing a drop in the intracellular pH, therefore inhibiting many of the essential enzymatic processes

(146). Interestingly, two-peptide bacteriocins show specificity with respect to the molecules they transfer across membranes (42). For example, the cation-conducting two-peptide bacteriocin lactococcin G renders target cells permeable to monovalent cations like Na+, K+, Li+ , Cs+, Rb+, and choline, but not to H+, divalent cations such as Mg2+ nor anions such as phosphate (156, 157). Conversely, the anion-conducting two-peptide bacteriocins like plantaricin J/K that allows the efflux of anions like glutamate but not potassium ions (156).

2.3.2 Inhibition of gene expression and protein production

Bacteriocins can interfere with DNA, RNA and protein metabolism, inhibiting gene expression or protein production and leading to death of target cells (16). Surface receptors for intracellular-acting bacteriocins include several outer membrane porins such as OmpF or siderophore-receptors such as FhuA (22, 23, 63).

2.3.2.1 Inhibition of the DNA gyrase activity

MccB17 is a TOMM produced by *E. coli* that targets the DNA gyrase subunit B, arresting DNA replication and inducing activation of the SOS response (158). The DNA gyrase is a topoisomerase composed of two subunits GyrA and two subunits of GyrB (A_2B_2 heterotetrameric complex) that introduces 2 negative supercoils into DNA by means of ATP hydrolysis (159). To induce the supercoling, GyrA induces double strand breaks (dsb) into DNA and then facilitates re-ligation of these dsb. MccB17 stabilizes the dsb covalent cleavage complex between the 5’ end of the DNA and the DNA gyrase subunit B, disrupting the re-ligation of the DNA dsb and leading to toxicity (160).

2.3.2.2 RNA transcription inhibition

MccJ25 inhibits the RNA polymerase activity by obstructing its secondary channel (161). The secondary channel or pore facilitates the diffusion of small molecules in and out of the active center of the enzyme, modifying the transcription properties of RNA polymerase (162). MccJ25 inhibits transcription by preventing the access of substrates to the enzyme active sites, acting as a “cork in a bottle”. The MccJ25 induces a filamentous phenotype on target cells due to the impaired transcription of genes coding for cell division proteins (161).

2.3.2.3 Protein synthesis inhibition

2.3.2.3.1 Inhibition of aminoacyl tRNAs

Microcin C (McC) inhibits translation by blocking the function of the aspartyl-tRNA synthetase. McC contains a modified adenosine monophosphate, covalently attached to a C-terminal aspartate, that is degraded inside the target bacteria into a modified aspartyl-adenylate containing a *N*-acylphosphoramidate linkage that blocks the aspartyl-tRNA synthetase activity (163). This leads to the accumulation of uncharged $tRNAs^{Asp}$, inhibiting protein synthesis and cell growth (164). This phenotype is also observed for the bottromycin A2, which binds to aminoacyl-tRNAs and blocks their interaction with the ribosomal A site (164).

2.3.2.3.2 Inhibition of the ribosomal activity

In general, thiopeptides bind to the 23S ribosomal RNA or to the Ef-Tu elongation complex, inhibiting ribosome activity and disrupting protein synthesis. Those biding the 23S ribosomal RNA are characterized by the small size of a macrocycle, and a conserved region essential for the interaction with the large ribosome subunit or GTP-ase associated center. The second group is characterized by a medium size of the macrocycle and the presence of a conserved Asn residue required for the interaction with EF-Tu (164).

Thiostrepton, nosiheptide and micrococcin belong to the first group. They bind a cleft formed by the N-terminal domain of the ribosomal protein L11 and the loops of the helices H43 and H44 of the 23s rRNA (165). Their binding sites overlap the binding sites of IF2, EF-G and EF-Tu, inhibiting therefore initiation, translocation and tRNA delivery to the ribosome (164). The thiopeptide thiopstrepton, prevents one or more conformational transitions critical to stimulate the GTPase action of the elongation factors (38).

GE2270A belongs to the thiopeptides that bind the elongation factor EF-Tu. GE2270A forms a complex with EF-Tu and GTP preventing the formation of the ternary complex with aminoacyl-tRNA (166). The binding site of this bacteriocin is located between the domains I and III of EF-Tu. Other thiopeptides that show similar modes of action are thiomuracin and GE37468A (164).

Recently, the TOMM klebsazolicin (KLB) was reported to target translation elongation by inhibiting the 70S ribosomal subunit (167). KLB binds to the upper part of the exit tunnel adjacent to the peptidyl-transferase center blocking the passage of the nascent peptide; only di- or tripeptides are synthetized and remained associated with tRNA and bound to the elongation ribosome (164). More recently a second TOMM called Phazolicin (PHZ) was discovered to also target the ribosome. In terms of amino acids composition, PHZ is identical to KLB but the PTMs are different (168). PHZ interacts with the loop regions of the 23S ribosomal proteins L4 and L22 conferring species-specific translation inhibition, mechanism absent in KLB (164).

2.4 Immunity mechanisms

Bacteria that produce bacteriocins need to develop self-immunity against the toxic effects of their own peptide in order to survive (108, 169). Immunity is acquired by the production of dedicated immunity proteins, which are usually encoded in the bacteriocin gene clusters (29, 39). Due to their conserved organization of these biosynthetic clusters, putative immunity genes for most bacteriocins have been already identified and their function has been confirmed by their heterologous expression in target cells, allowing them to acquire immunity against cognate bacteriocins (170). However, the mechanisms involved in immunity are poorly understood for most bacteriocins. Proposed immunity mechanisms include blocking the insertion of the bacteriocin into the membrane, or inhibiting the binding of the bacteriocin to its receptor (171–174).

2.4.1 Complex between the immunity protein and the receptor

For some class II bacteriocins, the immunity protein forms a strong complex with the bacteriocin bound to its receptor (bind-and-lock mechanism), preventing producer cells from being killed. This is the case for the immunity protein LciA, which binds lactococcin A in association with its receptor, the subunits IC and IID from the Man-PTS receptors. This also the case for lactococcin B and some pediocin-like bacteriocins that also target the man-PTS components IIC and IID (154).

2.4.2 Abi proteins with proteolytic activity

They are present in the biosynthetic clusters of several class IIb bacteriocins (two-peptide bacteriocins). The genes encoding for these immunity proteins are putative transmembrane CAAX proteases and bacteriocin-processing (CPBP) enzymes, also known as CAAX protease family or Abi family (175, 176). They are characterized by three conserved motifs: motif 1 consists of two glutamate residues and an arginine separated by three variable amino acids (EExxxR), motif 2 consists of a phenylalanine and a histidine separated by three variable amino acids (FxxxH) and motif 3 consists of a single histidine residue (170). In eukaryotes, these proteins have a proteolytic function and these 3 motifs are predicted to form the active site of the enzyme (177).

The Abi proteins have been shown to confer cross-immunity in different bacteria. The Abi immunity protein SkkI was shown to lose its function when the conserved motifs were mutated. The Abi gene *plnI* and the Abi-like gene *plnL* from *L. plantarum,* as well as the Abi gene *skkI* from *S. pyogenes* conferred cross-immunity against each other's bacteriocins, suggesting the recognition of a common receptor and a common proteolytic mechanism (177). The bacteriocin is not the target of the Abi proteolytic activity as it is not degraded; their substrates remain to be identified (177).

2.4.3 Multi-Drug transporter proteins

For some class II bacteriocins the immunity mechanism relies on multi-drug transporter proteins that export self-produced bacteriocins that re-enter through the cell membrane (178). For example, the multidrug transporter protein LmrB is involved in the efflux of the bacteriocins LsbA and LsbB (178). Producers of some cyclic bacteriocins such as enterocin AS-48 are also protected by ABC transporters which pump the bacteriocin out of the membrane of the producer cells (179).

2.4.4 ABC transporters that confer partial immunity

In some cases, immunity is a combined action of a cognate immunity protein that binds to the bacteriocin, and an ABC transporter that exports the bacteriocin from producer cells (174). Some lantibiotics and the aureocin A53 present this combined action where full immunity depends on both systems (172, 180, 181). Immunity to nisin depends partially on the NisFEG ABC transporter: it has been proposed that the transporter

functions by expelling nisin molecules which have entered the cytoplasmic membrane (before/during pore formation) and that its exporting capability is independent of NisI (dedicated immunity protein) (169). Sometimes a third molecule, called accessory factor, is involved in conferring this kind of immunity, and acts as an ancillary protein for the assembly and functioning of the ABC transporter. They are often involved in systems where the substrate requires immediate release to the extracellular medium. An example is EpiH involved in epidermin immunity, implicated in the assembly of a functioning EpiFEG ABC transporter system (169, 182).

2.4.5 Changes in the bacteriocin target

Some producers do not have specific immunity genes but resistance is acquired through modification of the peptidoglycan, by the incorporation of serine residues into the third and fifth positions of the penta-peptide cross-bridges, therefore avoiding the hydrolytic activity of the bacteriocin. For example, lysostaphin is unable to hydrolyse glycylserine and serylglycine peptide bonds introduced by the Lif protein (174, 183).

2.4.6 Quorum sensing-regulated immunity

Production of the NisI immunity protein is induced by nisin, which acts as a pheromone (169). QS allows neighbor cells to acquire immunity if they possess the *nisI* immunity gene (92). NisI is a peripherally membrane-anchored post-translationally modified protein. NisI possesses a hydrophobic N-terminal region containing a consensus lipoprotein sequence. The first 19 residues are removed at a putative signal peptidase II recognition site (LSGC) where palmitic acid is transferred to the new N-terminal Cys residue, and subsequently NisI is transported across the membrane. (184). Half of the NisI produced protein lacks the lipid modification and is secreted and acts extracellularly to aggregate nisin (185). The immunity for subtilin is similar, with a consensus lipoprotein signal sequence that is removed to be modified and inserted in the membrane (169).

2.4.7 Cross-immunity

Some bacteriocins and their associated immunity proteins are highly similar, such as nukacin ISK-1 and lacticin 481, and the immunity protein and ABC transporter for nukacin ISK-1 (NukH and NukFEG) provide cross-protection against lacticin 481 (186).

A second example is epicidin 280 and Pep5 immunity systems, where their immunity proteins provide protection to both lantibiotics (187). However, high levels of similarity are not always a good indicator of cross-immunity, since nisin and subtilin are closely related but cross-immunity is not present (169).

2.5 Role of bacteriocins in the regulation of interactions between bacterial communities

Bacteriocins play a critical role in mediating interactions in microbial populations and communities, inhibiting the invasion of other strains or species into an occupied niche (i.e the environment or a host) (17).

2.5.1 Role of bacteriocins in the environment

Several studies support the hypothesis that bacteriocin production has evolved as a competitive strategy under conditions of scarce resources to protect specific niches (188). Other studies have also demonstrated that, in the absence of competition, bacteriocin-producer strains may evolve and show a reduction in killing activities associated to an increase of fitness. This result is not surprising, due to the high energy cost associated to bacteriocin production, maintenance of a bacteriocin-encoding plasmid or the occurrence of autolysis of the producer cells (189). Interestingly, bacteriocin-resistant strains (possess specific immunity proteins) are found in much higher frequencies than producer strains. The abundance of resistant strains could be explained by the high frequency of horizontal transfer of resistance and the significant cost associated with bacteriocin production (190).

2.5.2 Role of bacteriocins in the intestinal microbiota

The human gut microbiota is inhabited by a large and diverse community of microbes and is dominated by Bacteroidetes and Firmicutes (191). The gut microbiota is controlled by host genetics and environmental factors. Additionally, microbiota diversity and composition is influenced by the host diet and also by positive and antagonistic interactions between gut bacteria (192). The most widely distributed weapons in the bacterial kingdom to outcompete and to establish within the microbiota are bacteriocins and CDI systems including T5SS, T6SS and T7SS discussed earlier (Section 2.2.4 Contact-dependent inhibition systems) (192).

In general, the microbiota is stable but the invasion or overgrowth of pathogens induces dysbiosis, an instability that may alter the composition of the microbiota and the host physiology (193, 194). More recently, the role of interbacterial competition in shaping gut bacterial communities has been studied, and some *in vivo* examples have been identified mainly by using T6SS as a weapon (195). In a dense microbial community such as the human colon, contact-dependent mechanisms such as T6SS should be an effective mean to antagonize competitors (196).

T6SS gene clusters are highly represented in Bacteroides species which are one of the phyla that dominates the gut microbiota (197). Several enteric pathogens use T6SSs to antagonize symbiotic gut bacteria facilitating colonization (196). The entero-pathogens *V. cholerae, S. typhimurium, C.* rodentium and *Shigella sonnei* have a functional T6SS to fight against other species (198, 199). The T6SS are highly expressed under gut conditions (200). For example, *V.cholerae* T6SS is activated by mucins and microbiota-modified bile salt (201); the *S. Typhimurium* T6SS is activated by bile salts (139); and the enteroaggregative *E. coli* Sci-1 T6SS is responsive to iron starvation (202).

More recently, a second CDI mechanism that relies on T7SS was identified in Firmicutes, a phylum that also dominates the gut microbiota. The LXG proteins are secreted by the T7SS and are able to kill diverse Firmicute species. These clusters are prevalent in the human gut microbiome and they are possibly responsible of shaping Firmicute-rich bacterial communities in the gut (116). Other mechanisms to persist in the gut used by *E. coli* is the use of ColE1, able to kill *E. coli* that does not produce colicins. The colicinogenic *E. coli* strains present an increased intestinal persistence compared to those strains unable to produce colicins (203, 204).

Antibacterial weapons are used by pathogens to colonize their host. As a consequence, to prevent the colonization by pathogens the gut microbiota exerts an important control by producing antibacterial weapons as well and protecting their niche against pathogens. For example, probiotic strain *E. coli* Nissle uses microcins M and H47 to compete against Enterobacteriaceae, including pathogens such as adherent-invasive *E. coli* (AIEC) and *S. Typhimurium* during intestinal inflammation (205). Another example is Thuricin CD produced by *B. thuringiensis* that directly targets

spore-forming Bacilli and Clostridia, including *C. difficile* (37). Altogether, these examples demonstrate that a broad range of competitive mechanisms occurs in the gut microbiota and they play a key role in shaping the microbiota composition, establishment, stability and evolution (192).

2.6 Bacteriocin applications

The majority of bacteriocins have a narrow-spectrum of activity, which may allow their use for the treatment of specific infections (16). For example, the bacteriocin Thuricin CD produced by *B. thuringiensis* is a narrow-spectrum bacteriocin that has activity against *C. difficile,* and its antimicrobial activity is comparable to that of vancomycin and metronidazole, which are the classical antibiotics used in clinics to treat *C. difficile* associated diarrhea (37). Most importantly, Thuricin CD does not alter the composition of the commensal microbiota, which is observed when vancomycin or metronidazole are used (206). Another example of ultra-narrow spectrum activity bacteriocin is PZN, produced by *B. methylotrophicus* and *B. pumilus* and which is active only against *B. anthracis* (207).

Interestingly, some bacteriocins display broad-spectrum activity, make them suitable for their use in the food industry. Nisin is the only bacteriocin licensed as a food additive/preservative over 45 countries for its activity against several Gram-positive bacteria. Pediocin PA-1 displays as well a wide-spectrum against Gram-positive bacteria, including those responsible for food spoilage or foodborne diseases such as *L. monocytogenes* (41).

Part III: Thiazole/Oxazole-Modified Microcins

Thiazole/Oxazole-Modified Microcins (TOMMs) are produced by biosynthetic gene clusters widely conserved in different bacterial phyla and in Archaea. These clusters allow the production of post-translationally modified ribosomal peptides with potential thiazole, oxazole and methyl-oxazole heterocycles. TOMMs display diverse activities, including DNA gyrase inhibition or membrane damage. As previously mentioned, this family includes MccB17 from *E. coli*, Listeriolysin S (LLS) from *L. monocytogenes*, SLS from *S. pyogenes*, Clostridiolysin S (CLS) from *Clostridium botulinum*, plantazolicin (PZN) from *Bacillus methylotropicus,* Staphylysin S (STS) from *S. aureus* and others (208–210).

3.1. Gene cluster organization

In general, TOMMs biosynthetic gene clusters encode for: (1) a pro-peptide (unmodified toxin), (2) an ABC transporter that exports the toxin once it is post-translationally modified, (3) an immunity protein, and (4) an enzymatic complex that allows the post-translational modification of the toxin with thiazole, oxazole and/or methyl-oxazole heterocycles (Figure 10) (56). The conservation of these biosynthetic genes across prokaryotes suggest that they play an important role in the survival of pathogenic and symbiotic bacteria within their specific niches (211).

3.1.1 Pro-peptide

The pro-peptide contains an amino-terminal leader region and a short carboxy-terminal structural peptide, rich in in potentially modifiable Cys, Ser, Thr and/or Gly residues (208). In the case of SLS, the pro-peptide possess a Gly-Gly leader cleavage site that yields a 23 amino acid leader peptide and a 30 amino acid structural peptide (212). A leaky Rho independent terminator sequence is present in SLS that acts as a regulator of *sagA* transcript abundance (213).

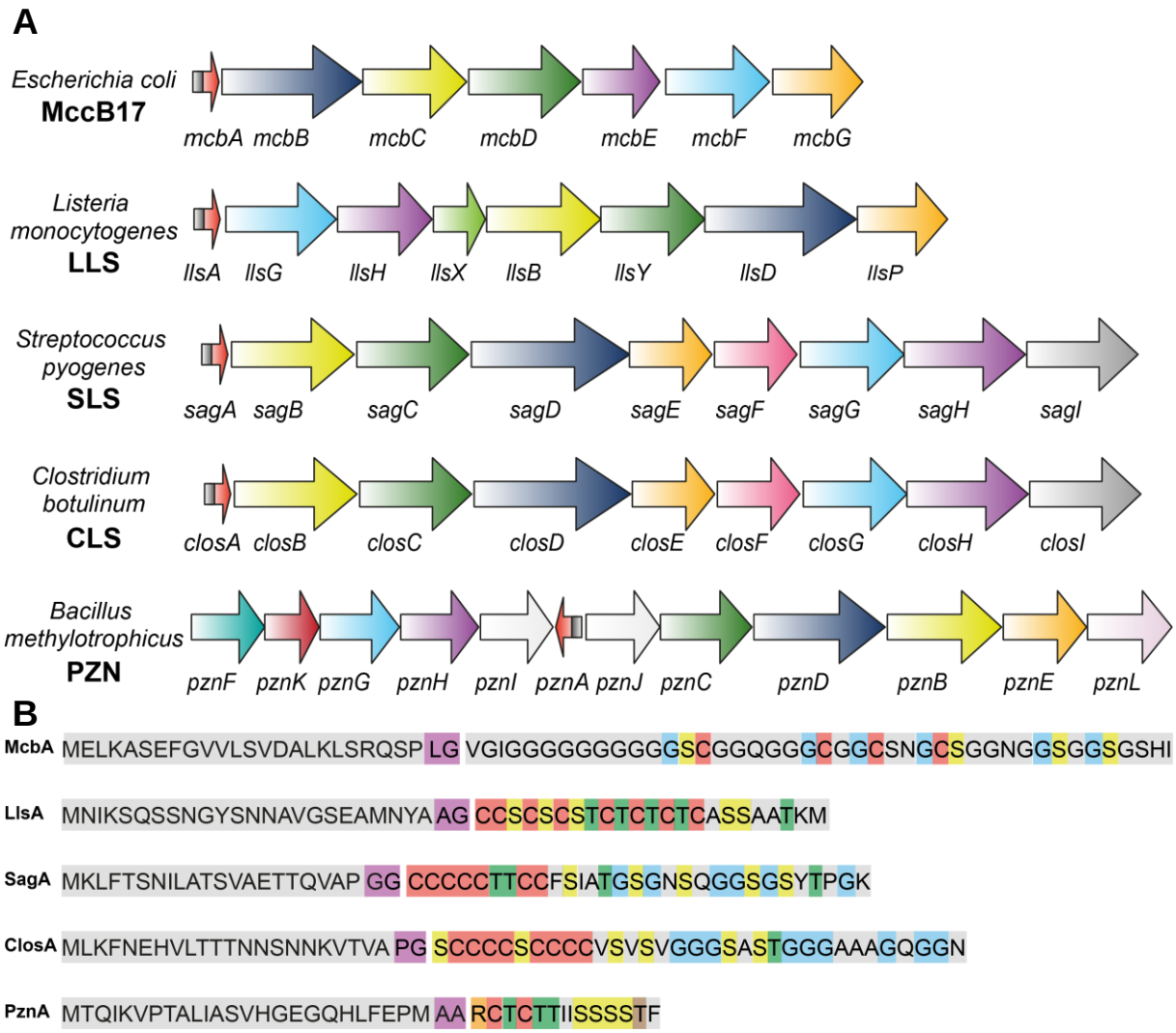

Figure 10. Operon organization and amino acid sequences of some TOMMs. (A) The gene cluster organization in *E. coli, L. monocytogenes, S. pyogenes, C. perfringens and B. methylotrophicus*. The related genes are indicated by colors as follows: in red the precursor peptide; in yellow the dehydrogenase gene; in dark green the cyclodehydratase gene; in dark blue the docking gene; in orange the CAAX protease; in light blue, purple and gray the ABC transporter genes; in turquoise the immunity gene; in dark red the transcriptional regulator (*pznK*) and in light pink a methyltransferase. The light green (*llsX*), pink (*sagF, closF* and *pznL*), and light grey (*pznI* and *pznJ*) are genes of unknown function. **(B)** Amino acid sequences of the unmodified microcin B17 precursor (McbA), Listeriolysin S precursor (LlsA), streptolysin S precursor (SagA), clostridiolysin S precursor (ClosA) and plantazolicin precursor (PznA). The predicted leader regions are to the left and terminate in putative leader cleavage sites (purple). Residues that are putatively modified are indicated in pink (Cys), yellow (Ser), green (Thr) and light blue (Gly). In the case of PZN the arginine is modified into a dimethylarginine (shown in orange) and the last threonine is modified into a methyloxazoline (shown in brown). Non-modified amino acids are shown in grey. Adapted from Lee *et al.* (2008), Molloy *et al.* (2011) and Molohon *et al.* (2016).

3.1.2 Posttranslational modifications enzymes

The posttranslational modification complex includes a dehydrogenase, a cyclodehydratase and a docking protein. This enzymatic complex is required for the posttranslational conversion of the Cys/Ser/Thr residues into oxazole, thiazole and methyloxazole heterocycles (Figure 11). The cyclodehydratase removes water from the peptide backbone to produce thiazoline, oxazoline and methyloxazoline rings. Then, a dehydrogenation reaction is catalyzed by the dehydrogenase via the removal of the hydrogen to generate the aromatic thiazole, axazole and methyloxazole heterocycles (Figure 11). The docking enzyme is proposed to support the enzymatic complex and also to regulate its enzymatic activity (59). The heterocycle synthetase complex displays functional promiscuity. The McbBCD from *E. coli* and SagBCD complex from *S. pyogenes* exhibit low sequence identity, however the SagBCD can catalyze the heterocycle formation of the MccB17 pro-peptide *in vitro.* In addition, the SagBCD complex can accept the ClosA pro-peptide from *C. botulinum,* leading to a cytotoxic phenotype (59).

The incorporation of thiazole, oxazole and methyloxazole heterocycles results in a net loss of 20 Da in peptide mass, and it has been explored by liquid chromatography-tandem mass spectrometry (LC-LMS/MS) for *in vitro*-modified SLS (212). These post-translational modifications are essential for the biological activity of the mature peptides, conferring a more rigid structure and allowing them to bind to their molecular targets efficiently (212, 214).

Most TOMMs gene clusters contain other ORFs that encode for additional modifying enzymes, suggesting that in addition to heterocycle formation, the pro-peptides may undergo further posttranslational modifications. For example, they can encode acetyl transferases, methyltransferases and lantibiotic dehydratases that could lead to acetylated, methylated and dehydrated amino acids (59).

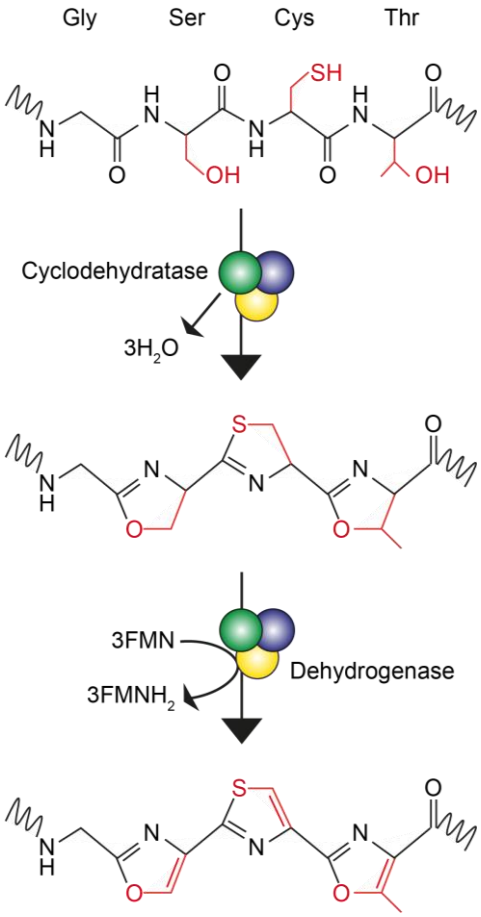

Figure 11. Post-translational modifications induced by the heterocycle synthetase complex in TOMMs. Heterocycles are formed in two steps: the activity of a zinc tetrathiolate-containing cyclodehydratase (in green) and a dehydrogenase (in yellow). Both enzymes form a three-enzyme complex together with the docking protein (in blue). The cyclodehydratase removes water from Cys, Ser and Thr residues in the peptide backbone to generate thiazoline, axazoline and methyloxazoline rings. Subsequently, a flavin mononucleotide (FMN)-dependent dehydrogenation reaction catalyzed by the dehydrogenase removes hydrogen to generate aromatic thiazole, oxazole and methyloxazole heterocycles. Adapted from Molloy *et al.* (2011).

3.1.3 ABC transporter

The ABC-type transporters are membrane proteins similar to those involved in bacteriocin export with ATP-binding pocket motifs (212). These transporters were previously explained in the Part II of the Introduction (see 2.2.1 ABC transporters).

3.1.4 Immunity protein

Immunity proteins are predicted to be peptidases and it has been suggested that they are also involved in the cleavage of the leader peptide (212). They are required for the viability of the producer bacteria (215). In the SLS cluster, the gene *sagE* encodes a predicted membrane-spanning immunity protein which shares weak homology with the candidate immunity protein PlnP from *Lactobacillus plantarum* (215). It has been suggested that in the case of *S. pyogenes*, the immunity provided by SagE is related only to the endogenous production of SLS and not to the exogenous exposure to SLS (215).

3.2 TOMMs in Gram-negative bacteria

3.2.1 Microcin B17 (MccB17)

MccB17, a 3.1 kDa pro-peptide produced by certain *E. coli* strains, is the prototype and first described TOMM. MccB17 was first described in 1986 as an antibacterial molecule that arrests DNA replication and induces the SOS response in target cells (159). In 1991, the specific mechanism of action of MccB17 was identified as inhibition of the DNA gyrase (216). Later, the proteins McbB, McbC and McbD (Figure 12) were shown to be responsible for introducing four oxazole (Ser40, Ser56, Ser62, and Ser65) and four thiazole rings (Cys41, Cys48, Cys51, and Cys55) in the MccB17 backbone (58, 217).

The process of introduction of thiazole and oxazole heterocycles was completely unknown until recently Ghilarov and colleagues (2019) succeed to solve MccB17 synthetase tridimensional complex, by taking advantage of the accidental observation that an N-terminal tagged MccB17 precursor peptide remained tightly associated with the MccB17 synthetase complex in *E. coli* cells that were unable to cleave off the leader sequence (218). This allowed this group to purify and subsequently crystallize the stable octameric complex together with its fully modified product pro-MccB17. The complex is described as an octameric assembly of $B_4C_2D_2$, where two McbB subunits interact to recognize the N-terminal part of the peptide while the C-terminal part of the peptide is trapped in the active site of McbC. The McbD (cyclodehydratase) and McbC (dehydrogenase) active sites are distant from each other, which necessitates alternative shuttling of the peptide substrate between them while they remain tethered

to the McbB dimer (docking protein) (218). Altogether the results provided by Ghilarov and colleagues show that the precursor peptide is subsequentially modified by shuttling between widely spaced heterocyclase and dehydrogenase catalytic sites prior to release of the mature peptide upon cleavage of the leader peptide by the TldD/E protease (encoded elsewhere in the chromosome), that yields the mature toxin (218, 219).

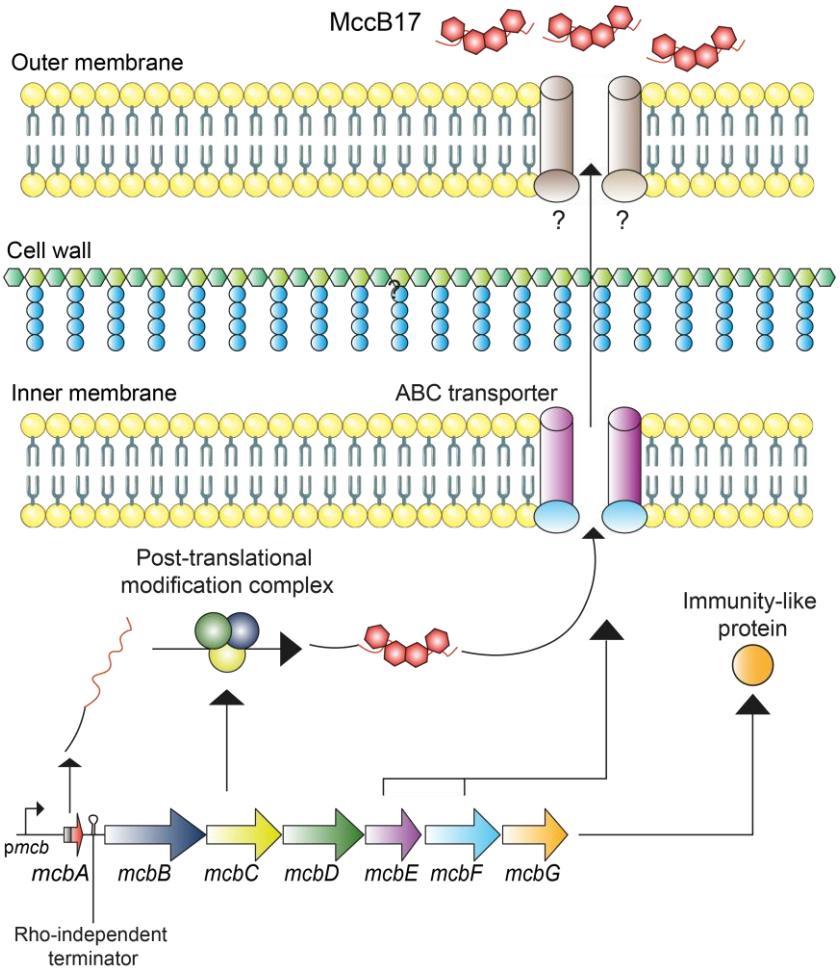

Figure 12. Production, processing and export of microcin B17. The carboxy-terminal core peptide of MccB17 produced *by E. coli* is post-translationally modified by the McbBCD complex to form biologically active MccB17. The amino-terminal leader sequence (represented in black) is cleaved from the mature core peptide after modification, resulting in aa mature peptide product. The Rho-independent terminator act as a regulatory mechanism, producing an excess of *mcbA* transcript compared to the quantity of transcripts for the genes encoding the modification and transport machinery. Adapted from Molloy *et al.* (2011).

3.3 TOMMs in Gram-positive bacteria

3.3.1 Streptolysin S (SLS)

SLS is a cytotoxic/hemolytic virulence factor produced by most group A *Streptococcus pyogenes* (GAS) responsible for skin disorders such as impetigo, respiratory tract infections such as pharyngitis, and the multisystem disorder streptococcal toxic shock syndrome (212, 220). SLS is also present in some Group C and Group G bacteria belonging to *S. dysgalactiae* subsp. *equisimilis.* The genetic cluster responsible for SLS production, maturation and export is *sagABCDEFGHI* (Figure 13) (212). SLS is a 2.7 kDa pro-peptide that is highly post-translationally modified before export (Figure 13) (212). Despite more than 100 years of research on SLS and recent findings providing insights into the structure-activity relationships of this toxin, the precise chemical structure of mature SLS has yet to be elucidated (212). However, site-directed mutagenesis with Ala (to reduce backbone rigidity) and Pro (to retain rigidity) suggests that oxazoles are formed at residues Ser34, Ser39, Ser46 and Ser48. Also, a thiazole is formed at Cys32 and Cys24 and Cys27 (57, 215, 221). SLS is not immunogenic due to its small size and its highly modified nature, which allows the removal of potential proteolytic sites required for antigen digestion and display (212, 222).

Cytotoxic activity remains active only when SLS is associated to the cell membrane or when it is extracted with carrier molecules like LTA, α-lipoprotein, RNA-core, and non-ionic detergents (223, 224). SLS cytotoxic activity targets erythrocytes, leucocytes, platelets, neutrophils, macrophages and subcellular organelles but excludes bacteria with intact cells walls (225–229). In erythrocytes, SLS leads to cell lysis by an influx of $Cl^{(-)}$ ions through disruption of the major erythrocyte anion exchange protein band 3 (230). SLS contributes to tissue injury, leading to cell death in soft tissues and vessels, promoting an influx of neutrophils and the development of necrotizing fasciitis (215, 231). It has been suggested that destruction of neutrophils and macrophages is a specific mechanism of virulence allowing the pathogen to evade the immune system (232). Furthermore, SLS is involved in GAS systemic dissemination through bacterial colonization of the pharynx or damaged skin (233), and it has been identified as a key factor in the paracellular penetration of the epithelial barrier (234).

SLS functions as a signaling molecule since the expression of the pro-peptide encoding gene *sagA* is up-regulated upon GAS exposure to SLS (235). It has been suggested that the untranslated *sagA* mRNA molecule is also involved in the pre- and post-translational control of other GAS virulence factors, including M proteins, the capsule protein SpeB and streptokinase (212, 236).

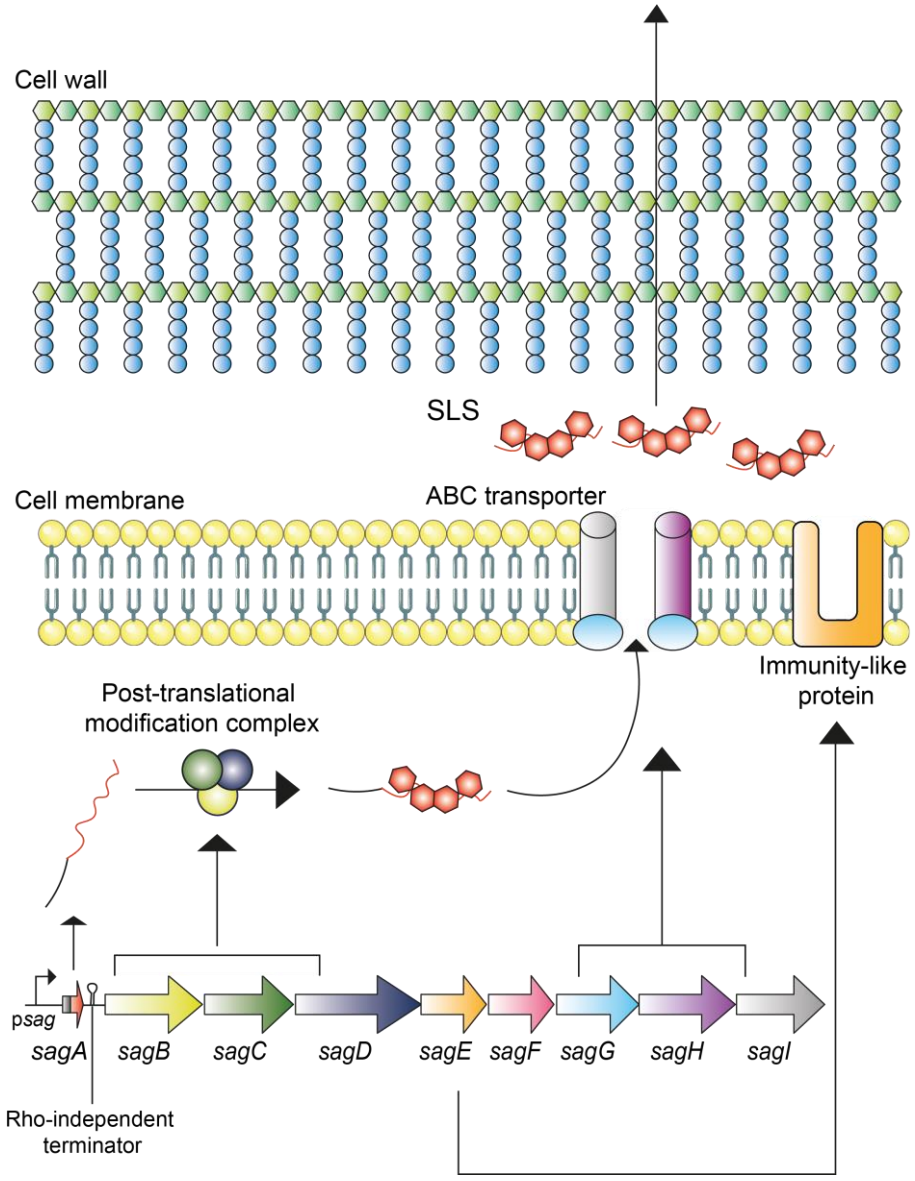

Figure 13. Production, processing and export of Streptolysin S. The carboxy-terminal core peptide of streptolysin S (SLS) produced *by S. pyogenes* is post-translationally modified by the SagBCD complex to form biologically active SLS. The amino-terminal leader sequence (represented in black) is cleaved from the mature core peptide after modification, resulting in aa mature peptide product. The Rho-independent terminator act as a regulatory mechanism, producing an excess of *sagA* transcript compared to the quantity of transcripts for the genes encoding the modification and transport machinery. Adapted from Molloy *et al.* (2011).

3.3.2 Clostridiolysin S (CLS)

CLS is produced by *C. botulinum* responsible of wound and food-borne botulism. CLS is also present in *C. sporogenes,* a related species that does not produce the botulinum toxin (214, 237). The genetic cluster *closABCDEFGHI* is the most closely related to the *sag* cluster of GAS and has the same organization (57). As SLS, CLS is also an hemolytic molecule (59). CLS is post-translationally modified, and an heterocycle was identified in Thr46 within CLS which is important for its hemolytic activity (221).

3.3.3 Plantazolicin (PZN)

The soil dwelling, plant growth-promoting bacterium *Bacillus amyloliquenfaciens* FZB42 produces the PZN. The molecular structure of PZN was recently elucidated by high-resolution mass spectrometry (MS), chemoselective modification and gene tools. PZN possess two thiazoles, four oxazoles and three methyl-oxazoles, as well as a dimethylarginine and a methyloxazoline (238). PZN has an ultra-narrow activity against *B. anthracis,* associating to cardiolipin micro-domains and inducing membrane depolarization, which ultimately results in cell lysis (207).

Part IV: *Listeria monocytogenes*

4.1. *L. monocytogenes* and the genus *Listeria*

The genus *Listeria* comprises actually 19 species, of which 17 are non-pathogenic environmental saprophytes which are often isolated from water, soil, and detritus (239–241). Only *L. monocytogenes* is pathogenic to humans and *L. ivanovii* is pathogenic to ruminants and sheep (242, 243). *Listeria* spp. belong to the Firmicutes phylum, are low guanine-cytosine Gram-positive rod-shaped, non-sporulating and facultative anaerobes. All *Listeria* spp. are motile below 30°C, can grow at low temperatures (4°C) and are resistant to environmental stresses such as low pH and high salt concentrations, which make *L. monocytogenes* problematic for the food industry (243).

4.2 *L. monocytogenes* lineages, serotypes and clonal complexes

Phylogenetic and subtyping studies have shown that *L. monocytogenes* (*Lm*) isolates belong to four divergent evolutionary lineages. The majority of *Lm* strains cluster into two lineages (I and II) first identified in 1989; subsequently, two additional lineages have been identified (III and IV). The assignation of an isolate into a lineage depends on genotypic and phenotypic approaches such as ribotyping, pulse-field gel electrophoresis (PFGE) and multilocus sequence typing (MLST) (239). The classical serotyping scheme is based on somatic (O) and flagellar (H) antigens which discriminate between 13 serotypes which represent genetically diverse groups of strains. Four serotypes (1/2a,1/2b, 1/2c and 4b) are usually associated to human listeriosis cases. As the serotyping discriminatory power is limited, this technique has been replaced by PFGE and MLST, as well as other approaches such as virulence gene variation, ribotyping and DNA arrays (244–248). Currently, whole-genome sequencing represents the gold standard for classification and diagnostics (242).

Lineage I include serotypes 4b, 1/2b, 3b 4d, 4e and 7, whereas lineage II includes serotypes 1/2a; 1/2c, 3a and 3c. Lineage III contains serotypes 4a and 4c. MLST applied on 360 strains demonstrated the existence of 63 clonal complexes (CCs) that helped to discriminate between different lineages (Figure 14). Most clinical isolates of *Lm* belong to seven distinct clonal complexes with an unique or dominant serotype (4b

for CC1, 2 and 4, 1/2b for CC3 and CC5, 1/2a for CC7, and 1/2c for CC9) (Figure 14) (249).

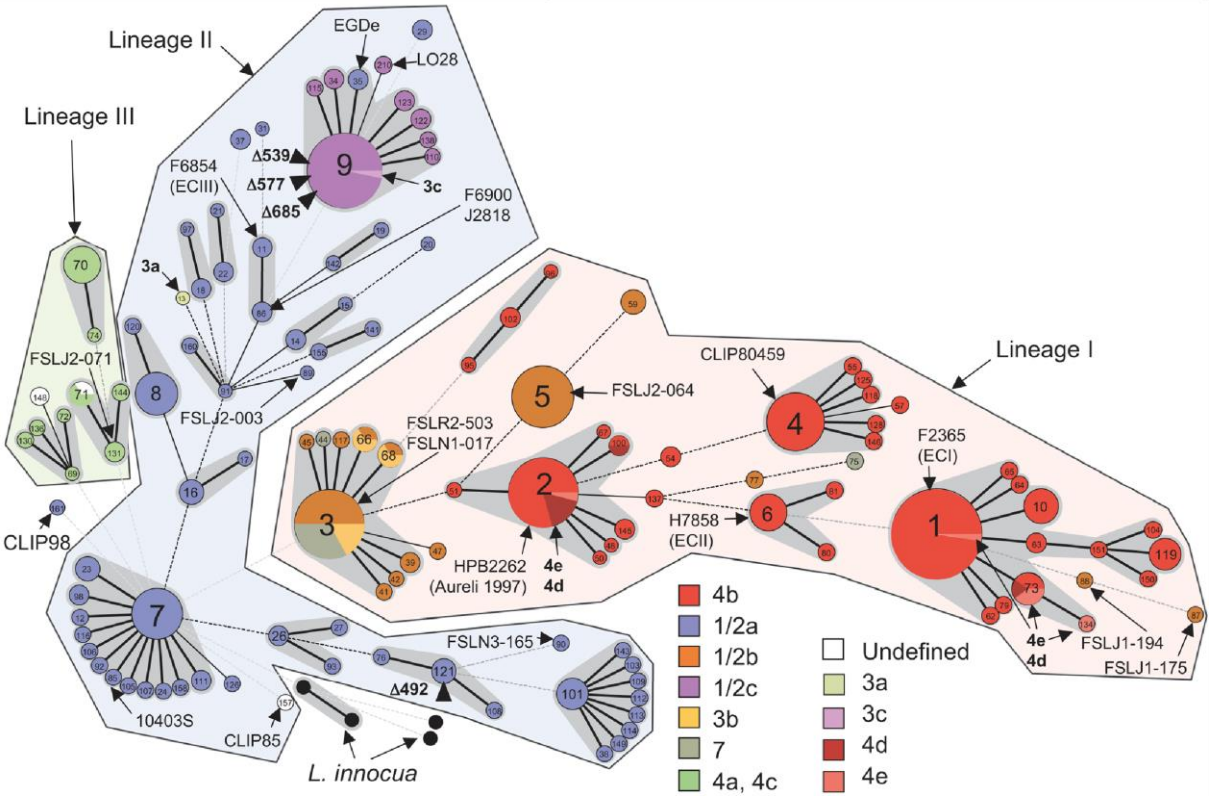

Figure 14. *L. monocytogenes* and *L. innocua* minimum spanning tree analysis based on MLST data. The three major lineages of *L. monocytogenes* are grouped. Each circle corresponds to a sequence type (ST) and the grey zones around STs belong to the same clonal complex (24 CC are visible). The ST numbers are inside the circles and are enlarged for the central genotypes that define the major CCs. The lines between STs indicate inferred phylogenetic relationships and are represented as bold, plain, discontinuous and light discontinuous depending on the number of allelic mismatches between profiles (1,2,3,4 or more, respectively). Circles were colored based on serotyping data. STs in which truncated forms of InlA were found are indicated by a black triangle and the positions of the premature stop codons are given after the Δ. Adapted from Ragon *et al.* (2008).

The most severe listeriosis outbreaks have been historically associated with a subset of *Lm* lineage I strains of serotype 4b (250, 251). More recently, specific lineage I CCs (mostly CC1, CC6, CC2 and CC4) have been associated with human clinical isolates, and have been shown to be more virulent in a humanized murine model of listeriosis (252). Genome sequencing revealed that these strains possess putative virulence loci that could potentially explain central nervous system tropism or materno-neonatal tropism (252). The Listeriolsyin S cluster, which encodes for a TOMM, has been also

identified in hyper-virulent *L. monocytogenes* CCs from lineage I (252, 253) (reviewed in Part V).

4.3 *L. monocytogenes,* a foodborne pathogen

Lm is a facultative intracellular Gram-positive pathogen responsible for listeriosis, a food-borne disease (254). After the ingestion of contaminated food (up to ~10^9 bacteria) healthy individuals may experience mild to severe gastroenteritis (255). In the case of children, elderly individuals, immunocompromised individuals and pregnant women, low levels of food contamination (~10^2-10^4 bacteria) can lead to disease (256, 257). Upon crossing the epithelial barrier, *Lm* may disseminate to the blood, liver, spleen, brain and placenta leading to meningitis in the newborn and in immunocompromised or elderly individuals, and to abortions in pregnant women (254). The mortality rate among infected individuals is very high (20-30%), however the number of cases worldwide is relatively low, estimated around 23 150 in 2010 (258).

4.3.1 *L. monocytogenes* infection cycle

Upon ingestion of contaminated food by the host, *Lm* interacts with the intestinal epithelial cells and crosses the intestinal epithelial barrier through two mechanisms: (1) invasion of ileal Peyer's patches via M cells, or (2) interaction with goblet cells and extruding enterocytes (259). Once in the lamina propria, *Lm* disseminates via the lymph nodes and blood vessels towards deep organs such as the liver and the spleen (Figure 15) (242). In pregnant women, *Lm* can cross the fetoplacental barrier, while in immunocompromised individuals it can cross the blood-brain barrier (243, 260).

L. monocytogenes capacity to invade diverse tissues and to cause disease relies on its ability to invade and proliferate within diverse host cells, including phagocytes and epithelial cells, from which bacteria disseminate intracellularly (cell-to-cell spread) without being exposed to extracellular host defenses such as antibodies or complement (261).

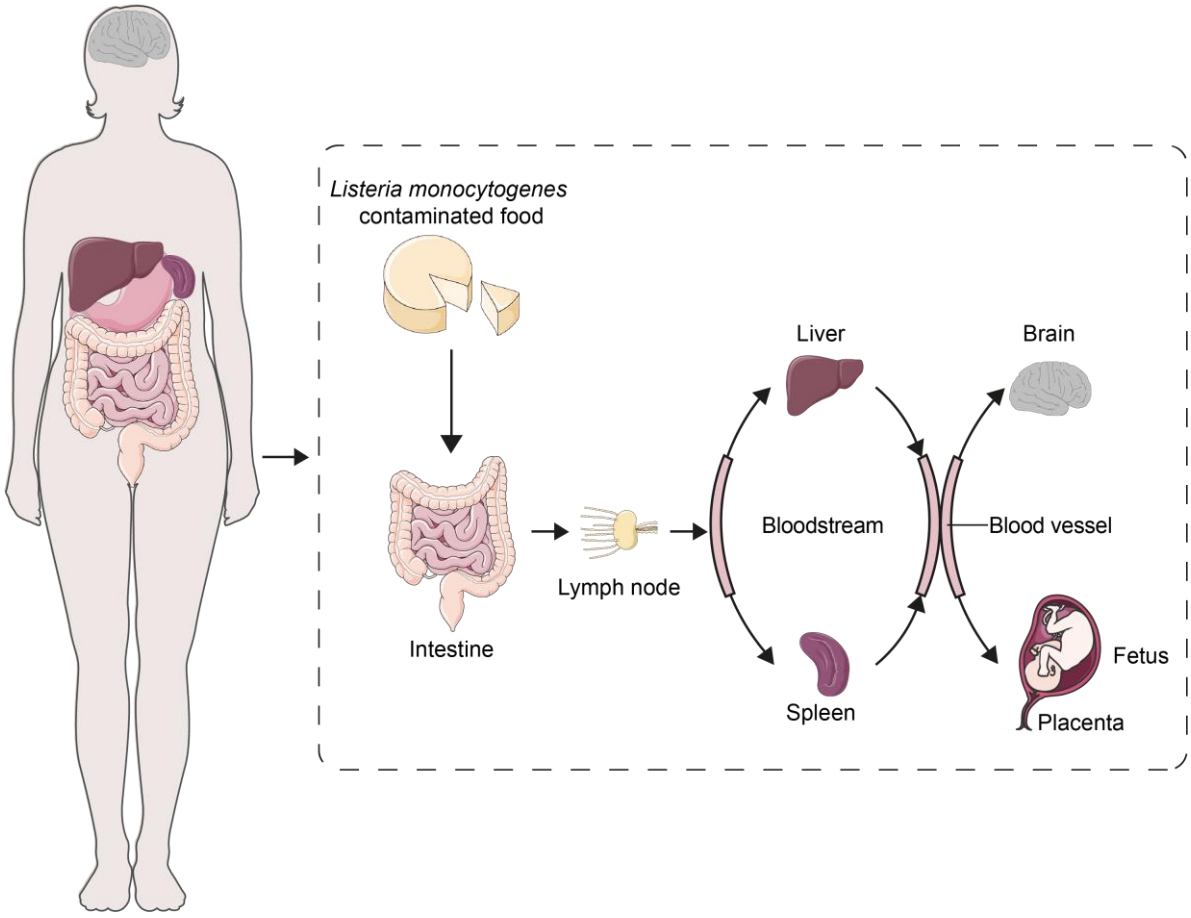

Figure 15. *L. monocytogenes* infection cycle in a human host. Upon ingestion of contaminated food, *Lm* traverse the intestinal barrier and spread throughout the bloodstream and lymph nodes to arrive to the target deep organs such as the liver and the spleen. In pregnant woman, the pathogen can cross the fetoplacental barrier leading to premature birth or abortion and in immunocompromised individuals can cross the blood-brain barrier causing fatal meningitis or sepsis. Adapted from Radoshevich and Cossart (2017)

4.3.1.1 Entry into cells

While *Lm* internalization in phagocytes is fully dependent on classical phagocytosis, invasion of epithelial cells is triggered upon interaction of bacterial surface molecules with host cell receptors (262). The bacterial surface leucine-rich repeat proteins InlA (cell wall-associated) and InlB (membrane-associated and potentially released as a soluble factor) (263) bind to the eukaryotic cell membrane receptors E-cadherin (involved in adherent junctions formation) and Met (the receptor of the hepatocyte growth factor) respectively, inducing bacterial uptake through receptor-mediated endocytosis (Figure 16). *Lm* possess several additional internalins and adhesins that support the function of InlA and InlB in cell invasion (264, 265). InlA is crucial for the

traversal of the intestinal barrier, while the synergy of InlA and InlB is required for invasion of the placenta (266, 267)

4.3.1.2 Escape from the vacuole

Upon cellular invasion, *Lm* resides temporally in a vacuole. However, vacuolar escape is essential for the bacterial intracellular survival. Listeriolysin O (LLO) as well as two phospholipases C (PlcA and PlcB) are key virulence factors that participate to vacuolar disruption and bacterial translocation to the host cell cytoplasm, where *Lm* replication takes place (Figure 16) (268).

LLO is a pore-forming toxin encoded by the *hly* gene which belongs to the cholesterol-dependent cytolysin (CDC) family (269). The LLO monomers are secreted and bind cholesterol-rich regions of eukaryotic membranes, form arc pores or slit-shaped assemblies which merge into complete rings, forming transmembrane pores leading to membrane disruption (270–272). LLO activity is regulated by acidic pH that triggers LLO oligomerization inside acidic phagosomes (273). PlcA is a secreted phosphatidylinositol-specific phospholipase C with an optimum pH of activity from 5.5 to 7. PlcB is a zinc-dependent broad range phospholipase C with an optimum pH of activity from 5.5 to 8. PlcB is secreted as an inactive proenzyme and the zinc-dependent metalloprotease Mpl processes the PlcB proenzyme into its active form (268). Secreted LLO together with PlcB disrupt the phagosomal membrane in primary infected cells. PlcA and PlcB cooperate with LLO in the disruption of double-membrane compartments generated during the process of cell-to-cell spread (242, 274, 275).

More recently, the secreted peptide pheromone-encoding lipoprotein A (PplA) was found to enhance the bacterial escape from host vacuoles (276). The type II secretion pseudopilus protein ComG was identified as a factor that potentially promotes vacuolar escape in phagocytes by physically disrupting the phagosome. The protein ComG is activated by the master activator gene *comK*, which becomes functional in phagosomes once the interrupted prophage A118 is excised (277). It is important to mention that in goblet cells, *Lm* can transcytose across the cell within a vacuole that is not disrupted, and in some macrophages, bacteria can replicate in spacious *Listeria*-containing phagosomes (SLAPs) (Figure 16) (243).

4.3.1.3 Intracellular and intercellular motility

Once *Lm* is located in the cytosol of host cells, it expresses the surface-anchored protein ActA, which recruits the cellular Arp2/3 complex and promotes actin-based bacterial motility and cell-to-cell spread (278). Bacterial spread between cells requires also the secreted virulence protein Internalin C (InlC) that binds to the host protein Tuba, a Cdc42 Rho-GTPase activator. By inhibiting Cdc42 activation and perturbing tight junctions formation, InlC relieves the cortical tension between cells and enhances the ability of motile bacteria to deform the plasma membrane into protrusions, increasing cell-to-cell spread (Figure 16) (279, 280). Protusion formation is also associated with plasma membrane damage due to LLO pore forming activity that generates membrane-derived vesicles with phosphatidylserine (PS) facing the surface. The PS-binding receptor mucin domain-containing protein 4 (TIM-4) mediates the uptake of these PS-positive protrusions, enabling cell-to-cell spread (281).

4.3.1.4 Changes in the organellar function

L. monocytogenes promotes infection of host cells by changing the function of several the host organelles including the mitochondria, the endoplasmic reticulum and the histones (243).

4.3.1.4.1 Broad range of cellular responses induced by LLO

LLO induces the formation of pores in cholesterol-containing membranes that lead to rapid Ca^{2+} influx and K^{+} efflux, triggering a wide range of host cell responses, including mitogen-activated protein kinase activation, histone modification, and caspase-1 activation (282). LLO is able to affect the mitochondria morphology and inducing mitochondrial fission independent of Dynamin-related protein 1, but dependent on Mic10 a component of the mitochondrial contact site and cristae organization system (MICOS) (283, 284). LLO also induces the ER stress upregulating the unfolded protein response and blocking translation and protein import into the ER, upregulating chaperones and ER-associated protein degradation to remove misfolded proteins (285). Moreover, LLO induces lysosome permeabilization leading to the release of cathepsins into the cytosol (Figure 16). Mitochondrial fragmentation, mitochondrial membrane potential loss, and drop in respiration and cellular ATP levels also correlate

with the LLO-induced calcium fluxes, altogether these processes promote efficient bacterial internalization (261, 286).

LLO leads to the degradation of the human, telomerase reverse transcriptase (TERT), an enzyme that maintains chromosomal integrity to promote infection (287). In addition, LLO degrade the DNA damage sensor meiotic recombination 11 homologue 1 (MRE11), eliciting the DNA damage response upon infection (288). The DNA damage is also induced upon infection which allow the extension of the cell cycle favoring the proliferation of *Lm* in the host cytoplasm (289).

4.3.1.4.2 Transcriptional and epigenetic modifications

Recent studies have identified a new class of virulence factors called nucleomodulins that can directly or indirectly modulate innate immune responses to invading pathogens. These factors are secreted from the bacterium into the host cell cytoplasm and then can reach the nucleus to exert their functions (290). The first identified nucleomodulin in *Lm* is the nuclear targeted protein A (LntA) which interacts directly with bromo adjacent homology domain-containing 1 protein (BAHD1), transcriptional repressor that affects the expression of interferon-stimulated genes) in order to derepress specific interferon-stimulated genes (ISGs) (Figure 16) (291, 292).

Lm infection can also induce changes in histone PTMs which control chromatin packing in the nucleus (293). Upon infection, the interaction of InlB with Met leads to the dephosphorylation of serine 25 and subsequent translocation of the protein NAD-dependent protein deacetylase sirtuin 2 (SIRT2) to the nucleus (Figure 16) (294). SIRT2 mediates the deacetylation of histone 3 at lysine 18 (H3K18) leading to the repression of several genes (295). *Lm* infection also affects other PTMs like the degradation of the SUMO-conjugating enzyme UBC9, the E2 enzyme required for sumoylation. Thus, sumoylated proteins are reduced upon infection, especially in the nucleus leading to an increase in the expression of antibacterial cytokines (296, 297). Host cell fight infection by upregulating a number of antibacterial effectors, for example ISG15 and the process of modification by ISG15 called ISGylation, which modulates cytokine secretion by covalent modification of ER and Golgi proteins (243).

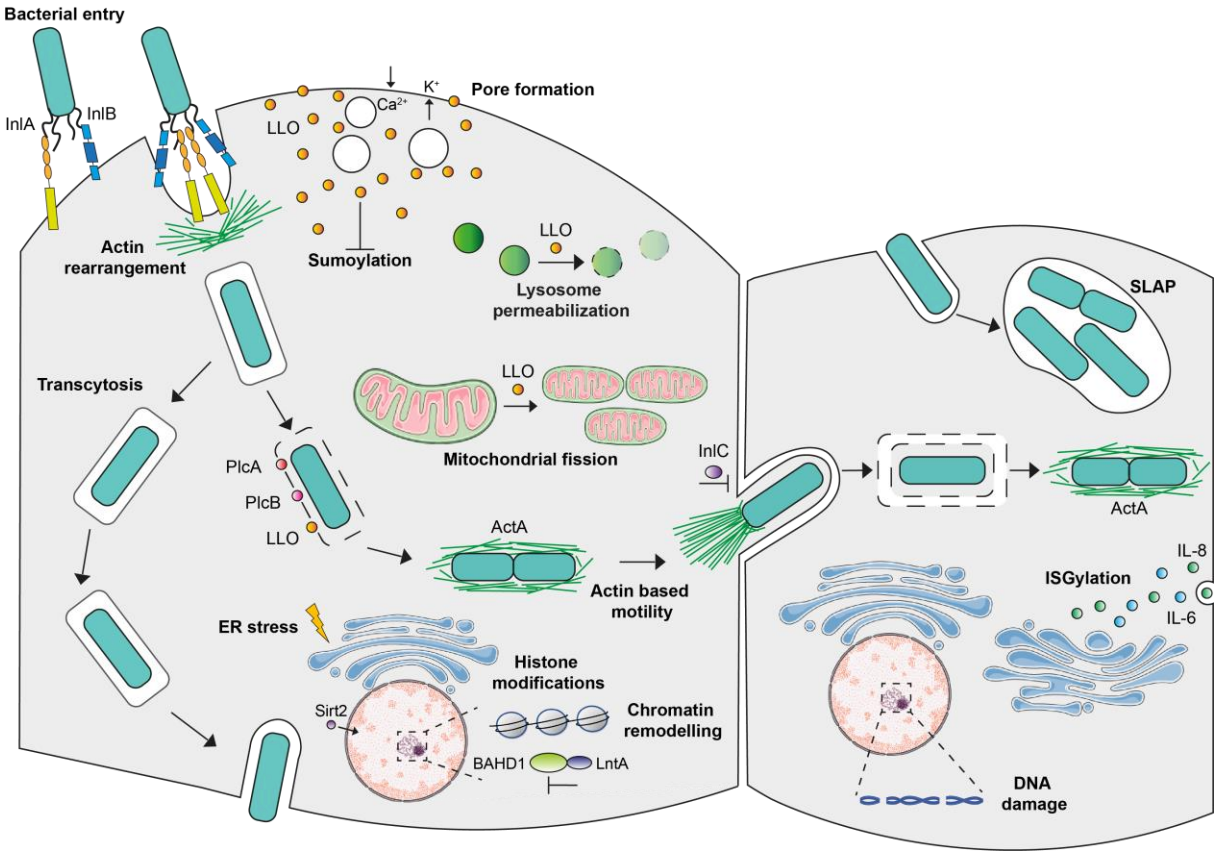

Figure 16. *Listeria monocytogenes* cellular infection cycle. *L. monocytogenes* invades non-phagocytic cells, such as epithelial cells, through receptor-mediated endocytosis, and in most cases, it escapes from the vacuole. In goblet cells, it can transcytose across the cell within a vacuole. In some macrophages, it can replicate in spacious *Listeria*-containing phagosomes (SLAPs). Upon vacuolar escape, *Lm* polymerizes actin and can spread from cell to cell. *Lm* infection has a plethora of effects on the cell through the activity of potent virulence factors. LLO, PlcA and PlcB mediate vacuolar escape. LLO also leads to changes in histone modification, desumoylation, mitochondrial fission, endoplasmic reticulum (ER) stress and lysosomal permeabilization, all of which can occur from the pore-forming activity of extracellular LLO. InlC interfere with tight junction's formation increasing *Lm* cell-to-cell spread. LntA interacts with BAHD1 protein complex to derepress interferon-stimulated genes (ISGs). SIRT2 shuttles into the nucleus to deacetylate histone 3 at lysine 18, leading to changes in chromatin packing that alter gene expression. Infection also leads to DNA damage, and the host cell upregulate a number of antibacterial effectors, for example, ISG15 and the process of modification by ISG15 (ISGylation) which modulates cytokine secretion by covalent modification of ER and Golgi proteins. Adapted from Radoshevich and Cossart (2017).

4.3.1.5 The virulence master regulator PrfA

The master virulence transcriptional regulator of *L. monocytogenes* is PrfA. It belongs to the cAMP receptor protein (Crp)/fumarate nitrate reductase regulator (Fnr) family of bacterial transcription factors and controls the transcription of two major virulence loci of *Lm*. The first locus (named the virulence regulon) includes the genes *hly, plcA, plcB, actA, mpI, orfX* and the second one includes *inlA* and *inlB* (242, 298).

PrfA also activates other genes harbouring a PrfA box in their promoter region and located elsewhere in the genome including *inlC* (298). PrfA is under the control of a 5'-UTR thermosensor which allows increased translation at 37°C when *Lm* is inside animal hosts (242). Also, PrfA is activated by the glutathione present in the host cells leading to a higher transcription of virulence genes (299).

4.3.1.6 *Sigma B a stress response activator of virulence genes*

The transcription of *L. monocytogenes* virulence genes is additionally controlled by the sigma factor SigmaB (σ^B), essential for the activation of virulence genes (300). These genes are essential for the survival of *Lm* in the intestine (301). The PrfA and σ^B regulons are significantly overlapping since σ^B regulates PrfA expression and other genes are regulated by both regulators (302, 303).

4.3.2 *L. monocytogenes* intestinal phase

Upon consumption of *L.* monocytogenes-contaminated food, bacteria reach the intestine and then cross the intestinal barrier to disseminate within the host (242). The host microbiota plays a critical role in resistance against colonization by entero-pathogens within the intestine (304). The commensal bacterial population can suppress directly intestinal pathogens by competitive exclusion and antimicrobial activities (305). In the case of *Lm,* the microbiota plays an important role, since germ-free mice (GFM) are much more susceptible to infection than conventional mice (306). Moreover, a diverse microbiota reduces significantly *Lm* colonization of the gut lumen and prevents systemic dissemination (307). Additionally, antibiotic administration to mice before oral inoculation increases *Lm* growth in the intestine (307).

However, the specific molecular mechanisms of *Lm* to compete with the host microbiota to survive in the intestine have been poorly studied. In 2016, Quereda and collaborators described Listeriolysin S (LLS) the first identified bacteriocin from epidemic *Lm* strains that is able to modulate the host microbiota in order to promote intestinal colonization and increased virulence (308).

Part V: Listeriolysin S

Listeriolysin S (LLS) is the first reported bacteriocin of *L. monocytogenes* and also the first bacteriocin reported for the Gram-positive bacteria genus *Listeria* (308, 309). LLS belongs to the TOMM family, which are highly post-translationally modified peptides, previously described in Part III of the Introduction. The first study on LLS was published in 2008, where this peptide was described as an hemolytic/cytotoxic virulence factor, associated with a subset of hyper-virulent lineage I *Lm* strains (253). Later, it was proposed instead that LLS is a bacteriocin that modifies the host gut microbiota, promoting intestinal colonization by *Lm* and deeper organ infection (308).

5.1 Distribution of LLS cluster in the *Listeria* genus

The LLS gene cluster has been also named as the *Listeria* pathogenicity island 3 (LIPI-3). The LIPI-3 is only present in a subset of *Lm* lineage I strains (52%, 23/44 strains) (310) which, as previously mentioned (Part IV of the Introduction), are more frequently associated with human listeriosis outbreaks (311). Interestingly, LIPI-3 is absent from the lineage II strains EGDe and 10403S, which have been historically referred as *Lm* reference strains, and have been recently characterized as hypovirulent strains (252)

The % of GC content and genome dissimilarity values indicate that LIPI-3 has been acquired by horizontal gene transfer (253). The variable nature of LIPI-3 within different lineage I sequence types (explained in Part 4 Figure 14) is more likely to reflect the LIPI-3 was lost in some STs as a consequence of recombination. This recombination events had place between two related glyoxalase-encoding genes (*lmof2365_1111* and *lmof2365_1121*); as a consequence the intervening genes were looped out and were lost from some lineage I STs (Figure 17) (253). In the strain EGDe, the LIPI-3 region is substituted by 17 kB encoding 17 ORFs (Figure 17) (253).These events happened frequently in the *Listeria* evolution, associated to the emergence of non-pathogenic *Listeria* species (312). Interestingly, LLS cluster is also present in a restricted group of strains of the non-pathogenic species *L. innocua*. Some *L. innocua* strains possess an intact LLS operon while other possess remnants of the LLS cluster. By placing the *L. innocua lls* genes under the control of a constitutive promoter, an hemolytic phenotype is observed, suggesting that the cluster encodes for a functional LLS (313).

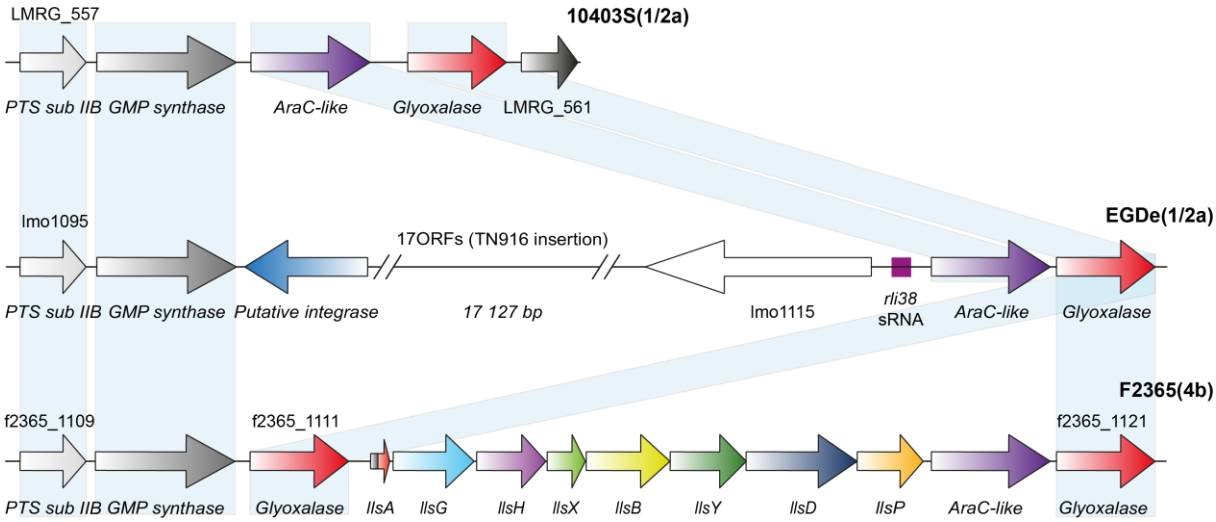

Figure 17. LIPI-3 and corresponding regions in LIPI-3 minus *L. monocytogenes*. Comparison of the LIPI-3 containing region in the strain F2365 (bottom) with the corresponding region of LLS$^-$ *L. monocytogenes* 10403S and EGDe (top). The strain name and serotype (in brackets) is indicated and the designation of the first gene in each case is the designation in the corresponding genome sequence. Homologous genes are presented by matching colours. Adapted from Cotter *et al*. (2008).

5.2 LLS gene cluster

The LLS gene cluster includes: (1) the gene *llsA* which encodes for the LLS pro-peptide with an N-terminal leader region, a C-terminal core region with an abundance of Cys, Ser and Thr residues, and a putative Ala-Gly leader cleavage motif; (2) the genes *llsG* and *llsH* that encode for a putative transporter; (3) the genes *llsB, llsY* and *llsD* that encode for a putative PTM complex involved in the generation of thiazole/oxazole/methyloxazole rings; (4) the *llsP* gene that encodes for a putative metalloprotease responsible for bacteriocin leader cleavage; and (5) the gene *llsX* which encode for a protein of unknown function, specific to the genus *Listeria* (Figure 18) (212, 253, 314). The LLS cluster is flanked by Rho-independent terminators. The predicted *llsA* promoter does not present motifs associated with virulence gene regulation in other *L. monocytogenes* strains, such as a PrfA box or σ^B binding sites (253).

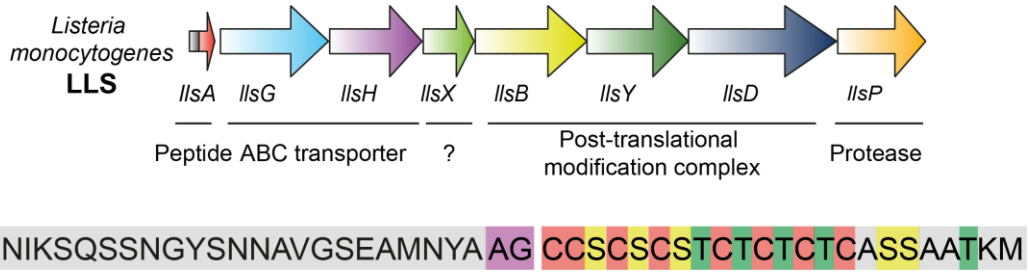

Figure 18. Operon organization and amino acid sequences of Listeriolysin S (A) The gene clusters organization of LLS in *Lm.* The genes are indicated by colors as follows: in red the precursor peptide; in yellow the dehydrogenase gene; in dark green the cyclodehydratase gene; in dark blue the docking gene; in orange the CAAX protease; in light blue, purple the ABC transporter genes; and in turquoise the immunity gene. The light green (*llsX*) is a *Listeria* unique gene of unknown function. **(B)** Amino acid sequences of Listeriolysin S precursor (LlsA). The predicted leader region is to the left and terminate in putative leader cleavage sites (purple). Residues that are putatively modified are indicated in pink (Cys), yellow (Ser), green (Thr) and light blue (Gly). Non-modified amino acids are shown in grey. Adapted from Molloy *et al.* (2011).

5.3 Functions of LLS

5.3.1 Hemolytic and cytotoxic activities

The LLS gene cluster was identified by Cotter and collaborators (253) upon genomic comparisons between the SLS gene cluster of *S. pyogenes* and a homologous region discovered in the *Lm* lineage I strain F2365 (CC1). Since SLS displays hemolytic activity, it was hypothesized that LLS could be a hemolytic peptide as well. As *Lm* produces the hemolysin LLO (encoded by the *hly* gene) that could mask any hemolytic activity from LLS, Cotter *et al.* generated an *hly* mutant in the F2365 background (F2365:*Δhly*) to investigate the biological function(s) of LLS. This F2365:*Δhly* mutant produced a non-hemolytic phenotype, but additional experiments using a bioluminescent reporter determined that the LLS gene cluster is not expressed under normal growth conditions. Expression of the LLS operon under the control of a strong constitutive promoter (pHelp) led the appearance of an hemolytic phenotype in the F2365 pHelp:*llsA Δhly* strain. Deletion mutagenesis established that six out of the seven genes of the LLS cluster are essential for the LLS hemolytic activity, with only *llsP* being non-essential (314). The LLS hemolytic activity, absent from supernatants of the F2365 pHelp:*llsA Δhly* strain, could be extracted from bacteria only when using

a RNA-based stabilizer, as it is the case for SLS. Cotter *et al.* also demonstrated that LLS was cytotoxic for mammalian epithelial and phagocytic cell lines (253).

5.3.2 Role in the virulence of *L. monocytogenes*

The contribution of LLS to the virulence of *Lm* was studied by Cotter *et al.* using a *llsB* mutant in the F2365 background. In a mouse intraperitoneal infection model, they demonstrated that the F2365 *ΔllsB* strain displays less bacterial numbers than the wild type strain in the liver and spleen of infected animals (253). This result suggests therefore that the LLS gene cluster plays a role in the virulence of *Lm*, and also that the putative PTMs introduced by the LlsBYD complex in the LLS peptide are important for its biological activity *in vivo*. Cotter *et al.* also mentioned that the survival of the F2365 *ΔllsB* strain in cultured human polymorphonuclear cells is hampered, suggesting that LLS is expressed *in vitro*; however, the authors did not verify the expression of LLS under these conditions.

Subsequently, Quereda and collaborators confirmed the importance of LLS for *Lm* virulence, but proposed that its role takes place at the intestinal level (308). Indeed, in a mouse oral infection model, they first showed that the GIT is more efficiently infected by the lineage I strain F2365 than by the lineage II strains EGE or 10403S. Secondly, by generating mutants of the *llsA* and *llsB* genes, they showed that the intestinal virulence of the F2365 strain is dependent on the function of the LLS gene cluster (308).

5.3.3 LLS expression and role in the regulation of the host microbiota

Using a bioluminescent reporter in which the *llsA* promoter was fused to the *lux* operon of *Photorhabdus luminescens,* Cotter and collaborators initially reported that expression of the LLS gene cluster is induced under oxidative stress conditions (253). However, using the same construct, Quereda *et al.* (2016) could not reproduce the induction of LLS expression *in vitro* by using different concentrations of H_2O_2 (308). Instead, the production of bioluminescence was detected only *in vivo* in the intestine of orally-infected mice, and not in other infected organs like the liver or spleen, though these organs contained higher bacterial loads than the intestine (308). The expression of LLS in the oral tract of infected animals prompted Quereda *et al.* to investigate its

potential impact on the intestinal microbiota. A metagenomic study identified a decrease in the representatives of the *Allobaculum, Streptococcus,* and *Alloprevotella* associated with LLS expression 24 hours post-infection (308). Interestingly, *Allobaculum* and *Alloprevotella* species produce butyric and acetic acid, respectively (315, 316). Butyrate is reported to inhibit virulence factors production in *Lm* and acetic acid inhibit *Lm* growth (308, 317, 318). It was therefore proposed that LLS is a bacteriocin that modulates the composition of the host intestinal microbiota, in order to favor *L. monocytogenes* intestinal colonization and infection of deeper organs (308).

5.3.4 LLS role as a bacteriocin

The hypothesis that LLS is as a bacteriocin was further explored *in vitro*. Using the F2365 pHelp:*llsA* (LLS^{+}) strain in co-culture assays, Quereda *et al.* showed that LLS is implicated in the killing of the *Lm* lineage II strains EGD and 10403S. Moreover, by investigating the impact of LLS on a collection of Gram-positive and Gram-negative bacteria, they showed that LLS is active only against Firmicutes, killing specifically *Lactococcus lactis* and *Staphylococcus aureus* (309).

THESIS OBJECTIVES

The discovery that the hyper-virulence of certain *L. monocytogenes* strains is associated to the modulation of the host intestinal microbiota by LLS opens new avenues in the understanding of listeriosis from a perspective that has been rarely explored so far concerning this disease. It also raises challenges and opens questions that remain to be investigated in relationship to the biology of this molecule, including the identification of its specific bactericidal mechanism of action, its structure, its activation signal(s), as well as the specific contribution of its cytotoxic and hemolytic activities to *L. monocytogenes* virulence *in vivo.*

The first goal of this Ph.D. thesis was to contribute to the characterization of the LLS cytotoxic role under physiological conditions. As mentioned in the previous chapter, LLS was initially reported as a novel *L. monocytogenes* hemolysin, displaying a cytotoxic activity that is important for bacterial virulence *in vivo* (253). Subsequently, LLS was described as a bacteriocin that modulates the composition of the gut microbiota, favoring *L. monocytogenes* colonization of the intestine (308). In this work, I investigated the importance of the LLS cytotoxic role by evaluating its contribution during *L. monocytogenes* infection of eukaryotic cells, as well as its damaging effects for macrophages and epithelial cells.

The second goal of this work was to understand the mechanism of action that allows the TOMM LLS to kill target bacteria. As reviewed in the introduction, bacteriocins may display diverse bactericidal activities that target different bacterial compartments and functions. TOMMs in particular have been shown to induce membrane damage or to inhibit the function of the DNA gyrase. By using a diversity of approaches (biochemical methods, microfluidics, flow cytometry) my work clarifies the killing mechanism displayed by this bacteriocin to outcompete gut commensal bacteria.

The third goal of this Ph.D. was to study the mechanisms that regulate the expression of LLS. We identified *in silico* transcriptional regulators and RNA regulatory elements that could be involved in LLS regulation. Also, we screened compounds or conditions present in the gut that could potentially induce LLS expression. In this work, we

performed a high-throughput screening (HTS) to try to identify the activation signal(s) by using a LLS transcriptional reporter.

The fourth goal was to characterize the LLS operon proteins LlsP and LlsX, in order to clarify their role in the production, maturation and export of LLS. We performed *in silico* analyses to predict their subcellular location and functions. Also, interaction studies were performed to study the LlsX subcellular location and interaction with LLS.

RESULTS

The results produced in this work are divided in 4 main parts:

Part I: LLS cytotoxic role during *L. monocytogenes* infection

The results obtained were published in *mBio,* where I figure as a third co-author (Quereda et al., 2017) (319).

Part II: Characterization of LLS mechanisms of action

The results obtained are under review in PNAS, where I figure as first author (Meza-Torres *et al.*) and include the characterization of LLS as a contact-dependent inhibition bacteriocin that impairs cell membrane integrity. Also includes proteomic analyses attempting to identify LLS specific molecular target(s). Finally, it includes the identification of a new LLS bacterial direct target.

Part III: Investigation of mechanisms regulating the expression of LLS

This part includes the *in silico* investigation of putative transcriptional regulators and putative regulatory RNA elements involved in LLS regulation. It also includes experiments attempting to characterize the transcription of LLS operon *in vivo.* Finally, it resumes the results from a high-throughput screen attempting to identify LLS *in vivo* activation signal(s) using a transcriptional reporter.

Part IV: Characterization of LLS operon products LlsX and LlsP

This part includes unpublished data from ongoing work that intends to clarify the role of the *L. monocytogenes* unique protein LlsX and *in silico* analyses to clarify the specific role of LlsP.

PART I: LLS cytotoxic role during *L. monocytogenes* infection

In addition to the antimicrobial activity displayed by bacteriocins, there are some cases where they also exhibit cytotoxic and hemolytic properties, as observed for the cytolysin produced by *E. faecalis* (320) and also the peptide BacSp222 from *Staphylococcus pseudintermedius* (321). SLS from GAS is a molecule that shares high homology with LLS, it exhibits cytotoxic and hemolytic properties but it does not kill intact bacteria (229, 322). SLS cytotoxic activity targets erythrocytes, leucocytes, platelets, neutrophils, macrophages and subcellular organelles (225–229). In epithelial cells, SLS causes lactate dehydrogenase (LDH) release into the medium, massive cytoskeletal collapse, loss of focal contacts, detachment of cells from the culture plates and severe membrane damage (59).

As presented in section 5.3.1 of the Introduction, LLS was initially described as an hemolytic and cytotoxic factor (253). Later, Quereda and collaborators characterized LLS as a bacteriocin that plays a critical role during *Lm* infection through modulation of the intestinal microbiota (308). In this context, it appeared therefore important to evaluate the specific role of the LLS hemolytic and cytotoxic activities during *Lm* infection *in vivo* and *in vitro*. Firstly, our group explored *in vitro* and *in vivo* whether LLS hemolytic activity was important for *Lm* survival in blood. The cytotoxic activity of LLS was then explored during *Lm* infection of macrophages and epithelial cells. Also, the expression of LLS was assessed during infection of eukaryotic cells *in vitro* or upon infection of deep organs *in vivo.* Later, the contribution of LLS for vacuolar escape during *L. monocytogenes* cell infection *in vitro* was investigated. Then, the individual role of LlsB and LLS for deeper organ colonization during *Lm* infection *in vivo* was studied. Finally, the activity of LLS on prokaryotic cells was explored by electron microscopy. The results obtained were published in *mBio* in a manuscript in which I figure as a third co-author (Quereda et al., 2017) (319).

My specific contributions to this study were:

1. To identify that LLS expressed by intracellular *L. monocytogenes* is not cytotoxic for macrophages or epithelial cells.
2. To determine that LLS expression does not confer an advantage to *L. monocyotogenes* during cell infection.

1.1 Results

1.1.1 LLS is not cytotoxic for eukaryotic cells during cellular infection by *L. monocytogenes*

Initial results from our laboratory differed from previous results published by Cotter *et al*. (2008) describing LLS as a cytotoxic molecule for epithelial cells, fibroblasts and macrophages (253). We therefore evaluated LLS cytotoxicity by measuring LDH release from RAW264.7 macrophages and enterocyte-like Caco-2 cells upon 24 hours of infection with the strains *Lm* F2365 (referred as WT), *Lm* F2365 *ΔllsA* (referred as LLS^-) and *Lm* F2365 pHELP::*llsA* (referred as LLS^+) which produces LLS under the control of the constitutive promoter pHelp (323). There were no differences in LDH release into culture supernatants from RAW264.7 and Caco-2 cells exposed to WT, LLS^-, or LLS^+ strains (Figure 19A). These results suggest that LLS expressed by intracellular *Lm* is not cytotoxic for eukaryotic host cells.

1.1.2 LLS does not confer an advantage to *L. monocytogenes* during cellular infection

Previous results from Cotter e*t al.* indicated that LLS contributed to *Lm* survival in polymorphonuclear neutrophils (253). These authors compared the difference between *Lm* F2365 (WT) and *Lm* F2365 Δ*llsB* (referred as Δ*llsB*) intracellular survival in purified human polymorphonuclear neutrophil granulocytes (PMNs) after 2 hours of infection. The WT survived better than the Δ*llsB* (253). However, Quereda et al (2016) showed that LLS is exclusively expressed *in vivo* and limited to the GIT (308). These results are contradictory and suggest that LLS is probably not expressed in PMNs *in vitro*. The differences in intracellular survival observed between WT and Δ*llsB* in PMNs could be associated to an additional function of the LlsB protein, which is part of the PTM complex that modifies LLS.

Since we could not exclude that LLS produced during intestinal infection could impact the capacity of bacteria to infect eukaryotic cells, we investigated the potential direct contribution of LLS to *Lm* infection *in vitro*. No differences in intracellular colony forming units (CFU) counts were observed between the WT, LLS^-, and LLS^+ strains at 2, 6, or 24 h post infection in RAW264.7, and Caco-2 cells (Figure 19B). These results show that LLS is not required during cellular infection by *Lm* (319).

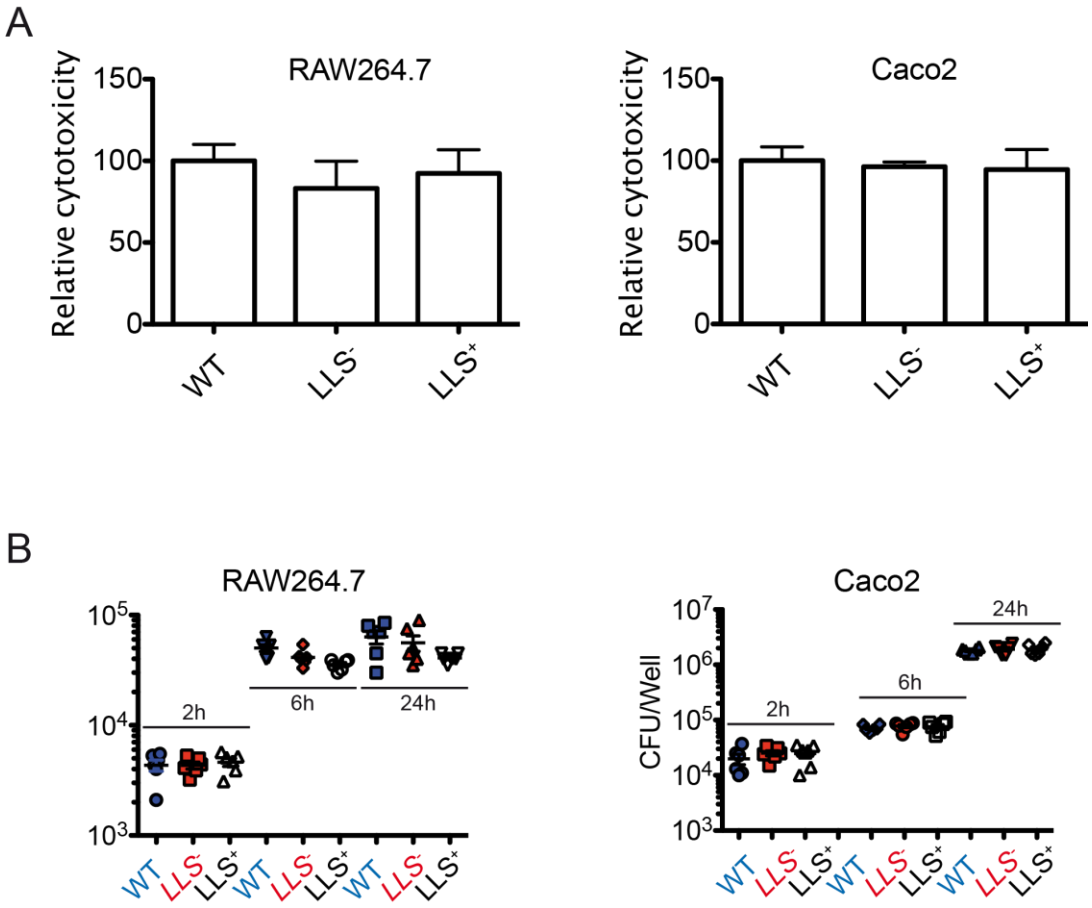

Figure 19. LLS is not cytotoxic for eukaryotic cells and does not confer an advantage during cell infection (A) Cytotoxicity (LDH release) relative to WT (100%) in RAW264.7 and Caco2 cells infected for 24 h. Error bars represent SD. (**B**) Numbers of viable intracellular *L. monocytogenes* F2365 (WT), *L. monocytogenes* F2365 Δ*llsA* (LLS$^-$), and *L. monocytogenes* pHELP::*llsA* (LLS$^+$) in Caco2 and RAW264.7 cells. The mean and standard error of the mean (SEM) are shown. CFU numbers were monitored at 2, 6, and 24 h p.i. (washed after 1 h of infection and with 40 μg/ml gentamicin added). Three independent experiments with 6 replicates in each experiment were performed. One representative experiment is shown.

1.2. Discussion

This work allowed to clarify LLS functions. Our results demonstrate that LLS has no contribution during *L. monocytogenes* cellular infection and that LLS is no cytotoxic for eukaryotic host cells as previously reported. Overall, we demonstrate that LLS is the first SLS-like virulence factor targeting exclusively prokaryotic cells during *in vivo* infections. Moreover, we describe that LlsB, a putative posttranslational modification enzyme encoded in the LLS operon, is necessary for murine inner organ colonization independently of the LLS activity. A previous study proposed a cytotoxic role of LLS in

epithelial and phagocytic cell lines (253). We attribute this cytotoxic effect due to the different experimental conditions used in this previous work, including the high number of bacteria used per cell in the absence of gentamycin. Indeed, unrestricted bacterial replication in the culture medium is probably associated to cellular damage, promoting an increase in the LDH release (20-30%) observed by the authors in their essay.

In the same study, it was claimed that LLS contributes to *Lm* virulence in a murine intraperitoneal model of infection (253). This conclusion was based on the reduced bacterial loads obtained in the livers and spleens of mice infected with a *llsB* mutant, compared to mice infected with the WT strain. Our present study suggests that it is LlsB and not LLS which plays an important role for the virulence of *Lm* in a murine intraperitoneal model of infection. This result indicates that LlsB performs an additional role *in vivo* different from the posttranslational modification of LLS, and we cannot exclude that a molecule outside the LLS cluster is posttranslationally modified by LlsB. To our knowledge, this is the first time that a TOMM posttranslational modification complex is involved in additional functions.

AMERICAN SOCIETY FOR MICROBIOLOGY | mBio®

RESEARCH ARTICLE

Listeriolysin S Is a Streptolysin S-Like Virulence Factor That Targets Exclusively Prokaryotic Cells *In Vivo*

Juan J. Quereda,[a,b,c] Marie A. Nahori,[a,b,c] Jazmín Meza-Torres,[a,b,c] Martin Sachse,[d] Patricia Titos-Jiménez,[e] Jaime Gomez-Laguna,[e] Olivier Dussurget,[a,b,c,f] Pascale Cossart,[a,b,c] Javier Pizarro-Cerdá[a,b,c]

Institut Pasteur, Unité des Interactions Bactéries-Cellules, Paris, France[a]; Institut National de la Santé et de la Recherche Médicale, U604, Paris, France[b]; Institut National de la Recherche Agronomique, USC2020, Paris, France[c]; Institut Pasteur, Ultrapole, Paris, France[d]; Anatomy and Comparative Pathology Department, University of Cordoba, International Excellence Agrifood Campus CeiA3, Cordoba, Spain[e]; Cellule Pasteur, Université Paris Diderot, Sorbonne Paris Cité, Paris, France[f]

ABSTRACT Streptolysin S (SLS)-like virulence factors from clinically relevant Gram-positive pathogens have been proposed to behave as potent cytotoxins, playing key roles in tissue infection. Listeriolysin S (LLS) is an SLS-like hemolysin/bacteriocin present among *Listeria monocytogenes* strains responsible for human listeriosis outbreaks. As LLS cytotoxic activity has been associated with virulence, we investigated the LLS-specific contribution to host tissue infection. Surprisingly, we first show that LLS causes only weak red blood cell (RBC) hemolysis *in vitro* and neither confers resistance to phagocytic killing nor favors survival of *L. monocytogenes* within the blood cells or in the extracellular space (in the plasma). We reveal that LLS does not elicit specific immune responses, is not cytotoxic for eukaryotic cells, and does not impact cell infection by *L. monocytogenes*. Using *in vitro* cell infection systems and a murine intravenous infection model, we actually demonstrate that LLS expression is undetectable during infection of cells and murine inner organs. Importantly, upon intravenous animal inoculation, *L. monocytogenes* is found in the gastrointestinal system, and only in this environment LLS expression is detected *in vivo*. Finally, we confirm that LLS production is associated with destruction of target bacteria. Our results demonstrate therefore that LLS does not contribute to *L. monocytogenes* tissue injury and virulence in inner host organs as previously reported. Moreover, we describe that LlsB, a putative posttranslational modification enzyme encoded in the LLS operon, is necessary for murine inner organ colonization. Overall, we demonstrate that LLS is the first SLS-like virulence factor targeting exclusively prokaryotic cells during *in vivo* infections.

IMPORTANCE The most severe human listeriosis outbreaks are caused by *L. monocytogenes* strains harboring listeriolysin S (LLS), previously described as a cytotoxin that plays a critical role in host inner tissue infection. Cytotoxic activities have been proposed as a general mode of action for streptolysin S (SLS)-like toxins, including clostridiolysin S and LLS. We now challenge this dogma by demonstrating that LLS does not contribute to virulence *in vivo* once the intestinal barrier has been crossed. Importantly, we show that intravenous *L. monocytogenes* inoculation leads to bacterial translocation to the gastrointestinal system, where LLS is specifically expressed, targeting the host gut microbiota. Our study highlights the heterogeneous modes of action of SLS-like toxins, and we demonstrate for the first time a further level of complexity for SLS-like biosynthetic clusters as we reveal that the putative posttranslational modification enzyme LlsB is actually required for inner organ colonization, independently of the LLS activity.

KEYWORDS *Listeria*, listeriolysin S, streptolysin S, cytotoxin, epidemics, infection

Received 15 February 2017 **Accepted** 7 March 2017 **Published** 4 April 2017

Citation Quereda JJ, Nahori MA, Meza-Torres J, Sachse M, Titos-Jiménez P, Gomez-Laguna J, Dussurget O, Cossart P, Pizarro-Cerdá J. 2017. Listeriolysin S is a streptolysin S-like virulence factor that targets exclusively prokaryotic cells *in vivo*. mBio 8:e00259-17. https://doi.org/10.1128/mBio.00259-17.

Editor Julian E. Davies, University of British Columbia

Address correspondence to Javier Pizarro-Cerdá, javier.pizarro-cerda@pasteur.fr.

Listeria monocytogenes is a foodborne pathogen and a facultative intracellular bacterium capable of causing severe disease in humans and animals. Upon ingestion of contaminated food, *L. monocytogenes* colonizes the intestine and crosses the intestinal barrier, disseminating via the blood to the liver, spleen, brain, and placenta (1, 2). The listeriosis fatality rate is estimated to be 20 to 30% of infected individuals despite antibiotic treatment (1). The most severe human listeriosis outbreaks are associated with a subset of *L. monocytogenes* lineage I strains that harbor a gene cluster encoding the bacteriocin and hemolytic factor listeriolysin S (LLS) (3, 4). Interestingly, the LLS gene cluster is absent from the most commonly studied *L. monocytogenes* lineage II strains EGD, EGDe, and 10403S (3), and its contribution to the intracellular lifecycle of *L. monocytogenes* is unknown (5).

LLS is homologous to streptolysin S (SLS [encoded by *sagA* in the *sag* operon]), a potent cytolytic toxin produced by most group A *Streptococcus pyogenes* (GAS) strains (6, 7). SLS is naturally expressed *in vitro* and is responsible for the classical β-hemolytic phenotype of *S. pyogenes* on blood agar plates (8). Using live-cell imaging, it has been shown that SLS activates the major erythrocyte anion exchange protein band 3 and favors a rapid influx of Cl^- ions into red blood cells (RBCs), leading to cellular rupture (9). In HEK-293 cells, SLS causes lactate dehydrogenase (LDH) release into the medium, massive cytoskeletal disassembly, loss of focal contacts, and detachment from the tissue culture plates (7). SLS promotes resistance to phagocytic killing in whole-blood killing assays and activates an inflammatory programed cell death pathway in macrophages (10, 11). *In vivo* studies have shown that SLS is required for *S. pyogenes* infection of skin and soft tissues (9, 12). The toxin encoded by an SLS-like gene cluster in *Clostridium botulinum* is named clostridiolysin S (CLS), and similarly to SLS, it is hemolytic and cytotoxic in HEK-293 cells (7, 13).

LLS, CLS, and SLS belong to the family of thiazole/oxazole-modified microcins (TOMMs) and are encoded by biosynthetic gene clusters characterized by the presence of cyclodehydratases/dehydrogenase genes (7). In the case of the LLS gene cluster, the genes *llsB*, *llsY*, and *llsD* code for putative posttranslational modification (PTM) enzymes that modify the product of the *llsA* gene coding for the structural LLS toxin (6, 7). Attempts to uncover the structural characteristics of the mature SLS-like toxins have been unsuccessful (7, 12, 13). The only direct structural insight available suggests that SLS contains two oxazole moieties observed at positions Ser^{46} and Ser^{48} and that CLS contains a methyloxazole at position Thr^{46} (13).

It has been suggested that given the genetic similarities of the TOMM operons in Gram-positive pathogens, it is likely that these TOMMs contribute to the pathogenic potential of each bacterial producer, similarly to SLS for *S. pyogenes* (6, 14). However, it is currently unknown if all SLS-like molecules of bacterial pathogens are cytotoxins, which play a role in tissue injury and contribute to virulence by targeting eukaryotic cells. By using an *llsB* deletion mutant, it has been previously concluded that LLS is a hemolysin and a cytotoxin that contributes to *L. monocytogenes* virulence in an intraperitoneal murine model of infection (3). We recently described that in orally infected mice, LLS behaves as a bacteriocin favoring *L. monocytogenes* gut colonization through modulation of the intestinal microbiota (4).

In the present study, we sought to deepen our insight into the functions of LLS during listeriosis, with a particular focus on its effects once the intestinal barrier has been crossed. Here, we show that while LLS kills prokaryotic targets, it does not impact infection of eukaryotic host cells *in vitro* and *in vivo*. Our present results demonstrate that, apart from its role as a bacteriocin in the host intestine, the structural product of the *llsA* gene has negligible activity on eukaryotic host cells, while the *llsB* gene product contributes to colonization of deep organs.

RESULTS

LLS causes weak RBC hemolysis *in vitro* and does not alter RBC counts *in vivo*. By growing *L. monocytogenes* colonies that constitutively express LLS in blood agar plates, or by using cell-free supernatants obtained from bacteria activated by the LLS

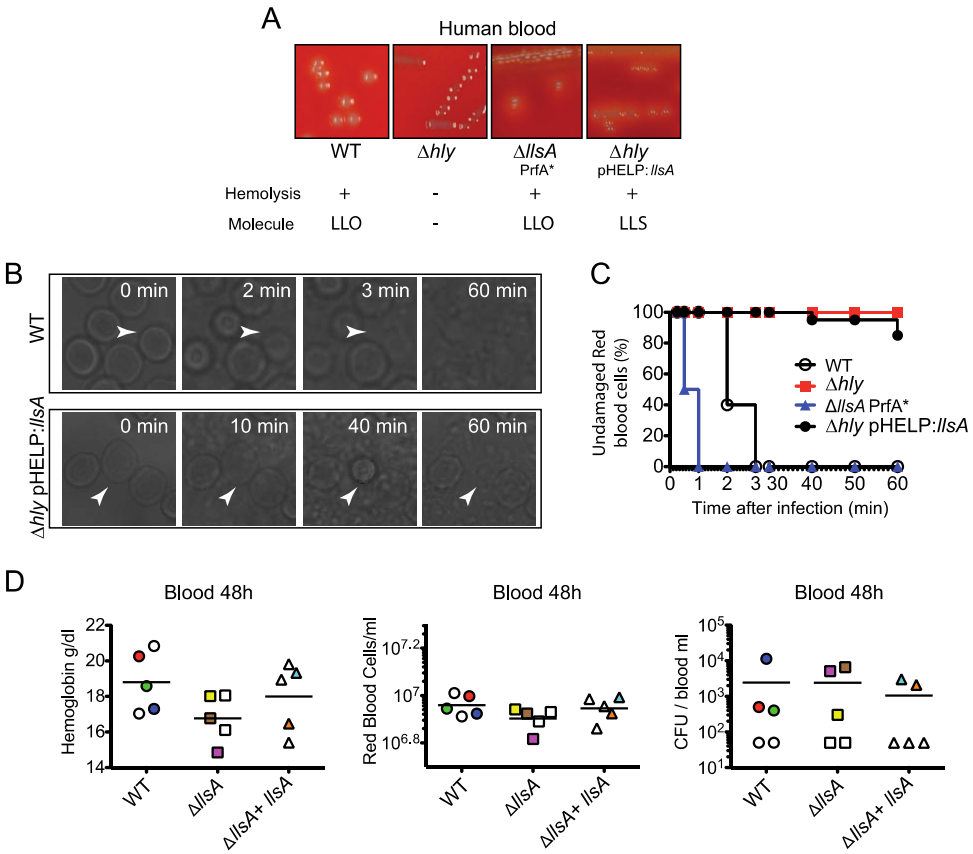

FIG 1 Hemolytic and cytolytic properties of LLS. (A) Hemolysis of human blood BHI agar plates by *L. monocytogenes* F2365, *L. monocytogenes* F2365 Δ*hly*, *L. monocytogenes* F2365 Δ*hly*(pHELP::*llsA*), and *L. monocytogenes* Δ*llsA* PrfA*. The lower panel shows the presence (+) or absence (−) of hemolysis and the *L. monocytogenes* molecule responsible for such hemolysis. LLO, listeriolysin O; LLS, listeriolysin S. (B and C) Live microscopy of RBC hemolysis using phase-contrast microscopy at different times posttreatment with the same strains used in panel A. Panel C shows quantification of the hemolysis over time. Data from one representative experiment out of the three performed are shown. (D) Concentration of hemoglobin (grams per deciliter), number of RBCs per milliliter of blood, and number of *L. monocytogenes* CFU per milliliter of blood of BALB/c mice injected intravenously with 10^4 CFU of the indicated strains. Mice were killed at 48 h p.i., and a blood sample was taken to assess the number of RBCs and the hemoglobin concentration. Mice whose blood contained more than 300 *L. monocytogenes* CFU/ml are colored to facilitate comparison of blood parameters.

inducer yeast RNA core, LLS has been previously shown to display hemolytic activity (3). In the case of SLS, real-time imaging indicated that the secreted toxin induces hemolysis of RBCs in 30 s (9). We investigated whether LLS exerts hemolysis as efficiently as SLS. First, we determined in brain heart infusion (BHI) agar plates with human or mouse blood the hemolytic activity of the *L. monocytogenes* F2365 wild type (WT), F2365 Δ*hly*, F2365 Δ*llsA* PrfA* (a strain that constitutively expresses listeriolysin O [LLO]), and F2365 Δ*hly*(pHELP::*llsA*) (a strain that does not produce LLO but expresses LLS). F2365 Δ*hly* was not hemolytic on human (Fig. 1A) or mouse (see Fig. S1 in the supplemental material) BHI blood agar plates. On the other hand, the F2365 WT and Δ*llsA* PrfA* strains caused hemolysis of both RBCs due to LLO activity, while the Δ*hly*(pHELP::*llsA*) strain also caused hemolysis in human and mouse RBCs due to LLS activity (Fig. 1A; Fig. S1). Second, we performed live-cell microscopy to visualize human RBC hemolysis caused by the same F2365 strains. Real-time imaging indicated 100% RBC hemolysis in 3 min due to LLO activity when incubated with the F2365 WT (Fig. 1B, upper panel, and C) or in 1 min when incubated with F2365 PrfA* Δ*llsA* (Fig. 1C). Hemolysis was marked by the visual rupture of the RBC membranes, as previously described for SLS (9). F2365 Δ*hly* caused no hemolysis, highlighting the potent activity of LLO (Fig. 1C). Surprisingly, only 15% of RBCs were lysed after 60 min of incubation with F2365 Δ*hly*(pHELP::*llsA*) (Fig. 1B,

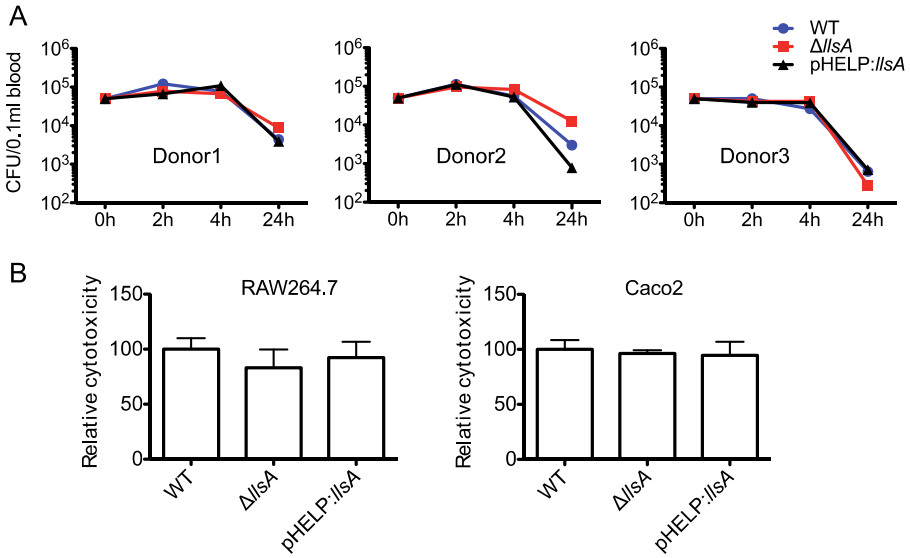

FIG 2 LLS expression does not confer resistance to phagocytic clearance and is not cytotoxic for eukaryotic cells. (A) Survival in human whole blood of the *L. monocytogenes* F2365 WT, *L. monocytogenes* F2365 Δ*llsA*, and *L. monocytogenes*(pHELP::*llsA*) strains. CFU numbers were monitored at 2, 4, and 24 h p.i. Experiments with three independent blood donors with 6 replicates in each experiment were performed. Error bars represent standard deviation (SD). (B) Cytotoxicity (LDH release) relative to F2365 WT (100%) in RAW264.7 and Caco-2 cells infected for 24 h (washed after 1 h of infection and with 40 μg/ml gentamicin added). Error bars represent SD.

lower panel, and C), suggesting that the hemolytic activity of LLS is much less efficient than that of LLO, as shown in our experiments and as reported in the literature for SLS.

In order to reveal the potential effects of the LLS hemolytic activity during *L. monocytogenes* infection *in vivo*, we infected intravenously conventional BALB/c mice with the F2365 WT, Δ*llsA* mutant strain, or its complemented strain and quantified the concentration of hemoglobin in blood, the number of RBCs, and the bacterial burden in blood at 48 h postinfection (p.i.). Consistent with real-time imaging performed *in vitro*, no significant changes in hemoglobin concentration (Fig. 1D, left panel) or RBC counts (Fig. 1D, center panel) were observed in mice infected with these three strains. Importantly, no correlation was observed between the number of *L. monocytogenes* cells in the blood (Fig. 1D, right panel) and the number of RBCs or hemoglobin (Fig. 1D; see Table S1 in the supplemental material). Taken together, these results show that LLS hemolytic activity is weak *in vitro* and that this activity does not affect RBC numbers during *L. monocytogenes* infection *in vivo*.

LLS expression does not confer resistance to phagocytic clearance. The weak hemolytic activity of LLS prompted us to evaluate its contribution to *L. monocytogenes* survival in blood. In the case of GAS, WT strains are able to proliferate in human blood, while SLS-negative mutants are cleared, demonstrating a crucial role for SLS in the resistance to phagocytic killing in human blood (10). To explore whether LLS contributes to phagocytic clearance, we incubated fresh human blood from three donors with *L. monocytogenes* F2365 WT, F2365 Δ*llsA*, and F2365(pHELP::*llsA*) strains. No significant difference could be observed between the three strains in phagocytic clearance (Fig. 2A). GAS can kill macrophages through the activation of an inflammatory programed cell death pathway mediated by SLS and streptolysin O (SLO) (11). Moreover, SLS induces alterations in keratinocyte inflammatory signaling cascades during GAS infection (15). These SLS properties prompted us to investigate a hypothetical role of LLS in cytokine secretion by macrophages infected by *L. monocytogenes*. We used an array kit detecting 111 different cytokines (Proteome Profiler mouse XL cytokine array) to compare the inflammatory responses of RAW264.7 macrophages infected with the F2365 WT strain (which does not express LLS *in vitro*, as shown above) to the responses

of cells infected with the Δ*llsA* deletion mutant or with the pHELP::*llsA* strain (which constitutively expresses LLS). No significant difference between the three groups (WT, Δ*llsA*, and pHELP::*llsA* strains) could be observed for secreted cytokine levels, including interleukin-1 (IL-1), IL-6, and tumor necrosis factor alpha (TNF-α), whose role is essential in the response to *L. monocytogenes* infection (see Fig. S2 in the supplemental material) (16), suggesting that LLS does not alter cytokine production in macrophages. Overall, our results indicate that LLS does not contribute to *L. monocytogenes* survival during the blood stage.

LLS expressed by intracellular *L. monocytogenes* is cytotoxic for neither macrophages nor epithelial cells. The absence of a role for LLS in macrophages contrasts with the previously published role of this molecule as cytotoxic for diverse cell lines, including professional phagocytes (3). To revisit this concept, we evaluated LLS cytotoxicity by measuring lactate dehydrogenase (LDH) release from RAW264.7 macrophages and enterocyte-like Caco-2 cells. No differences in LDH release into culture supernatants were observed between the WT, Δ*llsA*, and pHELP::*llsA* strains in RAW264.7 and Caco-2 cells (Fig. 2B). Taken together, these results suggest that LLS secreted by intracellular *L. monocytogenes* is not cytotoxic for eukaryotic host cells.

***llsA* promoter activity is undetectable during infection of eukaryotic cells *in vitro* or infection of deep organs, such as spleen or liver, *in vivo*.** Transcriptional fusion of the LLS promoter to a *lux* reporter plasmid previously demonstrated that LLS expression is specifically triggered in the intestine of orally infected mice and undetectable in other organs, such as liver and spleen (although these organs contained higher bacterial counts) (4). Bioluminescent signals in the intestine of germfree mice could also be detected, indicating that the intestine itself and not the gut microbiota activates the LLS promoter (4). Different compounds naturally present in the intestine, like mucin, gastric fluid, pepsin, $NaHCO_3$, short-chain fatty acids, ethanolamine, or even 6% O_2 or intestinal content of mice added *ex vivo* could not induce bioluminescence under *in vitro* conditions (4). In the present study, we investigated whether macrophages or epithelial cells could trigger LLS expression. We generated a transcriptional fusion of the LLS promoter to the promoterless green fluorescent protein gene (*gfp*), which is more sensitive as a reporter than the luciferase systems in other Gram-positive bacteria (17). A similar green fluorescent protein (GFP) transcriptional reporter was used for *hly*, a gene essential for the intracellular lifestyle of *L. monocytogenes*. We next infected Caco-2 epithelial cells and RAW264.7 macrophages with F2365^{InlB}(pAD-P*llsA*-GFP) or F2365^{InlB}(pAD-P*hly*-GFP) for 2, 6, and 24 h. Figure 3 shows intracellular bacteria that polymerize host cell actin (arrows) and bacteria not associated with actin (arrowheads), presumably inside vacuoles after 5 h of gentamicin treatment. Intracellular F2365^{InlB}(pAD-P*hly*-GFP) produced a green fluorescence at 2, 6, and 24 h p.i. in both cell lines tested, indicating that the GFP reporter is functional and that the *hly* promoter is active (Fig. 3A and B; see Fig. S3 and S4 in the supplemental material). Interestingly, the activity of the *llsA* promoter was undetectable at 2, 6, or 24 h p.i. in the cell lines tested (Fig. 3A and B; Fig. S3 and S4). No signal was observed for the *llsA* promoter at 2, 6, and 24 h p.i. in other cell lines (LoVo, HeLa, and Jeg-3) where the *hly* promoter was active (data not shown).

Furthermore, we investigated whether *L. monocytogenes* inoculated intravenously expresses LLS in deep organs, such as the spleen or the liver. We used the *L. monocytogenes* F2365$^{llsA::lux}$ strain in which we fused the LLS promoter to the *lux* reporter plasmid (4). Upon intravenous infection of BALB/c mice with 10^4 cells of F2365$^{llsA::lux}$, a bioluminescent signal was detected in the abdomen of infected animals at 72 and 96 h p.i. To uncover the origin of the bioluminescent signals, abdominal skin and peritoneum dissection was performed. The *ex vivo* images of the gastrointestinal system and the livers and spleens removed from the body are shown in Fig. 3C. Interestingly, bioluminescent signals were only detected in the stomach and the intestine of infected mice, while being absent from the liver and spleen (which are the main organs targeted by *L. monocytogenes*). Importantly, although the bioluminescent signals were specifically expressed in the gastrointestinal system, the liver and spleen contained at least

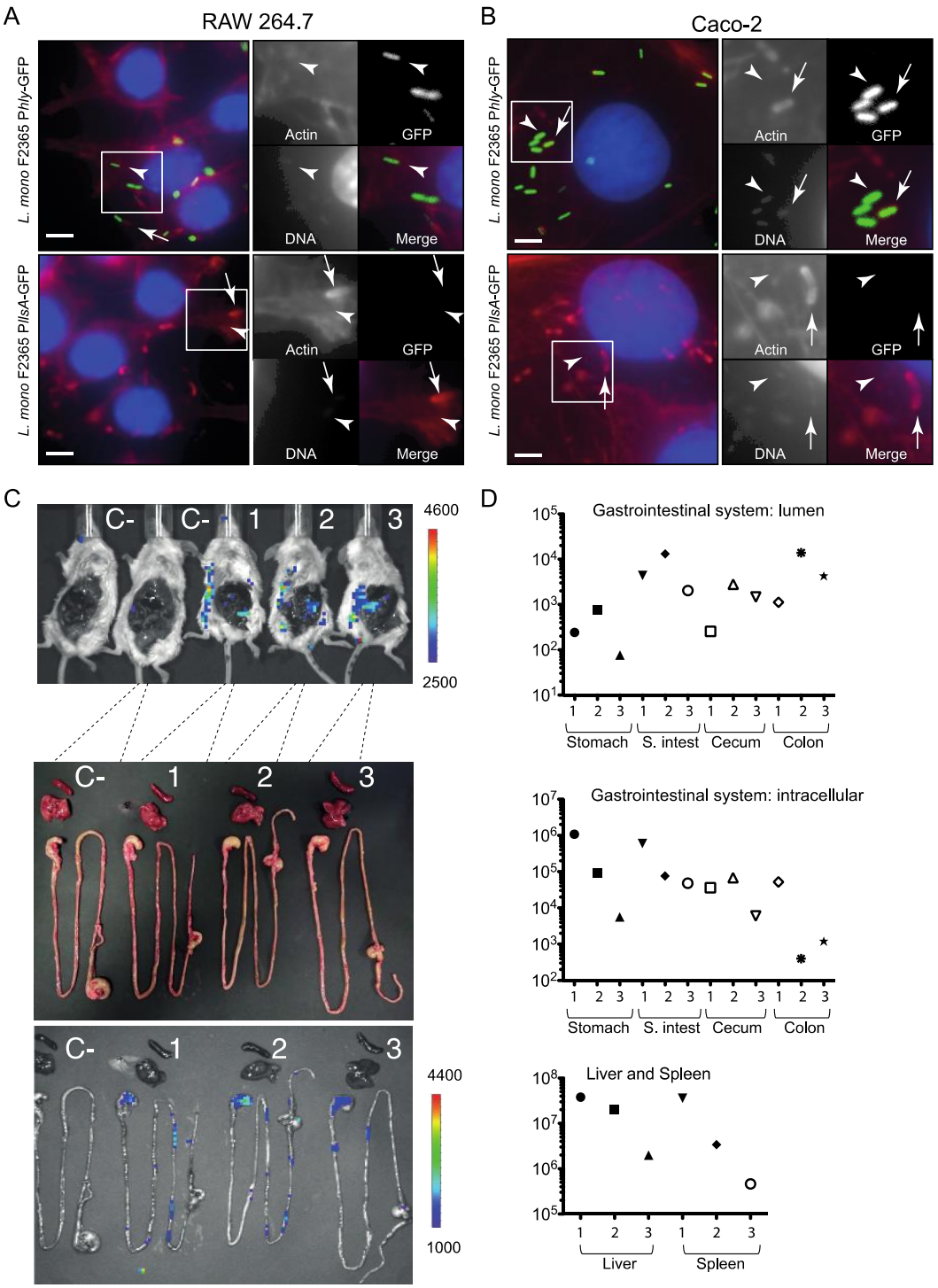

FIG 3 Fluorescence microscopy and bioluminescence assays to evaluate the promoter activity of llsA. RAW264.7 cells (A) and Caco-2 cells (B) were cultured in 96-well plates and infected with *L. monocytogenes* F2365^{InlB}(pAD-P*llsA*-GFP) or *L. monocytogenes* F2365^{InlB}(pAD-P*hly*-GFP). Host cells were infected for 6 h (washed after 1 h of infection and with 40 μg/ml gentamicin to kill extracellular bacteria) and fixed. GFP is shown in green. Actin (red) and nuclei (blue) were labeled with phalloidin conjugated to Alexa 546 and Hoechst, respectively. Scale bars, 5 μm. (C) Bioluminescence imaging showing induction of the LLS promoter in the gastrointestinal system after intravenous inoculation of three mice with 10^4 bacteria per BALB/c mouse. C−, noninfected control mice. Images were acquired at 96 h p.i. with an IVIS Spectrum imaging system. The false color bar indicates the number of photons/second. (D) Bacterial counts in the stomach, small intestine (S. intest), cecum, and colon content (top), as well as in the stomach, small intestine, cecum, colon, liver, and spleen tissues (middle and bottom), of the same mice at 96 h p.i.

more than 100-fold CFU than the stomach, small intestine, cecum, or colon (Fig. 3D). Altogether, these results demonstrate that the *llsA* promoter is not active or is expressed at very low levels during infection of host cells, suggesting that the activation of LLS expression in the gastrointestinal system is not triggered by the infection of eukaryotic cells.

LLS does not contribute to cell infection and is not sufficient for *L. monocytogenes* vacuolar escape. Since we could not exclude that LLS produced during intestinal infection could impact the capacity of bacteria to infect eukaryotic cells, we investigated the potential contribution of LLS to infection. No differences in intracellular CFU counts were observed between the F2365 WT, F2365 Δ*llsA*, and F2365(pHELP::*llsA*) strains at 2, 6, or 24 h p.i. in RAW264.7, HD11, and Caco-2 cells (Fig. 4A). These results show that LLS is not required during cellular infection by *L. monocytogenes*.

If LLS does not play a role in cell infection, this means that it should not affect vacuolar escape by *L. monocytogenes*. The capacity of LLS to mediate vacuolar rupture and to allow intracellular growth was evaluated in RAW264.7 macrophages. Extracellular and total *L. monocytogenes* numbers were distinguished by using inside-outside staining of fluorescently labeled bacteria, and cytosolic microorganisms were identified by actin staining. Approximately 80% of F2365 WT cells escaped from vacuoles and polymerized actin (Fig. 4B and E). As expected, LLO was required for vacuolar escape in macrophages, as no escape events were observed upon cell infection with F2365 Δ*hly* (Fig. 4C and E). Importantly, no F2365 Δ*hly*(pHELP::*llsA*) cells were found associated with actin (Fig. 4D and E), suggesting that these bacteria were trapped in phagosomes and that LLS expression is not sufficient to rupture the bacterial internalization vacuole in order to facilitate access to the host cytoplasm. Overall, our results indicate that LLS does not target eukaryotic membranes during infection.

LlsB, but not LLS, has a role in spleen and liver colonization. SLS causes extensive tissue disruption, inflammation, and necrosis of skin lesions and is required for *S. pyogenes* infection of skin and soft-tissues (9, 10, 12). Regarding LLS, as mentioned above we have shown that this molecule is specifically expressed in the intestine of intravenously and orally infected mice, where it alters the host intestinal microbiota and increases *L. monocytogenes* persistence (Fig. 3C and 4). LLS function in the intestine requires the activity of the LlsB enzyme, which is by homology with SLS putatively involved in the posttranslational modification of LLS. As reported, deletion of LlsB completely inactivates LLS hemolytic activity *in vitro* and decreases *L. monocytogenes* virulence in a mouse intraperitoneal infection model (3). To determine the impact of LLS on virulence once *L. monocytogenes* has crossed the intestine, we intravenously infected mice with the F2365 WT, F2365 Δ*llsA*, F2365 Δ*llsB*, F2365 Δ*llsA*, and F2365 Δ*llsB* complemented strains, and quantified the bacterial burdens in the liver and spleen. In agreement with the inactivity of LLS promoter in liver and spleen (4), and with the absence of a role for LLS in the blood and in the cell lines used in the present study, the Δ*llsA* mutant strain did not display significantly different bacterial loads in the spleen or liver compared with the WT strain (Fig. 5A). However, significant differences were observed between the WT and Δ*llsB* strains in the number of CFU isolated from these organs ($P < 0.05$) (Fig. 5A). Furthermore, histopathologic assessment of the liver and spleen of mice infected with WT, Δ*llsA* mutant, and Δ*llsA* complemented strains showed no differences in the numbers, locations, and inflammatory cell types of necrotic foci (Fig. 5B and C). Together, these results demonstrate that LLS does not play an essential role in *L. monocytogenes* deep organ colonization once the intestine has been crossed and strongly suggest that LlsB performs additional important functions for virulence apart from putatively driving LLS posttranslational modification.

LLS promotes killing of target bacteria. Our results suggest that during *in vivo* infections, LLS does not target eukaryotic cells. Our previous results (4) indicate that LLS is able to modulate the growth of *Lactococcus lactis*, *Staphylococcus aureus*, and *L. monocytogenes* lineage II strains as well as representatives of the *Allobaculum* and *Alloprevotella* genera during *in vivo* infection (4). To investigate a direct cytotoxic effect

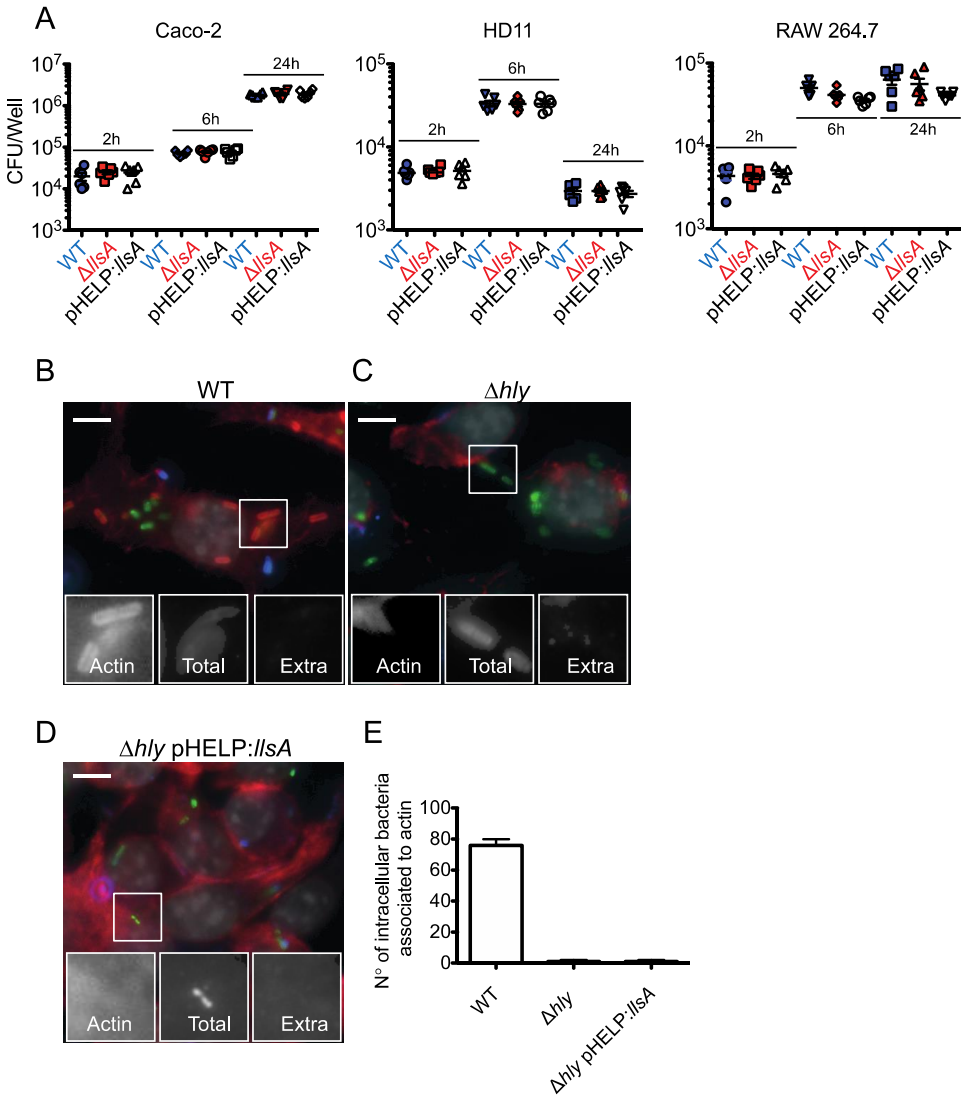

FIG 4 LLS expression does not confer an advantage during cell infection and is not sufficient to damage and rupture host cell vacuoles to access the host cytoplasm. (A) Numbers of viable intracellular *L. monocytogenes* F2365, *L. monocytogenes* F2365 Δ*llsA*, and *L. monocytogenes*(pHELP::*llsA*) cells in Caco-2, HD11, and RAW264.7 cells. The mean and standard error of the mean (SEM) are shown. CFU numbers were monitored at 2, 6, and 24 h p.i. (washed after 1 h of infection and with 40 μg/ml gentamicin added). Three independent experiments with 6 replicates in each experiment were performed. One representative experiment is shown. (B, C, and D) RAW264.7 cells were seeded into 96-well plates and infected with the *L. monocytogenes* F2365 WT (B), *L. monocytogenes* F2365 Δ*hly* (C), and *L. monocytogenes* F2365 Δ*hly*(pHELP::*llsA*) (D) strains. Differential immunofluorescence staining for identification of extracellular versus total *L. monocytogenes* numbers was performed. Extracellular bacteria (Extra) were labeled with a secondary goat anti-rabbit Alexa 647 (blue), and total bacteria (total) were labeled with a secondary goat anti-rabbit Alexa 488 (green) after cell permeabilization. Actin was labeled by using phalloidin conjugated to Alexa 546 (red). Nuclei were stained with Hoechst (gray). Bars, 5 μm. (E) Quantification of the number of bacteria of the *L. monocytogenes* strains used in panels B, C, and D that access the host cytosol.

of LLS on target bacteria, diluted overnight cultures of *L. monocytogenes* F2365 strains (WT and the pHELP::*llsA* strain) and the target *L. lactis* were grown in coculture. After 3 h of coculture, there was a reduction in the growth of *L. lactis* only when cocultured with *L. monocytogenes* F2365(pHELP::*llsA*) (Fig. 6A). The effect of LLS on *L. lactis* growth was even higher at 6 and 9 h of coculture (Fig. 6A). Under transmission electron microscopy, *L. lactis* cultured alone or cocultured with the *L. monocytogenes* F2365 WT (which does not produce LLS under *in vitro* conditions [4]) for 3, 6, or 9 h showed the typical structure of Gram-positive cocci, with a thick, uniform, smooth cell wall and intact

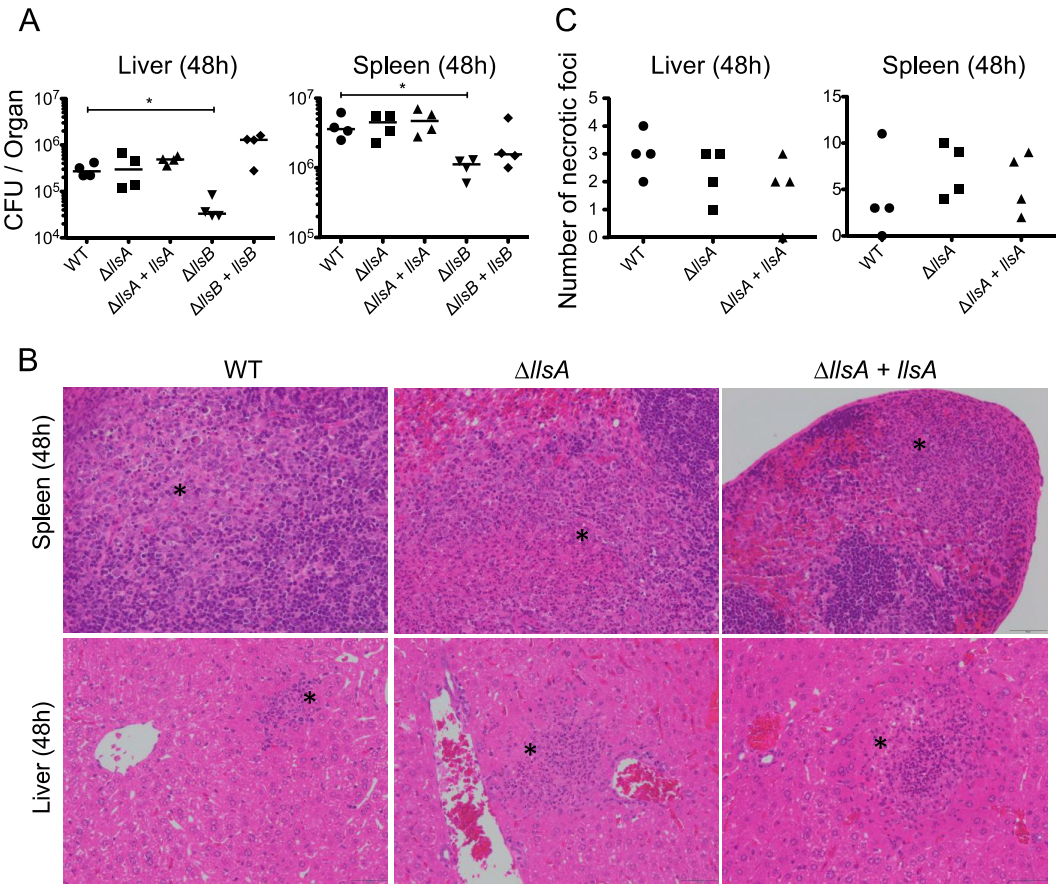

FIG 5 LLS role in spleen and liver colonization once the intestinal barrier has been crossed. (A) BALB/c mice were injected intravenously with 10^4 CFU of the indicated strains. Mice were killed at 48 h p.i., and spleens and livers were removed to assess the bacterial load per organ. (Note that these numbers of CFU correspond to the half-organ used to assess bacterial load. For details, see the Materials and Methods section.) (B) Examples of spleen and liver tissues from the same infected mice. Asterisks show necrotic foci. (C) The number of necrotic foci in spleen and liver tissues from the same infected mice was evaluated. (Note that these numbers of necrotic foci correspond to the half-organ used for histopathology. For details, see the Materials and Methods section.)

cytoplasmic membrane attached to the wall (Fig. 6B and C). The cytoplasm was granular and evenly distributed in the cell. Some of the cells demonstrated a dividing septum, indicative of bacterial growth (Fig. 6B and C). After 3 h of coculture with *L. monocytogenes* F2365(pHELP::*llsA*), disruption of *L. lactis* cell wall integrity was observed (Fig. 6C). At 6, 9, and 24 h of coculture with *L. monocytogenes* F2365(pHELP::*llsA*), increasing numbers of *L. lactis* cells showed more drastic changes, including cell wall wrinkles and even cellular lysis (Fig. 6C). These results confirm that LLS is the first SLS-like virulence factor of a bacterial pathogen able to promote death of target bacteria.

DISCUSSION

In 2008, SLS-like gene clusters were discovered in clinically relevant Gram-positive pathogens (including *S. aureus* and *C. botulinum*) and other nonpathogenic bacteria (7), leading to the identification of the LLS gene cluster in *L. monocytogenes*. SLS is a potent membrane-damaging agent and a major virulence factor contributing to GAS infection through rapid destruction of eukaryotic cells and tissue damage (6, 9–11, 15, 18–20). It has been proposed that SLS-like virulence factors from other Gram-positive pathogens also behave as potent cytotoxins (6, 14). Interestingly, functional experimental data of LLS activity on eukaryotic cells are scarce (3), despite the fact that LLS is almost exclusively detected within lineage I strains (the most frequent lineage among *L. mono-*

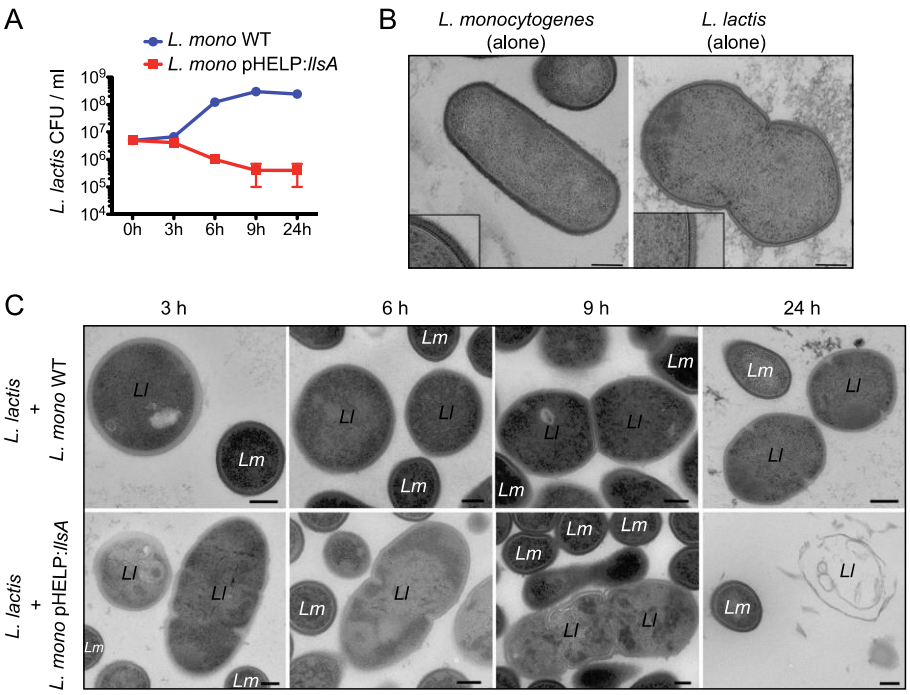

FIG 6 Effect of LLS on *L. lactis*. (A) Viable *L. lactis* at 3, 6, 9, and 24 h postinoculation in coculture with *L. monocytogenes* F2365 WT or *L. monocytogenes* F2365(pHELP::*llsA*). Error bars show SD. Data from one representative experiment out of the three performed are shown. (B) *L. lactis* and *L. monocytogenes* F2365 WT seen by electron microscopy when cultured alone. Bacteria were grown in BHI for 24 h. Insets present an enlargement of an area of the cell wall. Scale bars, 200 μm. (C) *L. lactis* cells cocultured with *L. monocytogenes* F2365 WT (upper panels) or *L. monocytogenes*(pHELP::*llsA*) (lower panels) in BHI for 3, 6, 9, or 24 h. Scale bars, 200 nm.

cytogenes clinical isolates) and that it has been related to the *L. monocytogenes* infectious potential in epidemiological and comparative genomic studies (21, 22). In the present work, we aimed to characterize the extent to which LLS potentially contributes to host infection by directly performing damaging activities on eukaryotic cells and tissues.

Using an array of molecular, cell biology, and histology techniques, we demonstrate that unlike SLS, (i) LLS causes very weak RBC hemolysis, (ii) it does not confer resistance to phagocytic clearance, (iii) it does not affect the levels of secreted cytokines by cells infected by *L. monocytogenes*, (iv) when expressed under the control of its native promoter or expressed through a constitutive promoter by intracellular *L. monocytogenes*, it is not cytotoxic for epithelial cells and macrophages, (v) its constitutive expression by *L. monocytogenes* in the confined space of a phagocytic vacuole is not sufficient to rupture this membrane compartment, (vi) its expression is undetectable within host cells due to inactivity of its promoter under both *in vitro* and *in vivo* conditions, (vii) it does not contribute to eukaryotic cell infection, and (viii) it does not contribute to virulence in an intravenous infection murine model. Altogether, our results clearly demonstrate that the biological activity of LLS is distinct from that of SLS or CLS, showing that LLS does not target eukaryotic host cells and is not involved in inner organ infection during systemic stages of listeriosis.

It has been previously proposed that LLS is hemolytic on blood agar plates and cytotoxic for epithelial and phagocytic cell lines (3). Importantly, experimental conditions *in vitro* used a ratio of 100 bacteria per cell for 6 h (without explicit use of gentamicin) to demonstrate the cytotoxic effect of LLS on J774, C2-Bbe, and CT26 cells (3). The fact that we did not observe the same cytotoxic effect on Caco-2 or RAW264.7 cells after the same infection period (making use of gentamicin after 1 h p.i.), using an MOI of 5 for Caco-2 cells or an MOI of 2 for RAW264.7 cells, leads us to believe that

TABLE 1 Bacterial strains used in this study[a]

BUG no.	Mutation/relevant genotype	Strain	Reference
3012	Wild type	*L. monocytogenes* 4b F2365	25
3651	PrfA*	*L. monocytogenes* 4b F2365	This study
3671	Δ*hly*	*L. monocytogenes* 4b F2365	This study
3781	Δ*llsA*	*L. monocytogenes* 4b F2365	4
3795	Δ*llsA*(pPl2::*llsA*)	*L. monocytogenes* 4b F2365	4
3817	pHELP::*llsA*	*L. monocytogenes* 4b F2365	4
3819	Δ*hly*(pHELP::*llsA*)	*L. monocytogenes* 4b F2365	This study
3672	Δ*llsB*	*L. monocytogenes* 4b F2365	4
3975	Δ*llsB*(pPl2::*llsB*)	*L. monocytogenes* 4b F2365	4
3783	Δ*llsA* PrfA*	*L. monocytogenes* 4b F2365	This study
3824	*inlB* corrected	*L. monocytogenes* 4b F2365	This study
4060	pAD-P*hly*-GFP	*L. monocytogenes* 4b F2365^{InlB}	This study
4058	pAD-P*llsA*-GFP	*L. monocytogenes* 4b F2365^{InlB}	This study
3763	LLS promoter fused to *lux* reporter system in pPL2 *lux*	*L. monocytogenes* 4b F2365	4
4048	pAD-P*llsA*-GFP	*E. coli*	This study
4052	pAD-P*hly*-GFP	*E. coli*	This study

[a]The strains shown are from the UIBC bacterial collection.

experimental conditions used in the previous study (3) may have influenced the *in vitro* cell system conditions, finally leading to an increase of ≈20 to 30% of LDH release to the medium due to LLS and also bacterial exposure. Moreover, the cytotoxic effect was only demonstrated by using a *L. monocytogenes* strain in which LLS was constitutively expressed using the pHELP promoter (3).

It has also been claimed that LLS contributes to virulence in a murine intraperitoneal model of infection (3). This conclusion was based on the reduced F2365 Δ*llsB* CFU numbers in the livers and spleens relative to those in the corresponding F2365 WT-infected mice. However, when we compared the virulence of the F2365 Δ*llsA* and F2365 Δ*llsB* mutants to that of the F2365 WT strain, we discovered an unexpected difference between these two deletion mutants: *llsB* but not *llsA* (the gene coding for the toxin LLS) contributed to virulence in our mouse intravenous model of infection, indicating that LlsB performs additional functions apart from the putative posttranslational modification of LLS. *llsB* is therefore the first gene from a dehydratase/dehydrogenase TOMM complex reported to perform additional functions apart from putative posttranslational modifications of the cluster-encoded toxin. An attractive hypothesis that remains to be validated is that LlsB participates in the posttranslational modification of another molecule outside the LLS operon.

Our present results show that although LLS constitutive expression [strain F2365(pHELP::*llsA*)] can damage RBCs in a blood agar plate or in a phosphate-buffered saline (PBS) suspension, the concentration of LLS produced by the epidemic *L. monocytogenes* F2365 WT strain during *in vivo* infection once the intestine has been crossed has minimal toxicity or even no effect on eukaryotic cells. On the contrary, LLS is highly toxic for prokaryotic targets such as *L. lactis in vitro* and modulates the host microbiota *in vivo* (4). These data demonstrate that LLS is the first SLS-like virulence factor of a bacterial pathogen that only targets prokaryotic cells *in vivo*. It is very important to highlight that in our present experiments, LLS expression is detected in the stomach and the intestine of mice after intravenous bacterial inoculation. Indeed, it has been previously shown that *L. monocytogenes* can be discharged back to the gastrointestinal system from the gallbladder (23, 24). Our results suggest that modulation of the host microbiota by LLS takes place not only during oral animal infection but also upon intravenous infection: this fact should be now taken into account during *in vivo* animal experiments with relevant epidemic *L. monocytogenes* strains expressing the LLS operon.

MATERIALS AND METHODS

Bacterial strains and cell lines. The epidemic lineage I *L. monocytogenes* strain F2365 of serotype 4b responsible for the 1985 California listeriosis outbreak (25) was used as parental strain (BUG3012; UIBC bacterial collection). The isogenic mutants and plasmids used in this study are listed in Table 1. Bacteria

were grown in brain heart infusion (BHI) medium with shaking at 200 rpm in tubes at 37°C. *E. coli* cells were grown in LB broth. When required, antibiotics were added (chloramphenicol at 35 μg/ml for *E. coli* or 7 μg/ml for *L. monocytogenes*). The tissue culture cells used in this study were from the RAW264.7 (BALB/c mouse macrophage cells; ATCC TIB-71), HD11 (avian macrophage cell line [26]), and Caco-2 (ATCC HTB-37) lines. Cells were maintained in Dulbecco's modified Eagle's medium (DMEM) (Gibco) with 2 mM GlutaMAX (4 mM for RAW264.7 cells) supplemented with 10% (20% for Caco-2) (vol/vol) fetal calf serum (BioWest). Cells were grown at 37°C with 10% CO_2.

Mutant construction. To construct *L. monocytogenes* F2365 Δ*hly*, fragments containing 500 bp DNA flanking the open reading frames (ORFs) of *hly* were amplified by PCR and cloned into the suicide integrative vector pMAD as previously described (see Table S2 in the supplemental material) (27). The F2365 PrfA* mutant strain was designed inserting a point mutation (G145S) in PrfA, which rendered it constitutively active. The prfA*-A/prfA*-B and prfA*-C/prfA*-D (Table S2) oligonucleotides were designed to introduce a silent mutation in Cys144 (codon TGC→TGT) and a missense mutation in Gly145 changing it to Ser145 (codon GGT→TCT). The DNA fragment generated after splicing by overlap extension (SOEing) PCR was inserted into pMAD.

L. monocytogenes F2365 has a premature stop codon in *inlB* (codon no. 34 is TAA) (28). To facilitate *in vitro* cell infection and imaging, we generated an *L. monocytogenes* F2365 strain with a functional *inlB* (*L. monocytogenes* F2365^{InlB}) by introducing a point mutation in codon 34 (TAA→CAA). The oligonucleotides InlB-new-A/InlB-new-B and InlB-new-C/InlB-new-D (Table S2) were used in SOEing PCR, and the PCR fragment was also cloned into pMAD.

To construct *L. monocytogenes* F2365 Δ*hly*(pHELP::*llsA*), we electroporated *L. monocytogenes* F2365 Δ*hly* with pMAD containing the promoter pHELP fused between two 500-nucleotide (nt) DNA fragments flanking the start codon of *llsA* (BUG3801 [4]). To construct the *L. monocytogenes* Δ*llsA* PrfA* strain, we electroporated *L. monocytogenes* F2365 PrfA*with pMAD-llsA from BUG3751 (4). Mutagenesis was performed by double recombination as described previously (27).

Bacterial cocultures and electron microscopy. Coculture assays of *L. monocytogenes* and *L. lactis* (Institut Pasteur Collection CIP 70.56T) were performed for 24 h in 6% O_2 as previously described (4). At 3, 6, 9, and 24 h, part of the coculture was fixed for transmission electron microscopy, and another part of the culture was used to determine viable CFU on BHI agar plates. For biosafety reasons, bacterial strains or cocultures were inactivated by fixation with 2% glutaraldehyde (Sigma-Aldritch) in PHEM (PIPES-HEPES-EGTA-$MgSO_4 \cdot 7H_2O$) buffer at pH 7.1. After inactivation, cells were washed with PHEM buffer and centrifuged. The pellet was resuspended in a small volume of PHEM buffer, and this suspension was taken up in capillary tubes (Wohlwendt Engineering) as described previously (29). The filled tube was separated by clamping into segments of less than 2 mm and placed into the 200-μm deep cavity of an aluminum planchette, type A (Wohlwendt Engineering) filled with 1-hexadecene. With the flat side of the complementary type B planchette, the filled planchette was closed and frozen with the HPM 010 (Abra fluid).

Freeze substitution was performed in anhydrous acetone containing 1% osmium tetroxide (Merck). 1-Hexadecene is insoluble at −90°C in dry acetone. To allow access of the substitution mix to the sample, small cracks were introduced under liquid nitrogen in the solid hexadecene by application of gentle pressure using a precooled fine-point forceps (Dumont). Substitution was carried out at −90°C for 24 h, at −30°C for 12 h, and at 0°C for 1 h each in a freeze substitution device FS8500 (RMC). Next, the samples were washed with dry acetone and embedded stepwise in Epon (29). After heat polymerization, thin sections were cut with a UC6 microtome (Leica Microsystems, Inc.). Sections were collected on 200-mesh Formvar-coated cupper grids and poststained with 4% aqueous uranyl acetate and Reynold's lead citrate. Images were taken at 120 kV with a Tecnai G2 transmission electron microscope (FEI) equipped with a US4000 camera (Gatan, Inc.).

Blood hemolysis assay on agar plates. Hemolysis was assessed by streaking 10 μl of frozen bacterial cultures to isolate single colonies onto BHI agar plus 5% mouse (BALB/c) or human blood (French National Blood Service) and incubating the cultures for 24 h at 37°C.

Live imaging of blood hemolysis. Fresh whole human blood (French National Blood Service) was centrifuged (2,000 × *g*, 10 min, 4°C). Three components were obtained at this stage: (i) the upper phase, a clear solution of blood plasma; (ii) a middle thin layer of platelets and leukocytes; and (iii) at the bottom RBCs. RBCs were collected and washed twice in cold 1× Dulbecco's PBS (DPBS; Gibco). An equivalent MOI of 40 bacteria was incubated with 2 ml of RBC suspension (≈10,000 RBCs) in 35-mm petri dishes (MatTek) at 37°C. Bacterial overnight cultures were directly added to the petri dishes during microscopy acquisition. Live-cell imaging was performed during 60 min on a Zeiss Axio Observer spinning-disk confocal microscope equipped with a 63×oil objective and driven by the MetaMorph software. Images were acquired every 5 s for 60 min. One hundred RBCs were counted for hemolysis for each of the strains tested during the duration of the experiment. Three independent experiments were performed.

Whole-blood killing assays. Fresh human whole blood (French National Blood Service) was diluted 1/5 into RPMI, and 96-well tissue culture plates were seeded with 100 μl of this suspension. The *L. monocytogenes* strains were grown overnight in BHI, washed in PBS, and diluted in RPMI medium. A total of 5×10^4 bacteria were added per well. The mixture of bacteria and blood was incubated at 37°C for 2, 4, and 24 h. The number of *L. monocytogenes* survivors was determined by serial dilution and colony counting on BHI agar plates. The experiments were repeated with blood from three independent human donors. Six technical replicates per bacterial strain and per blood donor were performed using independently derived clones of each of the strains. Statistical analyses were performed using the Student's *t* test.

Cell infection. Prior to infection, 96-well tissue culture plates were seeded with cells to attain 80% confluence on the day of infection. Overnight cultures of bacterial strains were washed three times in PBS and resuspended in infection medium (1% fetal bovine serum [FBS]) at an MOI of 2 (RAW264.7 and HD11) or 5 (Caco-2). Cells were centrifuged for 1 min at 1,000 rpm to synchronize infection. The cells were then incubated with the bacteria for 1 h at 37°C. Following this incubation, the cells were washed, and extracellular bacteria were neutralized by adding complete medium containing 40 μg/ml of gentamicin. At 2, 6, or 24 h postinfection, cells were washed with PBS and finally lysed in distilled water containing 0.1% Triton X-100. The number of viable intracellular *L. monocytogenes* cells was calculated by serial dilution and colony counting on BHI agar plates. These experiments employed 6 technical replicates per bacterial strain and were repeated three times with independent clones of each of the strains. Statistical analyses were conducted by using the Student's *t* test.

Cytotoxicity LDH release assays and cytokine measurements. RAW264.7 and Caco-2 cells were infected as indicated in the previous paragraph for 24 h (washed after 1 h of infection and with 40 μg/ml gentamicin added to kill extracellular bacteria) where the supernatant was recovered and filtered. LDH levels were assayed with the kit LDH BR (Linear Chemicals) according to the kit instructions. Supernatants from RAW264.7 cells were also used to measure cytokine levels by using the cytokine array kit (Proteome Profiler mouse XL cytokine array; Becton, Dickinson) according to the manufacturer's instructions.

Vacuolar escape. RAW264.7 cells were infected as indicated in the previous paragraphs for 6 h (washed after 1 h of infection and with 40 μg/ml gentamicin added to kill extracellular bacteria) and fixed with a paraformaldehyde (PFA) solution (4% in PBS) for 15 min at room temperature. Extracellular *L. monocytogenes* cells were labeled with a primary polyclonal goat anti-*Listeria* serum and with a secondary chicken anti-goat Alexa 647. Next, cells were permeabilized using 0.1% Triton X-100 for 4 min at room temperature, and total *L. monocytogenes* cells were labeled with the same primary antibody and a secondary chicken anti-goat Alexa 488 antibody. Actin was labeled by using phalloidin conjugated to Alexa 546. Nuclei were stained with Hoechst 33342 (dilution, 1/1,000). Samples were then rinsed four times in PBS and examined with a Zeiss Axiovert 135 epifluorescence microscope (Carl Zeiss, Inc.) associated with a charge-coupled device (CCD) camera. Images were obtained with a ×63 oil immersion objective and processed with MetaMorph software (Universal Imaging). Cytosolic bacteria were considered those stained with the Alexa 546 and Alexa 488 antibody but lacking Alexa 647 antibody labeling. Approximately 100 cells were counted in 3 representative fields to estimate the number of cytosolic *L. monocytogenes* cells.

Evaluation of *llsA* promoter expression with a GFP and a luciferase reporter system. A transcriptional fusion of the *llsA* promoter was created by cloning 500 bp upstream of the ATG of the respective gene with the gene encoding GFP-mut2 (30) (generating P*llsA*-GFP). This construct was cloned into SalI/SmaI-digested pAD vector (generating pAD-P*llsA*-GFP). Gene synthesis to construct P*llsA*-GFP was produced by Genecust (Luxembourg). pAD-P*llsA*-GFP was electroporated into *L. monocytogenes* F2365$^{\mathrm{InlB}}$. *hly* was used as a control gene, the expression of which is upregulated during infection of eukaryotic cells. The transcriptional fusion of the promoter of *hly* to GFP-mut 2 (pAD-P*hly*-GFP) was also cloned into *L. monocytogenes* F2365$^{\mathrm{InlB}}$.

For epifluorescence analysis of promoter activity, RAW264.7 and Caco-2 cells were infected for 6 h (washed after 1 h of infection and with 40 μg/ml gentamicin added) fixed with a PFA solution (4% in PBS) for 15 min at room temperature, and permeabilized (0.1% Triton X-100 for 3 min in PBS). Samples were then rinsed four times in PBS, incubated with Hoechst and phalloidin conjugated to Alexa 546 for 30 min at room temperature, and rinsed four times in PBS. Samples were examined with a Zeiss Axiovert 135 epifluorescence microscope (Carl Zeiss, Inc.) associated with a charge-coupled device (CCD) camera. Images were obtained with a ×63 oil immersion objective and processed with MetaMorph software (Universal Imaging).

For *in vivo* bioluminescence experiments, 8-week-old female BALB/c mice were infected by intravenous inoculation with 10^4 *L. monocytogenes* F2365$^{\mathit{llsA::lux}}$ (BUG3763) cells grown in BHI broth to an optical density (OD) of 1.0 at 37°C. Bioluminescence imaging was accomplished using an IVIS Spectrum *in vivo* imaging system (Perkin Elmer) with a 5-min exposure time. Mice were anesthetized with isoflurane. For CFU determinations, whole luminal contents from stomach, small intestine, cecum, and colon, as well as tissues from stomach, small intestine, cecum and colon, liver, and spleen, were obtained, homogenized, and serially diluted and plated on Oxford agar plates (Oxoid). In order to determine the CFU numbers in the tissues of the gastrointestinal system, the tissues were washed three times in DMEM, incubated for 2 h in DMEM supplemented with 40 μg/ml gentamicin, and finally washed three times in DMEM.

Mouse infections. Six- to 8-week-old female BALB/c mice (Charles River, Inc., France) were injected intravenously with 10^4 CFU of the indicated strain. Mice were sacrificed at 48 h after infection (four mice in each group), and livers and spleens were removed. Half of the organ was used to assess bacterial load, and the other half was used for histological analysis. To assess bacterial load, organs were homogenized and serially diluted. Dilutions were plated onto BHI plates and grown during 24 h at 37°C. Colonies were counted to assess bacterial load per organ. RBC and hemoglobin counts were determined using a Horiba scil Vet abc Plus veterinary hematology blood analyzer. Two independent experiments were carried out. Statistically significant differences were evaluated by the Mann-Whitney test. Pearson's correlation coefficients were computed to measure correlations between blood parameters and *L. monocytogenes* CFU in blood.

Histological analysis. Liver and spleen tissue sections from mice intravenously infected with the F2365 WT, Δ*llsA*, and Δ*llsA* complemented strains sacrificed at 48 h were fixed in 10% neutral buffered formalin and routinely processed for the histopathological analysis. Four-micrometer sections per organ were stained with hematoxylin and eosin (H&E). The number of necrotic foci and the main cell type

infiltrating necrotic areas were recorded. All of the slides were internally coded and analyzed blind. Statistically significant differences were evaluated by the Mann-Whitney test.

Ethics statement. This study was carried out in strict accordance with the French national and European laws and conformed to the Council Directive on the approximation of laws, regulations, and administrative provisions of the Member States regarding the protection of animals used for experimental and other scientific purposes (86/609/Eec). Experiments that relied on laboratory animals were performed in strict accordance with the Institut Pasteur's regulations for animal care and use protocol, which was approved by the Animal Experiment Committee of the Institut Pasteur (approval no. 03-49). All human blood samples were anonymized and collected from the French National Blood Service under IRB approval no. HS2008-3470.

SUPPLEMENTAL MATERIAL

Supplemental material for this article may be found at https://doi.org/10.1128/mBio.00259-17.

FIG S1, EPS file, 0.5 MB.

FIG S2, EPS file, 3 MB.

FIG S3, EPS file, 5.2 MB.

FIG S4, EPS file, 5.3 MB.

TABLE S1, DOC file, 0.1 MB.

TABLE S2, DOC file, 0.1 MB.

ACKNOWLEDGMENTS

We thank Esteban Chaves-Olarte for logistical support. P.C. is an International Senior Research Scholar of the Howard Hughes Medical Institute. The authors declare no conflict of interest.

This work was supported by the Institut Pasteur, the Institut National de la Santé et de la Recherche Médicale (INSERM Unité 604), the Institut National de la Recherche Agronomique (INRA Unité Sous Contrat 2020), Université Paris Diderot, grants from Région Île-de-France, the Institut Pasteur "Programmes Transversaux de Recherche" (PTR521 to J.P.C.), Agence Nationale de la Recherché (ANR-15-CE15-0017 StopBugEntry to J.P.C.), Fondation Le Roch Les Mousquetaires, European Research Council Advanced grant (670823 BacCellEpi to P.C.), and Région Île-de-France (DIM-MALINF to J.M.T.). The funders had no role in study design, data collection and interpretation, or the decision to submit the work for publication.

REFERENCES

1. Cossart P. 2011. Illuminating the landscape of host-pathogen interactions with the bacterium Listeria monocytogenes. Proc Natl Acad Sci U S A 108:19484–19491. https://doi.org/10.1073/pnas.1112371108.
2. Quereda JJ, García-Del Portillo F, Pucciarelli MG. 16 April 2016. Listeria monocytogenes remodels the cell surface in the blood-stage. Environ Microbiol Rep https://doi.org/10.1111/1758-2229.12416.
3. Cotter PD, Draper LA, Lawton EM, Daly KM, Groeger DS, Casey PG, Ross RP, Hill C. 2008. Listeriolysin S, a novel peptide haemolysin associated with a subset of lineage I Listeria monocytogenes. PLoS Pathog 4:e1000144. https://doi.org/10.1371/journal.ppat.1000144.
4. Quereda JJ, Dussurget O, Nahori MA, Ghozlane A, Volant S, Dillies MA, Regnault B, Kennedy S, Mondot S, Villoing B, Cossart P, Pizarro-Cerda J. 2016. Bacteriocin from epidemic Listeria strains alters the host intestinal microbiota to favor infection. Proc Natl Acad Sci U S A 113:5706–5711. https://doi.org/10.1073/pnas.1523899113.
5. Quereda JJ, Cossart P, Pizarro-Cerdá J. 7 September 2016. Role of Listeria monocytogenes exotoxins in virulence. Microb Toxins https://doi.org/10.1007/978-94-007-6725-6_24-1.
6. Molloy EM, Cotter PD, Hill C, Mitchell DA, Ross RP. 2011. Streptolysin S-like virulence factors: the continuing sagA. Nat Rev Microbiol 9:670–681. https://doi.org/10.1038/nrmicro2624.
7. Lee SW, Mitchell DA, Markley AL, Hensler ME, Gonzalez D, Wohlrab A, Dorrestein PC, Nizet V, Dixon JE. 2008. Discovery of a widely distributed toxin biosynthetic gene cluster. Proc Natl Acad Sci U S A 105:5879–5884. https://doi.org/10.1073/pnas.0801338105.
8. Alouf JE. 1980. Streptococcal toxins (streptolysin O, streptolysin S, erythrogenic toxin). Pharmacol Ther 11:661–717. https://doi.org/10.1016/0163-7258(80)90045-5.
9. Higashi DL, Biais N, Donahue DL, Mayfield JA, Tessier CR, Rodriguez K, Ashfeld BL, Luchetti J, Ploplis VA, Castellino FJ, Lee SW. 2016. Activation of band 3 mediates group A Streptococcus streptolysin S-based beta-haemolysis. Nat Microbiol 1:15004. https://doi.org/10.1038/nmicrobiol.2015.4.
10. Datta V, Myskowski SM, Kwinn LA, Chiem DN, Varki N, Kansal RG, Kotb M, Nizet V. 2005. Mutational analysis of the group A streptococcal operon encoding streptolysin S and its virulence role in invasive infection. Mol Microbiol 56:681–695. https://doi.org/10.1111/j.1365-2958.2005.04583.x.
11. Goldmann O, Sastalla I, Wos-Oxley M, Rohde M, Medina E. 2009. Streptococcus pyogenes induces oncosis in macrophages through the activation of an inflammatory programmed cell death pathway. Cell Microbiol 11:138–155. https://doi.org/10.1111/j.1462-5822.2008.01245.x.
12. Mitchell DA, Lee SW, Pence MA, Markley AL, Limm JD, Nizet V, Dixon JE. 2009. Structural and functional dissection of the heterocyclic peptide cytotoxin streptolysin S. J Biol Chem 284:13004–13012. https://doi.org/10.1074/jbc.M900802200.
13. Gonzalez DJ, Lee SW, Hensler ME, Markley AL, Dahesh S, Mitchell DA, Bandeira N, Nizet V, Dixon JE, Dorrestein PC. 2010. Clostridiolysin S, a post-translationally modified biotoxin from Clostridium botulinum. J Biol Chem 285:28220–28228. https://doi.org/10.1074/jbc.M110.118554.
14. Molloy EM, Casjens SR, Cox CL, Maxson T, Ethridge NA, Margos G, Fingerle V, Mitchell DA. 2015. Identification of the minimal cytolytic unit for streptolysin S and an expansion of the toxin family. BMC Microbiol 15:141. https://doi.org/10.1186/s12866-015-0464-y.
15. Flaherty RA, Puricelli JM, Higashi DL, Park CJ, Lee SW. 2015. Streptolysin S promotes programmed cell death and enhances inflammatory signaling in epithelial keratinocytes during group A Streptococcus

infection. Infect Immun 83:4118–4133. https://doi.org/10.1128/IAI.00611-15.
16. Stavru F, Archambaud C, Cossart P. 2011. Cell biology and immunology of *Listeria monocytogenes* infections: novel insights. Immunol Rev 240:160–184. https://doi.org/10.1111/j.1600-065X.2010.00993.x.
17. Guinane CM, Piper C, Draper LA, O'Connor PM, Hill C, Ross RP, Cotter PD. 2015. Impact of environmental factors on bacteriocin promoter activity in gut-derived Lactobacillus salivarius. Appl Environ Microbiol 81:7851–7859. https://doi.org/10.1128/AEM.02339-15.
18. Betschel SD, Borgia SM, Barg NL, Low DE, De Azavedo JC. 1998. Reduced virulence of group A streptococcal Tn916 mutants that do not produce streptolysin S. Infect Immun 66:1671–1679.
19. Fontaine MC, Lee JJ, Kehoe MA. 2003. Combined contributions of streptolysin O and streptolysin S to virulence of serotype M5 Streptococcus pyogenes strain Manfredo. Infect Immun 71:3857–3865. https://doi.org/10.1128/IAI.71.7.3857-3865.2003.
20. Engleberg NC, Heath A, Vardaman K, DiRita VJ. 2004. Contribution of CsrR-regulated virulence factors to the progress and outcome of murine skin infections by Streptococcus pyogenes. Infect Immun 72:623–628. https://doi.org/10.1128/IAI.72.2.623-628.2004.
21. Maury MM, Tsai YH, Charlier C, Touchon M, Chenal-Francisque V, Leclercq A, Criscuolo A, Gaultier C, Roussel S, Brisabois A, Disson O, Rocha EP, Brisse S, Lecuit M. 2016. Uncovering Listeria monocytogenes hypervirulence by harnessing its biodiversity. Nat Genet 48:308–313. https://doi.org/10.1038/ng.3501.
22. Moura A, Criscuolo A, Pouseele H, Maury MM, Leclercq A, Tarr C, Björkman JT, Dallman T, Reimer A, Enouf V, Larsonneur E, Carleton H, Bracq-Dieye H, Katz LS, Jones L, Touchon M, Tourdjman M, Walker M, Stroika S, Cantinelli T, Chenal-Francisque V, Kucerova Z, Rocha EP, Nadon C, Grant K, Nielsen EM, Pot B, Gerner-Smidt P, Lecuit M, Brisse S. 2016. Whole genome-based population biology and epidemiological surveillance of Listeria monocytogenes. Nat Microbiol 2:16185. https://doi.org/10.1038/nmicrobiol.2016.185.
23. Briones V, Blanco MM, Marco A, Prats N, Fernández-Garayzábal JF, Suárez G, Domingo M, Domínguez L. 1992. Biliary excretion as possible origin of Listeria monocytogenes in fecal carriers. Am J Vet Res 53:191–193.
24. Hardy J, Margolis JJ, Contag CH. 2006. Induced biliary excretion of Listeria monocytogenes. Infect Immun 74:1819–1827. https://doi.org/10.1128/IAI.74.3.1819-1827.2006.
25. Linnan MJ, Mascola L, Lou XD, Goulet V, May S, Salminen C, Hird DW, Yonekura ML, Hayes P, Weaver R, Audurier A, Plikaytis BD, Fannin SL, Kleks A, Broome CV. 1988. Epidemic listeriosis associated with Mexican-style cheese. N Engl J Med 319:823–828. https://doi.org/10.1056/NEJM198809293191303.
26. Beug H, von Kirchbach A, Döderlein G, Conscience JF, Graf T. 1979. Chicken hematopoietic cells transformed by seven strains of defective avian leukemia viruses display three distinct phenotypes of differentiation. Cell 18:375–390. https://doi.org/10.1016/0092-8674(79)90057-6.
27. Arnaud M, Chastanet A, Débarbouillé M. 2004. New vector for efficient allelic replacement in naturally nontransformable, low-GC-content, Gram-positive bacteria. Appl Environ Microbiol 70:6887–6891. https://doi.org/10.1128/AEM.70.11.6887-6891.2004.
28. Nightingale KK, Milillo SR, Ivy RA, Ho AJ, Oliver HF, Wiedmann M. 2007. Listeria monocytogenes F2365 carries several authentic mutations potentially leading to truncated gene products, including inlB, and demonstrates atypical phenotypic characteristics. J Food Prot 70:482–488. https://doi.org/10.4315/0362-028X-70.2.482.
29. Hohenberg H, Mannweiler K, Müller M. 1994. High-pressure freezing of cell suspensions in cellulose capillary tubes. J Microsc 175:34–43. https://doi.org/10.1111/j.1365-2818.1994.tb04785.x.
30. Balestrino D, Hamon MA, Dortet L, Nahori MA, Pizarro-Cerda J, Alignani D, Dussurget O, Cossart P, Toledo-Arana A. 2010. Single-cell techniques using chromosomally tagged fluorescent bacteria to study Listeria monocytogenes infection processes. Appl Environ Microbiol 76:3625–3636. https://doi.org/10.1128/AEM.02612-09.

PART II: Characterization of LLS mechanisms of action

LLS is a weak hemolytic factor that does not display cytotoxic effects on epithelial or phagocytic eukaryotic cells, that does not induce specific immune cell responses, and that has no impact on cellular infection by *L. monocytogenes* (319). Instead, LLS is a bacteriocin that targets Gram-positive bacteria *in vitro* including *L. lactis* as well as hypo-virulent *Lm* strains, and promotes intestinal colonization by *Lm in vivo* through modulation of the host gut microbiota composition (308, 309).

Our aim was to study the LLS transfer mechanism from LLS-producer to LLS-target bacteria, to characterize the LLS bactericidal mechanism(s) in target bacteria, to identify molecular targets or receptors of LLS in target bacteria, and to characterize additional bacterial species that are sensitive to the LLS bactericidal mechanism(s).

2.1 Results

2.1.1 LLS is a contact-dependent inhibition bacteriocin that impairs cell membrane integrity

TOMMs use diverse mechanisms to target other bacterial species. MccB17 inhibits the DNA gyrase activity (219), plantazolicin targets the cell membrane (207), klebsazolicin inhibits the ribosome by obstructing the peptide exit tunnel (167), phazolicin binds to the 23S rRNA and inhibits translation (168). Some bacteriocins also present a dual mechanism of action. For example, nisin binds to the lipid II peptidoglycan precursor and inhibits peptidoglycan formation, but it also inserts into the bacterial membrane to induce pore formation (324).

To characterize the mechanism of LLS transfer to target bacteria and its bactericidal function, we investigated its subcellular distribution in LLS-producer bacteria by using subcellular fractionation and transmission electron microscopy. Then, we characterize the specific conditions required for LLS-producer bacteria to display bactericidal activity by applying trans-well co-culture systems and microfluidic-coupled microscopy. We then propose a mechanism used by LLS to kill target bacteria. The results obtained are under review in the scientific journal PNAS, where I figured as first author.

In this work, we identified that LLS remains associated to the cell membrane and cytoplasm of producer bacteria, and is not secreted in the bacterial extracellular space. Only living LLS-producer bacteria (and not purified LLS-positive bacterial membranes) display bactericidal activity. We determined that LLS requires direct contact between LLS-producer and target bacteria in order to display bactericidal activity and thus is a contact-dependent bacteriocin. Moreover, we demonstrate that contact-dependent exposure to LLS leads to permeabilization of the target bacterial cell membrane. Finally, we show that a net increase in surface negative charges of target bacteria augments the susceptibility to LLS. Overall, our results demonstrate that LLS is the first TOMM that displays a contact-dependent inhibition mechanism.

PNAS
www.pnas.org

Main Manuscript for

Listeriolysin S is a contact-dependent inhibition bacteriocin from *Listeria monocytogenes* that impairs cell membrane integrity

Jazmin Meza-Torres[1,2,3], Juan J Quereda[4], Martin Sachse[5], Giulia Manina[6], Dmitry Ershov[7,8], Jean Yves Tinevez[7], Lilliana Radoshevich[9], Claire Maudet[10], Marc Lecuit[3,10,11,12], Olivier Dussurget[1,3], Pascale Cossart[2] & Javier Pizarro-Cerdá[1*]

[1]Yersinia Unit, Microbiology Department, Institut Pasteur, Paris, France

[2]Bacteria-Cell Interactions Unit, Cell Biology and Infection Department, Institut Pasteur, Paris, France

[3]Université de Paris, Sorbonne Paris Cité, Paris, France

[4]Departamento Producción y Sanidad Animal, Salud Pública Veterinaria y Ciencia y Tecnología de los Alimentos, Facultad de Veterinaria, Universidad Cardenal Herrera-CEU, CEU Universities Valencia, Spain

[5]Ultrastructural BioImaging, Institut Pasteur, Paris, France

[6]Microbial Individuality and Infection Group, Cell Biology and Infection Department, Institut Pasteur, Paris, France

[7]Image Analysis Hub, Cell Biology and Infection Department, Institut Pasteur, Paris, France
[8]Bioinformatics and Biostatistics HUB – Departement of Computational Biology, Institut Pasteur, USR 3756 CNRS, Paris, France

[9]Department of Microbiology and Immunology, University of Iowa, Iowa City, Iowa, USA

[10]Biology of Infection Unit, INSERM Unité 1117, Institut Pasteur, Paris, France

[11]Division of Infectious Diseases and Tropical Medicine, Necker-Enfants Malades University Hospital, Assistance Publique-Hôpitaux de Paris, Paris, France

[12]Institut Imagine, Paris, France

*Javier Pizarro-Cerdá

Email: javier.pizarro-cerda@pasteur.fr

Classification
Biological Sciences
Microbiology

Keywords
Listeriolysin S (LLS), bacteriocin, *Listeria monocytogenes*, contact-dependent inhibition, microfluidic microscopy

Author Contributions
JMT, JJQ, PC, OD, and JPC designed research. JMT, MS, GM, LR, CM and ML performed research. JMT, MS, GM, JPC, DE, and JYT analyzed data. JMT and JPC wrote the paper.

This PDF file includes:
Main Text
Figures 1 to 6

Abstract

Listeriolysin S (LLS) is a thiazole/oxazole modified microcin (TOMM) produced by hyper-virulent clones of *Listeria monocytogenes*. LLS targets specific Gram-positive bacteria and modulates the host intestinal microbiota composition. To characterize the mechanism of LLS transfer to target bacteria and its bactericidal function, we first investigated its subcellular distribution in LLS-producer bacteria. Using subcellular fractionation assays and transmission electron microscopy, we identified that LLS remains associated with the bacterial cell membrane and cytoplasm, and is not secreted in the bacterial extracellular space. Only living LLS-producer bacteria (and not purified LLS-positive bacterial membranes) display bactericidal activity. Applying trans-well co-culture systems and microfluidic-coupled microscopy, we determined that LLS requires direct contact between LLS-producer and target bacteria in order to display bactericidal activity and thus is indeed a contact-dependent bacteriocin. Moreover, we demonstrate that contact-dependent exposure to LLS leads to permeabilization of the target bacterial cell membrane. Finally, we show that a net increase in bacterial surface negative charges augments the susceptibility to LLS. Overall, our results demonstrate that LLS is the first TOMM that displays a contact-dependent inhibition mechanism.

Significance Statement

Listeria monocytogenes (*Lm*) is a bacterial pathogen that causes listeriosis, a foodborne disease characterized by gastroenteritis, meningitis, bacteremia, and abortions in pregnant women. The most severe human listeriosis outbreaks are associated with a subset of *Lm* hyper-virulent clones that encode a bacteriocin, which

modifies the gut microbiota and allows efficient *Lm* gut colonization and invasion of deeper organs. Our present work clarifies the killing mechanism displayed by this bacteriocin to outcompete gut commensal bacteria, demonstrating that it induces the membrane permeabilization of target bacteria. Moreover, we show that this is the first thiazole-oxazole modified microcin that displays a contact-dependent inhibition mechanism.

Main Text

Introduction

Listeria monocytogenes (*Lm*) is a Gram-positive food-borne pathogen responsible for listeriosis, a disease characterized by meningitis in the newborn, bacteremia in immunocompromised or elderly individuals, and abortions in pregnant women (1, 2). To date, the most severe human listeriosis outbreaks have been associated with a subset of *Lm* lineage I strains (3, 4). These hyper-virulent strains harbor a biosynthetic gene cluster that encodes for the small peptide Listeriolysin S (LLS) (3, 5). Though initially proposed to be a virulence factor via its hemolytic activity (3), it has since been shown that LLS is a weak hemolytic factor that does not display cytotoxic effects on eukaryotic cells, that does not induce specific immune cell responses, and that has no impact on cellular infection by *Lm* (6). Instead, LLS is a bacteriocin that targets Gram-positive bacteria *in vitro* including *Lactococcus lactis* as well as hypo-virulent *Lm* strains, and promotes intestinal colonization by *Lm in vivo* through modulation of the host gut microbiota composition (7, 8).

Biosynthetic gene clusters similar to the LLS operon are widely conserved in different bacterial phyla (9). They encode for: (1) a pro-peptide (unmodified toxin), (2) an ABC transporter that exports the toxin once it is post-translationally modified, (3) an immunity protein, and (4) an enzymatic complex that allows the post-translational modification of the toxin with thiazole, oxazole and/or methyl-oxazole heterocycles (10). This family of thiazole/oxazole-modified microcins (TOMMs) includes microcin B17 (MccB17) from *Escherichia coli*, streptolysin S (SLS) from *Streptococcus pyogenes* and plantazolicin (PZN) from *Bacillus methylotropicus* (10–12). MccB17 is an antimicrobial peptide that targets *E. coli* and acts as a DNA gyrase inhibitor (13), while PZN displays narrow activity against *B. anthracis* through bacterial membrane depolarization and association to cardiolipin micro-domains (11). In contrast, SLS is a

major cytotoxic and hemolytic virulence factor produced by group A *Streptococcus pyogenes* (GAS) (14, 15), which targets erythrocytes, leucocytes, platelets, subcellular organelles, and can display lytic activity against bacterial protoplasts (16–19).

We have previously shown that LLS kills specific Gram-positive bacteria (7) but its mechanism of action remains unknown. In the present study, we demonstrate that LLS remains associated to the bacterial cell membrane of LLS-producer bacteria, and exerts its killing mechanism via direct contact between LLS-producer and target bacteria, impairing the membrane integrity of target bacteria. Our previous findings demonstrate that LLS play a key role in the modulation of the host microbiota by *Lm* hyper-virulent strains. Our present work clarifies the specific mechanism used by *Lm* to interact and outcompete bacteria by means of LLS in a CDI manner.

Results

LLS is associated to the cell membrane of LLS-producer bacteria

We have previously demonstrated that LLS is not expressed *in vitro,* and that its production is detected only *in vivo* within the intestine of infected animals (7). In order to identify *in vitro* conditions that mimic the intestinal environment leading to LLS expression, we performed a screen exposing the *Lm* F2365 strain to libraries of molecules that mimic or are homologous to components present in the gastrointestinal tract, and we monitored LLS expression using a GFP fluorescent reporter. We also performed co-cultures of *Lm* F2365 with previously identified target bacterial species to explore whether target bacteria could be the LLS activating signal. Unfortunately, we did not find any molecule or condition that triggers LLS production *in vitro* (data not shown). Therefore, for the assessment of LLS activity, we introduced the constitutive promoter pHELP upstream of the LLS operon in the F2365 strain, as previously reported (3). The strain F2365: pHELP (designated as LLS^+) significantly expresses all the genes of the LLS operon (Fig. S1).

Production of antibodies against the biologically functional LLS represents a challenge due to the putative post-translational modifications of the mature LLS form and to its small size. Therefore, in order to label LLS we made a tag-protein fusion with FLAG and HA tags at its C-terminal region in the LLS^+ background strain (7). We confirmed that LLS^+-FLAG and LLS^+-HA constructs are fully functional, since they retain

bactericidal activity against target bacteria (Fig. S2A) and display weak hemolytic activity comparable to that of the parental strain (Fig. S2B). To study LLS distribution within bacteria and in the extracellular environment, we performed a fractionation experiment as previously described (20), leading to the separation of the bacterial cytoplasm, membrane and cell wall as well as the supernatant. An LLS$^+$ strain without FLAG or HA tags was used as a negative control (Fig. 1A and Fig. S2C). Our results clearly demonstrate that in our growth conditions LLS is detected only in the bacterial cell membrane and in the cytoplasm, and is neither secreted in the supernatant nor associated with the bacterial cell wall (Fig. 1A). In the cytoplasm, we detect a band of approximately 6 kDa corresponding to the expected molecular weight of a monomeric tagged LLS pro-peptide, but we also detect a higher molecular weight smear (between 50 and 250 kDa) which we hypothesize to be the LLS post-translational heterocyclic molecule (Fig. 1A). This smear is observed using the LLS$^+$-FLAG and LLS$^+$-HA constructs (Fig. 1A and Fig. S2C), suggesting that it is specific for the LLS structure.

To investigate whether the high molecular weight smear corresponds to the LLS post-translational heterocyclic molecule, we performed a bacterial subcellular fractionation assay with the tagged and non-tagged LLS$^+$ strains upon deletion of the *llsB* gene, which encodes a putative subunit of the LLS post-translational machinery (3) and is required for the biological activity of LLS (6). The high molecular weight smear is indeed absent in the LLS$^+$-FLAGΔ*llsB* strain (Fig. S3A), suggesting that it corresponds to a heterocyclic active molecule of LLS that has been post-translationally modified. Interestingly, the 6 kDa band corresponding to the monomeric tagged LLS pro-peptide also disappears in the LLS$^+$-FLAGΔ*llsB* strain (Fig. S3A). To determine whether deletion of the *llsB* gene leads to polar effects, we performed a qPCR of the LLS operon genes in the tagged and non-tagged LLS$^+$ strains. The deletion of the *llsB* gene did not cause expression defects on the upstream or downstream genes of the operon (Fig. S3B), indicating that the *llsA* gene is normally transcribed, but in the absence of the fully functional post-translational machinery, the LLS pro-peptide could be degraded or unstable.

To determine whether LLS is not detected in the supernatant due to its very low abundance, we performed an immunoprecipitation assay to concentrate the supernatant of the LLS$^+$-FLAG strain. These data confirm the total absence of LLS in

the media and its presence in the membrane fraction only (Fig. 1B). To verify the LLS subcellular location, employing a different methodological approach, we performed transmission electron microscopy using anti-HA colloidal gold-coupled antibodies to identify the distribution of LLS in the LLS^+-HA strain. We confirmed that the LLS is detected in both membrane and cytoplasm of producer bacteria, and is absent from the bacterial cell wall (Fig. 1C and Fig.1D). Overall, our results indicate that LLS is not actively secreted in the extracellular space and it is primarily localized to the cell membrane, and to a lesser extent in the cytoplasmic compartment of LLS-producer bacteria.

LLS bactericidal activity requires cell-to-cell contact between LLS-producer and target bacteria

To understand the mechanism of LLS transfer between LLS-producer and target bacteria, we first assessed the potential bactericidal activity of LLS^+ fractions on *L. lactis*, which we previously demonstrated as LLS sensitive (7). We incubated *L. lactis* for 24h with supernatant, cell wall, membrane and cytoplasmic fractions isolated from LLS^+ bacteria. Surprisingly, none of these fractions displayed bactericidal activity on *L. lactis* (Fig. 2A).

Therefore, we suspected that LLS activity might be dependent on proximity or direct contact between producer and target bacteria. To evaluate whether LLS activity requires bacterial cell-to-cell contact, LLS^+ and *L. lactis* were co-cultivated using a trans-well system in which bacteria are separated by a porous membrane (Fig. 2B). We compared two different trans-well systems with different membrane pore sizes: 0.4 µm and 8 µm. The 0.4 µm membrane allows the diffusion of media and molecules secreted by the bacteria, while the 8 µm membrane allows bacterial passage through the pore and thus direct contact of whole bacteria. Interestingly, the bactericidal effect of LLS was exerted exclusively when using the 8 µm membrane system (Fig. 2B), suggesting that direct contact between LLS-producer and target bacteria is required for LLS bactericidal activity. Indeed, this activity was absent using the 0.4 µm system, or when target bacteria were incubated with the negative control strain LLS^- (pHELP:Δ*llsA*) (Fig. 2B), rejecting the alternative hypothesis that reduction of *L. lactis* numbers could be due instead to dilution of target bacteria through the 8 µm porous membrane.

In the above experiments, we cannot exclude the possibility that LLS could form high molecular weight aggregates that do not cross the 0.4 µm membranes. To rule out this possibility and to further characterize LLS killing effect on target bacteria, we performed single-cell time-lapse microscopy employing a microfluidic culture system (21). The microfluidic device allows us to image the growth of single cells over time, and also to trap bacteria between a membrane and a coverslip, eliminating the possibility of cell movement and creating a bacterial monolayer (Fig. 3A). In this system, we co-cultured the target *Lm* 10403S strain constitutively expressing the GFP (mut2 variation) (22) protein together with the LLS^+ (or the negative control LLS^-) bacteria constitutively expressing the tdTomato. We used 10403S bacteria as a target because the antagonistic effect of LLS was previously assessed in *in vitro* co-cultures using this strain (7), and also because the F2365 and the 10403S cells have a very similar growth rate (Fig. S4).

We imaged LLS-producer and target bacteria every 15 min for a period of 10 hours. To measure the fluorescence intensities, two masks were outlined around the microcolony profile of each strain, and a third mask was extracted as their intersection, here referred to as the signal region of interest (sROI) (Fig. 3A and see Materials and Methods). Interestingly, an increase in the GFP fluorescence was solely detected in the contact points between the producer (LLS^+ tdTomato) and the target (10403S GFP) bacteria, but not between the *ΔllsA* (LLS^- tdTomato) and the target bacteria (Fig. 3B and Fig. 3C). Furthermore, we observed that only when the target bacteria encounter the producer LLS^+ strain (and not the LLS^-), the producer bacteria dominate over time (Fig. 3D).

We hypothesized that the increase in the GFP fluorescence in the target bacteria could be attributed to the accumulation of the GFP protein inside cells, due to a halted bacterial growth. To confirm this hypothesis, time-lapse experiments were performed in the microfluidic device and images were taken every 8 minutes over a period of 10 h. The growth rate and doubling time were then measured from the resulting image sequences. Our results confirm that the bacterial growth is halted for target cells that are in direct contact with the LLS^+ bacteria (Fig. 4A). This is not observed when target bacteria are physically distant from producer cells, or when they are in contact with LLS^- (*ΔllsA*) bacteria (Fig. 4A), demonstrating that the growth arrest of target cells is

dependent upon direct contact with bacteria producing LLS. Indeed, the *k* constant for target cells in direct contact with the LLS^+ strain was 0.0097 min^{-1}, with an average doubling time of 110 min. In contrast, the *k* constant of target cells, either not in contact with producer cells or in contact with LLS^-, was 0.02 min^{-1}, with an average doubling time of 40 min, which is expected for healthy growing *L. monocytogenes* bacteria.

We also found that LLS-target cells in contact with LLS^+ producer cells are unable to divide, and shrink before experiencing lysis (Fig. 4A). Remarkably, LLS-target cells that had more than one LLS^+ producer cell surrounding them were more likely to arrest growth and to die (Fig. 4B). Together, our results demonstrate that the LLS exerts a contact and concentration dependent growth inhibition mechanism on target cells impeding their cell division.

LLS induces cell membrane permeabilization exclusively on target cells that are in direct contact with LLS-producer bacteria

To understand the molecular mechanisms underlying the LLS contact-dependent bactericidal activity, we investigated whether LLS could impair peptidoglycan structure or cell membrane integrity.

To investigate a potential impact of LLS on peptidoglycan, we performed click chemistry and flow cytometry analysis. Briefly, target cells (*L. lactis*) were incubated overnight with 3-Azido D-alanine (ADA) to allow its incorporation into the peptidoglycan and then target bacteria were washed and co-cultivated during 3 h or 5 h with LLS^- or LLS^+ *Lm*. After, target bacteria were labelled with click chemistry reaction (reactive with ADA) to analyse fluorescence intensity of target cells by flow cytometry. The fluorescence intensity of labelled target cells is proportional to the ADA incorporated into the peptidoglycan. The fluorescence intensity levels of target bacteria incubated with LLS^- or LLS^+ after 3 h or 5 h was equivalent (Fig. S5), suggesting that the peptidoglycan structure was intact and that LLS does not affect the integrity or structure of peptidoglycan.

To investigate whether LLS could modify cell membrane permeabilization, we carried out time-lapse microfluidic microscopy and added the SYTOX blue dye, which exclusively penetrates and stains cells that have lost their membrane integrity (23).

Since Brain Heart Infusion (BHI) quenches the SYTOX signal (data not shown), after the first 2 h of cell growth in BHI medium, we performed the perfusion of SYTOX with PBS, which stopped bacterial growth due to the lack of nutrients. Using this specific setup, we found that SYTOX exclusively stains 10403S target cells that are in direct contact with LLS^+ bacteria, whereas 10403S target cells that are not in contact with LLS producers remain unstained (Fig. 5A and Fig. 5B). Interestingly, once the producer and the target bacteria are in intimate contact, the LLS killing effect is not immediate and requires an incubation period from 1 to 2 h to take place after the addition of the SYTOX dye (Fig. 5B). This is consistent with timing of GFP accumulation in the target cells that are in direct contact with the LLS-producer cells (Fig. 3B and Fig. 3C), where the bactericidal effect also takes place from 1 to 2 h after the contact. Together our results demonstrate that LLS is a contact-dependent bacteriocin that prevents cell division and growth, leading to cell membrane permeabilization on target cells.

Bacterial surface charges determine susceptibility to LLS

The contact-dependent bactericidal activity of LLS lead us to the hypothesis that the charge of the bacterial surface could influence susceptibility to LLS. To test this hypothesis, we assessed the bactericidal effect of LLS on a *Lm* EGD strain, which lacks the LLS operon and we have previously shown to be sensitive to LLS (7), and on a EGD Δ*dltA* mutant. This mutant strain cannot modify its lipoteichoic acids (LTA) with D-alanine, and therefore displays higher surface electronegativity, as well as increased susceptibility to antimicrobial peptides that exclusively target the cell membrane or the cell membrane and the peptidoglycan (24, 25). The wild type EGD and the Δ*dltA* mutant were cocultured with LLS^+ or LLS^- bacteria for 24 h to evaluate their susceptibility to LLS activity. Both strains were found to be susceptible to LLS^+, however, the Δ*dltA* mutant showed an increased susceptibility to LLS compared to the wild type EGD strain (Fig. 6). This result confirmed that increased net negative surface charges increase susceptibility to LLS. Moreover, by establishing that surface properties can alter susceptibility to LLS in a parallel manner to antimicrobial peptides (24, 25), our results further support that LLS could be acting at the bacterial membrane.

Discussion

Human listeriosis outbreaks are often caused by hyper-virulent *Lm* lineage I strains characterized by the presence of the LLS biosynthetic cluster (3, 4). LLS belongs to the TOMM family, which are present in pathogenic and non-pathogenic bacteria (9) with a diversity of functions such as cytotoxins (10, 26) or bacteriocins (7, 11, 12). The conservation and evolution of these biosynthetic clusters suggest that they present an advantage for the survival of pathogenic and symbiotic bacteria in very specific and different niches. In the case of *Lm,* we previously demonstrated that the presence of the LLS biosynthetic cluster represents an advantage in the gastrointestinal tract through modulation of the host microbiota composition, facilitating the colonization of the intestinal niche to allow further invasion of deeper tissues (7). Interestingly, some non-pathogenic *Listeria innocua* strains possess the intact LLS gene cluster (27) which suggest that this bacteriocin could also provide an advantage in the environment (28). In the present work, we explored the molecular mechanisms of action of LLS. Our results demonstrate that LLS is primarily associated with the bacterial cell membrane, and to a lesser extent with the cytoplasmic compartment of LLS-producer bacteria. Also, LLS is not actively secreted in the environment by LLS producer bacteria. We showed that LLS is detected within LLS-producer bacteria as a monomeric unit (in the cytoplasm) and is also present as a high molecular weight smear (in the cytoplasm and in the cell membrane) that is dependent on putative post-translational modifications. We show that LLS bactericidal activity requires direct cell-to-cell contact between living LLS-producer cells and target bacteria, whereas LLS activity is absent from purified subcellular compartments. We demonstrate that LLS induces a delayed cell growth arrest in target bacteria as well as cell membrane permeabilization. Finally, we showed that bacterial surface charges determine susceptibility to LLS.

LLS is retained at the cell membrane of LLS-producer bacteria

We were able to demonstrate the association of LLS to the bacterial cell membrane and to the cytoplasmic compartment by applying subcellular fractionation assays as well as immunogold-labelling transmission electron microscopy (TEM). It is worth mentioning that our study represents the first time that a TOMM has been immunodetected, to the best of our knowledge.

To our surprise, LLS was not secreted in the culture media of LLS-producer cells, and bacterial fractions harboring the LLS are inactive. The existence of other cell-associated bacteriocins have been previously reported (29–31). For example, the bovicin HC5 is associated with the producer cell and could be extracted with NaCl, however the cell-associated molecule is more active and stable than the cell-free molecule (29). Other cell-associated bacteriocins have been reported to be recovered after acid extraction at pH 2 (31). Although a contact-dependent inhibition (CDI) mechanism was not reported for these bacteriocins, their extraction from the bacterial membrane and their purification could be performed without the loss of bactericidal activity. In the case of LLS, our unpublished results indicate that LLS bactericidal activity is lost when is extracted from the bacterial membrane using a carrier molecule.

To our knowledge, there is just one other report describing a bacteriocin that remains attached to the cell membrane of the producer bacteria and displays a CDI mechanism. The Gram-negative bacterium, *Caulobacter crescentus,* makes a two-protein bacteriocin called CdzC/CdzD*,* which forms insoluble aggregates that are retained on the outer membrane of producer cells and has a CDI mechanism against other bacteria that lack the immunity protein CdzI. This bacteriocin uses a type I secretion system, an adhesion system encoded elsewhere in the genome (32). However, this is a two-peptide bacteriocin that is completely unrelated to TOMMs, which highlights the novelty of the mechanism of action used by LLS for this family of bacteriocins, and more generally for bacteriocins in Gram-positive bacteria.

Interestingly, the cytotoxic molecule SLS from *S. pyogenes* is a TOMM that is exported through an ABC transporter system and remains bound to the bacterial cell surface (19, 33, 34). SLS remains active (cytotoxic and hemolytic) only when is associated to the cell membrane or when it is extracted with carrier molecules like LTA, α-lipoprotein, RNA-core, and non-ionic detergents (33, 35). The LLS supernatant is also non-hemolytic, and only when it is extracted with RNA-core it is capable of producing an hemolytic phenotype (3). It has been proposed that the SLS precursor is a membrane bound molecule and LTA may be the binding site between streptococcal surface SLS and target cells (34). Considering the similarities between LLS and SLS, we cannot rule out the hypothesis that LLS could interact with LTA like SLS. Another interesting observation that supports this idea is that the LLS smear detected in the cytoplasm is

distinct from the membrane-localized LLS smear. This suggests that LLS could be post-translationally modified before being translocated across the membrane and once membrane-anchored, LLS could be associated with LTA. To verify whether this is the case, it would be interesting to generate a LTA mutant in the LLS^+ background to determine whether LLS is no longer associated to the membrane.

For other antimicrobial peptides, it is known that the export or secretion relies on diverse mechanisms: (1) releasing antimicrobial compounds into the milieu via an ABC transporter system (36), through the sec-dependent pathway (37), or by membrane vesicle shedding (38); (2) dependent on intimate physical contact between the producer and the target bacteria through Type V (two-partner secretion system) (39) or Type VI secretion systems (40) in Gram-negative bacteria, and Type VII secretion system in Gram-positive bacteria (41). In Gram-positive bacteria, the Type VII secretion system is responsible for the delivery of LXG domain proteins that have a CDI mechanism, however these proteins are detected in the supernatant and the killing activity is not observed in liquid media (41). Thus, again highlighting the novelty of the mechanism of action used by LLS since it is the first bacteriocin in Gram-positive bacteria that remains attached to the cell membrane and acts through a CDI mechanism.

We hypothesize that LLS is translocated to the membrane by the putative ABC-like transporter system encoded by the *llsGH* genes present in the *lls* gene cluster. To investigate this hypothesis, we attempted to generate a double Δ*llsGH* mutant in the LLS^+ background but this mutant was not viable. On the other hand, a double Δ*llsGH* mutant is viable in a F2365 wild-type background in which the LLS is not produced (data not shown). This result could indicate that once LLS is produced, it must be translocated through the membrane in order to avoid intoxication of producer cells. However, the precise mechanism of release of LLS from the membrane of the LLS-producer bacteria that allows transfer to target bacteria remains to be determined.

LLS compromises bacterial cell membrane permeability

Our microfluidics experiments show that LLS induces cell membrane permeabilization in target cells in a contact-dependent manner, suggesting that cell membrane integrity has been compromised in the LLS-sensitive bacteria. To our knowledge, the only

TOMM that has been reported so far to act on the bacterial cell membrane is the plantazolicin. The plantazolicin is an ultra-narrow spectrum antibiotic produced by *B. methylotrophicus* that acts against *B. anthracis* inducing cell membrane depolarization (11). There are however several non-TOMM bacteriocins that are able to form pores in target cell membranes, among them the lantibiotic nisin produced by *L. lactis* which targets several Gram-positive bacteria, including *Lm* (42, 43). It is interesting to highlight that nisin has two complementary bactericidal activities: it disrupts peptidoglycan synthesis through inhibition of lipid II activity and it forms pores in the bacterial cell membrane (44).

Our results do not allow us to determine whether the cell membrane is the primary and only target of LLS. We investigated whether LLS, as nisin, could target the peptidoglycan, and our results suggest that the peptidoglycan structure/composition is not affected in LLS-target bacteria. On the other hand, we demonstrated that increased net negative surface charges augment the bacterial susceptibility to LLS. This increased susceptibility of Δ*dltA* has been reported for other antimicrobial peptides such as bacitracin, colistin, polymyxin B, nisin and gallidermin that target exclusively the cell membrane or the cell membrane and the peptidoglycan (24, 25). Indeed, the absence of cell wall decorations in the Δ*dltA* decreases the cell wall density and increases the permeability to cationic antimicrobial peptides (45). Is important to mention that the LLS N-terminal part contains hydrophobic and charged amino acids (alanine, lysine and methionine) which is characteristic of cationic peptides (46).

LLS is the first TOMM that acts through a CDI mechanism

To our knowledge, LLS is the first described TOMM that acts through a CDI mechanism. Using trans-well assays and single-cell microfluidic-coupled microscopy, we demonstrated that target bacteria are killed only when they are in direct contact with LLS-producer cells. This mechanism of transfer differs considerably from family prototype, microcin B17 (MccB17) from *E. coli,* which has been described as a secreted bacteriocin (12). However, we do not exclude the hypothesis that other TOMMs including clostridiolysin S and plantazolicin could act as CDI bacteriocins since this approach has not been applied thus far to study these molecules (11, 47).

The potential advantages of a CDI mechanism for LLS-producing bacteria might be diverse. The LLS, as a narrow spectrum bacteriocin, could facilitate targeting the physically proximal members within a particular niche by having a CDI mechanism (28). This mechanism could be advantageous because the proximity between the producer and the target bacteria can assure the effective killing without risking loss of LLS (32). As reported before, the contact-dependent systems could limit the non-producer cells called 'cheaters' to benefit from the secreted products (48). This mechanism is highly effective since, as previously mentioned, LLS is displayed by hyper-virulent *Lm* strains responsible for the most important human listeriosis outbreaks (7, 49), and our previous results indicate that the absence of LLS significantly reduces the capacity of hyper-virulent *Lm* to colonize the intestine and to translocate to inner organs such as the liver and spleen (7).

In the context of *Lm* as an entero-pathogen, outcompeting the host intestinal microbiota is a critical step for the establishment of listeriosis. Our previous results demonstrate that *Lm* lacking LLS is impaired in its capacity to compete with intestinal microbiota and does not survive as efficiently as WT (LLS producer bacteria) in the intestinal lumen (7). Also strains which lack LLS such as EGD and EGD-e, rarely cause human disease (50). These previous findings demonstrate that LLS play a key role in the modulation of the host microbiota by *Lm* hyper-virulent strains. Our present work clarifies the specific mechanism used by *Lm* to interact and outcompete commensal bacteria by means of the LLS CDI activity.

Materials and Methods

Co-cultures and split-well co-culture bacterial assays

Co-culture assays were performed for 24 h statically at 37 °C in microaerophilic conditions (6% O_2 and 5-10% CO_2) as previously described (7). Briefly, 5×10^7 bacteria from overnight cultures were inoculated into 5 mL of fresh BHI either alone or in coculture with another strain as indicated. At 24 h after inoculation, cultures were serially diluted and plated on BHI and Oxford agar plates (Oxoid). Experiments were performed three times independently.

For the split-well co-culture assays 6-well polystyrene plates were used with Millicell hanging inserts (PET membrane, 0.4 or 8 µm pore size). The co-cultured strains were

split into the upper and lower chambers. In total, 1 mL of BHI broth was added to the upper chamber and 1 × 10^7 of each strain was inoculated from overnight cultures. Plates were covered with a lid and incubated during 24 h statically at 37°C in microaerophilic conditions.

Subcellular fractionation

The *Lm* fractionation was performed as described previously (20) with a few modifications. The cell wall, membrane and cytoplasm compartments were separated from 2 mL of stationary phase culture (OD_{600} = 2). The bacteria were pelleted and supernatant (SN) was precipitated at -20°C overnight with 16% of thricloracetic acid. The bacterial pellet was washed once with 2 mL of PBS and once with 2 mL of TS buffer (10 mM Tris-HCl pH 6.9, 10 mM $MgCl_2$ and 0.5 M sucrose). Then the bacteria were resuspended in 1 mL of TS buffer containing 45 µg mutanolysin (Sigma) and cOmplete protease inhibitor cocktail (Roche) overnight statically at 37 °C to digest completely the cell wall. Protoplasts were pelleted for 5 min at 15,000 *g* and the cell wall fraction was precipitated with TCA as indicated before for the supernatant. The protoplasts were lysed by four freeze-thaw cycles (liquid nitrogen and water bath at 37 °C) in 100 µl of protoplast buffer (100 mM Tris-HCl pH 7.5, 100 mM NaCl and 10 mM $MgCl_2$). The membrane and the cytoplasm fractions were centrifuged at 4 °C for 15 min at 16,000 *g*. The pellet corresponding to the membrane fraction was then resuspended in 100 µl of CHAPS lysis buffer (30 mM Tris-HCl pH 7.5, 150 mM NaCl and 1% CHAPS). The membrane fraction was sonicated (three cycles of 15 s, 20% amplitude).

Immunogold labelling and transmission electron microscopy

Bacteria were grown in BHI broth ON and the cultures were refreshed until bacteria reached and OD_{600nm} = 1. Strain *Lm* F2365 pHELP: *llsA*-HA was used to detect the LLS and the strain without the tag *Lm* F2365 pHELP: *llsA* was used as a negative control. Bacteria were fixed with 2% paraformaldehyde + 0.1% glutaraldehyde in PHEM buffer, pH 7 (60 mM Pipes, 25 mM Hepes, 2 mM $MgCl_2$, 10 mM EGTA) for 2 h at room temperature. After fixation, bacteria were washed with PHEM buffer and remaining free aldehydes were quenched with 50 mM NH_4Cl in PHEM buffer. Bacteria were pelleted down and embedded in 12% gelatin in PBS. After solidification on ice the bacterial pellet was cut into small cubes of $1mm^3$. The cubes were incubated

overnight in 2.1 M sucrose in PBS and mounted afterwards on metal pins for plunge freezing in liquid nitrogen. Cryo-sections with a nominal feed of 60 nm were cut with a Leica UC6/FC6 and picked up with a 1:1 mixture of 2.1 M sucrose in PBS and 2% methylcellulose in water. After thawing the sections were deposited on 200 mesh copper grids coated with a formvar and carbon film. Immunolabeling according to the protein A gold method was done as described (51). The rabbit monoclonal antibody anti-HA (clone 3F10 from Roche, 1:100 dilution) and the rat anti-rabbit conjugated antibody (from Epitomics, 1:200) followed by protein A gold 10 nm (CMC Utrecht) were used. Images were taken with a Tecnai G2 microscope run at 120kV, equipped with a Gatan US 4000.

Microfluidics and time-lapse microscopy

For the time lapse microscopy, a customized microfluidic device was used as described before with some modifications (21). Shortly, the customized microfluidics device consists of a PDMS chip with channels connected to an inlet and an outlet tubing. The bacteria are trapped between a glass coverslip and a semi-permeable cellulose membrane (Spectra/Por 6 Dialysis Tubing 25 kDa MWCO, Spectrum) for the growth rate assays or an agarose pad (1.5% w/v low-melting point agarose) for the cell membrane permeabilization assays. Before closing the device 2 µl of a mixture (target-producer and target-mutant) were inoculated in opposite sides of the device to avoid cross contamination (5×10^8 bacteria were inoculated for each strain). Once the microfluidics device was assembled, the silicone tubing connected to the two inlet ports of the microfluidic device were fixed to 50 mL syringes. The bacteria were fed by pumping the medium into the tubing, and by diffusion of the medium from the channels of the PDMS device through the membrane. For the growth rate assays BHI broth was pumped using a syringe pump set at a rate of 25 µl/min during 10 h, and for the cell membrane permeabilization assays BHI broth was pumped during 2 h and then changed to PBS 1x (Dulbeco PBS Gifco) with Blue Sytox dye (final concentration 1 µM) during 10 h.

Time-lapse microscopy was performed with an inverted Delta Vision Elite Microscope (GE Healthcare) equipped with an UPLFLN100XO2/PH3/1.30 objective (Olympus). An environmental chamber at 37°C was used enclosing the optical components of the microscope, the PDMS device and the stage (Weather station Precision Control,

Applied Precision). Images were recorded with a personal DV system equipped with a high-speed sCMOS camera. The exposure time and illumination power settings were: Phase contrast: 150 ms at 50% T; DAPI (Ex:360/40; Em:457/50): 100 ms at 32% T; FITC (Ex 475/28, Em 525/48): 100 ms at 32% T; mCherry (Ex:575/25; Em:632/60): 100 ms at 32% T. Images were recorded for 10 h at 15 min intervals for the SYTOX assays and at 8 min intervals for the growth rate assays.

Statistics

The Shapiro-Wilk test was used to test normal distribution of datasets. Normally distributed data with equal group variances were expressed as means ± standards errors of the means (SEM). Statistical tests were performed using Prism 8.0 (GraphPad Software) and differences were evaluated by an unpaired Student's *t*-test or unpaired Multiple *t*-tests as indicated. The level of significance was set at *p<0.05. Significant differences are represented by asterisks (*p<0.05, **p<0.01, *** p<0.001, **** p<0.0001).

Acknowledgments

We thank Mélodie Duval, Filipe Carvalho and Alessandro Pagliuso for useful advice, discussions and technical support; Fabrice Agou, Agnès Zettor and Sara Consalvi from Chemogenomic and Biological Screening Platform at Institut Pasteur for the technological and technical support; the help and training provided from the members of the Cytometry and biomarkers platform (UTECHS CB) at Institut Pasteur; the Centre de Ressources Biologiques de l'Institut Pasteur for providing strains; and Pr. Ivo Gomperts Boneca and Richard Wheeler for the help provided with click chemistry. This work received financial from Institut Pasteur, Institut Carnot Pasteur Microbes et Santé (PasteurInnov Grant LLS-Bact), from Région Ile-de-France (DIM-MALINF) and Fondation pour la Recherche Médicale to JMT. JJQ is supported by a "Ramón y Cajal" contract of the Spanish Ministry of Science, Innovation and Universities (RYC-2018-024985-I). The Yersinia Research Unit is a member of the LabEX IBEID (ANR LBX-62 IBEID).

References

1. P. Cossart, Illuminating the landscape of host-pathogen interactions with the bacterium *Listeria monocytogenes*. *Proceedings of the National Academy of Sciences* **108**, 19484–19491 (2011).
2. L. Radoshevich, P. Cossart, *Listeria monocytogenes*: towards a complete picture of its physiology and pathogenesis. *Nature Reviews Microbiology* **16**, 32–46 (2017).
3. P. D. Cotter, *et al.*, Listeriolysin S, a Novel Peptide Haemolysin Associated with a Subset of Lineage I *Listeria monocytogenes*. *PLoS Pathogens* **4**, e1000144 (2008).
4. R. H. Orsi, H. C. den Bakker, M. Wiedmann, *Listeria monocytogenes* lineages: Genomics, evolution, ecology, and phenotypic characteristics. *International Journal of Medical Microbiology* **301**, 79–96 (2011).
5. E. M. Clayton, C. Hill, P. D. Cotter, R. P. Ross, Real-time PCR assay to differentiate Listeriolysin S-positive and -negative strains of Listeria monocytogenes. *Appl. Environ. Microbiol.* **77**, 163–171 (2011).
6. J. J. Quereda, *et al.*, Listeriolysin S Is a Streptolysin S-Like Virulence Factor That Targets Exclusively Prokaryotic Cells *In Vivo*. *mBio* **8**, e00259-17, /mbio/8/2/e00259-17.atom (2017).
7. J. J. Quereda, *et al.*, Bacteriocin from epidemic *Listeria* strains alters the host intestinal microbiota to favor infection. *Proceedings of the National Academy of Sciences* **113**, 5706–5711 (2016).
8. J. J. Quereda, J. Meza-Torres, P. Cossart, J. Pizarro-Cerdá, Listeriolysin S: A bacteriocin from epidemic *Listeria monocytogenes* strains that targets the gut microbiota. *Gut Microbes* **8**, 384–391 (2017).
9. S. W. Lee, *et al.*, Discovery of a widely distributed toxin biosynthetic gene cluster. *Proceedings of the National Academy of Sciences* **105**, 5879–5884 (2008).
10. E. M. Molloy, P. D. Cotter, C. Hill, D. A. Mitchell, R. P. Ross, Streptolysin S-like virulence factors: the continuing sagA. *Nature Reviews Microbiology* **9**, 670–681 (2011).
11. K. J. Molohon, *et al.*, Plantazolicin Is an Ultranarrow-Spectrum Antibiotic That Targets the *Bacillus anthracis* Membrane. *ACS Infectious Diseases* **2**, 207–220 (2016).
12. Y. M. Li, J. C. Milne, L. L. Madison, R. Kolter, C. T. Walsh, From peptide precursors to oxazole and thiazole-containing peptide antibiotics: microcin B17 synthase. *Science* **274**, 1188–1193 (1996).
13. J. L. Vizán, C. Hernández-Chico, I. del Castillo, F. Moreno, The peptide antibiotic microcin B17 induces double-strand cleavage of DNA mediated by *E. coli* DNA gyrase. *EMBO J.* **10**, 467–476 (1991).
14. V. Datta, *et al.*, Mutational analysis of the group A streptococcal operon encoding streptolysin S and its virulence role in invasive infection: SLS operon and invasive GAS infection. *Molecular Microbiology* **56**, 681–695 (2005).
15. V. Nizet, Streptococcal beta-hemolysins: genetics and role in disease pathogenesis. *Trends Microbiol.* **10**, 575–580 (2002).
16. A. W. Bernheimer, Disruption of wall-less bacteria by streptococcal and staphylococcal toxins. *J. Bacteriol.* **91**, 1677–1680 (1966).
17. H. Keiser, G. Weissmann, A. W. Bernheimer, Studies on lysosomes. iv. solubilization of enzymes during mitochondrial swelling and disruption of lysosomes by streptolysin S and other hemolytic agents. *J. Cell Biol.* **22**, 101–113 (1964).

18. W. Hryniewicz, J. Pryjma, Effect of streptolysin S on human and mouse T and B lymphocytes. *Infect. Immun.* **16**, 730–733 (1977).

19. D. L. Higashi, *et al.*, Activation of band 3 mediates group A *Streptococcus* streptolysin S-based beta-haemolysis. *Nature Microbiology* **1**, 15004 (2016).

20. R. Jonquières, H. Bierne, F. Fiedler, P. Gounon, P. Cossart, Interaction between the protein InlB of *Listeria monocytogenes* and lipoteichoic acid: a novel mechanism of protein association at the surface of gram-positive bacteria. *Mol. Microbiol.* **34**, 902–914 (1999).

21. G. Manina, A. Griego, L. K. Singh, J. D. McKinney, N. Dhar, Preexisting variation in DNA damage response predicts the fate of single mycobacteria under stress. *EMBO J* **38** (2019).

22. D. Balestrino, *et al.*, Single-Cell Techniques Using Chromosomally Tagged Fluorescent Bacteria To Study *Listeria monocytogenes* Infection Processes. *Applied and Environmental Microbiology* **76**, 3625–3636 (2010).

23. H. Lee, E.-R. Woo, D. G. Lee, Glochidioboside Kills Pathogenic Bacteria by Membrane Perturbation. *Curr Microbiol* **71**, 1–7 (2015).

24. E. Abachin, *et al.*, Formation of D-alanyl-lipoteichoic acid is required for adhesion and virulence of *Listeria monocytogenes*. *Mol Microbiol* **43**, 1–14 (2002).

25. A. Peschel, *et al.*, Inactivation of the *dlt* Operon in *Staphylococcus aureus* Confers Sensitivity to Defensins, Protegrins, and Other Antimicrobial Peptides. *J. Biol. Chem.* **274**, 8405–8410 (1999).

26. D. A. Mitchell, *et al.*, Structural and Functional Dissection of the Heterocyclic Peptide Cytotoxin Streptolysin S. *Journal of Biological Chemistry* **284**, 13004–13012 (2009).

27. E. M. Clayton, *et al.*, Atypical *Listeria innocua* strains possess an intact LIPI-3. *BMC Microbiol.* **14**, 58 (2014).

28. M. A. Riley, "Bacteriocin-Mediated Competitive Interactions of Bacterial Populations and Communities" in *Prokaryotic Antimicrobial Peptides*, D. Drider, S. Rebuffat, Eds. (Springer New York, 2011), pp. 13–26.

29. B. M. Xavier, A. J. Houlihan, J. B. Russell, The activity and stability of cell-associated activity of bovicin HC5, a bacteriocin from *Streptococcus bovis* HC5: Bovicin HC5. *FEMS Microbiology Letters* **283**, 162–166 (2008).

30. A. Barbour, K. Philip, Variable Characteristics of Bacteriocin-Producing *Streptococcus salivarius* Strains Isolated from Malaysian Subjects. *PLoS ONE* **9**, e100541 (2014).

31. H. Daba, C. Lacroix, J. Huang, R. E. Simard, L. Lemieux, Simple method of purification and sequencing of a bacteriocin produced by *Pediococcus acidilactici* UL5. *Journal of Applied Bacteriology* **77**, 682–688 (1994).

32. L. García-Bayona, M. S. Guo, M. T. Laub, Contact-dependent killing by Caulobacter crescentus via cell surface-associated, glycine zipper proteins. *eLife* **6**, e24869 (2017).

33. I. Ginsburg, Is streptolysin S of group A streptococci a virulence factor? *APMIS* **107**, 1051–1059 (1999).

34. T. S. Theodore, G. B. Calandra, Streptolysin S activation by lipoteichoic acid. *Infect. Immun.* **33**, 326–328 (1981).

35. C. Loridan, J. E. Alouf, Purification of RNA-core Induced Streptolysin S, and Isolation and Haemolytic Characteristics of the Carrier-free Toxin. *Microbiology* **132**, 307–315 (1986).

36. K. Beis, S. Rebuffat, Multifaceted ABC transporters associated to microcin and bacteriocin export. *Research in Microbiology* **170**, 399–406 (2019).

37. S. Zheng, K. Sonomoto, Diversified transporters and pathways for bacteriocin secretion in gram-positive bacteria. *Appl Microbiol Biotechnol* **102**, 4243–4253 (2018).

38. L. Brown, J. M. Wolf, R. Prados-Rosales, A. Casadevall, Through the wall: extracellular vesicles in Gram-positive bacteria, mycobacteria and fungi. *Nat Rev Microbiol* **13**, 620–630 (2015).

39. S. K. Aoki, *et al.*, A widespread family of polymorphic contact-dependent toxin delivery systems in bacteria. *Nature* **468**, 439–442 (2010).

40. D. Unterweger, *et al.*, The Vibrio cholerae type VI secretion system employs diverse effector modules for intraspecific competition. *Nat Commun* **5**, 3549 (2014).

41. J. C. Whitney, *et al.*, A broadly distributed toxin family mediates contact-dependent antagonism between gram-positive bacteria. *eLife* **6**, e26938 (2017).

42. M. A. S. S. Ferreira, B. M. Lund, The effect of nisin on *Listeria monocytogenes* in culture medium and long-life cottage cheese. *Lett Appl Microbiol* **22**, 433–438 (1996).

43. T. Katla, K. Naterstad, M. Vancanneyt, J. Swings, L. Axelsson, Differences in Susceptibility of *Listeria monocytogenes* Strains to Sakacin P, Sakacin A, Pediocin PA-1, and Nisin. *Applied and Environmental Microbiology* **69**, 4431–4437 (2003).

44. I. Wiedemann, *et al.*, Specific Binding of Nisin to the Peptidoglycan Precursor Lipid II Combines Pore Formation and Inhibition of Cell Wall Biosynthesis for Potent Antibiotic Activity. *J. Biol. Chem.* **276**, 1772–1779 (2001).

45. R. Saar-Dover, *et al.*, D-Alanylation of Lipoteichoic Acids Confers Resistance to Cationic Peptides in Group B *Streptococcus* by Increasing the Cell Wall Density. *PLoS Pathog* **8**, e1002891 (2012).

46. K. Pane, *et al.*, Antimicrobial potency of cationic antimicrobial peptides can be predicted from their amino acid composition: Application to the detection of “cryptic” antimicrobial peptides. *Journal of Theoretical Biology* **419**, 254–265 (2017).

47. D. J. Gonzalez, *et al.*, Clostridiolysin S, a Post-translationally Modified Biotoxin from *Clostridium botulinum*. *J. Biol. Chem.* **285**, 28220–28228 (2010).

48. L. McNally, *et al.*, Killing by Type VI secretion drives genetic phase separation and correlates with increased cooperation. *Nat Comms* **8**, 14371 (2017).

49. M. J. Linnan, *et al.*, Epidemic Listeriosis Associated with Mexican-Style Cheese. *New England Journal of Medicine* **319**, 823–828 (1988).

50. M. M. Maury, *et al.*, Uncovering *Listeria monocytogenes* hypervirulence by harnessing its biodiversity. *Nature Genetics* **48**, 308–313 (2016).

51. J. W. Slot, H. J. Geuze, S. Gigengack, G. E. Lienhard, D. E. James, Immuno-localization of the insulin regulatable glucose transporter in brown adipose tissue of the rat. *The Journal of Cell Biology* **113**, 123–135 (1991).

Figures and Tables

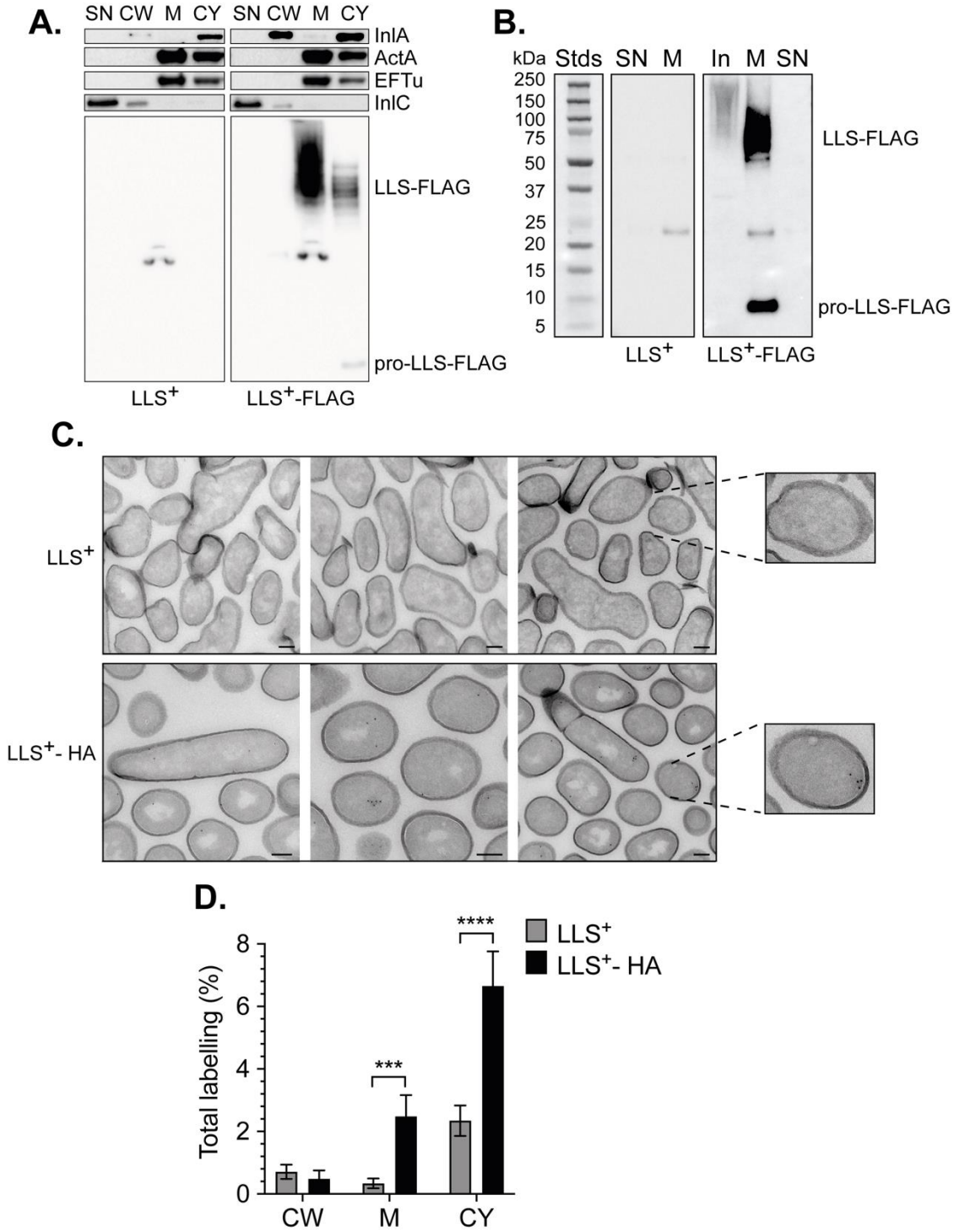

Figure 1. LLS is not actively secreted and is located at the cell membrane. (A) Localization of LLS by fractionation experiments. Western Blot analysis was performed on a strain expressing LLS$^+$ (negative control) and a strain expressing LLS$^+$-FLAG (FLAG at the C-terminus). Proteins were fractionated in four compartments supernatant (SN), cell wall (CW), membrane (M) and cytoplasm (CY). InlA, ActA, EF-Tu and InlC were used as controls for fractionation. Equivalent amounts of each fraction, corresponding to 100 µl of bacterial culture

were separated on SDS-PAGE and submitted to immuno-detection, using the indicated antibodies. Data from one representative experiment out of the three performed are shown. (B) LLS supernatant (SN) and membrane (M) fractions were immuno-precipitated on a strain expressing LLS^+ (negative control) and a strain expressing LLS^+-FLAG by using magnetic beads coupled to anti-FLAG antibodies. Equivalent amounts of each fraction, corresponding to 2.5 ml of bacterial culture were separated on SDS-PAGE and submitted to immune-detection, using the anti-FLAG antibody. Data from one representative experiment out of the three performed are shown. The pre-stained protein standards (Stds) are shown at the left with the respective molecular weight in kDa. (C) Location of LLS by TEM. An anti-HA colloidal gold-coupled antibody was used to detect LLS on a strain expressing LLS^+ (negative control) and a strain expressing LLS^+-HA (HA at the C-terminus). Insets present an enlargement of an area of LLS detected or not at the M. Scale bars, 200 nm. (D) Quantification of the total labelling (%) of LLS^+ (negative control) and LLS^+-HA in the CW, M and CY compartments obtained from TEM shown in C. Positive signal in the M and in the CY of the LLS^+-HA sample are significantly different from background noise present in the LLS^+ sample. Error bars show SEM. Multiple *t*-tests were performed to compare different compartments. M p value = 0.000143 and CY p value = 0.000069. LLS^+ n= 106 and LLS^+-HA n= 59.

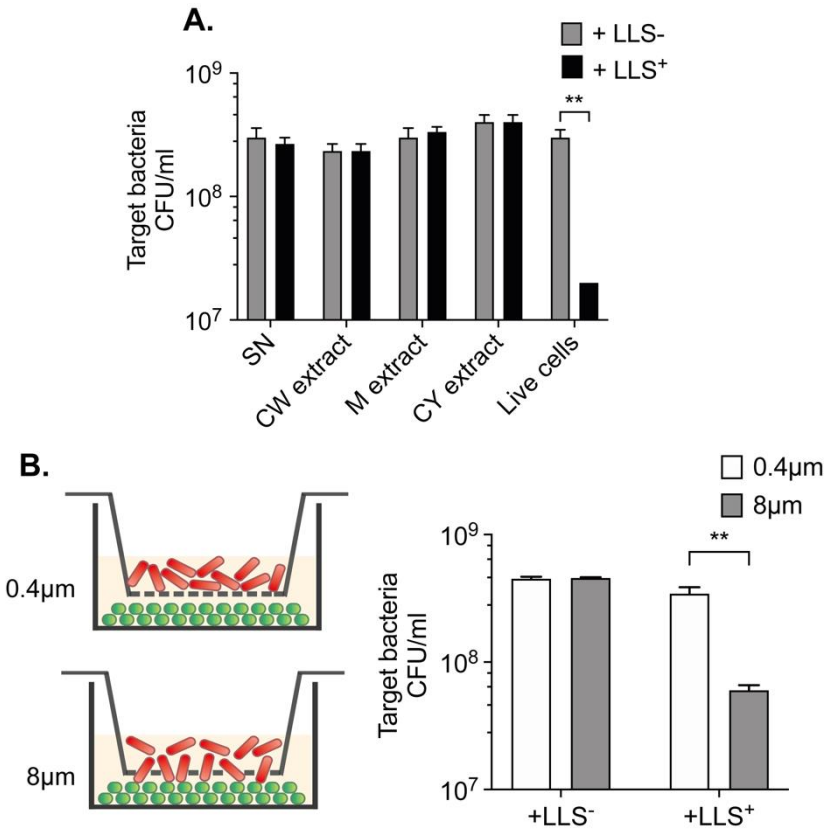

Figure 2. LLS bactericidal activity requires cell-cell contact between a producer and target bacteria. (A) Survival of target bacteria when co-cultured with live cells, Cell wall (CW), membrane (M) or cytoplasm (CY) fractions. Target bacteria were incubated 24h in BHI with LLS producer bacteria (LLS^+) or LLS mutant bacteria (LLS^-) live cells or fractions. (B) A co-culture was performed using the split well set-up shown (left). The membrane separating the producer bacteria (LLS^+ or LLS^-) from the target bacteria had a pore size of 8 or 0.4µm. Data from one representative experiment out of the three performed are shown. Error bars show SEM. Multiple two-tailed unpaired *t*-tests were performed p = 0.004066 (A) and p = 0.002921(B) n=3.

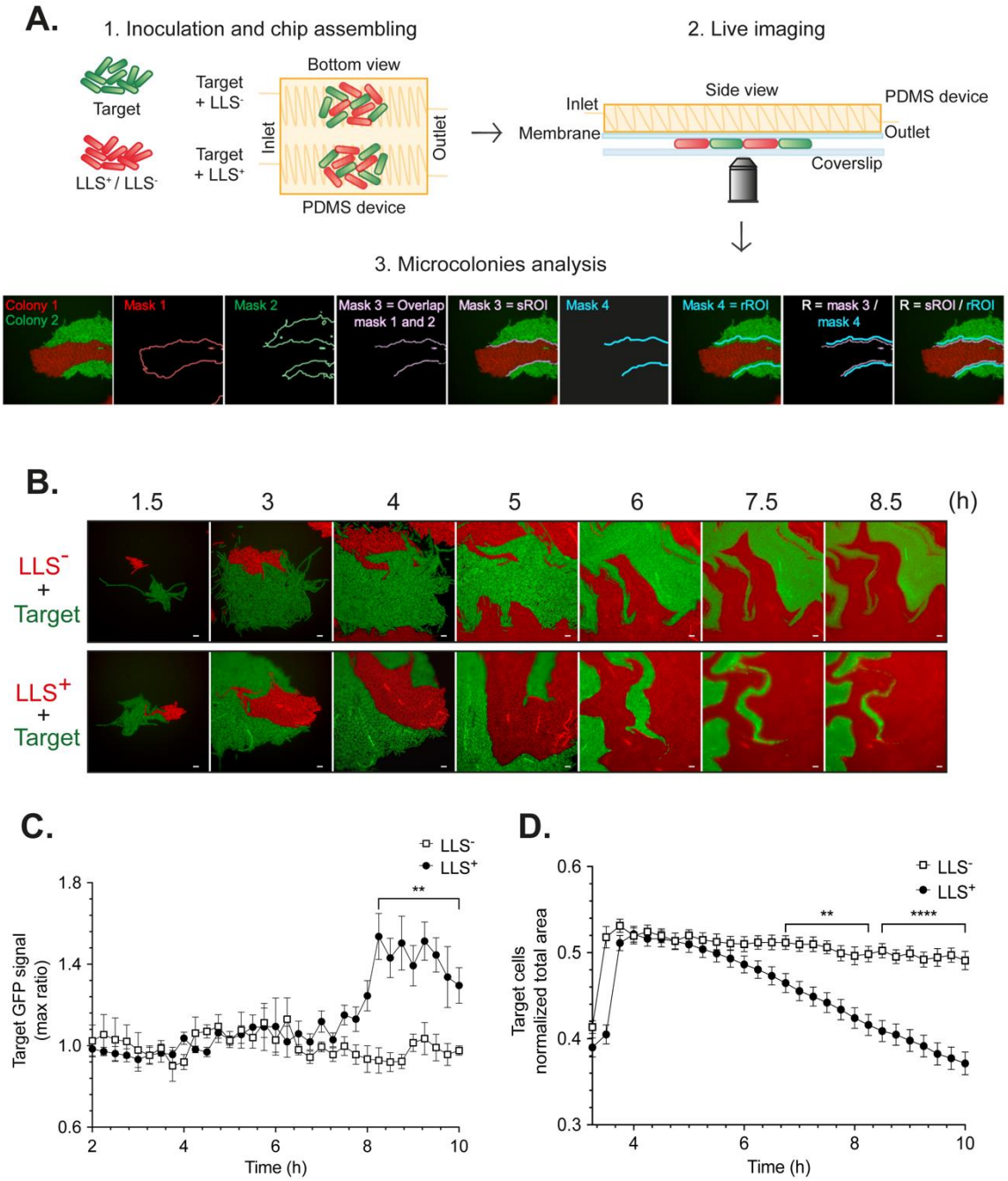

Figure 3. **LLS inhibits the growth of target cells over time** (A) Schematic representation of microfluidics experiments. Top view and side view of the assembled microfluidic device used for single-cell time-lapse microscopy. (1) *Listeria* LLS producer bacteria (LLS$^+$) and *Listeria* LLS mutant (LLS$^-$) express tdTomato constitutively and *Listeria* target bacteria express GFP constitutively from an integrative plasmid. (2) Bacteria are trapped between the coverslip and a semipermeable membrane, fed by diffusion of medium and imaged every 15 min during 10 h. (3) Microcolonies of the target and producer bacteria are segmented (Mask 1 and Mask 2) to obtain the intersection between them (Mask 3) which is the signal region of interest (sROI). The rROI (Mask 4) includes the target bacteria not in contact with LLS$^+$ or LLS$^-$ bacteria. The ratio (R) between the ROIs (R= sROI/rROI) is analyzed over time (B) Time-lapse microscopy

snapshots of LLS^+ or LLS^- (tdTomato) and target bacteria (GFP) over time. Data from one representative experiment out of the two performed are shown. Scale bar, 3µm. (C) Quantification of green fluorescence intensity of target bacteria in contact with LLS^+ or LLS^- bacteria obtained from R (shown in A) represented as ratios of intensities: Max. Multiple unpaired *t*-tests with Holm-Sidak correction were performed. P values are significant from 8h 15 min (**p< 0.01) LLS^- n=7 LLS^+ n=13. (D) Quantification of the target cells total area over time. The area is normalized according to the area occupied by LLS^+ or LLS^- bacteria. The area is represented as a percentage of the snapshot total area. Multiple unpaired *t*-tests with Holm-Sidak correction were performed. P values are significant from 6 h 45 min (**p< 0.01) and from 8h 30 min (****p<0.0001) LLS^- n=26 LLS^+ n=33. Error bars show SEM.

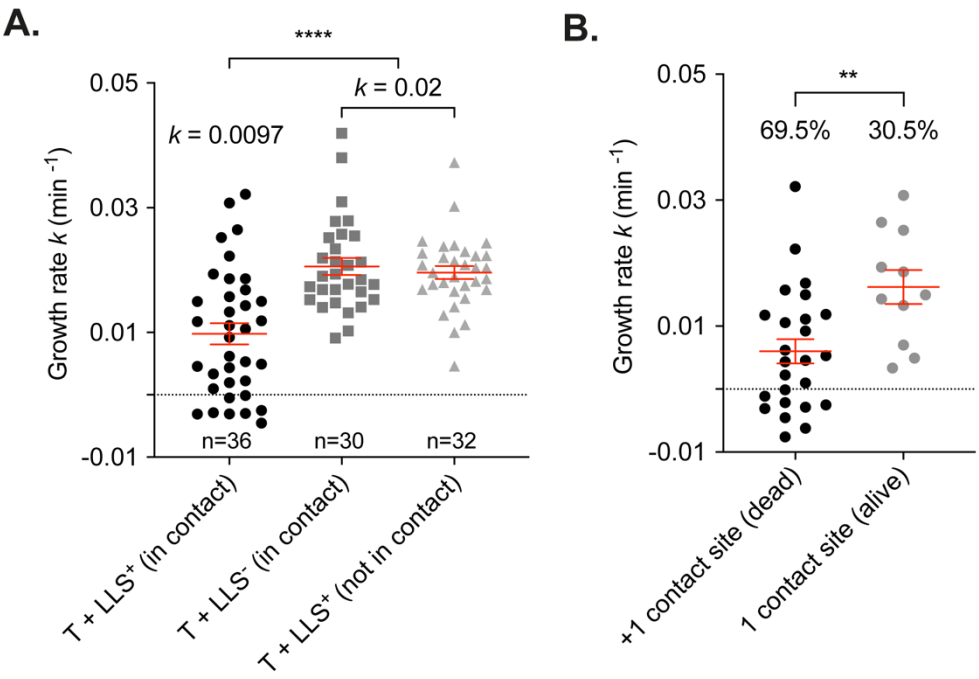

Figure 4. **LLS arrests the cell division on target cells in a contact-dependent manner.** (A) Growth rate of target bacteria in contact or not with LLS$^+$ bacteria or in contact with LLS$^-$ bacteria represented in min^{-1}(*k* constant). (B) Growth rate of target bacteria in contact with one LLS$^+$ bacteria (one contact site) or more LLS$^+$ bacteria (more than one contact site) represented in min^{-1}(*k* constant). The bacteria in contact with one LLS$^+$ bacteria represent the 30.5% of the population and do not die. The bacteria in contact with more LLS$^+$ bacteria represent the 69.5% of the population and die. The bacterial growth rate (*k* constant) was calculated by fitting an exponential curve to size measurements over the lifetime of the cells. Data from one representative experiment out of the two performed are shown. Error bars show SEM. Multiple two-tailed unpaired *t*-test were performed p****<0.0001(A) and p= 0.0053 (B).

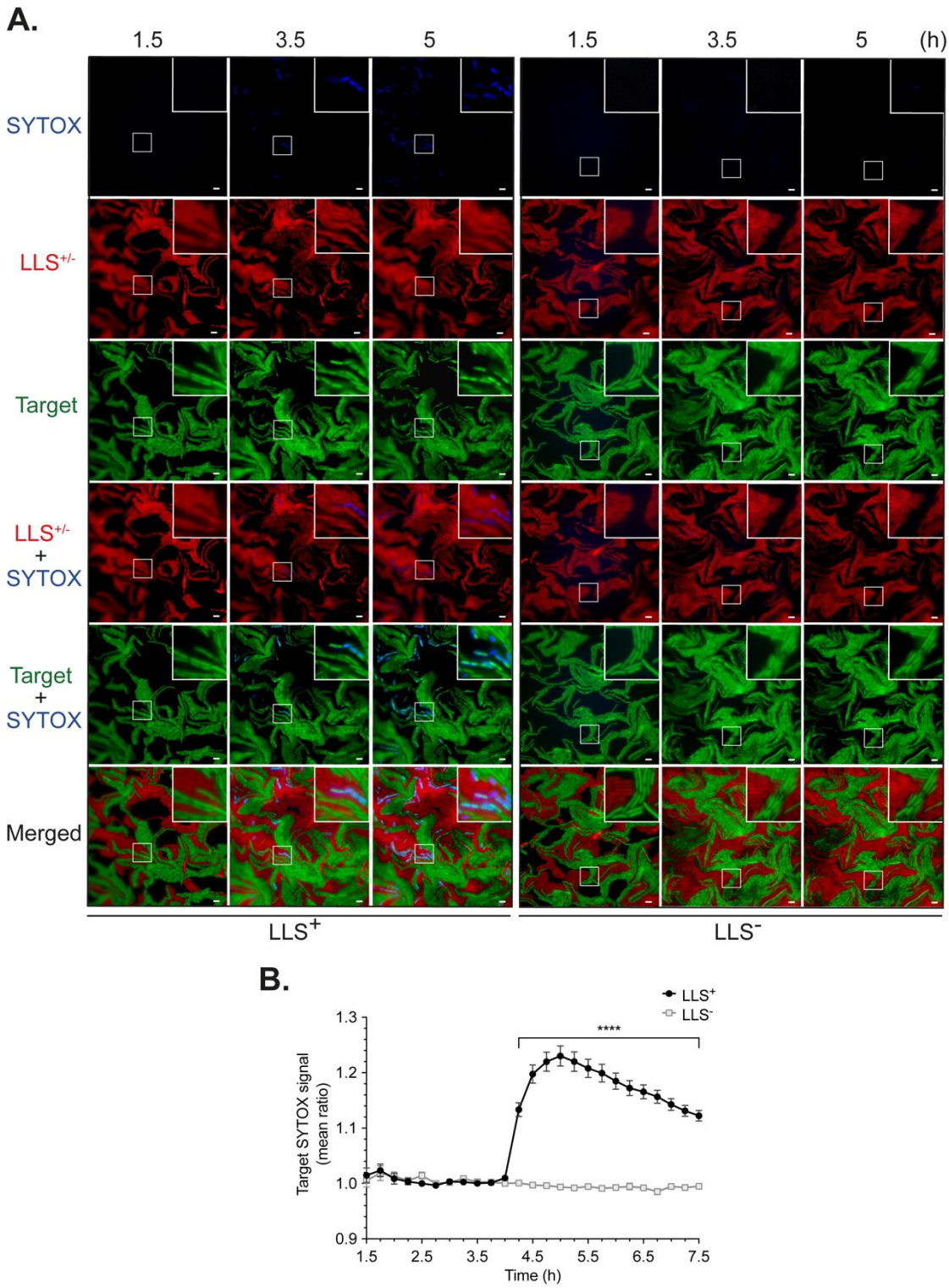

Figure 5. The LLS induces cell membrane permeabilization on the target bacteria that are into contact with LLS producer bacteria. (A) Time-lapse microscopy snapshots of LLS$^+$ or LLS$^-$ and target bacteria over time. *Listeria* LLS producer bacteria (LLS$^+$) and *Listeria* LLS mutant (LLS$^-$) express tdTomato constitutively and *Listeria* target bacteria express GFP constitutively from an integrative plasmid. BHI medium was perfused during 2 h and then SYTOX blue dye was diluted in PBS and added after 2 h to label dying bacteria (B) Quantification of SYTOX fluorescence intensity of target bacteria in contact with LLS$^+$ or LLS$^-$

bacteria obtained from R (shown in Fig. 3A) represented as ratios of intensities: mean. Data from one representative experiment out of the two performed are shown. Scale bar, 3µm. Error bars show SEM. Multiple unpaired *t*-tests with Holm-Sidak correction were performed. P values are significant from 4h 15 min (****p< 0.0001) LLS^- n=26 LLS^+ n=32.

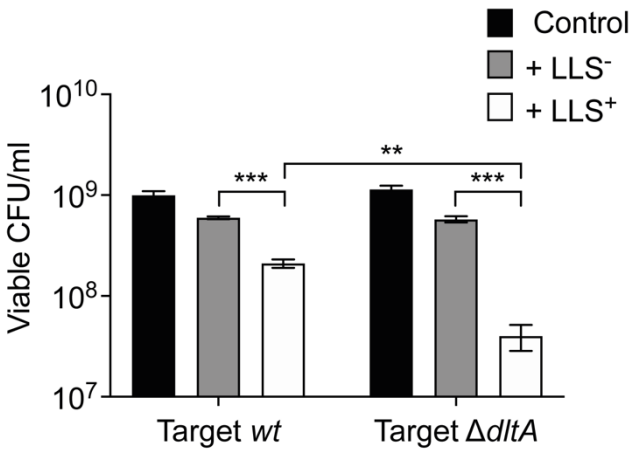

Figure 6. Increased net negative surface charges increase susceptibility to LLS. Target wt or Δ*dltA* EGD bacteria were cultivated alone or co-cultivated with LLS producer bacteria (LLS^+) or LLS mutant bacteria (LLS^-) during 24h in BHI. Data from three independent biological experiments are shown. Error bars show SEM. Multiple two-tailed unpaired *t*-test were performed, wt LLS^+ vs LLS^- p= 0.0001, Δ*dltA* LLS^+ vs LLS^- p= 0.0002 and wt LLS^+ vs *dltA* LLS^+ p= 0.0018.

PNAS
www.pnas.org

Supplementary Information for

Listeriolysin S is a contact-dependent inhibition bacteriocin from *Listeria monocytogenes* that impairs cell membrane integrity

Jazmin Meza-Torres[1,2,3], Juan J Quereda[4], Martin Sachse[5], Giulia Manina[6], Dmitry Ershov[7,8], Jean Yves Tinevez[7], Lilliana Radoshevich[9], Claire Maudet[10], Marc Lecuit[3,10,11,12], Olivier Dussurget[1,3], Pascale Cossart[2] & Javier Pizarro-Cerdá[1*]

Javier Pizarro-Cerdá
Email: javier.pizarro-cerda@pasteur.fr

This PDF file includes:

Supplementary Material and Methods
Tables S1 to S3
Figures S1 to S5
SI References

Supplementary Material and Methods

Bacterial strains and growth conditions

Bacterial strains and plasmids used in this study are listed in Table S1 and Table S2. The *Lm* and *L. lactis* strains were grown in tubes overnight at 200 rpm and 37°C in BHI broth (Difco). When required, antibiotics were added for *Listeria* chloramphenicol 7 µg/mL and erythromycin 5 µg/mL.

Mutant and strains construction

Lm F2365 *ΔllsA* and *Lm* F2365 pHELP: *llsA* were constructed as indicated previously (1). Briefly, fragments of ~500-bp DNA flanking the *llsA* gene were amplified by PCR using the chromosomal DNA of *Lm* F2365 as template and ligated into the pMAD by using *Xma*I/*Sal*I restriction sites. All the primers used are listed in Table S3. For the construction of the *Lm* F2365 pHELP: *llsA* strain, the pHELP promoter (2) was fused between two 500-ntd DNA fragments flanking the start codon of *llsA* and the DNA

construction was synthetically produced and cloned into SalI–EcoRI restriction sites of the the pMAD vector as indicated previously (1).

For the strains *Lm* F2365 pHELP: *llsA*-FLAG and *Lm* F2365 pHELP: *llsA*-HA the FLAG and HA tags were added in the C terminal of the *llsA* gene and the pHELP promoter was fused between two 500-ntd DNA fragments flanking the start codon of *llsA.* These DNA constructions were synthetically produced by gene synthesis (Genecust) and cloned into *Sal*I–*Eco*RI restriction sites of pMAD vector. Mutagenesis was performed by double recombination as described previously (3). For the construction of the *llsGH* double mutant DNA constructions were synthetically produced by IDT and cloned into SalI-SmaI restriction sites of pMAD vector. Approximately 800 -ntd DNA fragments upstream and downstream of the *llsGH* genes were used to design the DNA blocks. Mutagenesis was performed by double recombination as described previously (3). For the construction of the strains expressing constitutively GFPmut2 and tdTomato, the fragments were cloned into the pAD vector as described previously (4). The tdTomato protein was codon optimized for its expression in *Lm* (http://genomes.urv.es/OPTIMIZER/).

Immunoprecipitation

Stationary phase cultures (1L) of *Lm* F2365 pHELP: *llsA* and *Lm* F2365 pHELP: *llsA*-FLAG were pelleted. Bacteria were washed once with 50 ml of PBS and once with 50 ml of TS buffer. Bacteria were then resuspended into 25 mL of TS buffer containing 1250 µg mutanolysin (Sigma) and Complete protease inhibitor cocktail (Roche) overnight statically at 37 °C to digest completely the cell wall. Protoplasts were pelleted 5 min at 15,000 *g*, resuspendend in 15 mL of CHAPS lysis buffer and lysed by four freeze-thaw cycles. The lysed protoplasts were sonicated (four cycles of 15 s, 20% amplitude). Samples were centrifuged 45 min at 4°C at 16,000 *g*. Supernatant was collected and 100 µl of equilibrated M2 anti-flag beads (Sigma, washed three times with 1 mL of CHAPS lysis buffer) were added to both lysates. The lysates were incubated overnight at 4 °C on a rotating wheel. Beads were collected by centrifugation at 4 °C 1 min at 2,000 g and washed once with CHAPS lysis buffer and then three times with 5 mL of Elution buffer (50 mM Tris HCl pH 8.0, 150 mM NaCl and 2 mM $CaCl_2$). The FLAG tag protein was eluted by 3 serial elutions (150 µl twice and 100 µl

once) with the 3x FLAG peptide diluted in Elution buffer (final concentration of 100 µg/mL). The eluted fractions were analyzed by western Blot.

Antibodies

The following primary antibodies were used: mouse monoclonal anti-flag (M2, Sigma), mouse monoclonal anti-HA (6E2, Cell Signaling Technology) and home-made mouse monoclonal anti Internalin A (L7.7) (5), rabbit polyclonal anti-ActA (R32) (6) or rabbit monoclonal anti-ActA (A16) (7), rabbit polyclonal anti-EF-Tu (R114) (8) and rabbit polyclonal anti-Internalin C (R134) (9). Goat anti-mouse and anti-rabbit IgG HRP-conjugated antibodies (Abcam) were used as secondary antibodies. The primary antibodies were used in a 1:1000 dilution with exception of EF-Tu (1:40000) and Internalin C (1:2000) and the conjugated antibodies were used in a 1:5000 dilution.

SDS–PAGE and western blotting

Samples after cellular fractionation or immunoprecipitation were analyzed similarly. Equal amounts of each sample or fraction were then diluted with 100 µl of 2x Tricine Sample Buffer (Biorad) and 125 mM DTT to be analyzed by SDS–PAGE and western blotting. Samples were boiled 5 min at 95 °C and centrifuged at 15,000 *g* for 5 min and 20 µl (for subcellular fractions controls) or 35 µl (for LLS with tags) were loaded onto a NuPAGE 4-12% Bis-Tris Precast Protein Gels (Invitrogen). The samples were separated in Nu PAGE MOPS SDS Running Buffer (for protein controls) or MES SDS Running Buffer (for LLS) at 130 V and transferred onto a polyvinylidene fluoride (PVDF) membrane using the iBlot Dry Blotting System (Invitrogen) at 20 V for 8 min. The membranes were blocked with 5% skim milk in PBS 1X with 1% Tween-20 (PBST) and the primary antibodies were incubated overnight at 4 °C and the secondary antibodies at 37 °C during 1h at room temperature. The proteins were revealed with the Pierce ECL 2 Western Blotting Substrate or SuperSignal West Femto Maximum Sensitivity Substrate (Fisher Scientific) if necessary and image with Amersham Imager 680 (GE) or BioRad ChemiDoc MP.

RNA extraction and quantitative Real-Time PCR

Total RNA was extracted as previously described (10). Briefly, *Lm* F2365 strains were grown in BHI until stationary phase (OD_{600nm} =1.5) and pellets were resuspended in 1 mL TRIzol reagent (Ambion), transferred to 2 mL Lysing Matrix tubes and lysed with a

FastPrep apparatus (2 cycles of 45 s, speed 6.5). Tubes were centrifuged 5 min at 10 000 *g* for 10 min at 4 °C and the aqueous phase was transferred twice to an Eppendorf tube containing 200 µL of chloroform, lysates were shaken 30 s and incubated at room temperature for 10 min at room temperature and centrifuged 15 min at 13,000 × *g* at 4°C. The upper aqueous phase was removed and transfered to a new Eppendorf tube and RNA was precipitated by the addition of 500 µl Isopropanol and incubation at room temperature for 10 min. RNA was pelleted by centrifugation (10 min at 13,000 × *g* at 4°C). The supernatant was discarded and the pellet was washed twice with 75% ethanol. RNA pellets were resuspended in 40 µl water. Purified RNA (10 µg) was subjected to DNase treatment (Turbo DNase). cDNA was obtained by treating 500 ng of RNA with QuantiTect Reverse Transcription Kit following manufacturer's instructions. The quantitative Real-Time PCR was performed on CFX384 Touch Real-Time PCR Detection System (Bio-Rad) using SsoFast EvaGreen Supermix following manufacturer's instructions (Bio-Rad). Each reaction was performed in triplicate with 3 independent biological replicates. Data were analyzed by the ΔΔCt method. Gene expression levels were normalized to the *gyrA* gene.

Image analysis

To measure GFP signal dynamics and SYTOX uptake dynamics in target cells, we defined a set of regions of interest (ROI). First, the signal ROI (sROI) includes target cells that are in direct contact with producer cells (LLS^+) or *llsA* mutant cells (LLS^-); sROI signal reports the contact-dependent inhibition effect. Second, the reference ROI (rROI) includes target cells close to sROI but not in direct contact with LLS^+ or LLS^- (deeper into the microcolony); rROI signal reports the basal target microcolony signal. In addition, we defined a focus ROI (fROI) to include only those areas of an image that are focused.

To extract the sROI and the rROI, the microcolonies were smoothed (gaussian blur) and segmented (auto-threshold function, mode IsoData) using FIJI (11). Next, morphological operations were used (FIJI plugin MorpholibJ) (12) to extract the sROI and rROI. Briefly, the segmented $LLS^{+/-}$ microcolonies are dilated to get the external rim (mask 1) and the target bacteria microcolonies are eroded to get the inner rim (mask 2). The intersection between these rims gives the sROI (mask 3). The same procedure was used to get the rROI (mask 4), but to set it deeper into the target

microcolony (further from the producer) we use a larger size for dilation and erosion. The size used for dilation/erosion was 25 pixels (sROI) and 50 pixels (rROI). The width of the rim for sROI and rROI was limited to 25 pixels (length of one bacterial cell in our acquisition conditions).

Once the ROIs were identified, we calculated the fluorescence intensity (maximum signal intensity for GFP and the mean signal intensity for SYTOX) in these ROIs, and then the ratio (R) between them (R= sROI/rROI). If R is close to 1, the signal of the contact area is similar to the reference area, suggesting that target cells keep their integrity (for SYTOX) or there is no accumulation of the GFP protein. If R is >1 the signal is stronger in the area of contact, suggesting that there is membrane permeabilization (for SYTOX) and there is accumulation of GFP protein inside the target cells. The analyses were done for each time lapse with single values at each time point. The mean and the standard deviation were calculated for each time point.
To compare the growth rate of the target microcolonies as opposed to the producer or *llsA* mutant microcolonies, the relative microcolony area (RMA) was calculated. Briefly, the microcolonies were segmented and the area was normalized to the full area of the field of view 1024 x 1024 pixels to get the RMA. If both microcolonies grew at the same rate the average area of both microcolonies will occupy half of the field of view with RMA equal to 0.5.

To calculate the growth rate of bacteria in different conditions manual segmentation was performed using Icy software (13). A polygon (ROI) was drawn around a bacterium of interest to get its perimeter and the cell planar area (μm^2) (obtained from sum of the size of pixels within the ROI). The single bacterial growth rate was calculated by fitting an exponential curve to sequential size measurements of the ROIs over the lifetime of the cell as described before (14). Briefly, the values were fitted to a nonlinear regression, exponential growth equation (using Prism 8.0) to obtain the doubling time in minutes and the growth rate k (min^{-1}).

Click chemistry and flow cytometry analyses

Target bacteria were incubated with 1mM 3-Azido D-alanine ($C_3H_6N_4O_2$.HCl dissolved in DMSO) overnight. Bacteria were washed twice in PBS and co-cultured with LLS^- or LLS^+ cells for 3 or 5 h in BHI (as previously mentioned). After, the co-culture was

pelleted and cells were fixed with 200 µl ice cold pure methanol during 2 minutes. The samples were diluted with 200 µl cold PBS. Bacteria were centrifuged 3 min at 13,000 × *g* at 4°C and half of the supernatant was removed and replaced with cold PBS three times. Then tubes were centrifuged 3 min at 13,000 × *g* at 4°C and pellets were resuspended in 200 µl of PBS + 1% Bovine Serum Albumin. Samples were labelled with Click-iT® Cell Reaction Buffer Kit following manufacturer's instructions. Briefly, bacteria were resuspended in 200 µl reaction cocktail with or without (control mix) 500 µM of Alexa Fluor 594-alkyne. Samples were incubated 30 min in the dark at room temperature and bacteria were washed twice by centrifugation with PBS + 1% Bovine Serum Albumin. Bacteria were resuspended in PBS and diluted to perform flow cytometry analyses. Samples were acquired in a Cytoflex S (Beckman Coulter) and data were analyzed with FlowJo. Green Fluorescence was collected from 40 000 FSC/SSC-gated bacterial events in the FITC channel (525nm/40 nm bandpass filter). Fluorescence intensities were plotted in single-parameter histograms that were normalized to mode for the two populations (target bacteria incubated with LLS^- or LLS^+ after 3 or 5 h of co-culture).

Table S1. Strains used in this study

Strains	Description	Source	BUG or CIP no.
L. monocytogenes F2365	Strain associated with the California 1985 listeriosis outbreak	15	BUG 3012
L. monocytogenes F2365 Δ*llsA*	Deletion of the *llsA* gene	1	BUG 3781
L. monocytogenes F2365 Δ*llsB*	Deletion of the *llsB* gene	1	BUG 3668
L. monocytogenes F2365 pHELP: *llsA*	Strain that expresses the LLS operon constitutively under the control of the pHELP promoter	1	BUG 3817
L. monocytogenes F2365 pHELP: *llsA* Δ*llsB*	Strain *L. monocytogenes* F2365 pHELP: *llsA* where the *llsB* gene was deleted	This study	BUG 4314
L. monocytogenes F2365 pHELP: *llsA*-FLAG	Strain that expresses the LLS operon constitutively under the control of the pHELP promoter. The FLAG tag was added in the C terminal of the *llsA* gene.	This study	BUG 4177
L. monocytogenes F2365 pHELP: *llsA*-HA	Strain that expresses the LLS operon constitutively under the control of the pHELP promoter. The HA tag was added in the C terminal of the *llsA* gene.	This study	BUG 4179
L. monocytogenes F2365 pHELP: *llsA*-FLAG Δ*llsB*	Strain *L. monocytogenes* F2365 pHELP: *llsA*-FLAG where the *llsB* gene was deleted	This study	BUG 4315
L. monocytogenes F2365 Δ*llsGH*	Strain *L. monocytogenes* F2365 where the *llsGH* genes were deleted	This study	BUG4320
Lactococcus lactis lactis	Strain from the Institut Pasteur collection		CIP 70.56T
L. monocytogenes 10403S	Lineage II strain commonly used in laboratories (it lacks the LLS operon)	16	BUG 1361
L. monocytogenes EGD	Lineage II strain commonly used in laboratories (it lacks the LLS operon)	17	BUG 600
L. monocytogenes EGD Δ*dltA*	EGD *dltA* (LMON_0982) deletion mutant	18	BUG 2182
L. monocytogenes F2365 Δ*llsA* pAD-tdTomato	*L. monocytogenes* F2365 Δ*llsA* with tdTomato inserted into the chromosome using the plasmid pAD.	This study	BUG4339
L. monocytogenes F2365 pHELP: *llsA* pAD-tdTomato	*L. monocytogenes* F2365 pHELP: *llsA* with tdTomato inserted into the chromosome using the plasmid pAD.	This study	BUG4340
L. monocytogenes 10403S pAD-cGFP	*L. monocytogenes* 10403S with cGFP inserted into the chromosome using the plasmid pAD.	This study	BUG 4208

Table S2. Plasmids used in this study

Plasmids	Description	Source	BUG no.
pMAD	Shuttle vector used for mutagenesis	3	BUG1957
pMAD-llsA	Plasmid used to create the deletion Δ*llsA* mutant	1	BUG 3751
pMAD-llsB	Plasmid used to create the deletion Δ*llsB* mutant	1	BUG3668
pMAD-pHELP: llsA	Plasmid used to insert the pHELP promoter into the upstream region of the LLS operon	This study	BUG3801
pMAD-pHELP: llsA-FLAG	Plasmid used to insert the FLAG tag into the C terminal of the *llsA* gene	This study	BUG4142
pMAD-pHELP: llsA-HA	Plasmid used to insert the HA tag into the C terminal of the *llsA* gene	This study	BUG4143
pPL2	*L. monocytogenes* site-specific phage integration vector	4	BUG2176
pAD-GFPmut2	pPL2-P*hyper*-GFP (constitutive)	4	BUG2479
pAD-tdTomato	pPL2-P*hyper*-tdTomato (constitutive)	This study	BUG4337

Table S3. Primers used in this study

Name	Sequence 5'-3'	Purpose
llsAtag F	gcatattatcaaacggagggata	Verification of the tag insertion
llsAtag R	ctttcaagttcatatttgtgta	Verification of the tag insertion
pmad up	aagcgagaagaatcataatgg	Sequencing of the pMAD inserts
Pmad down v2	cataattattccccctagctaattttcgt	Sequencing of the pMAD inserts
llsB mut Fw	gtcaatatactgtttggct	Verification of the *llsB* gene mutation
llsB mut Rv	acagagaagattgaccat	Verification of the *llsB* gene mutation
llsGH clon Fw	atgccatggtacccgggatggtaataag	Amplification of DNA insert to clone into pMAD
llsGH clon Rv	catatgacgtcgacgtggttgattgtaagt	Amplification of DNA insert to clone into pMAD
llsGH pHELPFw	gcaattcactcgagatctgcaggat	Amplification of DNA insert to clone into pMAD
llsGH pHELP Rv	taggttgcgtctcgagtcaaatgcct	Amplification of DNA insert to clone into pMAD
Mut GH F	atgatgagcgtaacgcta	Verification of the *llsGH* gene mutation
Mut GH R	tccatggtttcgtataca	Verification of the *llsGH* gene mutation
pPL2-Fw	ttcgacccggtcgtcggttc	Sequencing insert in pAD-based plasmid
pPL2-Rv	cttagacgtcattaaccctcac	Sequencing insert in pAD-based plasmid
NC16	gtcaaaacatacgctcttatc	Verification of the plasmid integration into the chromosome
PL95	acataatcagtccaaagtagatgc	Verification of the plasmid integration into the chromosome
gyrA-RT-PCR-F	gcgatgagtgtaattgttg	For quantitative Real-Time PCRs
gyrA-RT-PCR-R	atcagaagtcatacctaagtc	For quantitative Real-Time PCRs
llsA-RT-PCR-F	tcacaatcatcaaatggctaca	For quantitative Real-Time PCRs
llsA-RT-PCR-R	caagaacatgagcaacatcca	For quantitative Real-Time PCRs
llsG-RT-PCR-F	gagagagcgcagtttttacaca	For quantitative Real-Time PCRs
llsG-RT-PCR-R	tcgttgtttttctccaccag	For quantitative Real-Time PCRs
llsH-RT-PCR-F	cccggatattgatgccagta	For quantitative Real-Time PCRs
llsH-RT-PCR-R	ggaagttccgaaaaagatgaaa	For quantitative Real-Time PCRs
llsX-RT-PCR-F	ttcacatgaatgatggcaca	For quantitative Real-Time PCRs
llsX-RT-PCR-R	ttcccaccatctcactacca	For quantitative Real-Time PCRs
llsB-RT-PCR-F	ggcaattcaccaatgctagg	For quantitative Real-Time PCRs
llsB-RT-PCR-R	tccatttctcttgcctcgtt	For quantitative Real-Time PCRs
llsY-RT-PCR-F	acatggagaaactggctgct	For quantitative Real-Time PCRs
llsY-RT-PCR-R	caaacatcaattcagctgtgg	For quantitative Real-Time PCRs
llsD-RT-PCR-F	ggatgcctttgcaatttgtt	For quantitative Real-Time PCRs
llsD-RT-PCR-R	gcagtgcctgttgatacagc	For quantitative Real-Time PCRs
llsP-RT-PCR-F	acagtttgtggtagttttatcgc	For quantitative Real-Time PCRs
llsP-RT-PCR-R	tcacgaatgaaaaggtggct	For quantitative Real-Time PCRs

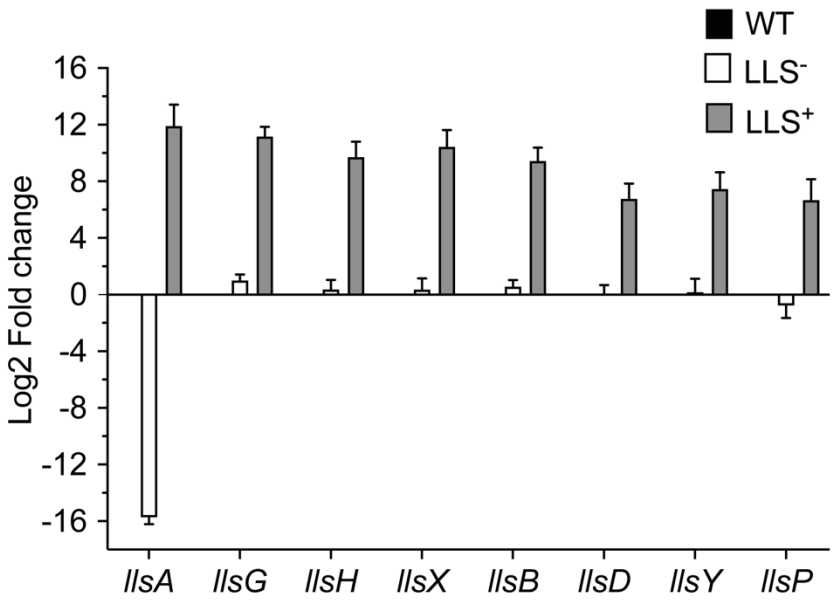

Figure S1. Transcription of LLS operon genes in the LLS$^+$ and LLS$^-$ strains. Expression of the LLS genes *in vitro* upon introduction of the strong constitutive promoter pHELP upstream of the *llsA* gene (LLS$^+$) or mutation of the *llsA* gene (LLS$^-$) in the *wt* strain. Values calculated by qPCR in comparison with the *wt* strain and normalized to the housekeeping gene *gyrA* represented as Log2 Fold change. Data from three independent biological experiments performed with three technical replicates are shown. Error bars show SEM.

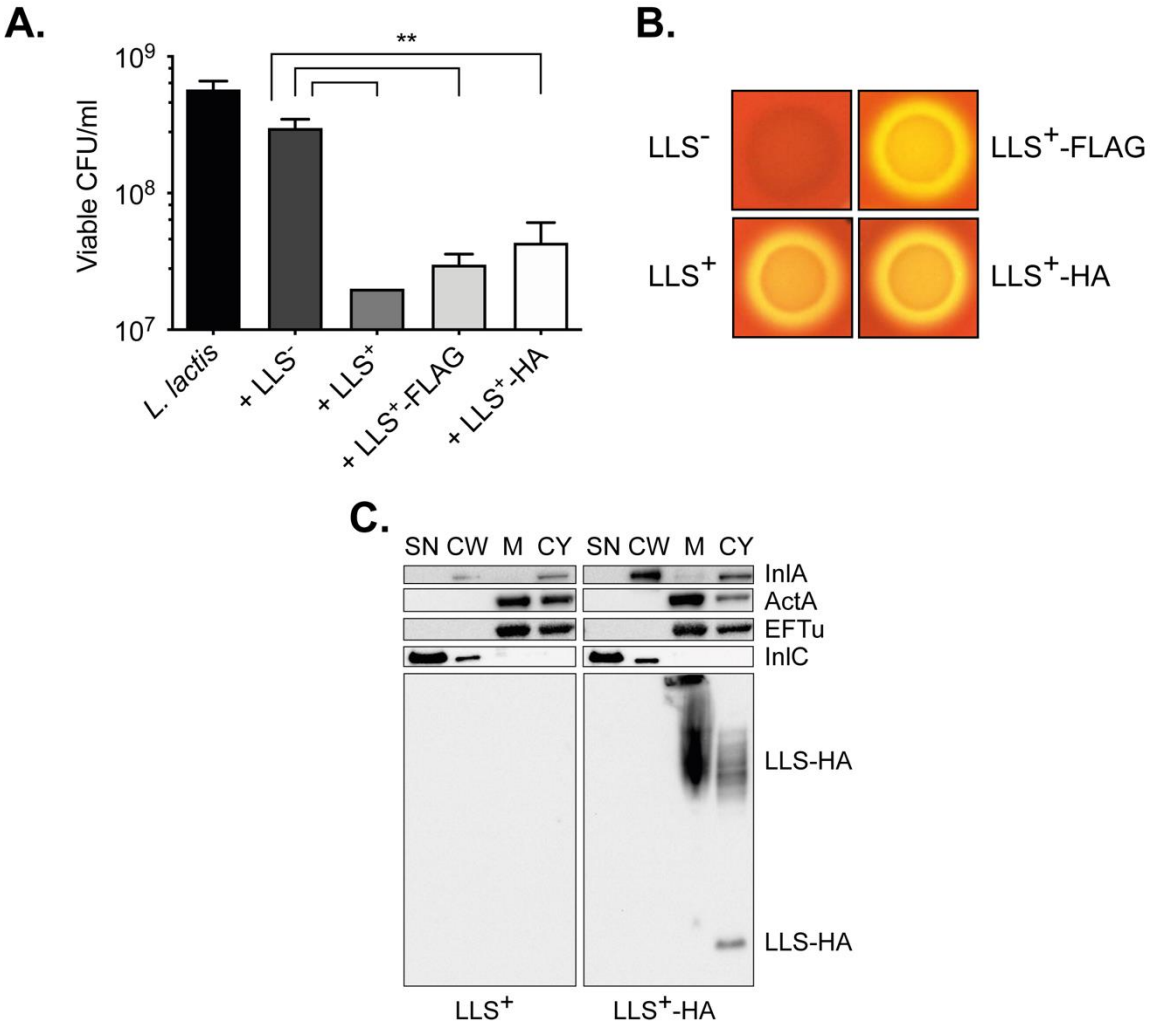

Figure S2. **LLS activity and localization upon addition of FLAG and HA tags.** (A) Target *L. lactis* bacteria were cultivated alone or co-cultivated with LLS mutant bacteria (LLS^-), LLS producer bacteria (LLS^+) or LLS producer bacteria with tags (LLS^+-FLAG and LLS^+-HA) during 24 h in BHI. Data from three independent biological experiments are shown. Error bars show SEM. Multiple two-tailed unpaired *t*-test were performed, LLS^- vs LLS^+ p= 0.0041, LLS^- vs LLS^+-FLAG p= 0.0048 and LLS^- vs LLS^+-HA p= 0.0070 (B) Assessment of hemolytic activity present in LLS^-, LLS^+, LLS^+-FLAG and LLS^+-HA strains in Columbia agar + 5% sheep blood. (C) Localization of LLS by fractionation experiments. Western Blot analysis was performed on a strain expressing LLS^+ (negative control) and a strain expressing LLS^+-HA (HA at the C-terminus). Proteins were fractionated in four compartments supernatant (SN), cell wall (CW), membrane (M) and cytoplasm (CY). InlA, ActA, EF-Tu and InlC were used as controls for fractionation. Equivalent amounts of each fraction, corresponding to 100 µl of bacterial culture were separated on SDS-PAGE and submitted to immuno-detection, using the indicated antibodies. Data from one representative experiment out of the three performed are shown.

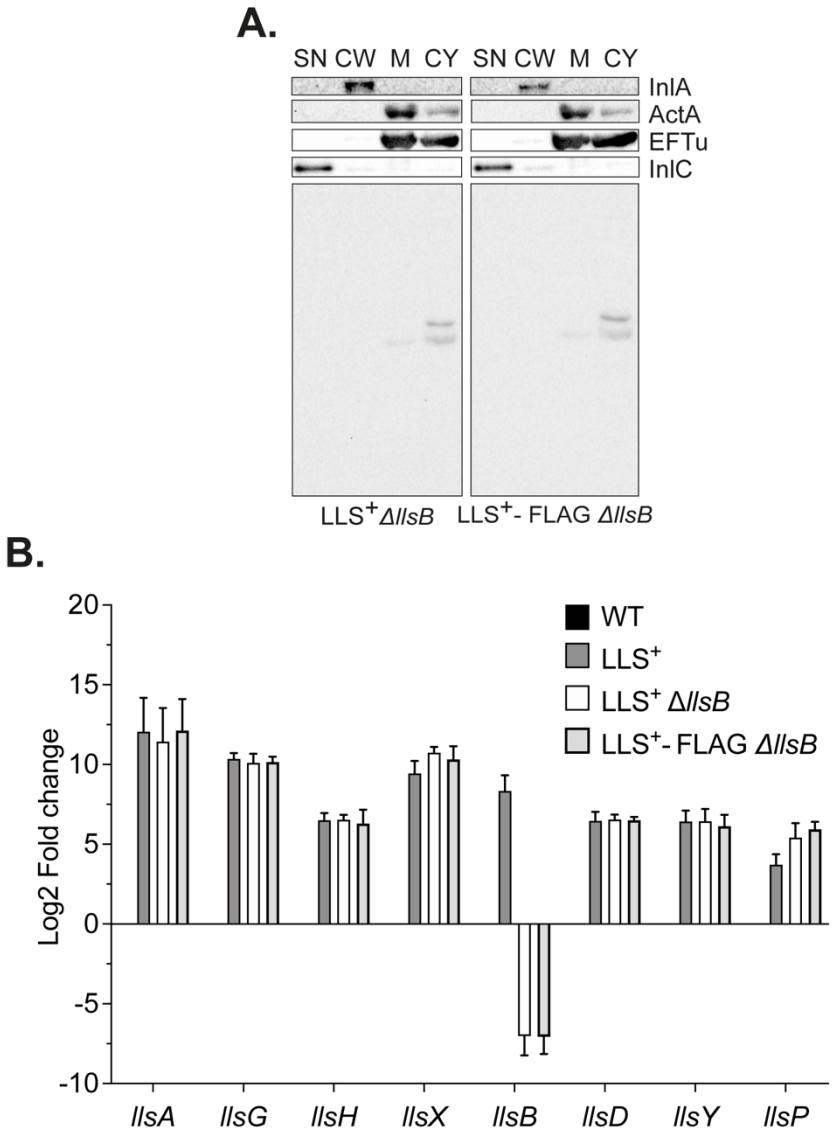

Figure S3. **Absence of LLS peptide and smear upon deletion of a putative subunit of the LLS post-translational machinery.** (A) Localization of LLS by fractionation experiments upon deletion of the *llsB* gene. Western Blot analysis was performed on LLS$^+$Δ*llsB* (negative control) and a LLS$^+$-FLAGΔ*llsB* strains. Proteins were fractionated in four compartments supernatant (SN), cell wall (CW), membrane (M) and cytoplasm (CY). InlA, ActA, EF-Tu and InlC were used as controls for fractionation. Equivalent amounts of each fraction, corresponding to 100 µl of bacterial culture were separated on SDS-PAGE and submitted to immuno-detection, using the indicated antibodies. Data from one representative experiment out of the three performed are shown. (B) Expression of the LLS genes *in vitro* in the *wt*, LLS$^+$ or LLS$^+$Δ*llsB* strains. Values calculated by qPCR in comparison with the *wt* strain and normalized to the housekeeping gene *gyrA* and represented as Log2 Fold change. Data from three independent biological experiments performed with three technical replicates are shown. Error bars show SEM.

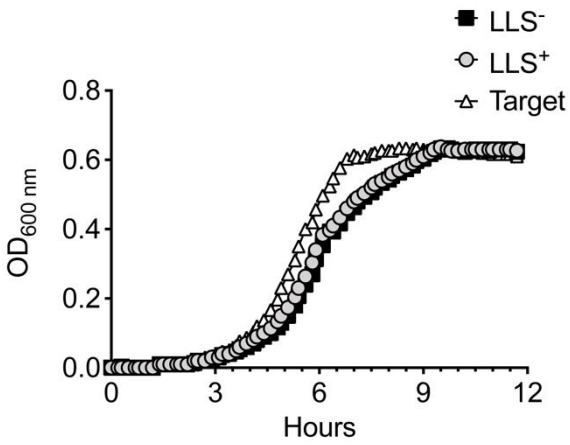

Figure S4. Growth curve of LLS$^-$, LLS$^+$ and target bacteria. *L. monocytogenes* F2365 (LLS$^-$ and LLS$^+$) and 10403S were grown in BHI media and OD_{600nm} measurements were taken every 20 minutes during 12 h in a Tecan's Sunrise absorbance microplate reader.

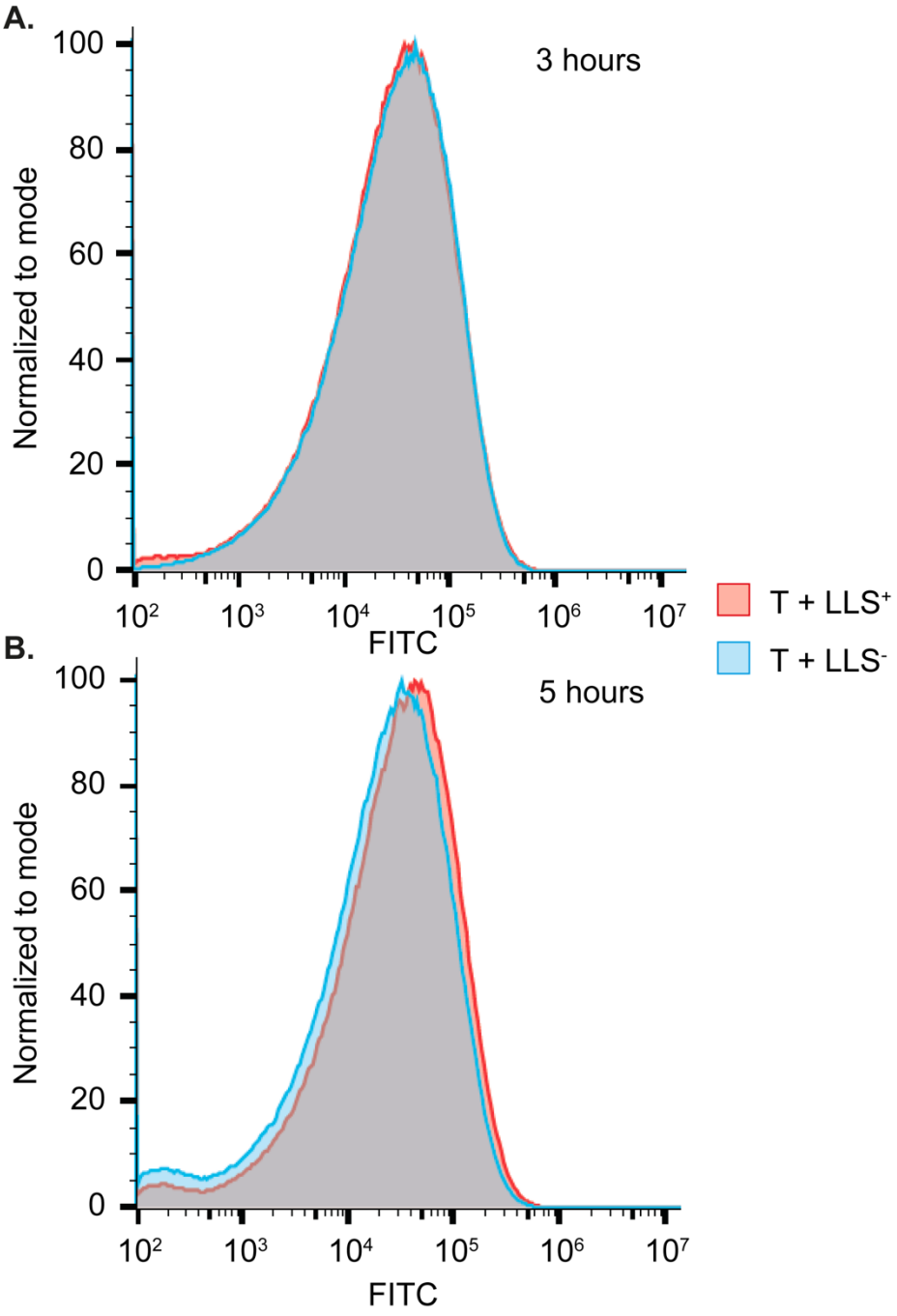

Figure S5. LLS does not affect the peptidoglycan synthesis of target cells. Click chemistry and flow cytometry analysis of 3-Azido D-Alanine labelled target bacteria (fluorescently labelled with Alexa fluor 594-alkyne via a copper-catalyzed click reaction). Labelled target bacteria were co-cultivated with LLS^- or LLS^+ cells during 3 h (A) and 5 h (B). Samples were acquired in a Cytoflex S and data were analyzed with FlowJo. Green fluorescence was collected from 40 000 FSC/SSC-gated bacterial events in the FITC channel and fluorescence intensities were plotted in single-parameter histograms that were normalized to mode for the two populations (target bacteria incubated with LLS^- or LLS^+). Data show one single experiment performed.

SI References

1. J. J. Quereda, *et al.*, Bacteriocin from epidemic *Listeria* strains alters the host intestinal microbiota to favor infection. *Proceedings of the National Academy of Sciences* **113**, 5706–5711 (2016).
2. C. U. Riedel, *et al.*, Improved Luciferase Tagging System for *Listeria monocytogenes* Allows Real-Time Monitoring In Vivo and In Vitro. *Applied and Environmental Microbiology* **73**, 3091–3094 (2007).
3. M. Arnaud, A. Chastanet, M. Debarbouille, New Vector for Efficient Allelic Replacement in Naturally Nontransformable, Low-GC-Content, Gram-Positive Bacteria. *Applied and Environmental Microbiology* **70**, 6887–6891 (2004).
4. D. Balestrino, *et al.*, Single-Cell Techniques Using Chromosomally Tagged Fluorescent Bacteria To Study *Listeria monocytogenes* Infection Processes. *Applied and Environmental Microbiology* **76**, 3625–3636 (2010).
5. J. Mengaud, *et al.*, Antibodies to the leucine-rich repeat region of internalin block entry of *Listeria monocytogenes* into cells expressing E-cadherin. *Infect. Immun.* **64**, 5430–5433 (1996).
6. P. Steffen, *et al.*, *Listeria monocytogenes* ActA protein interacts with phosphatidylinositol 4,5-bisphosphate in vitro. *Cell Motil. Cytoskeleton* **45**, 58–66 (2000).
7. R. Boujemaa-Paterski, *et al.*, *Listeria* Protein ActA Mimics WASP Family Proteins: It Activates Filament Barbed End Branching by Arp2/3 Complex. *Biochemistry* **40**, 11390–11404 (2001).
8. C. Archambaud, E. Gouin, J. Pizarro-Cerda, P. Cossart, O. Dussurget, Translation elongation factor EF-Tu is a target for Stp, a serine-threonine phosphatase involved in virulence of *Listeria monocytogenes*: EF-Tu, a target for the Listeria phosphatase Stp. *Molecular Microbiology* **56**, 383–396 (2005).
9. E. Gouin, *et al.*, The *Listeria monocytogenes* InlC protein interferes with innate immune responses by targeting the I B kinase subunit IKK. *Proceedings of the National Academy of Sciences* **107**, 17333–17338 (2010).
10. J. R. Mellin, *et al.*, Sequestration of a two-component response regulator by a riboswitch-regulated noncoding RNA. *Science* **345**, 940–943 (2014).
11. J. Schindelin, *et al.*, Fiji: an open-source platform for biological-image analysis. *Nat Methods* **9**, 676–682 (2012).
12. D. Legland, I. Arganda-Carreras, P. Andrey, MorphoLibJ: integrated library and plugins for mathematical morphology with ImageJ. *Bioinformatics*, btw413 (2016).
13. F. de Chaumont, *et al.*, Icy: an open bioimage informatics platform for extended reproducible research. *Nat Methods* **9**, 690–696 (2012).
14. I. Santi, N. Dhar, D. Bousbaine, Y. Wakamoto, J. D. McKinney, Single-cell dynamics of the chromosome replication and cell division cycles in mycobacteria. *Nat Commun* **4**, 2470 (2013).
15. M. J. Linnan, *et al.*, Epidemic Listeriosis Associated with Mexican-Style Cheese. *New England Journal of Medicine* **319**, 823–828 (1988).
16. D. K. Bishop, D. J. Hinrichs, Adoptive transfer of immunity to *Listeria monocytogenes*. The influence of in vitro stimulation on lymphocyte subset requirements. *J. Immunol.* **139**, 2005–2009 (1987).
17. E. G. D. Murray, R. A. Webb, M. B. R. Swann, A disease of rabbits characterised by a large mononuclear leucocytosis, caused by a hitherto undescribed bacillus *Bacterium monocytogenes* (n.sp.). *J. Pathol.* **29**, 407–439 (1926).

18. P. Mandin, *et al.*, VirR, a response regulator critical for *Listeria monocytogenes* virulence: Novel *Listeria* virulence regulon. *Molecular Microbiology* **57**, 1367–1380 (2005).

2.1.2 Investigation of LLS molecular targets

Some bacteriocins use cell envelope receptors as bacteriocin final targets and others use cell envelope receptors as docking molecules that allow bacteriocin internalization to target cytoplasmic bacterial molecules (38). In the case of LLS, our previous results suggest that the LLS target compartment is the cell envelope. Our hypothesis is that a specific molecular target is associated to the cell envelope of LLS sensitive bacteria.

Since LLS activity is dependent on cell contact between LLS producer and target bacteria, our first approach to identify the LLS molecular target was to perform proteomics of the target bacteria in contact with LLS^+ (producer bacteria) or with LLS^- (Δ*llsA*) as a negative control. The induced/repressed proteins could be indicative of the LLS target or of the LLS mechanism of action. For this, *Lm* 10403S GFP target bacteria were co-cultivated with LLS^+ or LLS^- bacteria during 4h, a time point where target bacteria are still viable but start to present some membrane permeabilization. After 4 hours of co-culture *Lm* 10403S GFP target bacteria were separated by using a cell sorter. Once a pure fraction of target bacteria was obtained, proteomics were performed in order to compare the differentially expressed proteins in target bacteria co-cultivated with LLS^+ or LLS^-. The proteins that were differentially expressed are shown in a volcano plot (Figure 20). Around 1000 proteins were identified for each sample which is around the half of *Lm* proteome.

In total 20 proteins were upregulated and 2 were downregulated in presence of LLS^+ cells (Figure 20). 6 out of 20 proteins are uncharacterized hypothetical proteins with domains of unknown function (not shown). Regarding the downregulated proteins, both of them are also hypothetical proteins with unknown functions (Annex 5, Table S6). The upregulated proteins were classified according to their functions. These proteins are mostly related to the energy metabolism, flagella proteins and osmotic shock response proteins (Table 8).

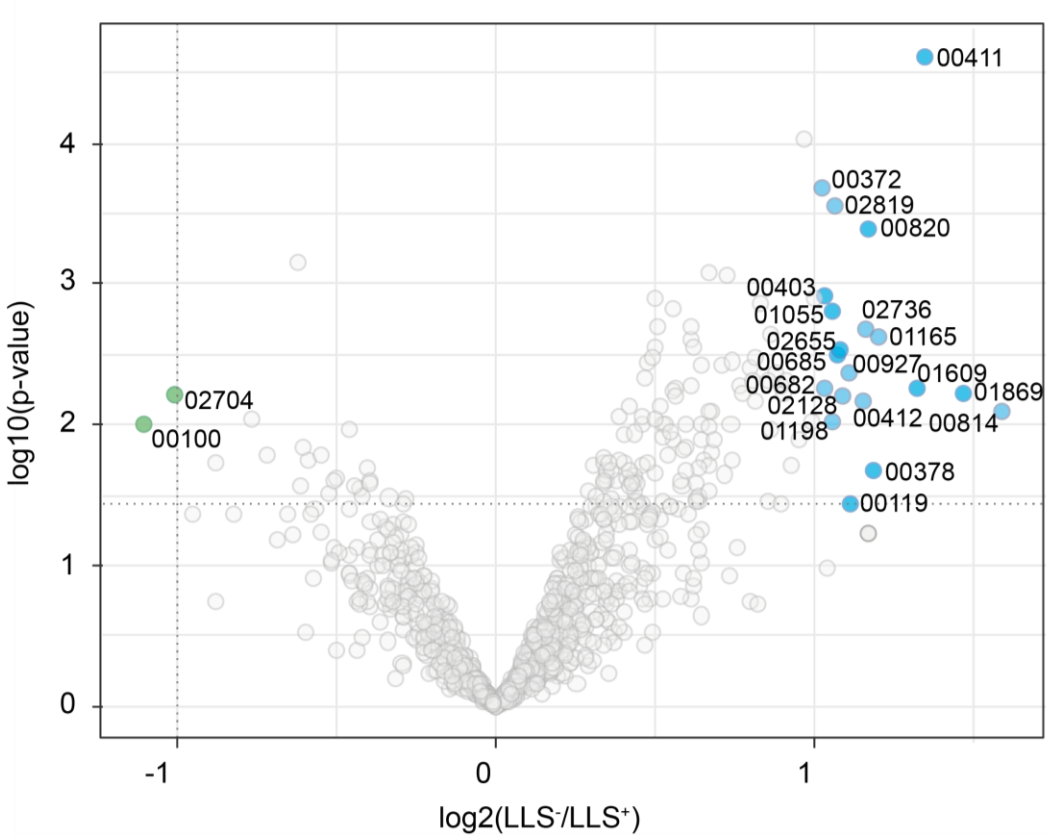

Figure 20. *Lm* 10403S proteins profile when co-cultivated with LLS$^+$ or LLS$^-$. A volcano plot represents the set of differentially regulated proteins in response to a 4 hours co-culture with LLS$^+$ or LLS$^-$. Blue (upregulated) and green (down-regulated) points are proteins with significantly altered expression in response to LLS$^+$, whereas gray points did not meet the q value (<0.01). Lm 10403S gene identifiers are indicated for the differentially upregulated and downregulated proteins. Experiments were performed 4 times independently.

In the absence of a specific response induced by LLS, we decided to analyze all the proteins that were exclusively present in the target cells incubated with LLS$^+$ but absent in target bacteria incubated with LLS$^-$ cells. A total of 38 proteins were exclusively present in target bacteria incubated with LLS$^+$ cells. We classified 28 proteins according to their functions (Table 9) and the rest 10 proteins were not classified because they contain domains of unknown function (Annex 5, Table S5). These proteins are involved in the energy metabolism, flagella proteins, antibiotics resistance, biosynthesis of amino acids and oxidative stress response. LLS target cells seem to counteract the LLS activity by producing energy, synthetizing amino acids and activating the production of proteins.

Table 8. Upregulated proteins in the target bacteria after co-culture with LLS^+

LMRG ID	Name	Function
Metabolism		
00411	Pyruvate oxidase	Piruvate metabolism energy production, amino acids or fatty acids production. Acetyl-P and CO_2 H_2O_2 products.
00820	Butyrate kinase	Increase in the presence of excess of glucose. ATP and butyrate products.
00119	Fructose-specific PTS IIB	Phosphorylated by phospho-IIA, before the phosphoryl group is transferred to the sugar substrate.
01055	MazG domain-containing protein	NTPs pyrophosphatases can hydrolyze rNTPs dNTPs to their respective NMPs and PP_i under amino acid starvation conditions.
00685	RdgB	Purine non-canonical NTPase hydrolyze nonstandard nucleotides such as XTP to XMP and ITP to IMP.
01869	Nitroreductase domain-containing protein	Metabolize nitro substituted compounds such as RNS. Involved in homeostasis and lipid signaling.
Flagella and chemotaxis		
00412	Methyl-accepting chemotaxis protein	Transduce the signal to swim towards nutrients and away from toxins.
00403	FliG	Flagellar motor switch protein.
00378	Flagellin	Polymerize flagellin to form flagella.
Osmotic shock response		
00927	Protein GrpE	Co-chaperone with capacity to stabilize proteins in their folded states under denaturing stress conditions.
01165	Cold shock protein	ssDNA or ssRNA binding to regulate transcription, translation and mRNA degradation.
00814	Cold shock-like protein cspLA	ssDNA or ssRNA binding to regulate transcription translation and mRNA degradation.
Cell wall remodelling		
02819	Glutamine amidotransferase	Peptidases C26 can hydrolyze bacterial cell wall peptides.
Translation		
02655	rplL	50S ribosomal protein L7/L12.

The general exposure to LLS induced general responses such as osmotic stress, metabolic responses, increase in the transcription and translation. Unexpectedly, the LLS increase the expression of flagellar proteins, for which the implications remain unclear. Interestingly, the membrane insertase protein YidC was overexpressed, a member of the Sec-dependent pathway that is involved in the entrance of newly synthesized proteins into the lipid bilayer (325). This could be an indication of the necessity to insert newly synthetized proteins into the membrane such as flagellar proteins, cytochrome C oxidase subunit II, and fructose-specific PTS IIB. Also, the Fur transcriptional regulator was upregulated, suggesting that the levels of iron are high and Fur represses siderophores synthesis and also avoid the formation of ROS (326).

Table 9. Proteins differentially expressed in the target bacteria after co-culture with LLS^+

LMRG ID	Name	Function
Metabolism		
02064	Adenylate cyclase	Conversion of ATP to 3',5'-cyclic AMP and PP_i
02442	Quinol oxidase polypeptide II	Cytochrome C oxidase subunit II
01434	Prephenate dehydratase	Phenylalanine biosynthesis
01775	Gluconeogenesis factor	Reduction of mannitol to fructose
02719	Aspartokinase	Synthesis of the essential amino acids Lys and Thr
00452	Lipoate--protein ligase	Adenylation of lipoic acid precursor BCAA
02001	Dihydroxyacetone kinase L subunit	Phosphorylate dihydroxyacetone, glyceraldehyde and other short-chain ketoses and aldoses.
02585	Aminotransferase	Carbohydrates and nitrogen metabolism
00819	Phosphate butyryltransferase	Produces CoA + butanoyl phosphate
Transcriptional regulators		
01103	Fur family transcriptional regulator	Metal ion uptake regulator proteins
01405	Transcriptional repressor NrdR	Unknown function
02363	Bacteriophage-type repressor	cro/C1-type HTH domain is a DNA-binding domain
01688	HTH gntR-type domain-containing protein	Transcriptional regulator
01929	RpiR family transcriptional regulator	Regulators of genes involved in phosphosugar metobolism.
Transcription translation		
01787	RNA polymerase sigma-54 factor	Transcription enhancer factor
00692	RNA helicase DbpA	Unwind short rRNA duplexes
01705	Glutamine N-methyltransferase (PrmC)	Stimulation of peptide chain release.
Transporters		
01944	ABC transporter	?
00831	Membrane protein insertase YidC	Membrane insertase
Flagella		
00405	FliI	Flagellar protein export ATPase for motor rotation
00404	FliH	Flagellum specific export
Antibiotics resistance		
01675	Lactamase_B domain-containing protein	Antibiotics resistance
00560	VOC domain-containing protein	Glyoxalase/Bleomycin resistance protein
Detoxification		
02403	HAD superfamily	Involved in amino acid biosynthesis and detoxification (IMP hydrolysis)
02083	Glutathione peroxidase	Reduction of hydroxyperoxides
01112	ADP-ribose pyrophosphatase	mutT homologue that degrade potentially mutagenic, oxidised nucleotides
02599	Haloacid dehydrogenase superfamily	Hidrolysis of IMP and GMP
Cell division		
00675	Cell division protein ZapA	Regulation of cell division

2.1.3 Identification of bacterial species sensitive to the LLS bactericidal mechanism(s)

The work from our group indicates that the significant reduction of *Alloprevotella* and *Allobaculum* populations in the gut microbiota of mice upon oral infection with *Lm* F2365 depends on the presence of LLS (308). These species are considered as protective microbiota species since they produce acetic and butyric acid that inhibit the growth and expression of *Lm* virulence factors (309). *Allobaculum* was previously identified as an early-life protective microbiota species and important for the immune development and response (327).

It is not clear whether *Lm* is capable of targeting *Allobaculum* and *Alloprevotella* in a direct manner. Since *Allobaculum* is a Gram-positive bacterium that belongs to the Firmicutes phyla, it might be a direct target of LLS (308). On the other hand, *Alloprevotella* is a Gram-negative bacterium from the Bacteroidetes phyla and is possible that it is not a direct target of LLS. Therefore, the decrease in *Alloprevotella* would be indirect as a result of the decrease of other microbiota bacterial species. Our objective was to determine whether *Allobaculum* and *Alloprevotella* are directely killed by LLS, and to identify additional bacterial species that are sensitive to the LLS bactericial mechanism(s).

To verify whether *Allobaculum* and *Alloprevotella* are direct LLS targets, we used *Allobaculum stercoricanis* (DSM 13633) isolated from canine feces (315) and *Alloprevotella rava* (DSM 22548) isolated from the human cavity (316). As shown in the previous results chapter (section 2.1.1), LLS is not actively secreted to the bacterial extracellular environment and we are obliged to used co-culture systems to explore the LLS bactericidal activity. However, both *Allobaculum* and *Alloprevotella* are fastidious anaerobic bacteria with a growth period of 3 days, and when co-cultivating these bacteria with LLS producers or LLS mutant bacteria under anaerobic conditions, their growth was completely inhibited in both conditions, making impossible to assess the LLS potential bactericidal effect *in vitro* (results not shown). Whether these microbiota species are directly targeted by LLS during *L. monocytogenes* lineage I infection remains therefore unknown.

The human gut microbiota is dominated by Bacteroidetes and Firmicutes (191) and so far, all the species that have been identified *in vitro* as targets of LLS belong to the Firmicutes phylum (*S. aureus, L. monocytogenes* and *L. lactis*) (308). In the Firmicutes, around 95% of gut commensal species are members of the *Clostridia* class (328). We were therefore interested in exploring the hypothesis that LLS could display bactericidal activity against pathogenic *Clostridium* species, for which narrow-spectrum antibiotics are needed. In co-culture experiments, while the *C. difficile* strain ATCC BAA-1382 did not display sensitivity towards LLS (results not shown), we were able to demonstrate LLS bactericidal activity against three strains of *C. perfringens* (Figure 21).

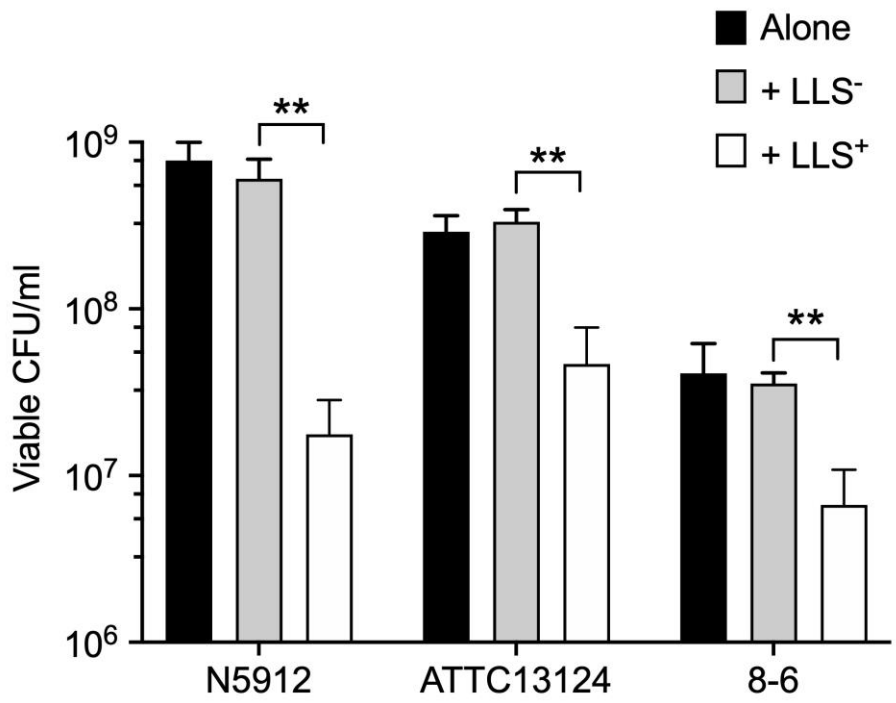

Figure 21. LLS inhibits the growth of *C. perfringens in vitro*. Survival of different strains of *C. perfringens* incubated during 24 h alone or in co-culture with LLS producer bacteria (LLS^+) or LLS mutant bacteria (LLS^-). Data from three independent experiments are presented. Error bar shows SD. Data were analyzed by using a Multiple *t*-test. **p < 0.01.

2.2 Discussion

2.1.2 Investigation of LLS molecular targets

After treatment with antimicrobial agents, bacteria experience changes in the expression of genes. These changes can be used to elucidate their mechanism of action (329). Some changes could be a direct consequence of target inhibition such as the SOS response after a treatment with a molecule that target DNA replication; and changes in tRNAs and nucleotides after exposure to molecules that inhibit RNA synthesis (330). Also, bacteria could experience some indirect effects such as general stress responses, metabolic changes and resistance mechanisms. Additionally, bacteria experience secondary effects due to downstream effects but not related to the mechanism of action and bystander effects of completely unrelated genes (329).

Interestingly, the formation of pores, induce efflux of metabolites such as amino acids, ATP or ions, favoring dissipation of the transmembrane electrical potential and causing a drop in the intracellular pH, therefore inhibiting many of the essential enzymatic processes (146, 331). Some active-membrane compounds are able to inhibit synthesis of RNA, DNA and proteins (332, 333). Is tempting to speculate that LLS induce pore formation and the several proteins involved in the ATP production and amino acids synthesis that were upregulated in target bacteria exposed to LLS are involved in counteracting LLS effects. The production of energy and excess of glycolysis products is confirmed by the presence of the glyoxalase/bleomycin resistance protein that is involved in the glyoxalase detoxification system against methylglyoxal and other aldehydes, which are metabolites derived from glycolysis (334).

We identified 3 proteins associated to the osmotic shock response. In general, stress responses such as the heat-shock response or osmotic shock responses are induced upon exposure to several antibiotics and have been related to stress conditions that are beyond the target and are considered indirect responses (335).

Intriguingly, the envelope stress response genes were not deregulated upon exposure to LLS^+ cells. For example, the LiaSR responds to cell wall antibiotics that interfere with the undecaprenol cycle and to perturbation of the cytoplasmic membrane (336). Enhanced resistance to nisin in *Lm* is associated with an increase in the LiaS HK (337,

338). Also, the VirRS TCS is involved in the regulation of genes that control surface charges that increase the resistance to cationic antimicrobial peptides in *Lm* (339–341). Additionally, the TCS CesRK is involved in the resistance of *Lm* to cell-wall acting antibiotics (342). None of these transcriptional regulators were upregulated in presence of LLS producer bacteria. Altogether, these results could indicate that LLS target is not associated to the cell wall.

Is worth to mention that since LLS is a CDI bacteriocin and not all target bacteria are exposed to LLS, the response dynamics of target bacteria could be heterogeneous in the bacterial target population. Also, the CDI make impossible to synchronize the contact of target bacteria to LLS making it hard to elucidate the specific changes induced by LLS. In future experiments, shorter times of exposure to LLS could be considered in order to obtain a more specific response rather than general stress responses that are indicative of indirect effects or downstream effects not associated to the LLS specific mechanism of action (329).

2.1.3 Identification of bacterial species sensitive to the LLS bactericidal mechanism(s)

Our group has identified for LLS a narrow-spectrum of activity against Gram-positive bacteria, specifically against Firmicutes. We were not able to clarify whether *L. monocytogenes* is capable of targeting *Allobaculum* and *Alloprevotella* in a direct manner. However, we managed to identify a new target of LLS which is *C. perfringens*. The narrow spectrum of bacteriocins makes them ideal candidates for their potential use as antibiotics (16). It has been shown that commensal species that produce bacteriocins are effective against enteropathogenic infections. For example, bacteriocin production by *Lactobacillus salivarus* UCC118 allows mice protection against oral *Lm* infection (343). Also, the bacteriocin Thuricin CD produced by *B. thuringiensis* is a narrow-spectrum bacteriocin that has activity against *C. difficile.* Thuricin CD was able to target *C. difficile in vivo* without changing dramatically the composition of the microbiota contrary to the changes observed during vancomycin and metronidazole antibiotics treatment (206).

Another example of ultra-narrow spectrum activity bacteriocin is the TOMM plantazolicin produced by *B. methylotrophicus* and *B. pumilus* and active against *B. anthracis* by the depolarization of its membrane leading to cell lysis (207). However, for its clinical use, the potential activity of plantazolicin *in vivo* needs to be evaluated. Interestingly, some bacteriocins display a broad-spectrum of activity allowing their potential use as broad-spectrum antibiotics when the infection agent is unknown in advance, for example in the food industry. Nisin displays a broad-spectrum of activity, and is the only bacteriocin licensed as a food additive over 45 countries for its activity against Gram-positive bacteria to preserve food. Pediocin PA-1 displays as well a wide-spectrum against Gram-positive bacteria including those responsible for food spoilage or foodborne diseases as *L. monocytogenes* (41). These broad-spectrum activities make them suitable for their use in the food industry (16).

To date, the most interesting LLS targets identified *in vitro* are the human pathogens *S. aureus* and *C. perfringens.* The bactericidal effect of LLS against these pathogens highlights its potential use as an alternative antibiotic. However, our results indicate that LLS is highly hydrophobic, making it not a good candidate to use as an antibiotic. On the other hand, engineering of LLS may potentially render it more soluble and suitable to potentially use it as antibiotic to treat infections caused by multi-resistant microorganisms such as *S. aureus.* In the same line, other Firmicutes that are causing agents of infection such as *Bacillus, Streptococcus*, and *Enterococcus* could be potential targets of LLS (220, 344–348).

In order to consider LLS as a potential antibiotic it is crucial to assess its activity in more clinically relevant circumstances. Additionally, is possible to consider the option of administration of a non-pathogen *L. innocua* that produces LLS at the site of infection as a probiotic. Eventually, the potential clinical application of LLS as an antibiotic will depend on the complete understanding of its mechanism of action.

2.3 Materials and methods

Co-culture bacterial assays

Co-culture assays were performed for 24 h statically at 37 °C in anaerobic conditions (AnaeroGen, Oxoid) as previously described (349). Briefly, 5 × 10^7 bacteria from

overnight cultures were inoculated into 5 mL of fresh BHI either alone or in coculture with another strain as indicated. At 24 h after inoculation, cultures were serially diluted and plated on BHI and Oxford agar plates (Oxoid) under anaerobic conditions. *Alloprevotella rava* was cultivated under strict anaerobic conditions in fastidious anaerobe agar and *Allobaculum stercoricanis* was cultivated under anaerobic conditions in PYG medium (modified) as recommended by the DSMZ German Collection of Microorganisms and Cell Cultures GmbH. Experiments were performed three times independently.

Flow cytometry and cell sorting

After 4 hours of co-culture bacteria were centrifuged, washed once and resuspended in PBS. GFP target bacteria were purified with a FACSAria III (Becton Dickinson), a nozzle of 70 µm was used. Bacteria were positively selected at 4°C with the FITC channel (530nm/40nm bandpass filter) collecting a maximum 10 000-FSC/SSC-gated bacterial events per second in a 15 mL tube. Approximately 1 x 10^8 bacteria were isolated after 5 hours. Collected bacteria were centrifuged, washed twice and resuspended in 250 µL of HEPES buffer (20 mM HEPES pH 8.0, 1 mM $MgCl_2$) in low binding eppendorf tubes. Approximately 25 ng of mutanolysin was added to each suspension and samples were incubated for 1hr at 37˚C. Ureum was added dry to both samples to a final concentration of 8 M. Lysates were sonicated by four bursts of 15 seconds at an amplitude of 20%. Then, lysates were cleared by centrifugation for 15 min at 16000g at RT. The protein concentration in the supernatans was measured by BCA. Experiments were performed four times for each condition, independently.

Proteomics

Equal amount of proteins from target bacteria exposed to LLS^+ or LLS^- were precipitated by using a TCA-Acetone approach. Briefly, a volume of ice-cold TCA was added to the sample, vortex and 1 volume of ice-cold acetone was added. Samples were incubated at 4°C for 30 min and proteins were pelleted at 16 000 g for 15 min at 4°C. Resulting pellet was washed twice in ice-cold acetone and spin down. Remaining acetone was removed under hood. Pellet of proteins was resuspended in ammonium bicarbonate 50 mM and reduced using TCEP 10mM for 30 min at RT with sonication steps. Alkylation of reduced disulfide bridges was done using iodoacetamide 20mM for 30 min at room temperature in the dark. Digestion of protein was performed using 500

ng of trypsin (Promega) and performed at 37°C overnight. Digestion was stopped adding 1% final of TFA and resulting peptides were desalted using homemade stage tips and lyophilized until further LC-MS analysis. Peptides were resuspended in loading buffer (0.1% FA). LC-MS/MS analysis of digested peptides was performed on an Orbitrap Q Exactive Plus mass spectrometer (Thermo Fisher Scientific, Bremen) coupled to an EASY-nLC 1200 (Thermo Fisher Scientific). A home-made column was used for peptide separation (C18 40 cm capillary column picotip silica emitter tip 75 µm diameter filled with 1.9 µm Reprosil-Pur Basic C18-HD resin, Dr. Maisch GmbH, Ammerbuch-Entringen, Germany). The column was equilibrated and peptide were loaded in solvent A (0.1 % FA) at 800 bars. Peptides were separated at 250 $nl.min^{-1}$. Peptides were eluted using a gradient of solvent B (ACN, 0.1 % FA) from 3% to 22% in 140 min, 22% to 42% in 61 min, 42% to 60% in 15 min, 60% to 75% in 15 min (total length of the chromatographic run was 240 min including high ACN level steps and column regeneration). Mass spectra were acquired in profile mode in data-dependent acquisition mode with the XCalibur 2.2 software (Thermo Fisher Scientific, Bremen) with automatic switching between MS and MS/MS scans using a top-10 method. MS spectra were acquired at a resolution of 70000 (at m/z 400) with a target value of 3×10^6 ions. The scan range was limited from 200 to 2000 m/z. Peptide fragmentation was performed using higher-energy collision dissociation (HCD) with the energy set at 26 NCE. Intensity threshold for ions selection was set at 1×10^6 ions with charge exclusion of $z = 1$ and $z > 7$. The MS/MS spectra were acquired in profile mode at a resolution of 17500 (at m/z 400). Isolation window was set at 1.6 Th. Dynamic exclusion was employed within 35s.

Acquired MS data were searched using MaxQuant (version 1.5.3.8) (with the Andromeda search engine) against homer made database proteome of *Listeria monocytogenes* 10403S. The following search parameters were applied: carbamidomethylation of cysteines was set as a fixed modification, oxidation of methionine and protein N-terminal acetylation were set as variable modifications. The mass tolerances in MS and MS/MS were set to 5 ppm and 20 ppm respectively. Maximum peptide charge was set to 7 and 7 amino acids were required as minimum peptide length. Two miss cleavages for trypsin were allowed. A false discovery rate of 1% was set up for both protein and peptide levels. The iBAC feature was also search by the search engine.

Proteomics statistical analysis

Quantification of each identified protein was performed by summing the intensities of its associated peptides if at least 1 unique peptide was identified per protein. For the statistical analysis of one condition versus another, proteins identified in the reverse and contaminant databases and proteins “only identified by site” (with an identification score too low - not exceeding the 1% FDR threshold) were first discarded from the list. Then, proteins exhibiting fewer than 2 summed intensities in at least one condition were discarded from the list to avoid misidentified proteins. After log2 transformation of the leftover proteins, summed intensities were normalised by median centering within conditions (normalizeD function of the R package DAPAR) (350). Remaining proteins without any summed intensities in one of both conditions have been considered as proteins present in a condition and absent in another. They have therefore been set aside and considered as differentially abundant proteins. Next, missing values were imputed using the impute.slsa function of the R package imp4p (351). Proteins with a fold-change inferior to 1.5 (log2(FC) inferior to 0.58) have been considered as proteins which are not significantly differentially abundant. Statistical testing of the remaining proteins (having a log2 (fold-change) superior to 1) was conducted using a limma t-test thanks to the R package limma (352). An adaptive Benjamini-Hochberg procedure was applied on the resulting p-values thanks to the function adjust.p of R package cp4p (353) using the robust method of Pounds and Cheng (2006) to estimate the proportion of true null hypotheses among the set of statistical tests (354). The proteins associated to an adjusted p-value inferior to a FDR level of 1% have been considered as significantly differentially abundant proteins. Finally, the proteins of interest are therefore those which emerge from this statistical analysis supplemented by those which are considered to be absent from one condition and present in another.

Statistics

The Shapiro-Wilk test was used to test normal distribution of datasets. Normally distributed data with equal group variances were expressed as means ± standards deviation (SD). Statistical tests were performed using Prism 8.0 (GraphPad Software) and differences were evaluated by Multiple *t*-tests as indicated. The level of significance was set at *$p<0.05$. Significant differences are represented by asterisks (**$p<0.01$).

PART III: Investigation of mechanisms regulating the expression of LLS

The transcriptional factors or signals involved in the activation of the LLS operon during the *in vivo* infection are unknown and whether the activation of LLS is also triggered in environmental conditions or only during host infections requires further investigation. Moreover, the predicted *llsA* promoter does not contain motifs associated with virulence gene regulation in other *L. monocytogenes* strains such as PrfA box or σ^B binding site (253), which suggest that the LLS regulators are different from the classical virulence regulators described for lineage II strains since the LLS operon is absent in these strains.

Quereda *et al*. (2016) demonstrated that LLS is not expressed under standard *in vitro* growth conditions and that its production is detected only *in vivo* within the intestine of infected mice (308). The expression of some bacteriocins is triggered in the presence of other bacteria (355), so it was hypothesized that the expression of LLS could be triggered in presence of the gut microbiota. However, the expression of LLS is induced in GFM (308), suggesting that there should be a host-derived combination of signals triggering the expression of LLS. None of the compounds that could induce LLS expression that are present in the gut tested by Quereda *et al.* (mucin, gastric fluid, trypsin, pepsin, $NaHCO_3$, bile salts, detergents, succinic acid, butyric acid, propionic acid, valeric acid, octanoid acid, ethanolamine, different antibiotics and microaerophilic conditions) activated the expression of LLS *in vitro* (308). Our aim was to study the transcriptional factors and the mechanisms underlying LLS regulation including the LLS specific activation signal(s).

3.1 Results

3.1.1 *In silico* investigation of the *llsA* promoter region

To analyze the *llsA* promoter region, we performed *in silico* analyses to identify DNA motifs recognized by transcription factors, using the MEME suite database of known motifs present in prokaryotes (356). The scanning algorithm TOMTOM allowed us to scan for transcription factors motifs, by comparing one or more motifs against the MEME database and to produce an alignment for the significant matches (357). We looked for motifs around 150 base pairs upstream from the *llsA* start codon site. We

found 3 significant matches: the CcpA box from *S. pneumoniae* (E-value 5.03^{-05}), the CodY box from *S. pyogenes* (E-value 2.99^{-01}) and the MogR box from *L. monocytogenes* (E-value=3.76^{-02}) (Figure 22).

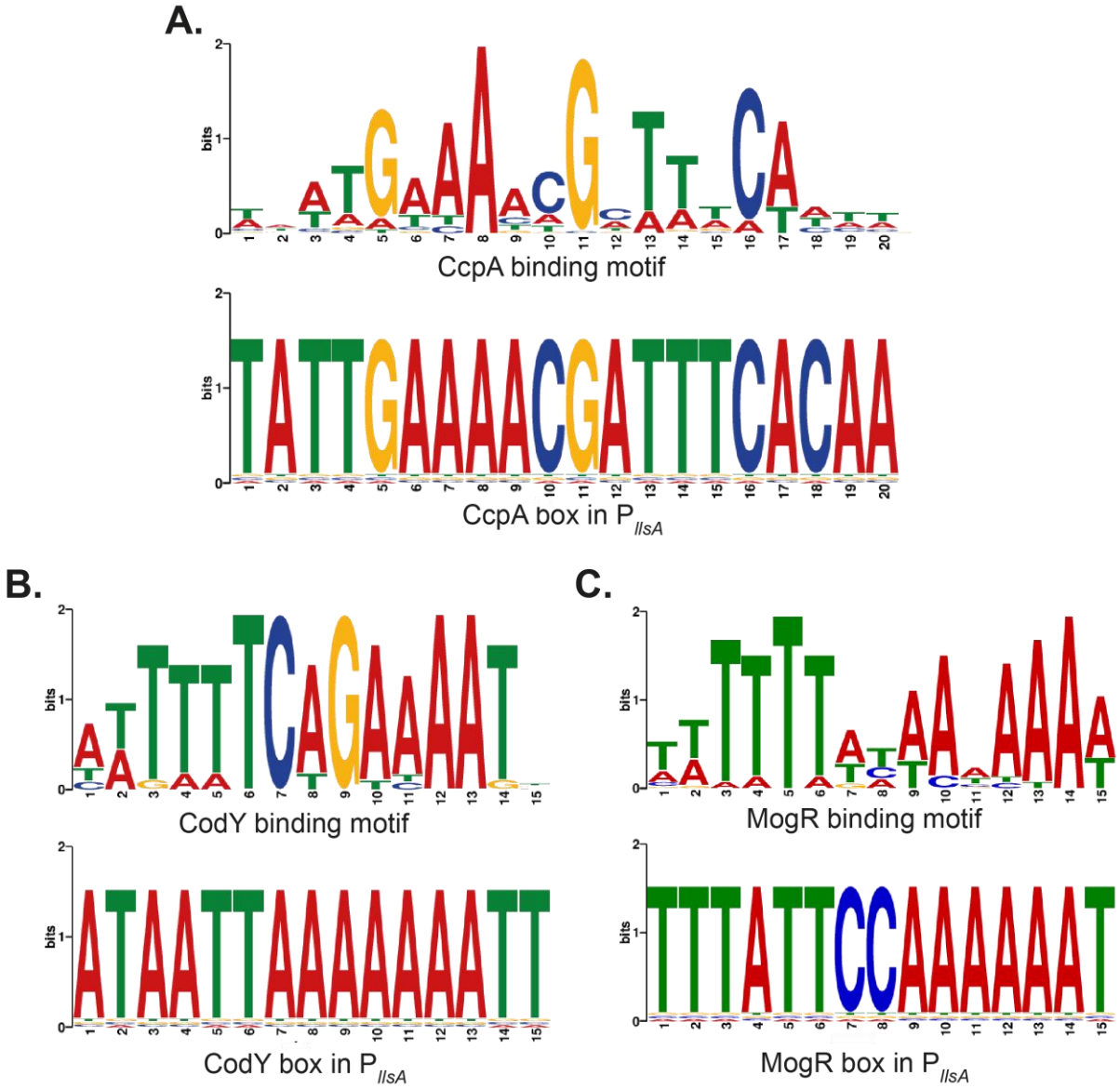

Figure 22. Putative transcription factors motifs present in the P_{llsA}. A. A CcpA binding motif from *S. pneumoniae* is present from -77 to –58 upstream from the start codon site (p-value=5.99^{-07}, E-value =5.03^{-05} and q-value=5.03^{-05}) **B.** A CodY binding motif from *S. pyogenes* is present from -139 to -125 upstream from the start codon site (p-value=3.56^{-03}, E-value=2.99^{-01} and q-value=1.85^{-01}). **C**. A MogR binding motif from *L. monocytogenes* is present from -32 to -18 upstream from the start codon site (p-value=4.47^{-04}, E-value=3.76^{-02} and q-value=3.76^{-02}).

CcpA is the main global regulator of carbon catabolite repression, it belongs to the LcI/GalR family of transcription factors and influences the expression of a wide range of catabolic operons in Gram-positive bacteria (358). CcpA allows the utilization of

preferred available sugars (359) and is also important for the regulation of virulence genes. For example, is required for *S. pneumoniae* colonization of the nasopharynx, survival and multiplication in the lung (360). In GAS, CcpA is responsible for repressing around 6% of the genome (124 genes) including SLS. CcpA repress SLS activity and virulence during systemic infection in mice, important process for GAS pathogenesis (361). In *L. monocytogenes*, CcpA is not involved in controlling virulence (362). PrfA is inhibited in the presence of glucose or other PTS substrates. However, the mechanism that inhibits PrfA upon sugar availability is unknown and independent from CcpA. Though, PTS-dependent transport activity seems to be crucial for PrfA signaling (363).

CodY is a global transcriptional regulator. CodY can regulate negatively or positively the expression of genes. For example, in *S. pyogenes*, CodY controls the expression of about 17% (250 genes) of the genome (364). The low levels of branched-chain amino acids (BCAAs) render CodY a more active repressor. In general, CodY downregulates the negative regulator CovRS, which is a negative transcriptional regulator of the SLS operon (365). Increases in CodY levels through BCAA starvation, indirectly enhance SLS expression (366). In *L. monocytogenes*, CodY is a global transcriptional regulator that controls directly or indirectly the metabolism, motility and virulence genes, including PrfA and SigB (367). In *Lm,* the BCAAs and isoleucine serve as ligands for CodY and modulate its activity. When the bacteria are starved, BCAAs levels increase and bind CodY, CodY functions as an activator of virulence genes, including *prfA* (368). On the other hand, when isoleucine is present it bounds CodY, which works as a repressor of metabolic pathways, including BCAA biosynthesis (369).

In *L. monocytogenes,* MogR represses the expression of flagellin during the extracellular growth at 37°C and during intracellular infection. MogR is also required for virulence *in vivo* in the murine model. MogR represses transcription of all known flagellar motility genes by binding directly to a minimum of two TTTT-N_5-AAAA recognition sites positioned within promoter regions such that RNA polymerase binding is occluded (370).

3.1.2 *In silico* investigation of potential regulatory RNA elements

Besides transcriptional regulators, *cis* or *trans* antisense regulatory RNA elements or 5'UTR *cis*-acting RNA (riboswitches) can control gene expression (371, 372). In *L. monocytogenes* around 50 sRNAs and 40 riboswitches have been identified in EGD-e (301). To explore whether we could predict a 5'UTR *cis*-acting RNA in the LLS promoter region, we used the tool PASIFIC, created to predict regulatory elements or premature termination sites in bacteria (373). We were able to predict two potential riboswitches, both with a score above 0.5 which is considered reliable. The first riboswitch with a score 0.67 upstream the *llsA* region (from -272 to -217). A second one with a 0.63 score predicted inside the *llsA* gene region (from +55 +149) (Figure 23). We hypothesize that the first riboswitch is involved in the inhibition of the *llsA* gene and the second one in the inhibition of the downstream genes (*llsGHXBDYP*).

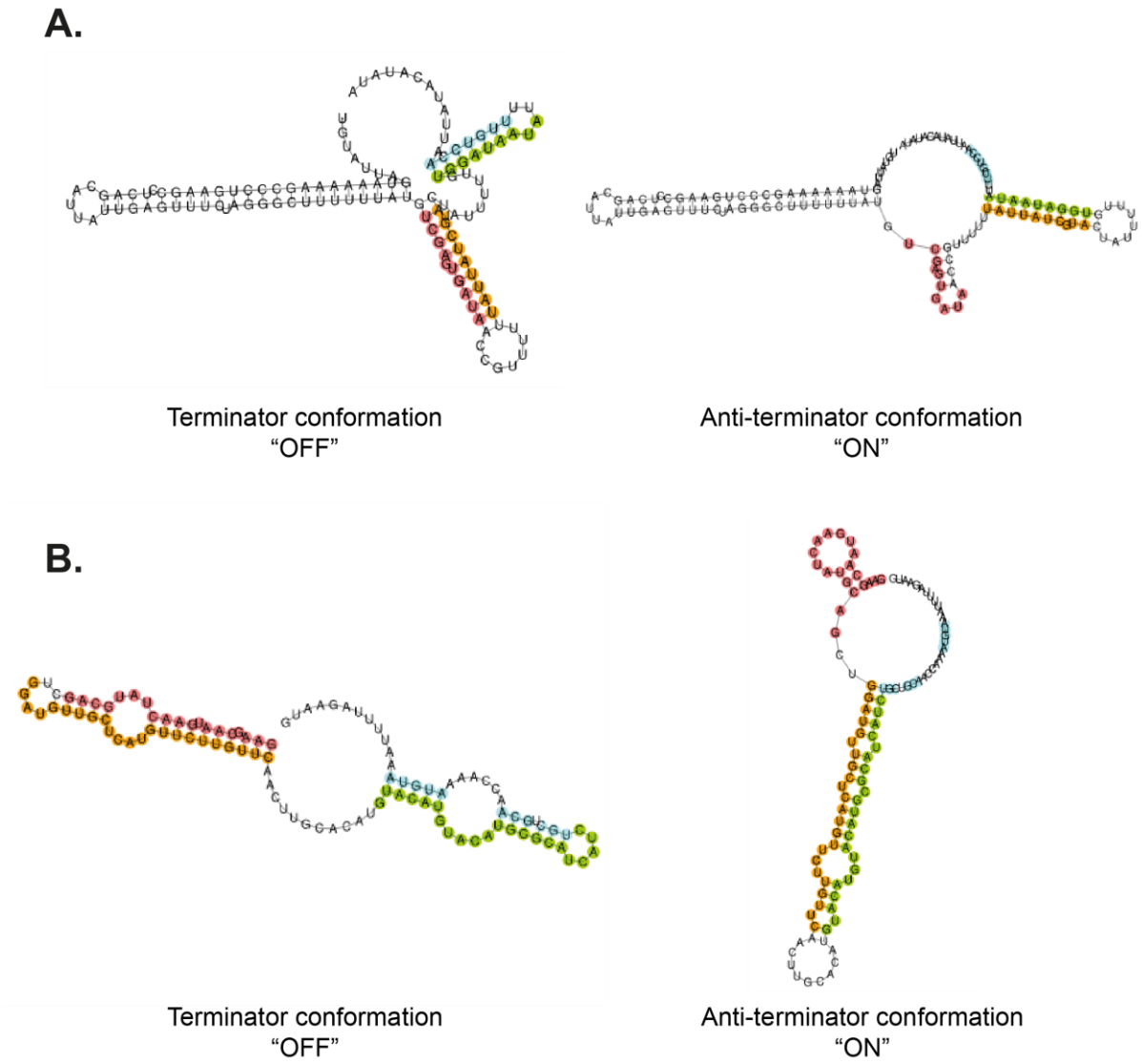

Figure 23. Predicted *cis*-acting regulatory RNA structures present in the P_{llsA}. Riboswitches were predicted using the PASIFIC algorithm, and two alternative conformations were anticipated for both riboswitches, one with an intrinsic terminator (left) and one with an anti-terminator (right). **A.** Predicted terminator (Free energy: -34.80 kcal/mol) and anti-terminator (Free energy: -30.60 kcal/mol) for the *llsA* upstream region. **B.** Predicted terminator (Free energy: -21.30 kcal/mol) and anti-terminator (Free energy: -18.90 kcal/mol) for the *llsA* region.

3.1.3 *In vivo* investigation of the LLS gene cluster transcription

To study whether these predicted transcriptional factors and/or regulatory RNA elements are involved in LLS regulation we planned to perform transcriptomics of *Lm* F2365 *in vivo,* specifically in the GIT of orally infected mice where the LLS operon is active. This technique could allow us to identify potential transcriptional regulators that are overexpressed in the GIT, sRNAs and/or riboswitches that could be involved in LLS operon regulation. This approach has been used before with success for the *L. monocytogenes* strain EGD-e (301).

First, C57BL/6J female GFM were orally infected with an inoculum of 5 $x10^{10}$ *L. monocytogenes* F2365 per mice. RNA was then extracted from the small intestine content after 24 and 48 hours of infection. Unfortunately, this strain caused epithelial intestinal cell shedding and lysis, and we obtained mostly eukaryotic RNA and no prokaryotic RNA (Figure 24A). In order to avoid the epithelial intestinal cell shedding and lysis, we performed oral infection of C57BL/6J female and male GFM with a lower dose (5 $x10^9$ bacteria per mice) and performed the RNA extraction 24h after infection. Possibly male mice were more resistant to *Lm* infection because we observed less eukaryotic RNA, but still we did not obtain prokaryotic RNA (Figure 24B). When using a lower infection dose (5 $x10^8$ bacteria per mice) in germ-free male C57BL/6J mice, we obtained a much lower quantity of eukaryotic RNA at 7h of infection and almost no eukaryotic RNA at 24h of infection (Figure 24C). However, the quantity of extracted prokaryotic RNA was still too low to perform a transcriptomic analysis (10-15 ng/µl).

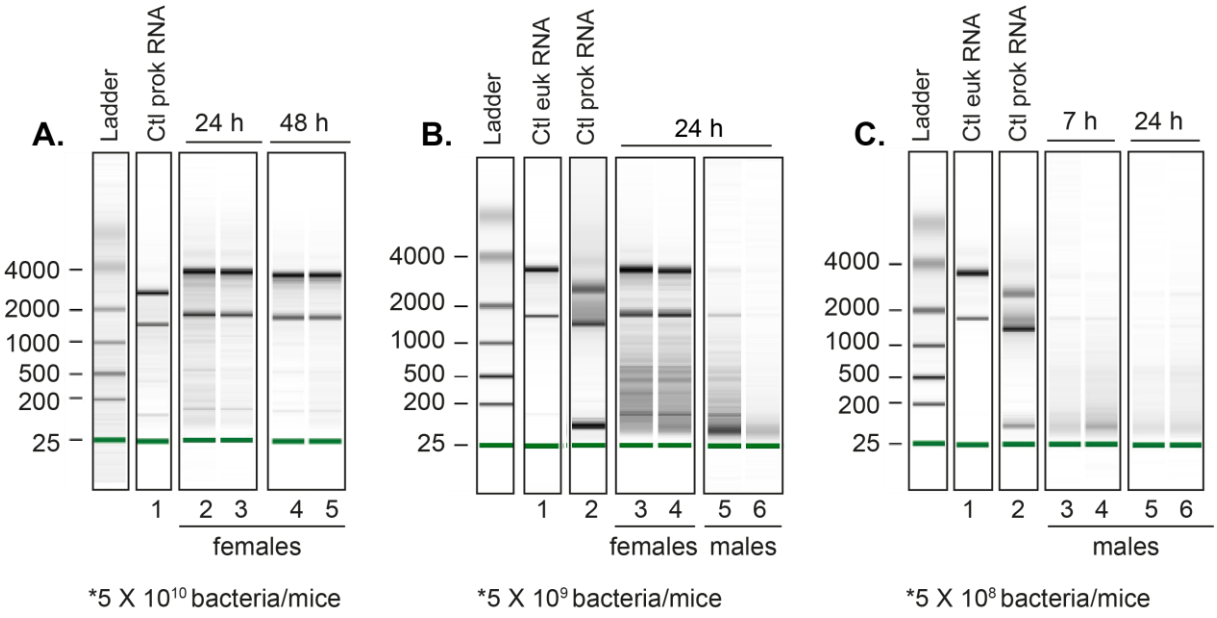

Figure 24. RNA extraction from the small intestine content of GFM after *Lm* F2365 oral infection. Female or male C57BL/6J mice were orally infected with *Lm* F2365. The total RNA from the intestinal content was extracted after different times after infection (7, 24 and 48h). Different inoculums were used: (A) 5 x10^{10} bacteria per mice, (B) 5 x10^{9} bacteria per mice and, (C) 5 x10^{8} bacteria per mice. As control, prokaryotic RNA or eukaryotic was extracted from *in vitro* cultivated bacteria or intestinal epithelial cells, respectively.

3.1.4 *In vitro* investigation of the LLS activation signal (s)

We performed an *in vitro* screen to identify molecules that could activate the LLS gene expression, in collaboration with the Chemogenomic and Biological Screening Platform at Institut Pasteur. To perform the screen, molecules from thwo different libraries were used: Sigma LOPAC library and an internal library with FDA approved compounds from Sigma, Enzo Life Sciences and Selleckchem. Only molecules that mimic or are homologous to components present in the GIT were tested.

A bioluminescent reporter was used before to explore the LLS activation signal in discrete experiments, however this reporter is not suited for medium- or high-throughput screens. For this reason we construct a different transcriptional reporter, the *llsA* promoter region was fused to the GFP protein and placed in a plasmid that integrates into the chromosome of *Lm* F2365 (WT pAD::P_{llsA}-GFPmut2) (374). As positive control for the high-throughput screen, the previously constructed reporter pKSV7::$P_{lmo2230}$-eGFP was used (375). This gene encodes for a putative arsenate

reductase, is regulated by σ^B and is induced under stress conditions during the stationary phase or under high osmotic conditions such as 0.5 M of NaCl (Figure 25) (375).

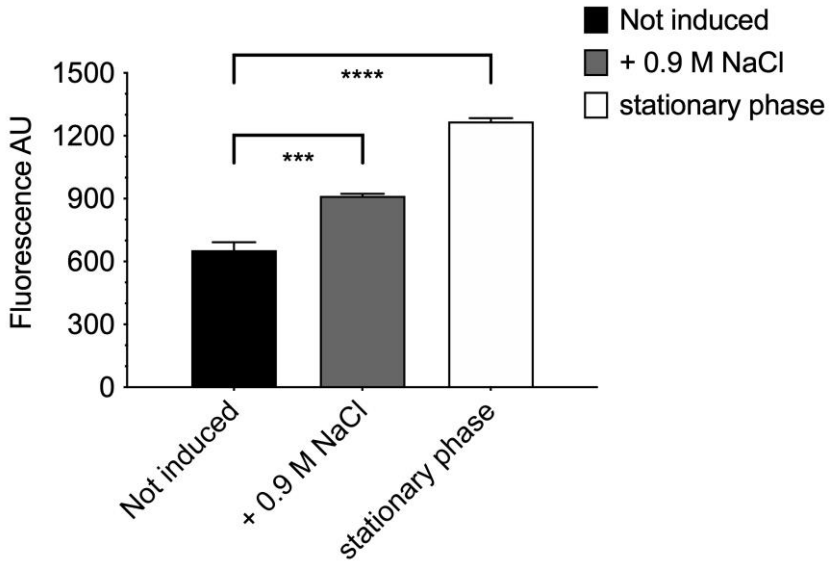

Figure 25. Induction of the $P_{lmo2230}$ during stress conditions. Cells were grown in BHI until an OD_{600nm} =1(not induced), incubated 30 min with BHI + 0.9 M NaCl or grown overnight in BHI OD_{600nm} =2.5. Error bars show SD. Multiple unpaired were performed. ***p< 0.001, ****p< 0.0001) n=3.

In total 927 molecules were tested at a 10 micromolar final concentration and were plated by a liquid acoustic dispenser (Echo550, labcyte) in 384 well plates. Bacteria were resuspended in NaCl 0.8 M buffer and fluorescence was detected in a Cytation5 Each 30 minutes during 10 hours. From all tested molecules, only 8 showed an increase in the GFP fluorescence (Figure 26). These molecules are: idarrubicin, ergotamine, amrinone, reserpine, emodin, quinacrine dihydrochloride, CRANAD 2, and sunitinib malate. For all the molecules there is sustained increase in the GFP fluorescence over time, except for Idarubicin (Figure 26). The idarubicin could be toxic to bacteria, inhibiting bacterial growth (376).

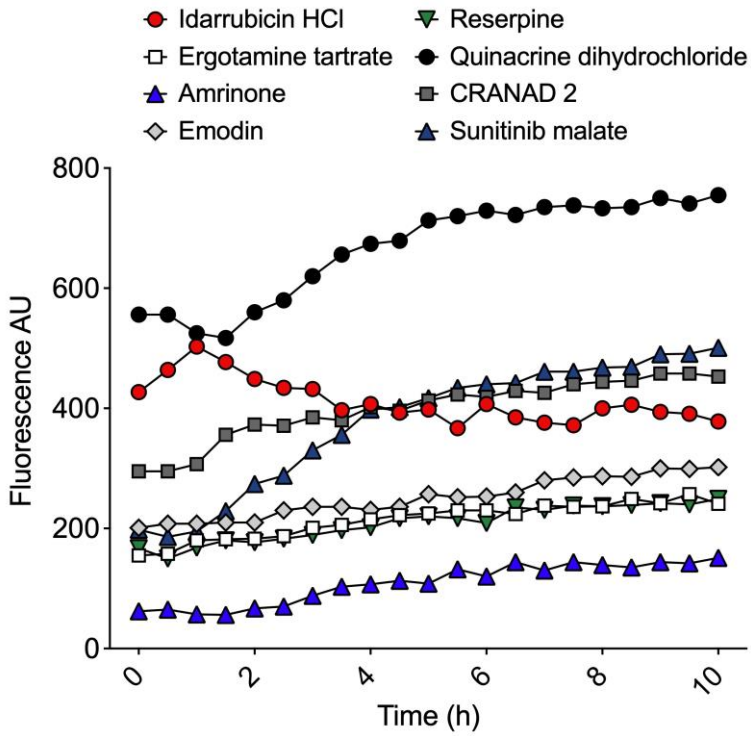

Figure 26. Induction of the P_{llsA} promoter after incubation with different compounds. Bacteria harboring pAD::P_{llsA}-GFPmut2 reporter were grown in BHI until an OD_{600nm} =1. Plates were incubated during 10 hours and read every 30 min (37°C, 5% CO_2).

To confirm that this activation was specific to the *llsA* promoter activation and not due to autofluorescence of the compounds, a validation test was performed. The fluorescence of the the WT strain (*Lm* F2365) lacking the reporter (Figure 27A) was compared with the reporter strain (WT pAD::P_{llsA}-GFPmut2) (Figure 27B). The fluorescence values from both strains were very similar suggesting that the fluorescence observed was exclusively due to autofluorescence emitted by the compounds and not specific to the *llsA* promoter activation (Figure 27). Therefore, we did not find any molecule or condition that triggers LLS production *in vitro.*

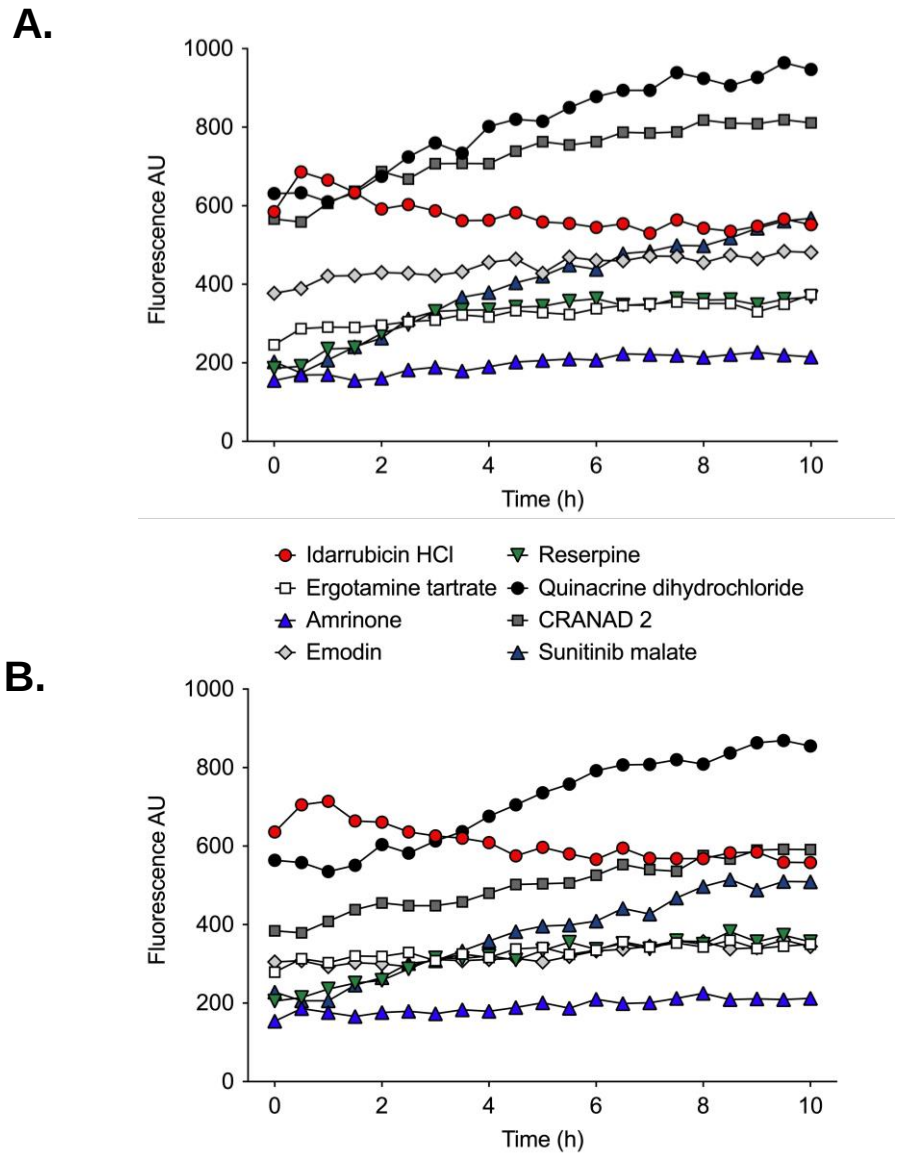

Figure 27. Induction of the P_{llsA} promoter compared to the WT strain lacking the reporter after incubation with different compounds. Bacteria lacking the reporter (WT) (A) or harboring the GFP reporter (pAD::P_{llsA}-GFPmut2) (B) were grown in BHI until an OD_{600nm} =1. Plates were incubated during 10 hours and read every 30 min (37°C, 5% CO_2).

3.2 Discussion

Our *in silico* work allowed to predict potential regulatory regions in the LLS gene cluster. Unfortunately, *in vitro* as well as *in vivo* experiments intended to perform transcriptomic analyses were not successful, hampering our possibilities to further investigate the regulation of LLS production.

Concerning our high-throughput *in vitro* screen, we performed the analysis of LLS activation using a restricted set of conditions, including a discrete concentration of

tested compounds. We cannot discard the possibility that a higher concentration of the used compounds is required or that a combination of signals is able to activate the LLS expression, making it challenging to find the right concentration and combination of conditions. It is tempting to speculate that a combination of signals in the gut could activate the LLS expression including: anaerobic conditions, acidic conditions, limitation of iron and nutrients, and others. Due to the complexity and richness of the gut environment, the possibilities are vast.

A limitation with the GFP fluorescent reporter used in our assays is that we had to used NaCl 0.8 M buffer to resuspend bacteria because minimal media generates auto-fluorescence, masking all the specific fluorescence signals. In the future, a non-fluorescent minimal media could be designed in order to be able to resuspend the different compounds in a minimal media that allow the growth of bacteria over time. The drawback of resuspending compounds in a complex media is that some compounds could precipitate making them unavailable for bacteria.

Significant efforts were also performed to isolate RNA from the intestinal content of orally infected germ-free mice. However, the amounts of RNA obtained were too low to perform transcriptomics or high quantities of eukaryotic RNA were recovered when we inoculated mice with higher inoculum of bacteria. Good quality and quantity RNA isolation might be technically complicated due to the higher virulence observed for the lineage I strain *L. monocytogenes* F2365 compared to lineage II strains such as EGD-e. Indeed, the isolation of prokaryotic RNA from the intestinal content of EGD-e orally-infected mice was successfully achieved by Toledo-Arana *et al.* (301). The best result we obtained was with male mice inoculated with 5 $x10^8$ bacteria. Though the RNA quantities are still low, it could be possible to pool the RNA obtained from 3 or more mice in order to obtain 1-2 µg of RNA required per condition in order to perform transcriptomics.

Another possibility that we explored to study the expression levels of the LLS operon genes *in vivo*, was to isolate RNA from the intestinal content of orally-infected conventional mice and to perform qPCR with the already designed and validated primers that amplify the different LLS operon genes (data not shown). Though good quantities and quality of prokaryotic RNA was obtained from conventional mice, there

was no amplification of the LLS operon genes. One possibility for the absence of amplification in these samples is interference by the high quantities of RNA from different gut microbiota species present in the samples of intestinal content from conventional mice.

Several transcriptional factors and riboswitches could regulate the expression of LLS to allow the specific activation in the GIT. The expression of bacteriocins is tightly regulated and could be controlled at several levels: transcriptional, translational, and post-translational (77, 78). In general, the activation and regulation of these systems is complex and depends on several signals and regulatory networks (200). Several studies demonstrate the activation of toxins by several compounds that are present in the gut, these systems are able to kill commensal bacteria and facilitate entero-pathogens' colonization of the gut (139, 377). For example, the T6SS of *V. cholerae* is functional under anaerobic conditions, the mucins present in the gut are able to activate this system and bile acids can modulate its activity. Interestingly, microbiota modify bile-acids to inhibit T6SS-mediated killing of commensal bacteria (201). The enteropathogenic bacteria *Salmonella Typhimurium* that kills commensal bacteria in a T6SS-dependent manner, also requires bile salts to increase T6SS expression (139). The T6SS-1 of Enteroaggregative *E. coli* is activated in minimal media or in iron depletion conditions (202).

Interestingly, recent studies in *Lm* showed that exposure to indole substantially downregulated the transcriptional regulator CodY, virulence genes such as *sigB* and *prfA* and virulence-associated genes such as flagellar genes, *hly* and *agrA*. The only upregulated gene upon indole exposure is MogR (378). Additionally, the CodY motif in *Lm* was confirmed recently and a model of interaction has been proposed between two CodY dimers and two overlapping CodY-binding sites (AATTTTCWGAAWW TTCWGAAAATT) (367) .

It is tempting to speculate that CodY is a major transcriptional repressor of LLS and in the presence of indole, the levels of CodY significantly decreased leading to an expression of LLS operon genes in the intestinal lumen. The pattern of gene expression in indole-treated *Lm* was comparable to that of the bacterium colonizing in the intestinal lumen, in particular the downregulation of *dltA, flaA, fliI* and *gmaR* genes

(379). This indicate that is possible that *L. monocytogenes* may acquire indole from gut microbiota as a signaling molecule for the adaptation and transition to the GIT.

Indeed, indole has been characterized as a signaling molecule produced by the gut microbiota and its concentrations are higher in the lumen, where the microbiota is present. For some pathogens such as enterohemorrhagic *E. coli* and *Citrobacter rodentium* the indole is used as a signaling molecule to downregulate the expression of virulence genes in the luminal compartment (380). Also the indole has shown to inhibit the *Salmonella* virulence, by decreasing the expression of virulence genes (381).

Is worth to explore whether indole regulates LLS operon expression through CodY or other genes. The indole compounds or indole derivates that we have tested to date were in a 10 micromolar concentration. The reported concentration of indole in human stool is between 250 and 1 000 micromolar (382, 383). Higher concentrations of indole could be tested by using the GFP fluorescent reporter that we generated in our work.

3.3 Material and methods

In silico analyses

To analyze the *llsA* promoter region, we performed *in silico* analyses to identify DNA motifs recognized by transcription factors, using the MEME Suite 5.1.1 database (http://meme-suite.org/tools/meme) of known motifs present in prokaryotes (356). First, the scanning algorithm MEME allowed us to scan for transcription factors motifs present in the *lls* promoter region. Once these motifs were identified in the *lls* promoter region, we compared these motifs against the Tomtom motif comparison tool (http://meme-suite.org/tools/tomtom), in order to produce an alignment for the significant matches (357). We looked for motifs around 150 base pairs upstream from the *llsA* start codon site and the selection criteria was Prokaryote DNA using the Collect TF database and the Pearson Correlation Coefficient with an E-value threshold <10.

We used the tool PASIFIC (http://www.weizmann.ac.il/molgen/Sorek/PASIFIC) to predict regulatory elements or premature termination sites in the *lls* promoter region

(373). For this the *lls* promoter region (-300 to -1) and *llsA* gene region (+1 to +150) were included and the default parameters were used.

Bacterial strains and growth conditions

Bacterial strains and plasmids used in this study are listed in Table S1 and Table S2 (Annex 3). All the primers used are listed in Table S3 (Annex 3). The *Lm* strains were grown in tubes overnight at 200 rpm and 37°C in BHI broth (Difco). When required, antibiotics were added for *Listeria* chloramphenicol 7 µg/mL and erythromycin 5 µg/mL.

Strains and constructs

The promoter of the *llsA* gene (500 pb upstream of the LLS operon) and the GFPmut2 gene fusion was synthesized by Genecust, digested and cloned into SmaI and SalI restriction sites of pAD-ActA-YFP as described (374). The resultant plasmid pAD::P_{llsA}-GFPmut2 was isolated from *E. coli* and introduced into *Lm* F2365 (Table S1). As positive control for the assays, the previously constructed reporter pKSV7::$P_{lmo2230}$-eGFP (σ^B-dependent promoter region of lmo2230 induced by osmotic shock) was used (375). This integrative plasmid was electroporated into *Lm* F2365 (Table S1, Annex 3).

High-throughput screen

A total of 927 molecules were tested *in vitro* from three different libraries: Sigma LOPAC library and an internal library with FDA approved compounds from Sigma, Enzo Life Sciences and Selleckchem. To perform the screening, we selected only homologues of compounds that are present in the gut or that are bacteria metabolic products such as: short-chain fatty acids, bile acids, mucins, choline metabolites, phenol and indole derivatives, vitamins, polyamines, lipids, some sugars, co-enzymes, antimicrobial peptides, antibiotics, amino acids and nucleobases (384). The compounds were tested at a 10 micromolar final concentration and were plated by a liquid acoustic dispenser (Echo550, labcyte). Briefly, daughter 384 multiwell plates were prepared from 96 multiwell library plates (cherry-picking method). Compounds were resuspended in 80 µl of NaCl 0.8 M buffer. Then, 20µl of resuspended bacterium were added to the plates (previously resuspended in NaCl 0.8 M buffer, OD_{600nm} =1) to reach a final volume of 100 µl per well. The complete list of library compounds used in the HTS can be consulted in Annex 4 Table S4.

The fluorescence was detected in a Cytation5 (Excitation: 485, Emission: 507, Light Source: Xenon Flash, Lamp Energy: High, Extended Dynamic Range, Read Speed: Normal, Delay: 100 msec, Read Height: 7 mm). Plates were incubated during 10 hours and read every 30 min (37°C, 5% CO_2).

Mice Infections

C57BL/6J mice were purchased from Charles River. GFM generated from C57BL/6J mice were obtained from the Gnotobiology Platform of the Institut Pasteur and kept in isolators. Ten to twelve-week-old C57BL/6J mice were infected by intragastric inoculation with 5 $\times 10^{8\text{-}10}$ bacteria as indicated. The bacterial inoculum was prepared in a total volume of 200 µL. The bacterial inoculum was mixed with 300 µL of $CaCO_3$ (50 mg/mL) before oral gavage. Bacterial numbers in the inocula were verified by plating different dilutions onto BHI plates before and after inoculation. Mice were killed at different time points, and intestines were removed and opened to recover the intestinal content. The intestinal contents were immediately frozen in liquid nitrogen and kept at -80°C until the RNA extraction. All animal experiments were approved by the committee on animal experimentation of the Institut Pasteur and by the French Ministry of Agriculture.

RNA extraction

Total RNA was extracted as previously described with some modifications (385). The intestinal content from one mouse were divided in two and each sample was resuspended in 1 mL TRIzol reagent (Ambion), transferred to 2 mL Lysing Matrix tubes containing 600µL of RLT-Beta-mercaptoethanol solution (10µL beta-mercaptoethanol/mL de RLT, kit RNeasy Qiagen) and lysed with a FastPrep apparatus (2 cycles of 45 s, speed 6.5, 4°C). Tubes were incubated 5 min at room temperature and centrifuged at 13 000 *g* for 10 min at 4 °C and the aqueous phase was transferred twice to an Eppendorf tube containing 200 µL of chloroform, lysates were shaken 60 s, incubated at room temperature for 3 min at room temperature and centrifuged 15 min at 13 000 *g* at 4°C. The upper aqueous phase was carefully removed and transferred to a new Eppendorf tube containing 1 volume of 70% ethanol. Samples were incubated 5 min at room temperature and the following steps were performed with the RNeasy minikit (Qiagen) according to the manufacturer's instructions. The Dnase digestion was performed in the RNeasy minikit columns with the RNAse free

DNAse set (Qiagen) according to the manufacturer's instructions. Purified RNA was resuspended in 40 µl water.

Quantification of RNA and quality control

Purified RNA was quantified at 260 nm using a NanoDrop ND-1000 spectrophotometer (NanoDrop Technologies). The quality of the RNA was analyzed with a 2100 bioanalyzer (Agilent) using RNA 6000 NANO chips according to the manufacturer's instructions.

PART IV: Characterization of LLS operon products LlsX and LlsP

All the LLS cluster genes present homology to SLS genes, except for the gene *llsX*. In fact, *llsX* does not share homology to any known gene. The *llsX* gene is located downstream of the *llsGH* genes that encode for a putative ABC transporter (253), and is essential for LLS hemolytic activity (314). Our aim was to study the potential function(s) of LlsX within the LLS biosynthetic cluster.

The LLS putative immunity protein LlsP shares weak homology (26,60% identity) with a candidate bacteriocin immunity protein PlnP from *L. plantarum* (177). The PnlP immunity protein is an Abi-like protein, that encodes for putative transmembrane proteases CPBP also known as Abi family (Pfam PF02517) (175, 176). Our goal was to investigate whether LlsP is an immunity protein and confers immunity against LLS.

4.1 Results

4.1.1. LlsX is associated to the cell membrane of producer bacteria

First, *in silico* analyses of the *llsX* protein sequence were performed to investigate the predicted topology of the protein. The ExPASy TMPDB database predicts a topology that involves 2 transmembrane helixes (386) and Interpro predicts two transmembrane domains, a non-cytoplasmic domain and two cytoplasmic domains (387) (Figure 28). The N-terminal side of the protein is predicted to be inside with two transmembrane helixes (Figure 28). When entering the protein sequence into Motif Scan database, to find all known motifs that occur in a sequence, it presents 1 putative *N*-glycosylation site and several putative phosphorylation sites. However, the score is weak and to determine the validity of these motifs additional biological evidence is required (388).

When entering LlsX sequence into the Pfam protein database, to look for protein families, there are no significant matches (389). However, there are some similarities with: (1) a domain found in lipopolysaccharide assembly protein A that functions in the export and assembly of lipopolysaccharide (390) (2) a domain that belongs to the FtsX-like permease family which are transmembrane permeases that require ATP to transport substrates as the tripartite efflux system MacAB-TolC and bacitracin export permease protein BcbE (391, 392).

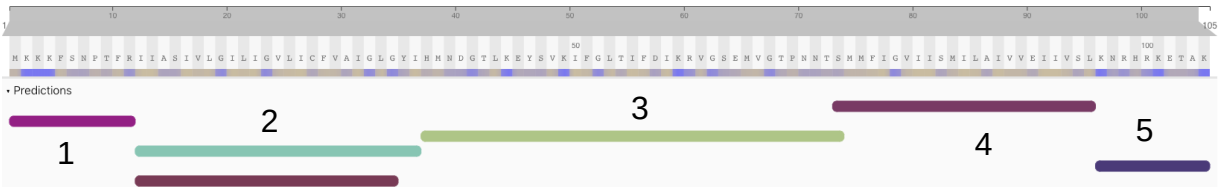

Figure 28. Topology prediction for LlsX. (1) From position 1 to 11 a cytoplasmic domain is predicted. (2) From amino acid 13-36 a transmembrane region forming a helix is predicted. (3) From position 37 to 73 a non-cytoplasmic domain is predicted. (4) From amino acid 73 to 95 a transmembrane region forming a helix is predicted. (5) Fom 96 to 105 position a cytoplasmic domain is predicted. Adapted from InterPro Jones *et al.* (2014).

Based on these *in silico* analyses, our hypothesis is that LlsX is a membrane protein that could act as a chaperone. Our first aim was to explore LlsX subcellular location. For this goal, we buy commercially produced polyclonal antibodies (Covalab) against LlsX by using the LlsX peptide (amino acids 15 to 58). Afterwards, we performed a subcellular fractionation (as described earlier, PART II) to elucidate LlsX subcellular location in producer cells *Lm* F2365 pHELP::*llsA* (referred to as LLS$^+$ bacteria). We detected a band of approximately 12 kDa which corresponds to the expected molecular weight of monomeric LlsX protein (Figure 29).

Our results clearly demonstrate that LlsX is detected only in the bacterial cell membrane. The LLS protein shows the same subcellular location at the membrane level; when the protein is fused to FLAG and HA tags (LLS$^+$-FLAG and LLS$^+$-HA), a high molecular weight smear is observed at the cell membrane (Figure 29). The membrane distribution of LlsX is not changed when a FLAG or HA tag are added to LLS, indicating that the addition of LlsX is not altered when a tag is added to LLS (Figure 29).

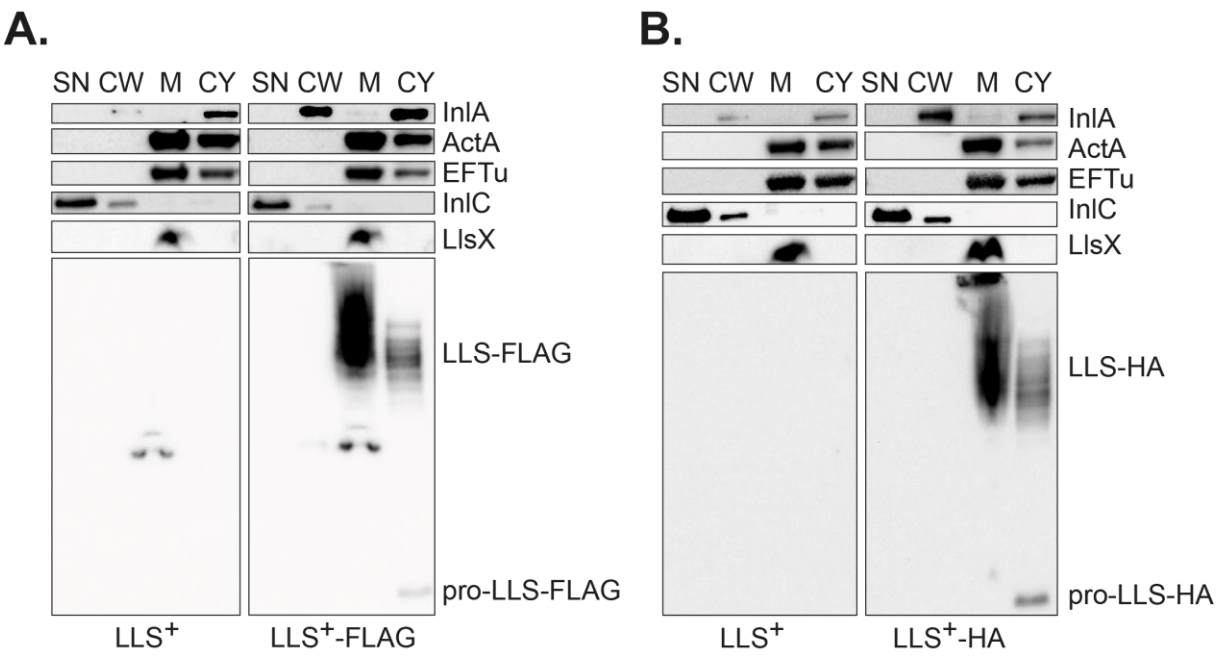

Figure 29. LlsX is located at the cell membrane. (A) Localization of LlsX by fractionation experiments. Western Blot analysis was performed on a strain expressing LLS$^+$ and a strain expressing LLS$^+$-FLAG or LLS$^+$-HA. Proteins were fractionated in four compartments supernatant (SN), cell wall (CW), membrane (M) and cytoplasm (CY). InlA, ActA, EF-Tu, InlC and LLS with or without FLAG and HA tags were used as controls for fractionation. Equivalent amounts of each fraction, corresponding to 100 µl of bacterial culture were separated on SDS-PAGE and submitted to immuno-detection, using the indicated antibodies. Data from one representative experiment out of the three performed are shown.

4.1.2 LlsX interacts with LLS

Since LlsX is located at the membrane of producer bacteria as LLS (Figure 29), we investigated whether these two proteins could interact. Immunoprecipitated (IP) LlsX pulled down LLS$^+$-FLAG (Figure 30A) from bacterial lysates. Interestingly, not only the LLS pro-peptide interacts with LlsX but also the LLS higher molecular weight smear (Figure 30A). Additionally, immunoprecipitated LLS-FLAG pulled down the LlsX protein from bacterial lysates (Figure 30B).

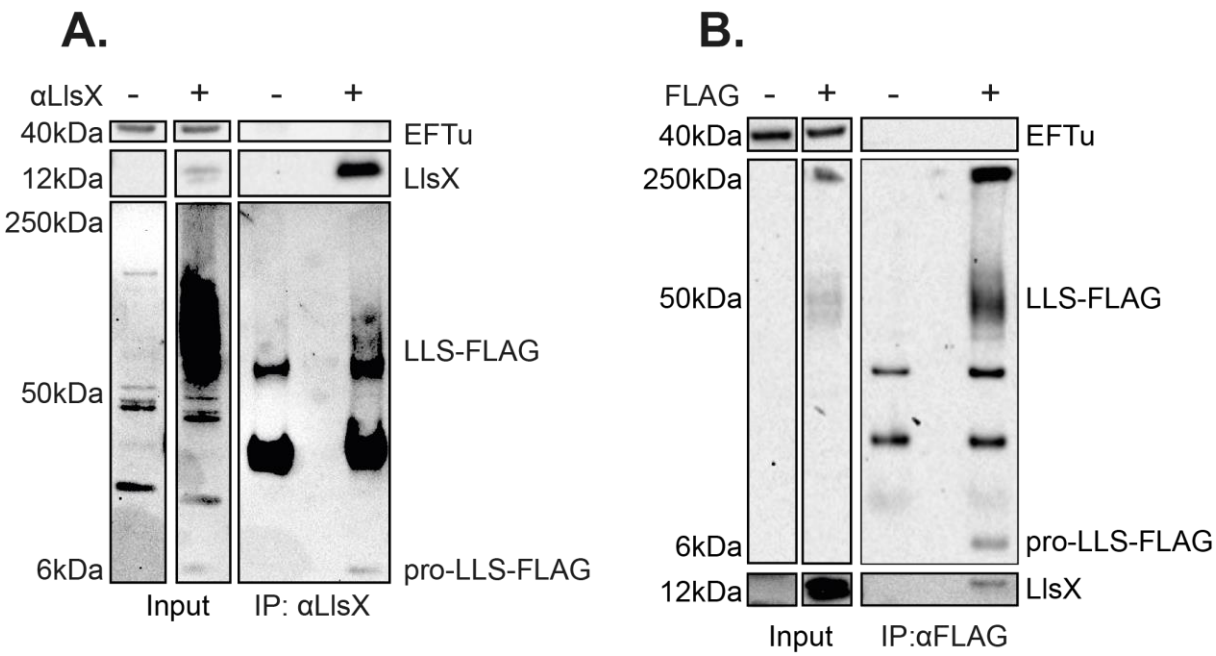

Figure 30. LlsX interacts with LLS. coIP between LlsX and LLS-FLAG from overnight bacterial cultures. Cells were suspendend in CHAPS buffer and sonicated. (A) Bacterial lysates from LLS$^+$-FLAG$^+$ were immunoprecipitated with LlsX antibody or pre-immune αIgG serum coupled to protein G. (B) Bacterial lysates from a strain expressing LLS$^+$ (negative control) and a strain expressing LLS$^+$-FLAG were immunoprecipitated with magnetic beads coupled to anti-FLAG antibody. Immunoprecipitated fractions were separated on SDS-PAGE and submitted to immune-detection, using the anti-llsX and the anti-FLAG antibodies. Data from one representative experiment out of the three performed are shown.

Immunoprecipitated LLS-FLAG was submitted to MS analyses to identify the co-immunoprecipitated partners. The identified LLS$^+$-FLAG co-immunoprecipitated proteins were compared to LLS$^+$ co-immunoprecipitated proteins and only those that were present in the LLS$^+$-FLAG condition were considered (32 proteins in total) (complete list of proteins in Annex 5, Table S7). These 32 proteins were analyzed based on the Intensity Based Absolute Quantification (iBAQ) values, which are proportional to the molar quantities of the proteins present in the analyzed samples. The 10 proteins with the highest iBAQ values are presented in Table 10. The second most abundant LLS-FLAG co-immunoprecipitated protein was LlsX.

Table 10. LLS-FLAG co-immunoprecipitated proteins identified by MS.

Protein ID	LMOf2365 ID	iBAQ*	Protein name	Protein function	REF
WP_009917805.1	1958	3398600	Nucleoside diphosphate kinase (NDk)	Catalyzes the formation of NTP from ATP and NDP, protein histidine phosphorylation	(393)
WP_003730943.1	1115	2486100	LlsX	Unknown function, part of LLS operon	(253)
WP_010958846.1	1117	2220400	LlsY	Putative cyclodehydratase involved in LLS PTMs	(253)
WP_003723533.1	1548	1992600	YajC (SecDF)	Sec-dependent pathway translocase subunit, stimulates pre-protein translocation	(136)
WP_010958772.1	0630	1605100	Putative adhesin	Putative all-β structure with a twenty-residue repeat with a highly conserved repeating gly-asp motif	(339)
WP_003725873.1	2006	1125900	Dihydroxy-acid dehydratase	Biosynthesis of isoleucine and valine, the dehydratation of 2,3-dihydroxy-isovaleic acid into alpha-ketoisovaleric acid	(339)
WP_003721799.1	0715	904340	FlhB	Membrane protein responsible for substrate specificity switching from rod/hook-type export to filament-type export	(394)
WP_003728076.1	0264	890580	Hypothetical protein	Possess a domain with methyltransferase activity	(253)
WP_003725828.1	1904	805150	Thymidylate synthase	Catalyzes the conversion of dUMP to dTMP	(253)
WP_003720130.1	1843	627970	Asp23/Gls24 family envelope stress response protein	Homologous to alkaline shock protein associated to cell envelope homoeostasis	(395)

*iBAQ (Intensity Based Absolute Quantification) iBAQ values are proportional to the molar quantities of the proteins.

Based on these results, we confirmed the interaction between LlsX and LLS (Table 10). Interestingly, LlsY was identified as the third most abundant co-immunoprecipitated protein, LlsY belongs to the LLS operon and is a putative cyclodehydratase involved in the LLS putative PTMs (Table 10). We can speculate that LlsX interacts with LLS before and during the introduction of PTMs.

The other proteins that were pulled down with LLS-FLAG are not associated with the LLS operon. Interestingly, the most abundant protein is a nucleoside diphosphate kinase (Table 10). This protein is involved in the formation of dNTPs but also in the phosphorylation of histidine residues. Is tempting to speculate that since LlsX has two histidine residues at positions 37 and 99, LlsX could be phosphorylated to regulate its interaction with LLS.

Interestingly, the protein YajC is abundantly pulled-down with LLS-FLAG (Table 10). YajC is a Sec-dependent pathway translocase subunit responsible to stimulate pre-protein translocation. Somehow, YajC could help to translocate LlsX. The other co-immunoprecipitated proteins are enzymes (a dehydratase, a methyltransferase, and a thymidylate synthase) which association with LLS is not clear and need further studies. The additional co-immunoprecipitated hits include membrane proteins: a putative adhesin, a flagella protein and an alkaline shock protein homologue (Table 10). However, the relationship of these proteins with LLS and/or LlsX is not clear.

4.1.3 LLS is absent in a *llsX* mutant

Since LLS and LlsX interact and both are located at the membrane level we hypothesized that LlsX could help to stabilize and keep LLS at the cell membrane of the producer bacteria before being translocated to the target bacteria. To better study the role of LLS we created a *llsX* mutant in LLS$^+$ and LLS$^+$-FLAG strains. First, to investigate whether the absence of *llsX* could disrupt LLS location at the cell membrane, we performed a bacterial subcellular fractionation assay with the tagged and non-tagged LLS$^+$ strains upon deletion of the *llsX* gene. The high molecular weight smear and the LLS pro-peptide are completely absent in the LLS$^+$-FLAG Δ*llsX* strain (Figure 31A). To determine whether deletion of the *llsX* gene leads to polar effects, we performed a qPCR of the LLS operon genes in the tagged and non-tagged LLS$^+$ strain. The deletion of the *llsX* gene did not cause expression defects on the upstream or downstream genes of the operon (Figure 31B), suggesting that the *llsA* gene is normally transcribed, but in the absence of LlsX, the LLS pro-peptide could be degraded or unstable.

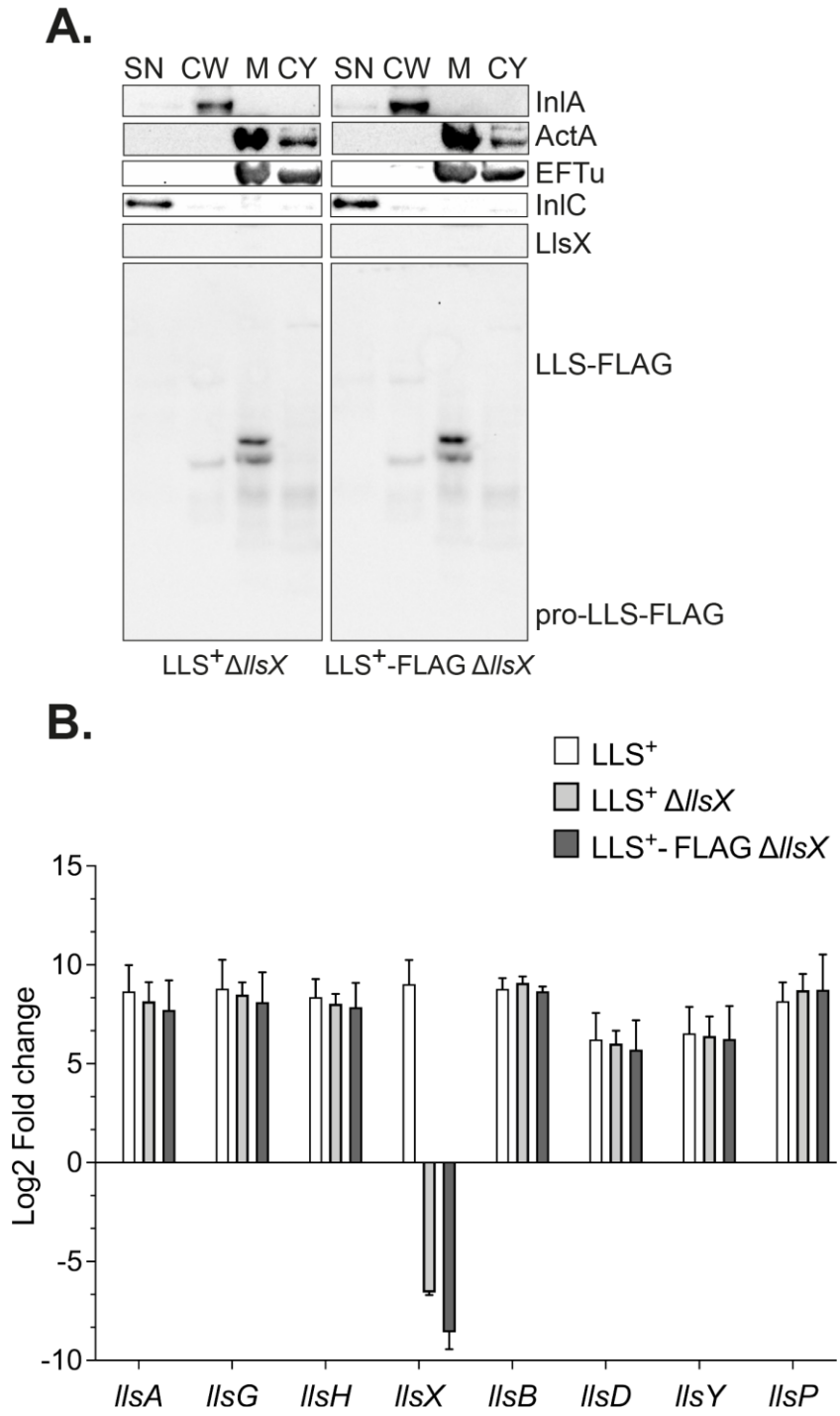

Figure 31. **Absence of LLS peptide and smear upon deletion of the *llsX gene*.** (A) Localization of LLS by fractionation experiments upon deletion of the *llsX* gene. Western Blot analysis was performed on LLS$^+$Δ*llsX* (negative control) and LLS$^+$-FLAG Δ*llsX* strains. Proteins were fractionated in four compartments supernatant (SN), cell wall (CW), membrane (M) and cytoplasm (CY). InlA, ActA, EF-Tu and InlC were used as controls for fractionation. Equivalent amounts of each fraction, corresponding to 100 µl of bacterial culture were separated on SDS-PAGE and submitted to immuno-detection, using the indicated antibodies. Data from one representative experiment out of the three performed are shown. (B) Expression of the LLS

genes *in vitro* in the LLS$^+$ or LLS$^+$Δ*llsX* and LLS$^+$-FLAG Δ*llsX* strains. Values calculated by qPCR in comparison with the *wt* strain and normalized to the housekeeping gene *gyrA* and represented as Log2 Fold change. Data from two independent biological experiments performed with three technical replicates are shown. Error bars show SEM.

4.1.4 LlsP possess CAAX proteases conserved motifs

First, *in silico* analyses of the LlsP protein sequence were performed to investigate the predicted topology of the protein. The ExPASy TMPDB database predicts a membrane-spanning protein, the topology involving 6 transmembrane helixes (386). Interpro predicts as well six transmembrane domains, three non-cytoplasmic domains and three cytoplasmic domains (387) (Figure 32). The N-terminus side of the protein is predicted to be extracellular (Figure 32).

When entering the protein sequence into the Motif Scan database, it presents CAAX amino terminal protease family motifs with a high score (388). These family of proteins are characterized by three conserved motifs: motif 1 consists of two glutamate residues and an arginine separated by three variable amino acids (EExxxR), motif 2 consists of a phenylalanine and a histidine separated by three variable amino acids (FxxxH) and motif 3 consists of a single histidine residue (170). These 3 motifs are present in the LlsP protein: motif 1 EEIIFR, motif 2 FVIAH, and motif 3 histidine residue.

When entering the LlsP sequence into the Pfam family protein database and Interpro to search for protein families, there is one significant match with the CBPB family (CAAX proteases and bacteriocin-processing enzymes) (389). Members of this family are present in all domains of life and the eukaryotic type II CAAX proteases and their related bacterial and archaeal homologues have a CAAX-box in which the last three amino acids of the processed protein (AAX) are removed by proteolysis remove the C-terminal tripeptide AAX. This tripeptide is bound directly to a cysteine residue modified with a farnesyl (C_{15}) or geranylgeranyl (C_{20}) prenyl chain, which facilitates membrane localization (396). Interpro predicts that the protein has intramembrane metalloendoprotease activity (387).

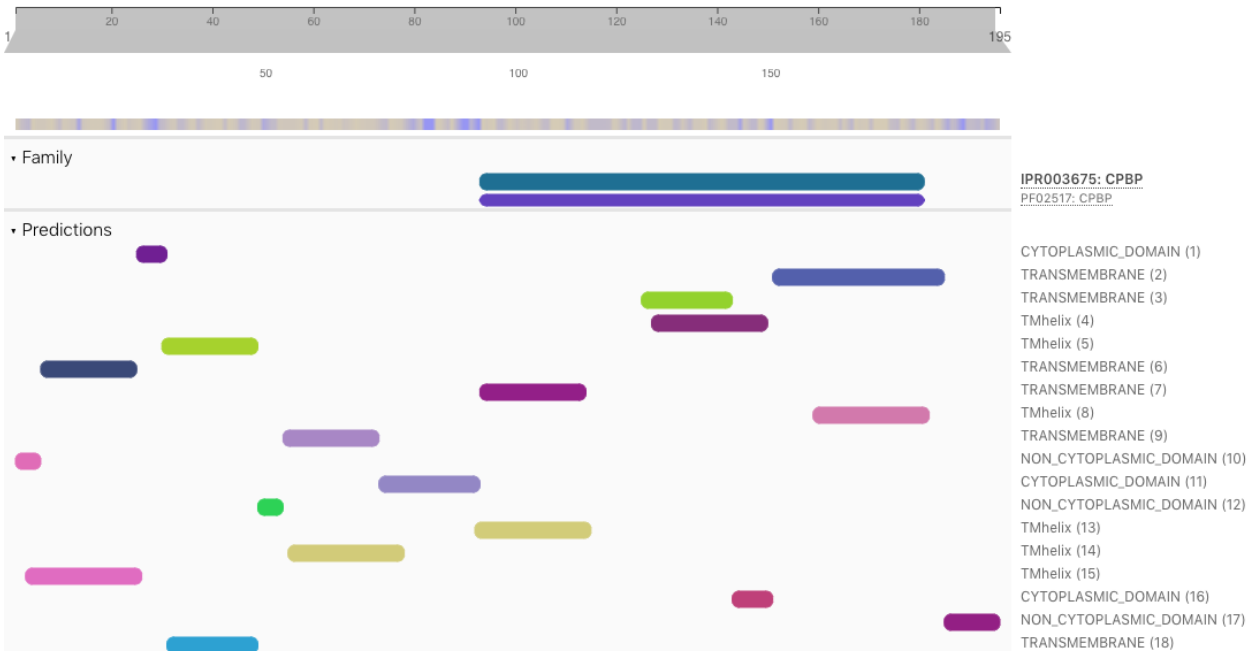

Figure 32. Topology prediction for LlsP. The 6 transmembrane regions are predicted to be located in positions: 6 to 24, 31 to 48, 54 to 72, 93 to 113, 125 to 142, and 151 to 184. From amino acid 25 to 30, 73 to 92 and 143 to 150 three cytoplasmic domains are predicted. From position 1 to 5, 114 to 124 and 185 to 195 three non-cytoplasmic domain are predicted. The protein is predicted to belong to the CBPB family. Adapted from InterPro Jones *et al.* (2014).

Based on these *in silico* analyses, our hypothesis is that LlsP is a membrane protein that could act as an intramembrane metalloprotease that inactivates LLS to confer immunity to the producer bacteria. Alternatively, we hypothesize that LlsP could cleave LLS signal peptide.

4.1.5 LlsP protein does not confer immunity against LLS when expressed in a target bacterium

Our first aim was to explore LlsP subcellular location. For this goal, we intended to produced polyclonal antibodies (Covalab) against LlsP by immunizing rabbits with two non-hydrophobic LlsP regions: KLLTIYKKNKIFIQSI (amino-acids 83-98) and VYIVRTSKYENHRNW (amino-acids 181-195). Unfortunately, these peptides were not immunogenic (data not shown). Since LlsP is a multi-spanning membrane protein it is more difficult to generate antibodies that recognize exposed regions of the protein.

We decided then to express the LlsP protein in a target bacterium to explore whether LlsP could protect the target bacteria against LLS activity. For this goal, the *llsP* gene

from *Lm* F2365 was inserted into the chromosome of *Lm* 10403S, a previously identified LLS target bacteria (308). Briefly, the *llsP* was cloned into the pAD vector and expressed under the control of a constitutive promoter (*Lm* 10403S pAD::*llsP*), as described previously (374). Additionally, the plasmid pAT18-cGFP was added to this strain (referred to as LlsP$^+$) in order to add resistance to a second antibiotic and select the strain after 24 hours of co-culture with a producer LLS$^+$ bacteria expressing the tdTomato protein (referred to as LLS$^+$) or with a non-producer LLS$^-$ bacteria expressing the tdTomato protein (referred to as LLS$^-$) (described in Results Part II). After 24h of co-culture the target bacteria expressing the LlsP protein (LlsP$^+$) did not confer any protection against the LLS activity (Figure 33). However, we cannot confirm that the LlsP protein is correctly expressed in target bacteria and displays the correct subcellular location. In general, LlsP$^+$ target bacteria grew less in comparison to the LlsP$^-$. We hypothesize that the difference of growth is due to the loss of the pAT18-cGFP plasmid in some bacteria as LlsP$^+$ bacteria were plated on BHI with antibiotics (chloramphenicol and erythromycin).

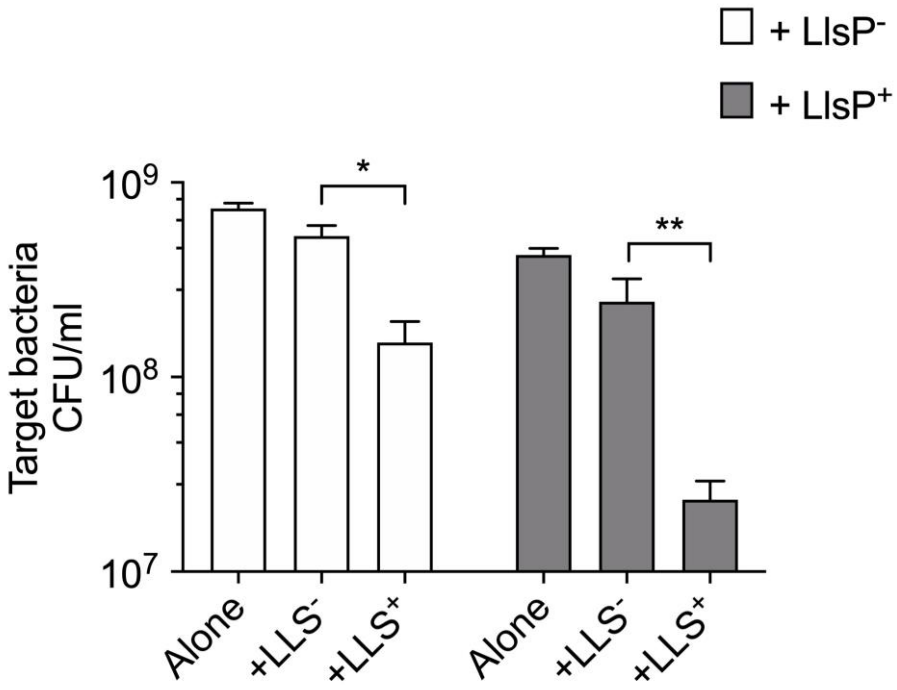

Figure 33. LlsP protein does not confer immunity against LLS when expressed in a target bacterium. Target LlsP$^-$ or LlsP$^+$ bacteria were cultivated alone or co-cultivated with LLS producer bacteria (LLS$^+$) or LLS mutant bacteria (LLS$^-$) during 24h in BHI. Data from three independent biological experiments are shown. Error bars show SD. Multiple two-tailed unpaired *t*-test were performed, LlsP$^-$ + LLS$^-$ vs LlsP$^-$ + LLS$^+$ p= 0.0227, and LlsP$^+$ + LLS$^-$ vs LlsP$^+$ + LLS$^+$ p= 0.0072.

4.2 Discussion

The *llsX* gene does not share significant homology with any known gene. Clayton *et al*. (2011) showed that *llsX* is essential for LLS hemolytic activity (314). Our results highlight the cell membrane location of LLsX and the interaction between LLS and LlsX. Additionally, LlsX is required for expression and/or stabilization of LLS. In the absence of LlsX the LLS pro-peptide is unstable or degraded, thus the post-translationally modified LLS is not produced. Additionally, LlsY (PTM putative enzyme) is pulled-down with LlsX and LLS suggesting that the interaction between LLS and LlsX occurs during the LLS maturation process that could take place at the membrane level. Altogether these results support that LlsX activity is essential for LLS maturation and stability, supporting the hypothesis that LlsX could act as a chaperone before and during the LLS maturation process.

As mentioned before, there are no significant protein matches with the LlsX sequence in the Pfam family protein database (389). However, when entering the LlsX protein into the NCBI database and doing a BLASTP (refseq_protein database) two different proteins show homology to LlsX (1) LysE family translocator with 37.31% of identity and (2) FKBP-type peptidyl-prolyl-cis-trans isomerase with 32.14% of identity (397).

The protein from the LysE family is identified as a threonine/homoserine/homoserine lactone efflux protein. Interestingly, this family of proteins is known to catalyze solute export of amino acids or ions (398). More recently, new transporters that belong to this family were identified, they are involved in transport of electrons, calcium, peptidoglycolipids, and others. In the case of Peptidoglycolipid Addressing Protein Family (GAP), is found in bacteria and are prominent in mycobacterial genus. They are predicted to have 6 transmembrane α-helical segments (399). For example, the GAP protein from *Mycobacterium smegmatis* is required for the transport of phenoglycolipids or peptidoglycolipids attached to the cell surface (400).

The second protein (FKBP) is a peptidyl-prolyl cis/trans isomerase (PPIase), PPIases are chaperones that catalyze the isomerization of peptide bonds to achieve conformational changes in native folded proteins allowing protein refolding (401). The

identity of LlsX with these two proteins is lower than 40% with no putative conserved domains identified.

The general idea of LlsX having a dual activity acting as a chaperone and a transporter for LLS could be explored in the future by adding point mutations to LlsX and detecting the specific domains that could contribute to stabilize LLS or to transport LLS. Also, producing antibodies against the proteins of the ABC transporter and the PTM enzymatic complex could help to better understand the specific role of LlsX. Coupled to this, microscopy techniques such as high-resolution microscopy, can help to understand the interactions of LlsX with LLS and other proteins of the operon.

CPBP protease activity has been associated with maturation and secretion of bacteriocins and/or helping to confer immunity against self-produced bacteriocins (176). Interestingly, the CPBP proteins are frequent in Firmicutes and Actinobacteria. It is possible to find 5-20 CPBP family members in a single genome. For example, *Streptococcus sanguinis* has 21 copies of CPBP members within its genome (176). These proteins have been associated to operons that produce bacteriocins in *L. plantarum* (402, 403). Aditionally, *K. pneumoniae* protein CPBP MceF protein has been shown to be important for the microcin E492 export (404). The MlrA protein from *Sphingomomunas sp*. is responsible for the cleavage of the peptide bond present in microcystin LR, opening its cyclic structure and rendering it linear; after this cleavage microcystin LR is degraded by the peptidases MlrB and MlrC (405). In *Streptococcus pneumoniae*, CPBP proteins PncO and PncP were found in the *pnc* locus that encodes for bacteriocins (406). In all the TOMMs a CAAX protease is present in the biosynthetic gene clusters from Gram-positive pathogens such as *C. botulinum, L. monocytogenes* and *S. aureus* suggesting its essential role for the bacteriocin maturation and/or immunity (59, 176).

Unfortunately, we could not confirm whether LlsP is an immunity protein that protects target bacteria against LLS. However, we attempted to generate a Δ*llsP* mutant in the LLS^+ background but this mutant was not viable. On the other hand, a Δ*llsP* mutant is viable in a F2365 wild-type (LLS^-) background in which the LLS is not produced. This result suggest that the LlsP is in fact an immunity protein that protects the producer bacteria from the LLS activity. However more experimental data is required to confirm

this idea. There is a possibility that LlsP is an immunity protein for the LLS producer cells that confers self-immunity but not for the target cells exposed to LLS. This concept of self-immunity has been suggested for SLS, where the provided immunity by SagE is only for SLS producer cells and not for the exogenous exposure to SLS (215).

Limited functional experiments have been carried out to completely understand the enzymatic mechanism of CPBP proteins. Site-directed mutagenesis demonstrated that conserved motifs that constitute the putative proteolytic active site of *L. sakei* immunity protein SkkI are essential for its immunity function. Double mutants of the two conserved glutamates (E133A/E134A or E133Q/E134Q) in the first motif or a single mutant of the conserved histidine in the fourth motif (H214D) abolished completely the immunity function of SkkI (177). Two site-directed mutagenesis studies of the Rce1p CAAX protein from yeast, showed that mutation of any one of the conserved glutamates and histidines (E156A or E157A in the first motif, H194A in the second motif, or H248A in the fourth motif) inactivated Rce1p's enzymatic activity (396, 407).

Some intramembrane zinc metalloproteases enzymatic processes have been better characterized such as those of site-2 protease (S2P) in bacteria. For example, the S2P membrane-embedded metalloprotease YaeL from *E. coli*, required for the RseA degradation. The RseA, is an anti-sigma factor that inhibits the transcriptional activity of σ^E, the pathway that responds to protein misfolding in the envelope. This mechanism is similar to the mechanism of activation of the mammalian unfolded protein response transcription factor ATF6 by site-1 protease and S2P (408).

Further functional studies are required to understand the specific mechanism of CPBP proteins. However, CPBP proteins are neighbors of genes encoding ABC transporters, as revealed in several bacteriocin gene clusters; suggesting that these proteins could couple leader peptide cleavage with transport (176, 402, 409). Certain ABC transporters possess a protease domain (SunT-type transporters) that removes the leader peptide sequence of the transported substrates (discussed in the section 2.2 Export and Secretion mechanisms) (121). We can hypothesize that LlsP works concomitantly with LlsGH ABC transporter to cleave LLS leader peptide and transport mature LLS.

4.3 Materials and Methods

Bacterial strains and growth conditions

Bacterial strains and plasmids used in this study are listed in Table S1 and Table S2 (Annex 3). All the primers used are listed in Table S3 (Annex 3). The *Lm* strains were grown in tubes overnight at 200 rpm and 37°C in BHI broth (Difco). When required, antibiotics were added for *Listeria* chloramphenicol 7 µg/mL and erythromycin 5 µg/mL.

Mutant and strains construction

For the strains *Lm* F2365 pHELP: *llsA*-FLAG and *Lm* F2365 pHELP: *llsA*-HA the FLAG and HA tags were added in the C terminal of the *llsA* gene and the pHELP promoter was fused between two 500-ntd DNA fragments flanking the start codon of *llsA.* These DNA constructions were synthetically produced by gene synthesis (Genecust) and cloned into *Sal*I–*Eco*RI restriction sites of pMAD vector. Mutagenesis was performed by double recombination as described previously (410). For the construction of the Δ*llsX* mutants (LLS$^+$Δ*llsX* and a LLS$^+$-FLAG Δ*llsX*) DNA constructions were synthetically produced by IDT and cloned into SalI-SmaI restriction sites of pMAD vector. Approximately 800 -ntd DNA fragments upstream and downstream of the *llsX* genes were used to design the DNA blocks. Mutagenesis was performed by double recombination as described previously (410).

The *llsP* and the tdTomato genes were synthesized by IDT, digested and cloned into SmaI and SalI restriction sites of pAD-ActA-YFP as described previously (374). The tdTomato protein was codon optimized for its expression in *L. monocytogenes* (http://genomes.urv.es/OPTIMIZER/). The resultant integrative plasmids pAD::*llsP* and pAD::*tdTomato* were isolated from *E. coli* and electroporated into *Lm* 10403S (pAD::*llsP*), LLS$^+$ and LLS$^-$ (pAD::*tdTomato*) as described before (PART II). For the strain *Lm* 10403S pAD::*llsP* (LlsP$^+$) the plasmid pAT18-cGFP was electroporated as described before (374).

Subcellular fractionation

The fractionation of *Listeria* bacterial cells was performed as described previously (263) with a few modifications. The cell wall, membrane and cytoplasm compartments were separated from 2 mL of stationary phase culture (OD_{600nm} = 2). The bacteria were

pelleted and supernatant (SN) was precipitated at -20°C overnight with 16% of thricloracetic acid. The bacterial pellet was washed once with 2 mL of PBS and once with 2 mL of TS buffer (10 mM Tris-HCl pH 6.9, 10 mM $MgCl_2$ and 0.5 M sucrose). Then the bacteria were resuspended in 1 mL of TS buffer containing 45 µg mutanolysin (Sigma) and cOmplete protease inhibitor cocktail (Roche) overnight statically at 37 °C to digest completely the cell wall. Protoplasts were pelleted for 5 min at 15,000 *g* and the cell wall fraction was precipitated with TCA as indicated before for the supernatant. The protoplasts were lysed by four freeze-thaw cycles (liquid nitrogen and water bath at 37 °C) in 100 µl of protoplast buffer (100 mM Tris-HCl pH 7.5, 100 mM NaCl and 10 mM $MgCl_2$). The membrane and the cytoplasm fractions were centrifuged at 4 °C for 15 min at 16,000 *g*. The pellet corresponding to the membrane fraction was then resuspended in 100 µl of CHAPS lysis buffer (30 mM Tris-HCl pH 7.5, 150 mM NaCl and 1% CHAPS). The membrane fraction was sonicated (three cycles of 15 s, 20% amplitude).

Immunoprecipitation

Overnight cultures (100mL) of *L. monocytogenes* F2365 pHELP: *llsA*-FLAG and *L. monocytogenes* F2365 pHELP: *llsA*-FLAG Δ*llsX* (IP αLlsX) or *L. monocytogenes* F2365 pHELP: *llsA* and *L. monocytogenes* F2365 pHELP: *llsA*-FLAG (IP αLLS-FLAG) were pelleted. Bacteria were washed once with 50 mL of PBS and resuspended in 2 mL of CHAPS lysis buffer and sonicated (four cycles of 30 s, 20% amplitude). Samples were then transferred to Lysing Matrix tubes and lysed with a FastPrep apparatus (2 cycles of 45 s, speed 6.5). Samples were centrifuged 15 min at 4°C at 16,000 *g*. Supernatant was collected and protein concentrations were measured with a bicinchoninic acid (BCA) protein assay kit (ThermoFisher) and supplemented with protease inhibitors mixture (Roche).

For the immunoprecipitation of LlsX, 1 mg of bacterial lysates, 50 µl of equilibrated Dynabeads protein G (Invitrogen, washed two times with 1 mL of CHAPS lysis buffer) and 6 µg of αLlsX antibody or 6 µg of pre-immune serum (negative control) were added per sample. Samples were incubated at least 1h at 4°C on a rotating wheel. Beads were washed 4 times in CHAPS buffer during 5 min. After the washes, the bound protein was eluted from the Dynabeads beads by boiling (10 min) in 50 µL of NuPAGE

loading sample buffer with β-mercapto-ethanol. Samples were then subjected to immunoblotting.

For the immunoprecipitation of LLS-FLAG, 1 mg of bacterial lysates, and 25 µl of equilibrated M2 anti-flag beads (Sigma, washed three times with 1 mL of CHAPS lysis buffer) were added per sample. Samples were incubated overnight at 4 °C on a rotating wheel. Beads were collected by centrifugation at 4 °C 1 min at 2,000 g and washed once with CHAPS lysis buffer and then three times with 1 mL of Elution buffer (50 mM Tris HCl pH 8.0, 150 mM NaCl and 2 mM $CaCl_2$). The FLAG tag protein was eluted by 2 serial elutions (25 µl each elution) with the 3x FLAG peptide diluted in Elution buffer (final concentration of 100 µg/mL). Samples were diluted by boiling with 50 µl of 2x Tricine Sample Buffer (Biorad) and 125 mM DTT and then subjected to immunoblotting.

SDS–PAGE and western blotting

Samples were loaded onto a NuPAGE 4-12% Bis-Tris Precast Protein Gels (Invitrogen). The samples were separated in Nu PAGE MOPS SDS Running Buffer (for LlsX) or MES SDS Running Buffer (for LLS) at 130 V and transferred onto a polyvinylidene fluoride (PVDF) membrane using the iBlot Dry Blotting System (Invitrogen) at 20 V for 8 min. The membranes were blocked with 5% skim milk in PBS 1X with 1% Tween-20 (PBST) and the primary antibodies were incubated overnight at 4 °C and the secondary antibodies at 37 °C during 1h at room temperature. The proteins were revealed with the Pierce ECL 2 Western Blotting Substrate or SuperSignal West Femto Maximum Sensitivity Substrate (Fisher Scientific) if necessary and image with Amersham Imager 680 (GE) or BioRad ChemiDoc MP.

Antibodies

The following primary antibodies were used: mouse monoclonal anti-flag (M2, Sigma), mouse monoclonal anti-HA (6E2, Cell Signaling Technology) and home-made mouse monoclonal anti Internalin A (L7.7) (411), rabbit polyclonal anti-ActA (R32) (412) or rabbit monoclonal anti-ActA (A16) (278), rabbit polyclonal anti-EF-Tu (R114) (413), rabbit polyclonal anti-Internalin C (R134) (414), and rabbit polyclonal anti-LlsX (Covalab, this study). Goat anti-mouse and anti-rabbit IgG HRP-conjugated antibodies (Abcam) were used as secondary antibodies. The primary antibodies were used in a

1:1000 dilution with exception of EF-Tu (1:40000), Internalin C and LlsX (1:2000) and the conjugated antibodies were used in a 1:5000 dilution.

Mass spectrometry

The immunoprecipitated LLS^+-FLAG and LLS^+ (negative control) samples (50µl) were denatured in 4M urea, reduced in TCEP 5mM (30 min at RT) and alkylated using iodoacetamide 20mM (30 min at RT in the dark). Proteins were digested using LysC (500ng, 4h at 30°C). Second digestion with trypsin (500ng, overnight at 37°C) was done after dilution down to 1M urea. Digestion was stopped using 1% final formic acid and peptides were desalted using SepPak column according to manufacturer recommendations. Digested peptides were resuspended in loading buffer (0.1% formic acid). LC-MS/MS analysis of digested peptides was performed on an Orbitrap Q Exactive HF mass spectrometer (Thermo Fisher Scientific, Bremen) coupled to an EASY-nLC 1200 (Thermo Fisher Scientific). A home-made column was used for peptide separation (C18 50 cm capillary column picotip silica emitter tip 75 µm diameter filled with 1.9 µm Reprosil-Pur Basic C18-HD resin, (Dr. Maisch GmbH, Ammerbuch-Entringen, Germany)). The column was equilibrated and peptides were loaded in solvent A (0.1 % FA) at 800 bars. Peptides were separated at 250 $nl.min^{-1}$. Peptides were eluted using a gradient of solvent B (ACN, 0.1 % FA) from 3% to 9% in 5 min, 9% to 29% in 130 min, 29% to 56% in 26 min, 56% to 100% in 5 min (total length of the chromatographic run was 180 min including high ACN level steps and column regeneration).

Mass spectra were acquired in profile mode in data-dependent acquisition mode with the XCalibur 2.2 software (Thermo Fisher Scientific, Bremen) with automatic switching between MS and MS/MS scans using a top-10 method. MS spectra were acquired at a resolution of 60000 (at m/z 400) with a target value of 3 × 106 ions. The scan range was limited from 300 to 1700 m/z. Peptide fragmentation was performed using higher-energy collision dissociation (HCD) with the energy set at 27 NCE. Intensity threshold for ions selection was set at 1×10^5 ions with charge exclusion of z = 1 and z > 7. The MS/MS spectra were acquired in profile mode at a resolution of 15000 (at m/z 400). Isolation window was set at 1.6 Th. Dynamic exclusion was employed within 30s.

Acquired MS data were searched using MaxQuant (version 1.5.3.8) (with the Andromeda search engine) against homer made database proteome of *Listeria monocytogenes* F2365 (6404 entries). The following search parameters were applied: carbamidomethylation of cysteines was set as a fixed modification, oxidation of methionine and protein N-terminal acetylation were set as variable modifications. The mass tolerances in MS and MS/MS were set to 5 ppm and 20 ppm respectively. Maximum peptide charge was set to 7 and 7 amino acids were required as minimum peptide length. Two miss cleavages for trypsin were allowed. A false discovery rate of 1% was set up for both protein and peptide levels. The iBAC feature was also search by the search engine.

RNA extraction and quantitative Real-Time PCR

Total RNA was extracted as previously described (385). Briefly, *L. monocytogenes* F2365 strains were grown in BHI until stationary phase (OD_{600nm} =1.5) and pellets were resuspended in 1 mL TRIzol reagent (Ambion), transferred to 2 mL Lysing Matrix tubes and lysed with a FastPrep apparatus (2 cycles of 45 s, speed 6.5). Tubes were centrifuged at 10 000 *g* for 10 min at 4 °C and the aqueous phase was transferred twice to an Eppendorf tube containing 200 µL of chloroform, lysates were shaken 30 s and incubated at room temperature for 10 min at room temperature and centrifuged 15 min at 13 000 *g* at 4°C. The upper aqueous phase was removed and transferred to a new Eppendorf tube and RNA was precipitated by the addition of 500 µl Isopropanol and incubation at room temperature for 10 min. RNA was pelleted by centrifugation (10 min at 13 000 *g* at 4°C). The supernatant was discarded and the pellet was washed twice with 75% ethanol. RNA pellets were resuspended in 40 µl water. Purified RNA (10 µg) was subjected to DNase treatment (Turbo DNase). cDNA was obtained by treating 500 ng of RNA with QuantiTect Reverse Transcription Kit following manufacturer's instructions. The quantitative Real-Time PCR was performed on CFX384 Touch Real-Time PCR Detection System (Bio-Rad) using SsoFast EvaGreen Supermix following manufacturer's instructions (Bio-Rad). Each reaction was performed in duplicate with 3 independent biological replicates. Data were analyzed by the ΔΔCt method. Gene expression levels were normalized to the *gyrA* gene.

Co-cultures assays

Co-culture assays were performed for 24 h statically at 37 °C in microaerophilic conditions (6% O_2 and 5-10% CO_2) as previously described (349). Briefly, 5×10^7 bacteria from overnight cultures were inoculated into 5 mL of fresh BHI either alone or in coculture with another strain as indicated. At 24 h after inoculation, cultures were serially diluted and plated on BHI and Oxford agar plates (Oxoid). Experiments were performed three times independently.

DISCUSSION AND PERSPECTIVES

Our results provide a better understanding of the LLS biological role and illustrate its mechanism of action. We demonstrate that LLS is no cytotoxic for eukaryotic host cells, targeting exclusively prokaryotic cells. We identified that LLS remains associated to the cell membrane and cytoplasm of LLS-producer bacteria. We determined that LLS is a contact-dependent bacteriocin that leads to permeabilization of the cell membrane in LLS-target bacteria. We also revealed the direct interaction between LLS and the *Lm*-specific protein LlsX at the cell membrane of LLS-producer bacteria, and we show that LlsX is required for expression and/or stabilization of LLS. Moreover, we identified *C. perfringens* as a new LLS target bacterial species *in vitro*. Overall, our results demonstrate that LLS is the first TOMM that displays a contact-dependent inhibition mechanism, impairing the target cell membrane integrity and targeting exclusively prokaryotic cells during *in vivo* infections.

LLS biological function and expression

LLS belongs to the TOMM family, which are present in pathogenic and non-pathogenic bacteria (59) with a diversity of functions such as cytotoxins (56, 57) or bacteriocins (209, 210, 349). The conservation and evolution of these biosynthetic clusters suggest that they present an advantage for the survival of pathogenic and symbiotic bacteria in very specific and different niches. In the case of *Lm,* our group previously demonstrated that the presence of the LLS biosynthetic cluster represents an advantage in the GIT through modulation of the host microbiota composition, facilitating the colonization of the intestinal niche to allow further invasion of deeper tissues (349). Interestingly, some non-pathogenic *Listeria innocua* strains possess a functional LLS gene cluster (313), which suggests that this bacteriocin provides an advantage to these non-pathogenic bacteria in the environment, and raises the question of whether LLS also provides an advantage to *L. monocytogenes* lineage I strains in specific environmental niches.

Is interesting to mention that, while in *L. monocytogenes* the LLS gene cluster is either fully present in some lineage I strains or fully absent in all the other strains, in the case of *L. innocua*, beside these two scenarios there are also some strains which possess

remnants of the cluster (313). At this stage is not possible to determine whether this difference is the result of divergent evolutionary pressures for each bacterial species due to different biological functions of the LLS gene cluster in different niches (415). The identification of signals activating the expression of the LLS gene cluster would have been critical to experimentally address this question. However, our *in vivo* work as well as our *in vitro* HTS experiments did not allow to identify the specific molecular environment that drives LLS activation, suggesting that several signals might be acting in parallel.

The identification of the signal and/or mechanisms involved in LLS regulation is also important because it should allow the study of LLS activity under natural induction conditions as it happens in the GIT, and providing a better understanding of the mechanism(s) of action of LLS. For the assessment of LLS activity, in our study we introduced the constitutive promoter pHELP upstream of the LLS operon. Though this system allowed us to characterize a role for LLS in membrane permeabilization of target bacteria in a contact-dependent manner, we are aware that LLS overexpression could alter its subcellular location. Therefore, identification of the activation signal(s) for LLS and study of LLS in natural induction conditions remains a crucial task.

LLS mechanism of action

Our study allowed to identify that LLS inhibits cell growth and induces cell membrane permeabilization of target cells in a contact-dependent manner. However, we cannot reject the possibility that the membrane permeabilization is a consequence of LLS primary activity in a different bacterial compartment, and not the direct target of LLS. A second possibility we may consider is that LLS displays a dual mechanism of action, targeting several bacterial compartments or activities (as observed for example for nisin, which targets the lipid II and also forms pores in the target bacterial cell membrane).

However, because LlsP, the putative LLS biosynthetic cluster immunity protein, is predicted to localize at the cell membrane of LLS-producer cells, it is tempting to speculate that the LLS target compartment is the cell membrane, in analogy to what has been observed for other TOMMs. Indeed, SLS and MccB17 immunity-like proteins are located in the same subcellular compartment that is targeted by these bacteriocins.

MccB17 targets the cytoplasmic DNA gyrase and the immunity-like protein McbG is located at the cytoplasm of MccB17-producer cells. In the absence of McbG, endogenous MccB17 can partially inhibit DNA synthesis, however the specific immunity mechanism of McbG is still unknown (416, 417). In the case of SLS, the immunity-like protein SagE is predicted to be a membrane spanning peptidase. Though SLS is not a bacteriocin but a cytotoxin that exerts membrane disruption of eukaryotic cells (418), SagE is required for SLS-producer cells viability and is similar to the PnlP immunity protein from *L. plantarum* (177, 212).

High-resolution imaging techniques should be instrumental in confirming the cell membrane as the target compartment for LLS. We performed electron microscopy studies to investigate the distribution of tagged LLS in target bacteria, however immuno-labelling techniques for LLS detection were incompatible with the morphological discrimination of LLS-producer *Lm* and LLS-target *L. lactis* in our co-culture assays. Photonic super-resolution microscopy is another alternative to investigate the subcellular localization of LLS in target cells. Once more, the fact that purified LLS is not active obliges the use of co-culture bacterial systems. However, the use of a short TC tag containing a tetracysteine motif (4Cys) should allow to track LLS in living target bacteria by using the biarsenic organometallic FlAsH reagent, which becomes fluorescent when complexed with the tetracysteine motifs (419–421). The use of different fluorophores in LLS-producer and LLS-target bacteria would also allow to distinguish among these two bacterial populations.

Recently, four PTMs were identified by MS in LLS (Cys^{27}, Cys^{28}, Cys^{30}, and Cys^{35}) (see Annex 1). Though the solubility of the modified LLS is low, its bactericidal activity could be tested. The confirmation of its bactericidal activity could allow to synthetize a mature LLS peptide and also to improve its solubility, in order to perform functional studies on target bacteria with a pure molecule. A purified and active LLS could allow to characterize in a direct and dynamic manner its membrane permeabilization properties by investigating the distribution of specific probes for membranes such as $DiSC_3(5)$ and DiOC2(3), in order to measure changes in the membrane potential of LLS treated cells (422–424).

LLS maturation, self-immunity and export

In our fractionation studies to investigate the distribution of LLS in producer cells, our results showed that in the absence of one of the synthetase complex proteins (LlsB), the LLS precursor peptide is unstable and degraded. Further studies are required to better understand the LLS maturation process by the LlsBYD complex. In general, TOMMs modification mechanisms are still poorly understood. Some of the constraints that hamper the study of these complexes are the difficulty to purify and assemble their components into macromolecular complexes, as well as their low *in vitro* activity levels. However, recent studies with MccB17 suggest that the process of introduction of PTMs could occur co-translationally while the C-terminus of the nascent peptide is still bound to the ribosome. These results indicate that the process of maturation of TOMMs is spatio-temporally regulated with one process leading to the next, suggesting that the MccB17 synthetase complex is stabilized in presence of the peptide and the peptide is also stabilized by the synthetase complex. We hypothesize that LLS maturation process is similar to that of MccB17, since our results suggest that in the absence of the LlsB dehydrogenase the LLS precursor peptide is completely absent (218).

The precise bacterial subcellular location where the LLS is modified by the LlsBYD complex also remains to be identified. We have detected by western blot a LLS smear that disappears in the absence of the LlsB protein, leading us to propose that the smear corresponds to the LLS PTMs. However, we ignore whether LLS is modified before the export through the membrane or after the export, since the smear present in the membrane is different from the smear present in the cytosol. One possibility to approach this question is to block LLS export though the introduction of specific mutations in the LLS leader peptide. In the case of the TOMMs SLS and CLS, the leader peptides that are recognized by their synthetase complexes have been identified: the motif FXXXB (where X is any amino acid and B is a branched chain amino acid) present in the leader peptide of CLS and SLS is important for directing the cyclodehydratase substrate binding. Besides the FXXXB motif, the motif TQV is also important for the synthetase complex binding affinity. Mitchell and colleagues, demonstrated that both motifs present within the SLS N-terminal leader peptide synergize to provide a high affinity binding site to SagC, a component of the PTM complex (57). While the FXXXB and TQV motifs are absent in the LLS signal peptide, we identified two other motifs which are shared between the LLS and STS signal

peptides: NGYS and SEAMXYAAG (where X is Q in STS and N in LLS). Mutation of these motifs could allow to investigate whether they are required for recognition by the LlsBYD synthase complex, and also to investigate whether LLS is modified before or after the export through the membrane.

Recent findings lead us to hypothesize that LlsP putative intramembrane metalloprotease could be also responsible to cleave the signal peptide of mature pro-LLS. In MccB17, the heterodimeric metalloprotease TldDE processes the signal peptide of mature MccB17acting as a ‘‘molecular pencil sharpener’’ (425). Intriguingly, the MccB17 precursor peptide is resistant to proteolysis unless it is completely modified. (425). TldD contains a conserved metalloprotease-like HExxxH motif that requires Zn or Fe as cofactors for its proteolytic activity (425). Interestingly, TldDE is encoded elsewhere in the genome and is capable of processing other unfolded peptides (425). LlsP on the other hand is located in the same operon as LLS, suggesting that it could be a more specific protease capable of processing only modified pro-LLS. LlsP metalloprotease activity could be investigated by using metalloprotease inhibitors such as O-phenanthroline, EDTA, phosphoramidon or bestatin. These inhibitors should be able to block LlsP activity and thus LLS bactericidal activity should be absent and/or producer bacteria might dye due to LLS effect.

Our results suggest that the ABC transporter LlsGH and the LlsP protein are both involved in conferring self-immunity to the LLS-producer bacteria, since both mutants are not viable in the LLS^+ background. Interestingly, both mutants are viable in a F2365 WT (LLS^-) background in which the LLS is not produced. This result suggests that LLS must be produced and translocated through the membrane in order to avoid intoxication of producer cells. As previously mentioned, several ABC transporters are involved in self-immunity (121, 123, 124). For example, the McjD ABC transporter, which transports MccJ25 and also provides self-immunity to producer cells (60). This could be the case for the ABC transporter LlsGH. However, the potential contribution of LlsGH and LlsP to LLS immunity still requires formal demonstration.

The precise mechanism of secretion of LLS also remains to be identified. Recently, a two-step secretion model has been identified in *Pseudomonas fluorescens*, where an

ABC transporter and a protease work together to release a membrane protein. The LapBC (ABC transporter) and LapE (TolC-like OM pore) retain the LapA adhesin involved in biofilm formation at the IM (426). A cysteine protease called LapG is linked to the ABC transporter LapBC. LapG is responsible for the post-translational cleavage of LapA. When LapA is cleaved by LapG at the N-terminal di-alanine motif, LapA is removed from the cell surface (427). LapA is then released through LapBC (ABC-like transporter) (427). This two-step secretion model has been only identified in Gram-negative bacteria but could be a strategy used by Gram-positive bacteria as well.

Other aspect that remains unsolved is how the LLS is tethered to the cell membrane of producer bacteria. We hypothesize that LLS could be tethered to the LTA as it has been proposed for SLS which is also a membrane bound molecule, and LTA may be the binding site between streptococcal surface SLS and target cells (34). The construction of *lafAB* mutant (it cannot assemble LTA) (428) could be used to address this question. This mutant was previously used to prove that LTA contribute to the surface association of the *Lm* surface protein InlB (429). The possibility that LLS is tethered to other molecules such as lipoproteins can be also explored by generating a deletion mutant for the prolipoprotein diacylglyceryl transferase Lgt, which catalyzes the transfer of a diacylglyceryl moiety to the N-terminal cysteine of the mature lipoproteins (430).

Our results suggest that LlsX interacts with LLS at the membrane level and could act as a chaperone stabilizing LLS. It is tempting to speculate a two-step secretion model, where LlsX act as a chaperone that stabilizes LLS while the peptide is being modified, Then, LlsX transfer mature LLS to the LlsP intramembrane metalloprotease that cleaves LLS signal peptide. This proteolytic cleavage could lead to the release of LLS from the membrane through the LlsGH ABC transporter. Subsequently, mature LLS could be tethered to the membrane of producer bacteria by interactions with the LTA until delivery to the target bacteria in a contact-dependent manner. However, more functional and biochemical studies are required to understand the molecular interplay between the LLS operon gene products.

Proposed model of LLS activity

Based on our results, we propose a working model of LLS production, maturation and activity:

1. Once *Lm* reach the GIT within the host, an unknown signal allows the activation of LLS operon genes.

2. LLS pro-peptide is transcribed and stabilized by LlsX at the cell membrane level.

3. The LLS signal peptide is recognized by the synthetase complex LlsBYD and thiazole heterocycles are introduced.

5. Modified LLS peptide is transferred to the membrane metalloprotease LlsP that cleaves the LLS signal peptide.

6.Mature LLS is transported by LlsGH ABC transporter.

7. The LLS transport through the LlsGH ABC transporter allows LLS tethering to the cell membrane through potential interactions with LTA.

8. LLS is delivered to the target bacteria in a contact-dependent manner interacting with target bacteria surface negative charges.

9. LLS target specific microbiota species from the Firmicutes phyla leading to cell growth arrest, cell membrane permeabilization and lysis of target bacteria.

10. LLS leads to the alteration of the host intestinal microbiota and promotes intestinal colonization by *Lm*.

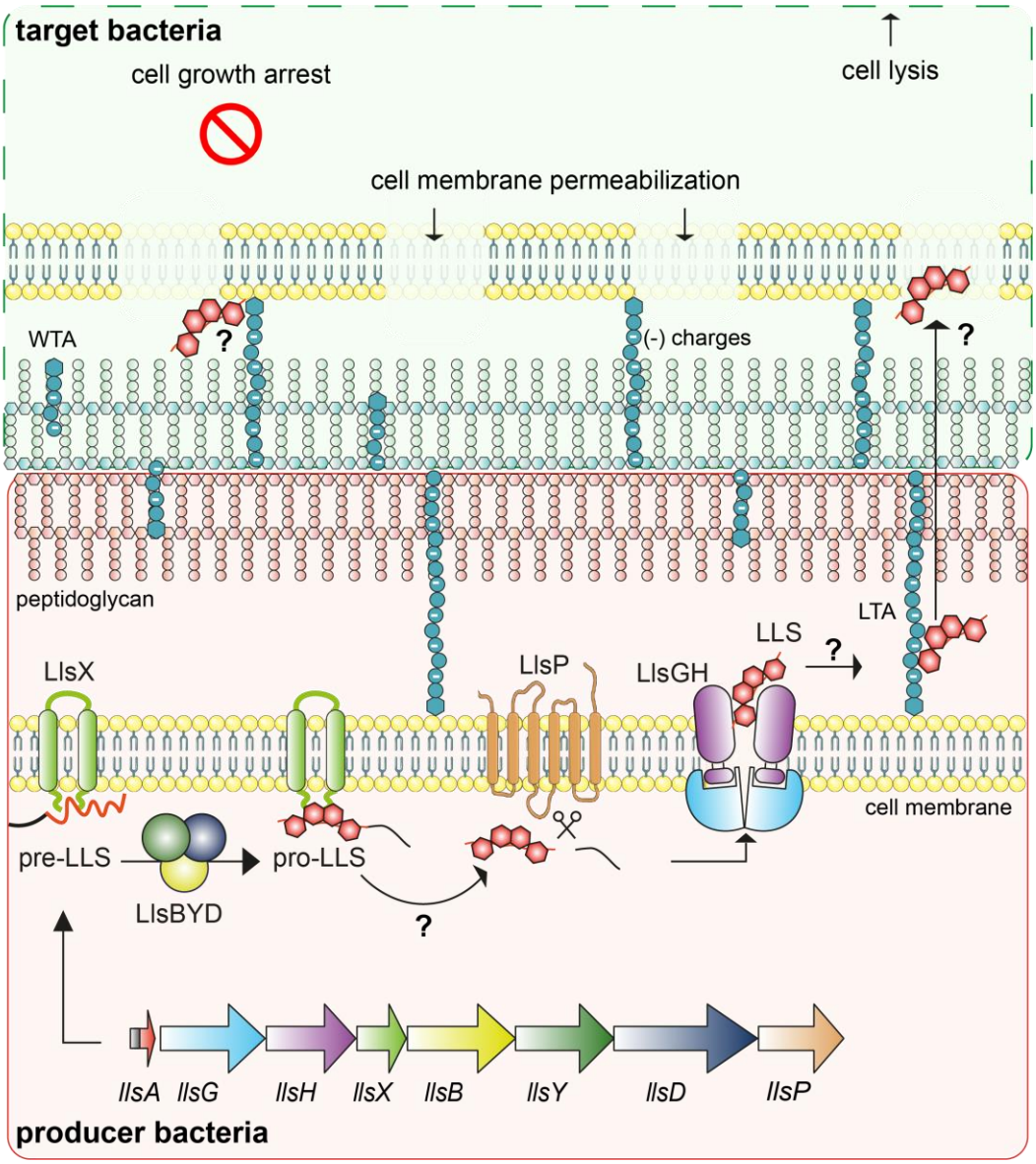

Figure 34. Working model on LLS production, maturation and CDI activity. LLS pro-peptide is transcribed and stabilized by LlsX at the cell membrane level (?). LLS is modified by the synthetase complex LlsBYD. Modified LLS peptide is transferred to the membrane metalloprotease LlsP that cleaves the LLS signal peptide (?). LLS is exported though the LlsGH ABC transporter and tethered to the cell membrane through interactions with the LTA (?). Subsequently, LLS is delivered to the target bacteria in a contact-dependent manner interacting with target bacteria surface negative charges. LLS induces cell membrane permeabilization, cell growth arrest and cell lysis. Consequently, LLS leads to the alteration of the host intestinal microbiota promoting intestinal colonization by *Lm*.

REFERENCES

1. Arnison PG, Bibb MJ, Bierbaum G, Bowers AA, Bugni TS, Bulaj G, Camarero JA, Campopiano DJ, Challis GL, Clardy J, Cotter PD, Craik DJ, Dawson M, Dittmann E, Donadio S, Dorrestein PC, Entian K-D, Fischbach MA, Garavelli JS, Göransson U, Gruber CW, Haft DH, Hemscheidt TK, Hertweck C, Hill C, Horswill AR, Jaspars M, Kelly WL, Klinman JP, Kuipers OP, Link AJ, Liu W, Marahiel MA, Mitchell DA, Moll GN, Moore BS, Müller R, Nair SK, Nes IF, Norris GE, Olivera BM, Onaka H, Patchett ML, Piel J, Reaney MJT, Rebuffat S, Ross RP, Sahl H-G, Schmidt EW, Selsted ME, Severinov K, Shen B, Sivonen K, Smith L, Stein T, Süssmuth RD, Tagg JR, Tang G-L, Truman AW, Vederas JC, Walsh CT, Walton JD, Wenzel SC, Willey JM, van der Donk WA. 2013. Ribosomally synthesized and post-translationally modified peptide natural products: overview and recommendations for a universal nomenclature. Nat Prod Rep 30:108–160.
2. Nes IF. 2011. History, Current Knowledge, and Future Directions on Bacteriocin Research in Lactic Acid Bacteria, p. 3–12. *In* Drider, D, Rebuffat, S (eds.), Prokaryotic Antimicrobial Peptides. Springer New York, New York, NY.
3. Zasloff M. 2002. Antimicrobial peptides of multicellular organisms. Nature 415:389–395.
4. Pasteur L, Joubert J. 1877. Charbon et septicemie. C R Soc Biol Paris 101–115.
5. Rea MC, Ross RP, Cotter PD, Hill C. 2011. Classification of Bacteriocins from Gram-Positive Bacteria, p. 29–53. *In* Drider, D, Rebuffat, S (eds.), Prokaryotic Antimicrobial Peptides. Springer New York, New York, NY.
6. Rebuffat S. 2011. Bacteriocins from Gram-Negative Bacteria: A Classification?, p. 55–72. *In* Drider, D, Rebuffat, S (eds.), Prokaryotic Antimicrobial Peptides. Springer New York, New York, NY.
7. Gratia JP. 2000. André Gratia: a forerunner in microbial and viral genetics. Genetics 156:471–476.
8. Jacob F, Lwoff A, Siminovitch A, Wollman E. 1953. [Definition of some terms relative to lysogeny]. Ann Inst Pasteur 84:222–224.
9. Tagg JR, Dajani AS, Wannamaker LW. 1976. Bacteriocins of gram-positive bacteria. Bacteriol Rev 40:722–756.
10. Klaenhammer TR. 1988. Bacteriocins of lactic acid bacteria. Biochimie 70:337–349.
11. Riley MA. 1998. MOLECULAR MECHANISMS OF BACTERIOCIN EVOLUTION. Annu Rev Genet 32:255–278.
12. Klaenhammer TR. 1988. Bacteriocins of lactic acid bacteria. Biochimie 70:337–349.

13. Gordon DM, O'Brien CL. 2006. Bacteriocin diversity and the frequency of multiple bacteriocin production in Escherichia coli. Microbiology 152:3239–3244.

14. O'Shea EF, Gardiner GE, O'Connor PM, Mills S, Ross RP, Hill C. 2009. Characterization of enterocin- and salivaricin-producing lactic acid bacteria from the mammalian gastrointestinal tract. FEMS Microbiol Lett 291:24–34.

15. Cotter PD, Hill C, Ross RP. 2005. Bacteriocins: developing innate immunity for food. Nat Rev Microbiol 3:777–788.

16. Cotter PD, Ross RP, Hill C. 2013. Bacteriocins — a viable alternative to antibiotics? Nat Rev Microbiol 11:95–105.

17. Riley MA. 2011. Bacteriocin-Mediated Competitive Interactions of Bacterial Populations and Communities, p. 13–26. *In* Drider, D, Rebuffat, S (eds.), Prokaryotic Antimicrobial Peptides. Springer New York, New York, NY.

18. Rebuffat S. 2011. Microcins from Enterobacteria: On the Edge Between Gram-Positive Bacteriocins and Colicins, p. 333–349. *In* Drider, D, Rebuffat, S (eds.), Prokaryotic Antimicrobial Peptides. Springer New York, New York, NY.

19. Cascales E, Buchanan SK, Duche D, Kleanthous C, Lloubes R, Postle K, Riley M, Slatin S, Cavard D. 2007. Colicin Biology. Microbiol Mol Biol Rev 71:158–229.

20. Braun V, Patzer SI, Hantke K. 2002. Ton-dependent colicins and microcins: modular design and evolution. Biochimie 84:365–380.

21. Ghazaryan L, Tonoyan L, Ashhab AA, Soares MIM, Gillor O. 2014. The role of stress in colicin regulation. Arch Microbiol 196:753–764.

22. Jakes KS, Cramer WA. 2012. Border Crossings: Colicins and Transporters. Annu Rev Genet 46:209–231.

23. Cramer WA, Sharma O, Zakharov SD. 2018. On mechanisms of colicin import: the outer membrane quandary. Biochem J 475:3903–3915.

24. Housden NG, Kleanthous C. 2012. Colicin translocation across the Escherichia coli outer membrane. Biochem Soc Trans 40:1475–1479.

25. de Zamaroczy M, Chauleau M. 2011. Colicin Killing: Foiled Cell Defense and Hijacked Cell Functions, p. 255–287. *In* Drider, D, Rebuffat, S (eds.), Prokaryotic Antimicrobial Peptides. Springer New York, New York, NY.

26. Duquesne S, Destoumieux-Garzón D, Peduzzi J, Rebuffat S. 2007. Microcins, gene-encoded antibacterial peptides from enterobacteria. Nat Prod Rep 24:708.

27. Piper C, Cotter P, Ross R, Hill C. 2009. Discovery of Medically Significant Lantibiotics. Curr Drug Discov Technol 6:1–18.

28. Klaenhammer TR. 1993. Genetics of bacteriocins produced by lactic acid bacteria. FEMS Microbiol Rev 12:39–85.

29. Heng NCK, Wescombe PA, Burton JP, Jack RW, Tagg JR. 2007. The Diversity of Bacteriocins in Gram-Positive Bacteria, p. 45–92. *In* Riley, MA, Chavan, MA (eds.), Bacteriocins. Springer Berlin Heidelberg, Berlin, Heidelberg.

30. Acedo JZ, Chiorean S, Vederas JC, van Belkum MJ. 2018. The expanding structural variety among bacteriocins from Gram-positive bacteria. FEMS Microbiol Rev 42:805–828.

31. Kuipers A, Rink R, Moll GN. 2011. Genetics, Biosynthesis, Structure, and Mode of Action of Lantibiotics, p. 147–169. *In* Drider, D, Rebuffat, S (eds.), Prokaryotic Antimicrobial Peptides. Springer New York, New York, NY.

32. Willey JM, van der Donk WA. 2007. Lantibiotics: Peptides of Diverse Structure and Function. Annu Rev Microbiol 61:477–501.

33. Knerr PJ, van der Donk WA. 2012. Discovery, Biosynthesis, and Engineering of Lantipeptides. Annu Rev Biochem 81:479–505.

34. Goto Y, Li B, Claesen J, Shi Y, Bibb MJ, van der Donk WA. 2010. Discovery of Unique Lanthionine Synthetases Reveals New Mechanistic and Evolutionary Insights. PLoS Biol 8:e1000339.

35. Meindl K, Schmiederer T, Schneider K, Reicke A, Butz D, Keller S, Gühring H, Vértesy L, Wink J, Hoffmann H, Brönstrup M, Sheldrick GM, Süssmuth RD. 2010. Labyrinthopeptins: A New Class of Carbacyclic Lantibiotics. Angew Chem Int Ed 49:1151–1154.

36. Kawulka K, Sprules T, McKay RT, Mercier P, Diaper CM, Zuber P, Vederas JC. 2003. Structure of Subtilosin A, an Antimicrobial Peptide from *Bacillus s ubtilis* with Unusual Posttranslational Modifications Linking Cysteine Sulfurs to α-Carbons of Phenylalanine and Threonine. J Am Chem Soc 125:4726–4727.

37. Rea MC, Sit CS, Clayton E, O'Connor PM, Whittal RM, Zheng J, Vederas JC, Ross RP, Hill C. 2010. Thuricin CD, a posttranslationally modified bacteriocin with a narrow spectrum of activity against Clostridium difficile. Proc Natl Acad Sci 107:9352–9357.

38. Bagley MC, Dale JW, Merritt EA, Xiong X. 2005. Thiopeptide Antibiotics. Chem Rev 105:685–714.

39. Nissen-Meyer J, Rogne P, Oppegard C, Haugen H, Kristiansen P. 2009. Structure-Function Relationships of the Non-Lanthionine-Containing Peptide (class II) Bacteriocins Produced by Gram-Positive Bacteria. Curr Pharm Biotechnol 10:19–37.

40. Belguesmia Y, Naghmouchi K, Chihib N-E, Drider D. 2011. Class IIa Bacteriocins: Current Knowledge and Perspectives, p. 171–195. *In* Drider, D, Rebuffat, S (eds.), Prokaryotic Antimicrobial Peptides. Springer New York, New York, NY.

41. Rodríguez JM, Martínez MI, Kok J. 2002. Pediocin PA-1, a Wide-Spectrum Bacteriocin from Lactic Acid Bacteria. Crit Rev Food Sci Nutr 42:91–121.

42. Nissen-Meyer J, Oppegård C, Rogne P, Haugen HS, Kristiansen PE. 2011. The Two-Peptide (Class-IIb) Bacteriocins: Genetics, Biosynthesis, Structure, and Mode of Action, p. 197–212. *In* Drider, D, Rebuffat, S (eds.), Prokaryotic Antimicrobial Peptides. Springer New York, New York, NY.

43. Rogne P, Fimland G, Nissen-Meyer J, Kristiansen PE. 2008. Three-dimensional structure of the two peptides that constitute the two-peptide bacteriocin lactococcin G. Biochim Biophys Acta BBA - Proteins Proteomics 1784:543–554.

44. Rogne P, Haugen C, Fimland G, Nissen-Meyer J, Kristiansen PE. 2009. Three-dimensional structure of the two-peptide bacteriocin plantaricin JK. Peptides 30:1613–1621.

45. Martin-Visscher LA, van Belkum MJ, Vederas JC. 2011. Class IIc or Circular Bacteriocins, p. 213–236. *In* Drider, D, Rebuffat, S (eds.), Prokaryotic Antimicrobial Peptides. Springer New York, New York, NY.

46. Iwatani S, Zendo T, Sonomoto K. 2011. Class IId or Linear and Non-Pediocin-Like Bacteriocins, p. 237–252. *In* Drider, D, Rebuffat, S (eds.), Prokaryotic Antimicrobial Peptides. Springer New York, New York, NY.

47. Oman TJ, Boettcher JM, Wang H, Okalibe XN, van der Donk WA. 2011. Sublancin is not a lantibiotic but an S-linked glycopeptide. Nat Chem Biol 7:78–80.

48. Stepper J, Shastri S, Loo TS, Preston JC, Novak P, Man P, Moore CH, Havlíček V, Patchett ML, Norris GE. 2011. Cysteine S-glycosylation, a new post-translational modification found in glycopeptide bacteriocins. FEBS Lett 585:645–650.

49. Wang H, van der Donk WA. 2011. Substrate Selectivity of the Sublancin S-Glycosyltransferase. J Am Chem Soc 133:16394–16397.

50. Wiebach V, Mainz A, Siegert M-AJ, Jungmann NA, Lesquame G, Tirat S, Dreux-Zigha A, Aszodi J, Le Beller D, Süssmuth RD. 2018. The anti-staphylococcal lipolanthines are ribosomally synthesized lipopeptides. Nat Chem Biol 14:652–654.

51. Minami Y, Yoshida K, Azuma R, Urakawa A, Kawauchi T, Otani T, Komiyama K, Ōmura S. 1994. Structure of cypemycin, a new peptide antibiotic. Tetrahedron Lett 35:8001–8004.

52. Claesen J, Bibb M. 2010. Genome mining and genetic analysis of cypemycin biosynthesis reveal an unusual class of posttranslationally modified peptides. Proc Natl Acad Sci 107:16297–16302.

53. Hamada T, Matsunaga S, Yano G, Fusetani N. 2005. Polytheonamides A and B, Highly Cytotoxic, Linear Polypeptides with Unprecedented Structural Features, from the Marine Sponge, *Theonella s winhoei*. J Am Chem Soc 127:110–118.

54. Iwamoto M, Shimizu H, Muramatsu I, Oiki S. 2010. A cytotoxic peptide from a marine sponge exhibits ion channel activity through vectorial-insertion into the membrane. FEBS Lett 584:3995–3999.

55. Freeman MF, Gurgui C, Helf MJ, Morinaka BI, Uria AR, Oldham NJ, Sahl H-G, Matsunaga S, Piel J. 2012. Metagenome Mining Reveals Polytheonamides as Posttranslationally Modified Ribosomal Peptides. Science 338:387–390.

56. Molloy EM, Cotter PD, Hill C, Mitchell DA, Ross RP. 2011. Streptolysin S-like virulence factors: the continuing sagA. Nat Rev Microbiol 9:670–681.

57. Mitchell DA, Lee SW, Pence MA, Markley AL, Limm JD, Nizet V, Dixon JE. 2009. Structural and Functional Dissection of the Heterocyclic Peptide Cytotoxin Streptolysin S. J Biol Chem 284:13004–13012.

58. Li YM, Milne JC, Madison LL, Kolter R, Walsh CT. 1996. From peptide precursors to oxazole and thiazole-containing peptide antibiotics: microcin B17 synthase. Science 274:1188–1193.

59. Lee SW, Mitchell DA, Markley AL, Hensler ME, Gonzalez D, Wohlrab A, Dorrestein PC, Nizet V, Dixon JE. 2008. Discovery of a widely distributed toxin biosynthetic gene cluster. Proc Natl Acad Sci 105:5879–5884.

60. Maksimov MO, Pan SJ, James Link A. 2012. Lasso peptides: structure, function, biosynthesis, and engineering. Nat Prod Rep 29:996–1006.

61. Bierbaum G, Jansen A. 2007. Tying the knot: making of lasso peptides. Chem Biol 14:734–735.

62. Rosengren KJ, Craik DJ. 2009. How bugs make lassos. Chem Biol 16:1211–1212.

63. Rebuffat S, Blond A, Destoumieux-Garzón D, Goulard C, Peduzzi J. 2004. Microcin J25, from the macrocyclic to the lasso structure: implications for biosynthetic, evolutionary and biotechnological perspectives. Curr Protein Pept Sci 5:383–391.

64. Sivonen K, Leikoski N, Fewer DP, Jokela J. 2010. Cyanobactins—ribosomal cyclic peptides produced by cyanobacteria. Appl Microbiol Biotechnol 86:1213–1225.

65. Donia MS, Schmidt EW. 2011. Linking Chemistry and Genetics in the Growing Cyanobactin Natural Products Family. Chem Biol 18:508–519.

66. Amagai K, Ikeda H, Hashimoto J, Kozone I, Izumikawa M, Kudo F, Eguchi T, Nakamura T, Osada H, Takahashi S, Shin-ya K. 2017. Identification of a gene cluster for telomestatin biosynthesis and heterologous expression using a specific promoter in a clean host. Sci Rep 7:3382.

67. Weiz AR, Ishida K, Makower K, Ziemert N, Hertweck C, Dittmann E. 2011. Leader peptide and a membrane protein scaffold guide the biosynthesis of the tricyclic peptide microviridin. Chem Biol 18:1413–1421.

68. Philmus B, Christiansen G, Yoshida WY, Hemscheidt TK. 2008. Post-translational modification in microviridin biosynthesis. Chembiochem Eur J Chem Biol 9:3066–3073.

69. Oman TJ, van der Donk WA. 2010. Follow the leader: the use of leader peptides to guide natural product biosynthesis. Nat Chem Biol 6:9–18.

70. Müller WM, Ensle P, Krawczyk B, Süssmuth RD. 2011. Leader Peptide-Directed Processing of Labyrinthopeptin A2 Precursor Peptide by the Modifying Enzyme LabKC. Biochemistry 50:8362–8373.

71. Sprules T, Kawulka KE, Gibbs AC, Wishart DS, Vederas JC. 2004. NMR solution structure of the precursor for carnobacteriocin B2, an antimicrobial peptide from Carnobacterium piscicola. Implications of the alpha-helical leader section for export and inhibition of type IIa bacteriocin activity. Eur J Biochem 271:1748–1756.

72. Dutton JL, Renda RF, Waine C, Clark RJ, Daly NL, Jennings CV, Anderson MA, Craik DJ. 2004. Conserved Structural and Sequence Elements Implicated in the Processing of Gene-encoded Circular Proteins. J Biol Chem 279:46858–46867.

73. Patton GC, Paul M, Cooper LE, Chatterjee C, van der Donk WA. 2008. The Importance of the Leader Sequence for Directing Lanthionine Formation in Lacticin 481 †. Biochemistry 47:7342–7351.

74. Furgerson Ihnken LA, Chatterjee C, van der Donk WA. 2008. *In Vitro* Reconstitution and Substrate Specificity of a Lantibiotic Protease †. Biochemistry 47:7352–7363.

75. Cheung WL, Pan SJ, Link AJ. 2010. Much of the Microcin J25 Leader Peptide is Dispensable. J Am Chem Soc 132:2514–2515.

76. Gonzalez D, Mavridou DAI. 2019. Making the Best of Aggression: The Many Dimensions of Bacterial Toxin Regulation. Trends Microbiol 27:897–905.

77. Kuhar I, Zgur-Bertok D. 1999. Transcription regulation of the colicin K cka gene reveals induction of colicin synthesis by differential responses to environmental signals. J Bacteriol 181:7373–7380.

78. Kuhar I, Van Putten JPM, Žgur-Bertok D, Gaastra W, Jordi BJAM. 2001. Codon-usage based regulation of colicin K synthesis by the stress alarmone ppGpp: Translational regulation of colicin K by ppGpp. Mol Microbiol 41:207–216.

79. Niehus R, Mitri S, Fletcher AG, Foster KR. 2015. Migration and horizontal gene transfer divide microbial genomes into multiple niches. Nat Commun 6:8924.

80. Mulec J, Podlesek Z, Mrak P, Kopitar A, Ihan A, Žgur-Bertok D. 2003. A cka-gfp Transcriptional Fusion Reveals that the Colicin K Activity Gene Is Induced in Only 3 Percent of the Population. J Bacteriol 185:654–659.

81. Žgur-Bertok D. 2012. Regulating colicin synthesis to cope with stress and lethality of colicin production. Biochem Soc Trans 40:1507–1511.

82. van Raay K, Kerr B. 2016. Toxins go viral: phage-encoded lysis releases group B colicins: Toxins go viral. Environ Microbiol 18:1308–1311.

83. Shanker E, Federle M. 2017. Quorum Sensing Regulation of Competence and Bacteriocins in Streptococcus pneumoniae and mutans. Genes 8:15.

84. Papenfort K, Bassler BL. 2016. Quorum sensing signal–response systems in Gram-negative bacteria. Nat Rev Microbiol 14:576–588.

85. Monnet V, Juillard V, Gardan R. 2014. Peptide conversations in Gram-positive bacteria. Crit Rev Microbiol 1–13.

86. Eijsink VGH, Axelsson L, Diep DB, Håvarstein LS, Holo H, Nes IF. 2002. Production of class II bacteriocins by lactic acid bacteria; an example of biological warfare and communication. Antonie Van Leeuwenhoek 81:639–654.

87. Kleerebezem M, Quadri LE. 2001. Peptide pheromone-dependent regulation of antimicrobial peptide production in Gram-positive bacteria: a case of multicellular behavior. Peptides 22:1579–1596.

88. Parkinson JS, Kofoid EC. 1992. Communication Modules in Bacterial Signaling Proteins. Annu Rev Genet 26:71–112.

89. Kuipers OP, Beerthuyzen MM, Siezen RJ, Vos WM. 1993. Characterization of the nisin gene cluster nisABTCIPR of Lactococcus lactis. Requirement of expression of the nisA and nisIgenes for development of immunity. Eur J Biochem 216:281–291.

90. Kuipers OP, Beerthuyzen MM, de Ruyter PGGA, Luesink EJ, de Vos WM. 1995. Autoregulation of Nisin Biosynthesis in *Lactococcus lactis* by Signal Transduction. J Biol Chem 270:27299–27304.

91. Ra R, Beerthuyzen MM, de Vos WM, Saris PEJ, Kuipers OP. 1999. Effects of gene disruptions in the nisin gene cluster of Lactococcus lactis on nisin production and producer immunity. Microbiology 145:1227–1233.

92. Li H, O'Sullivan DJ. 2006. Identification of a nisI Promoter within the nisABCTIP Operon That May Enable Establishment of Nisin Immunity Prior to Induction of the Operon via Signal Transduction. J Bacteriol 188:8496–8503.

93. Quadri LE, Sailer M, Roy KL, Vederas JC, Stiles ME. 1994. Chemical and genetic characterization of bacteriocins produced by Carnobacterium piscicola LV17B. J Biol Chem 269:12204–12211.

94. Quadri LEN, Yan LZ, Stiles ME, Vederas JC. 1997. Effect of Amino Acid Substitutions on the Activity of Carnobacteriocin B2: OVERPRODUCTION OF THE ANTIMICROBIAL PEPTIDE, ITS ENGINEERED VARIANTS, AND ITS PRECURSOR IN *ESCHERICHIA COLI*. J Biol Chem 272:3384–3388.

95. Worobo RW, Henkel T, Sailer M, Roy KL, Vederas JC, Stiles ME. 1994. Characteristics and genetic determinant of a hydrophobic peptide bacteriocin,

carnobacteriocin A, produced by Carnobacterium piscicola LV17A. Microbiology 140:517–526.

96. Saucier L, Poon A, Stiles ME. 1995. Induction of bacteriocin in *Carnobacterium piscicola* LV17. J Appl Bacteriol 78:684–690.

97. Kies S, Vuong C, Hille M, Peschel A, Meyer C, Götz F, Otto M. 2003. Control of antimicrobial peptide synthesis by the agr quorum sensing system in Staphylococcus epidermidis: activity of the lantibiotic epidermin is regulated at the level of precursor peptide processing. Peptides 24:329–338.

98. Johnston C, Martin B, Fichant G, Polard P, Claverys J-P. 2014. Bacterial transformation: distribution, shared mechanisms and divergent control. Nat Rev Microbiol 12:181–196.

99. Havarstein LS, Coomaraswamy G, Morrison DA. 1995. An unmodified heptadecapeptide pheromone induces competence for genetic transformation in Streptococcus pneumoniae. Proc Natl Acad Sci 92:11140–11144.

100. Guiral S, Mitchell TJ, Martin B, Claverys J-P. 2005. From The Cover: Competence-programmed predation of noncompetent cells in the human pathogen Streptococcus pneumoniae: Genetic requirements. Proc Natl Acad Sci 102:8710–8715.

101. Knutsen E, Ween O, Håvarstein LS. 2004. Two Separate Quorum-Sensing Systems Upregulate Transcription of the Same ABC Transporter in Streptococcus pneumoniae. J Bacteriol 186:3078–3085.

102. Chiuchiolo MJ, Delgado MA, Farías RN, Salomón RA. 2001. Growth-Phase-Dependent Expression of the Cyclopeptide Antibiotic Microcin J25. J Bacteriol 183:1755–1764.

103. Boyer AE, Tai PC. 1998. Characterization of the cvaAand cvi Promoters of the Colicin V Export System: Iron-Dependent Transcription of cvaA Is Modulated by Downstream Sequences. J Bacteriol 180:1662–1672.

104. Zaini PA, Fogaça AC, Lupo FGN, Nakaya HI, Vêncio RZN, da Silva AM. 2008. The Iron Stimulon of Xylella fastidiosa Includes Genes for Type IV Pilus and Colicin V-Like Bacteriocins. J Bacteriol 190:2368–2378.

105. Dingemans J, Ghequire MGK, Craggs M, De Mot R, Cornelis P. 2016. Identification and functional analysis of a bacteriocin, pyocin S6, with ribonuclease activity from a *Pseudomonas aeruginosa* cystic fibrosis clinical isolate. MicrobiologyOpen 5:413–423.

106. Diep DB, Axelsson L, Grefsli C, Nes IF. 2000. The synthesis of the bacteriocin sakacin A is a temperature-sensitive process regulated by a pheromone peptide through a three-component regulatory system. Microbiology 146:2155–2160.

107. Hindré T, Pennec J-P, Haras D, Dufour A. 2004. Regulation of lantibiotic lacticin 481 production at the transcriptional level by acid pH. FEMS Microbiol Lett 231:291–298.

108. Beis K, Rebuffat S. 2019. Multifaceted ABC transporters associated to microcin and bacteriocin export. Res Microbiol 170:399–406.

109. Gebhard S. 2012. ABC transporters of antimicrobial peptides in Firmicutes bacteria - phylogeny, function and regulation. Mol Microbiol 86:1295–1317.

110. Zheng S, Sonomoto K. 2018. Diversified transporters and pathways for bacteriocin secretion in gram-positive bacteria. Appl Microbiol Biotechnol 102:4243–4253.

111. Aoki SK. 2005. Contact-Dependent Inhibition of Growth in Escherichia coli. Science 309:1245–1248.

112. Aoki SK, Diner EJ, de Roodenbeke C t'Kint, Burgess BR, Poole SJ, Braaten BA, Jones AM, Webb JS, Hayes CS, Cotter PA, Low DA. 2010. A widespread family of polymorphic contact-dependent toxin delivery systems in bacteria. Nature 468:439–442.

113. Ruhe ZC, Low DA, Hayes CS. 2013. Bacterial contact-dependent growth inhibition. Trends Microbiol 21:230–237.

114. Unterweger D, Miyata ST, Bachmann V, Brooks TM, Mullins T, Kostiuk B, Provenzano D, Pukatzki S. 2014. The Vibrio cholerae type VI secretion system employs diverse effector modules for intraspecific competition. Nat Commun 5:3549.

115. Garcia EC. 2018. Contact-dependent interbacterial toxins deliver a message. Curr Opin Microbiol 42:40–46.

116. Whitney JC, Peterson SB, Kim J, Pazos M, Verster AJ, Radey MC, Kulasekara HD, Ching MQ, Bullen NP, Bryant D, Goo YA, Surette MG, Borenstein E, Vollmer W, Mougous JD. 2017. A broadly distributed toxin family mediates contact-dependent antagonism between gram-positive bacteria. eLife 6:e26938.

117. Locher KP. 2016. Mechanistic diversity in ATP-binding cassette (ABC) transporters. Nat Struct Mol Biol 23:487–493.

118. Jones PM, O'Mara ML, George AM. 2009. ABC transporters: a riddle wrapped in a mystery inside an enigma. Trends Biochem Sci 34:520–531.

119. Moussatova A, Kandt C, O'Mara ML, Tieleman DP. 2008. ATP-binding cassette transporters in Escherichia coli. Biochim Biophys Acta BBA - Biomembr 1778:1757–1771.

120. Wright J, Muench SP, Goldman A, Baker A. 2018. Substrate polyspecificity and conformational relevance in ABC transporters: new insights from structural studies. Biochem Soc Trans 46:1475–1484.

121. Zheng S, Sonomoto K. 2018. Diversified transporters and pathways for bacteriocin secretion in gram-positive bacteria. Appl Microbiol Biotechnol 102:4243–4253.

122. Kazakov T, Vondenhoff GH, Datsenko KA, Novikova M, Metlitskaya A, Wanner BL, Severinov K. 2008. Escherichia coli Peptidase A, B, or N Can Process Translation Inhibitor Microcin C. J Bacteriol 190:2607–2610.

123. Ishii S, Yano T, Hayashi H. 2006. Expression and Characterization of the Peptidase Domain of *Streptococcus pneumoniae* ComA, a Bifunctional ATP-binding Cassette Transporter Involved in Quorum Sensing Pathway. J Biol Chem 281:4726–4731.

124. Bobeica SC, Dong S-H, Huo L, Mazo N, McLaughlin MI, Jiménez-Osés G, Nair SK, van der Donk WA. 2019. Insights into AMS/PCAT transporters from biochemical and structural characterization of a double Glycine motif protease. eLife 8:e42305.

125. Romano M, Fusco G, Choudhury HG, Mehmood S, Robinson CV, Zirah S, Hegemann JD, Lescop E, Marahiel MA, Rebuffat S, De Simone A, Beis K. 2018. Structural Basis for Natural Product Selection and Export by Bacterial ABC Transporters. ACS Chem Biol 13:1598–1609.

126. Sushida H, Ishibashi N, Zendo T, Wilaipun P, Leelawatcharamas V, Nakayama J, Sonomoto K. 2018. Evaluation of leader peptides that affect the secretory ability of a multiple bacteriocin transporter, EnkT. J Biosci Bioeng 126:23–29.

127. Veenendaal AKJ, van der Does C, Driessen AJM. 2004. The protein-conducting channel SecYEG. Biochim Biophys Acta BBA - Mol Cell Res 1694:81–95.

128. Schneewind O, Missiakas D. 2014. Sec-secretion and sortase-mediated anchoring of proteins in Gram-positive bacteria. Biochim Biophys Acta BBA - Mol Cell Res 1843:1687–1697.

129. Aoki SK. 2005. Contact-Dependent Inhibition of Growth in Escherichia coli. Science 309:1245–1248.

130. Angkawidjaja C, Kanaya S. 2006. Family I.3 lipase: bacterial lipases secreted by the type I secretion system. Cell Mol Life Sci 63:2804–2817.

131. Thomas S, Holland IB, Schmitt L. 2014. The Type 1 secretion pathway — The hemolysin system and beyond. Biochim Biophys Acta BBA - Mol Cell Res 1843:1629–1641.

132. Létoffé S, Delepelaire P, Wandersman C. 1996. Protein secretion in gram-negative bacteria: assembly of the three components of ABC protein-mediated exporters is ordered and promoted by substrate binding. EMBO J 15:5804–5811.

133. García-Bayona L, Guo MS, Laub MT. 2017. Contact-dependent killing by Caulobacter crescentus via cell surface-associated, glycine zipper proteins. eLife 6:e24869.

134. Morse RP, Nikolakakis KC, Willett JLE, Gerrick E, Low DA, Hayes CS, Goulding CW. 2012. Structural basis of toxicity and immunity in contact-dependent growth inhibition (CDI) systems. Proc Natl Acad Sci 109:21480–21485.

135. Russell AB, Peterson SB, Mougous JD. 2014. Type VI secretion system effectors: poisons with a purpose. Nat Rev Microbiol 12:137–148.

136. Pukatzki S, Ma AT, Sturtevant D, Krastins B, Sarracino D, Nelson WC, Heidelberg JF, Mekalanos JJ. 2006. Identification of a conserved bacterial protein secretion system in Vibrio cholerae using the Dictyostelium host model system. Proc Natl Acad Sci 103:1528–1533.

137. Hood RD, Singh P, Hsu F, Güvener T, Carl MA, Trinidad RRS, Silverman JM, Ohlson BB, Hicks KG, Plemel RL, Li M, Schwarz S, Wang WY, Merz AJ, Goodlett DR, Mougous JD. 2010. A Type VI Secretion System of Pseudomonas aeruginosa Targets a Toxin to Bacteria. Cell Host Microbe 7:25–37.

138. Schwarz S, West TE, Boyer F, Chiang W-C, Carl MA, Hood RD, Rohmer L, Tolker-Nielsen T, Skerrett SJ, Mougous JD. 2010. Burkholderia Type VI Secretion Systems Have Distinct Roles in Eukaryotic and Bacterial Cell Interactions. PLoS Pathog 6:e1001068.

139. Sana TG, Flaugnatti N, Lugo KA, Lam LH, Jacobson A, Baylot V, Durand E, Journet L, Cascales E, Monack DM. 2016. *Salmonella* Typhimurium utilizes a T6SS-mediated antibacterial weapon to establish in the host gut. Proc Natl Acad Sci 113:E5044–E5051.

140. Chatzidaki-Livanis M, Geva-Zatorsky N, Comstock LE. 2016. *Bacteroides fragilis* type VI secretion systems use novel effector and immunity proteins to antagonize human gut Bacteroidales species. Proc Natl Acad Sci 113:3627–3632.

141. Hecht AL, Casterline BW, Earley ZM, Goo YA, Goodlett DR, Bubeck Wardenburg J. 2016. Strain competition restricts colonization of an enteric pathogen and prevents colitis. EMBO Rep 17:1281–1291.

142. Ates LS, Houben ENG, Bitter W. 2016. Type VII Secretion: A Highly Versatile Secretion System. Microbiol Spectr 4.

143. Rashid R, Veleba M, Kline KA. 2016. Focal Targeting of the Bacterial Envelope by Antimicrobial Peptides. Front Cell Dev Biol 4.

144. López-Lara IM, Geiger O. 2017. Bacterial lipid diversity. Biochim Biophys Acta BBA - Mol Cell Biol Lipids 1862:1287–1299.

145. Kumariya R, Garsa AK, Rajput YS, Sood SK, Akhtar N, Patel S. 2019. Bacteriocins: Classification, synthesis, mechanism of action and resistance development in food spoilage causing bacteria. Microb Pathog 128:171–177.

146. Moll GN, Konings WN, Driessen AJ. 1999. Bacteriocins: mechanism of membrane insertion and pore formation. Antonie Van Leeuwenhoek 76:185–198.

147. Hasper HE, Kramer NE, Smith JL, Hillman JD, Zachariah C, Kuipers OP, de Kruijff B, Breukink E. 2006. An Alternative Bactericidal Mechanism of Action for Lantibiotic Peptides That Target Lipid II. Science 313:1636–1637.

148. Brotz H, Bierbaum G, Reynolds PE, Sahl H-G. 1997. The Lantibiotic Mersacidin Inhibits Peptidoglycan Biosynthesis at the Level of Transglycosylation. Eur J Biochem 246:193–199.

149. Wiedemann I, Böttiger T, Bonelli RR, Schneider T, Sahl H-G, Martínez B. 2006. Lipid II-Based Antimicrobial Activity of the Lantibiotic Plantaricin C. Appl Environ Microbiol 72:2809–2814.

150. Ramnath M, Arous S, Gravesen A, Hastings JW, Héchard Y. 2004. Expression of mptC of Listeria monocytogenes induces sensitivity to class IIa bacteriocins in Lactococcus lactis. Microbiology 150:2663–2668.

151. Kjos M, Salehian Z, Nes IF, Diep DB. 2010. An Extracellular Loop of the Mannose Phosphotransferase System Component IIC Is Responsible for Specific Targeting by Class IIa Bacteriocins. J Bacteriol 192:5906–5913.

152. Ríos Colombo NS, Chalón MC, Navarro SA, Bellomio A. 2018. Pediocin-like bacteriocins: new perspectives on mechanism of action and immunity. Curr Genet 64:345–351.

153. Drider D, Fimland G, Héchard Y, McMullen LM, Prévost H. 2006. The Continuing Story of Class IIa Bacteriocins. Microbiol Mol Biol Rev 70:564–582.

154. Diep DB, Skaugen M, Salehian Z, Holo H, Nes IF. 2007. Common mechanisms of target cell recognition and immunity for class II bacteriocins. Proc Natl Acad Sci 104:2384–2389.

155. Nissen-Meyer J, Oppegård C, Rogne P, Haugen HS, Kristiansen PE. 2010. Structure and Mode-of-Action of the Two-Peptide (Class-IIb) Bacteriocins. Probiotics Antimicrob Proteins 2:52–60.

156. Moll GN, van den Akker E, Hauge HH, Nissen-Meyer J, Nes IF, Konings WN, Driessen AJM. 1999. Complementary and Overlapping Selectivity of the Two-Peptide Bacteriocins Plantaricin EF and JK. J Bacteriol 181:4848–4852.

157. Moll G, Ubbink-Kok T, Hildeng-Hauge H, Nissen-Meyer J, Nes IF, Konings WN, Driessen AJ. 1996. Lactococcin G is a potassium ion-conducting, two-component bacteriocin. J Bacteriol 178:600–605.

158. Parks WM, Bottrill AR, Pierrat OA, Durrant MC, Maxwell A. 2007. The action of the bacterial toxin, microcin B17, on DNA gyrase. Biochimie 89:500–507.

159. Herrero M, Moreno F. 1986. Microcin B17 Blocks DNA Replication and Induces the SOS System in Escherichia coli. Microbiology 132:393–402.

160. Heddle JG, Blance SJ, Zamble DB, Hollfelder F, Miller DA, Wentzell LM, Walsh CT, Maxwell A. 2001. The antibiotic microcin B17 is a DNA gyrase poison: characterisation of the mode of inhibition. J Mol Biol 307:1223–1234.

161. Vincent P, Morero R. 2009. The Structure and Biological Aspects of Peptide Antibiotic Microcin J25. Curr Med Chem 16:538–549.

162. Nickels BE, Hochschild A. 2004. Regulation of RNA Polymerase through the Secondary Channel. Cell 118:281–284.

163. Metlitskaya A, Kazakov T, Kommer A, Pavlova O, Praetorius-Ibba M, Ibba M, Krasheninnikov I, Kolb V, Khmel I, Severinov K. 2006. Aspartyl-tRNA Synthetase Is the Target of Peptide Nucleotide Antibiotic Microcin C. J Biol Chem 281:18033–18042.

164. Travin DY, Bikmetov D, Severinov K. 2020. Translation-Targeting RiPPs and Where to Find Them. Front Genet 11:226.

165. Harms JM, Wilson DN, Schluenzen F, Connell SR, Stachelhaus T, Zaborowska Z, Spahn CMT, Fucini P. 2008. Translational Regulation via L11: Molecular Switches on the Ribosome Turned On and Off by Thiostrepton and Micrococcin. Mol Cell 30:26–38.

166. Heffron SE, Jurnak F. 2000. Structure of an EF-Tu Complex with a Thiazolyl Peptide Antibiotic Determined at 2.35 Å Resolution: Atomic Basis for GE2270A Inhibition of EF-Tu †,‡. Biochemistry 39:37–45.

167. Metelev M, Osterman IA, Ghilarov D, Khabibullina NF, Yakimov A, Shabalin K, Utkina I, Travin DY, Komarova ES, Serebryakova M, Artamonova T, Khodorkovskii M, Konevega AL, Sergiev PV, Severinov K, Polikanov YS. 2017. Klebsazolicin inhibits 70S ribosome by obstructing the peptide exit tunnel. Nat Chem Biol 13:1129–1136.

168. Travin DY, Watson ZL, Metelev M, Ward FR, Osterman IA, Khven IM, Khabibullina NF, Serebryakova M, Mergaert P, Polikanov YS, Cate JHD, Severinov K. 2019. Structure of ribosome-bound azole-modified peptide phazolicin rationalizes its species-specific mode of bacterial translation inhibition. Nat Commun 10:4563.

169. Draper LA, Ross RP, Hill C, Cotter PD. 2008. Lantibiotic immunity. Curr Protein Pept Sci 9:39–49.

170. Kjos M, Borrero J, Opsata M, Birri DJ, Holo H, Cintas LM, Snipen L, Hernández PE, Nes IF, Diep DB. 2011. Target recognition, resistance, immunity and genome mining of class II bacteriocins from Gram-positive bacteria. Microbiology 157:3256–3267.

171. Dubois J-YF, Kouwen TRHM, Schurich AKC, Reis CR, Ensing HT, Trip EN, Zweers JC, van Dijl JM. 2009. Immunity to the bacteriocin sublancin 168 Is determined by the SunI (YolF) protein of Bacillus subtilis. Antimicrob Agents Chemother 53:651–661.

172. Bierbaum G, Sahl H-G. 2009. Lantibiotics: Mode of Action, Biosynthesis and Bioengineering. Curr Pharm Biotechnol 10:2–18.

173. Coelho MLV, Coutinho BG, Cabral da Silva Santos O, Nes IF, Bastos M do C de F. 2014. Immunity to the Staphylococcus aureus leaderless four-peptide bacteriocin aureocin A70 is conferred by AurI, an integral membrane protein. Res Microbiol 165:50–59.

174. Bastos M do C de F, Coelho MLV, Santos OC da S. 2015. Resistance to bacteriocins produced by Gram-positive bacteria. Microbiology 161:683–700.

175. Pei J, Grishin NV. 2001. Type II CAAX prenyl endopeptidases belong to a novel superfamily of putative membrane-bound metalloproteases. Trends Biochem Sci 26:275–277.

176. Pei J, Mitchell DA, Dixon JE, Grishin NV. 2011. Expansion of Type II CAAX Proteases Reveals Evolutionary Origin of γ-Secretase Subunit APH-1. J Mol Biol 410:18–26.

177. Kjos M, Snipen L, Salehian Z, Nes IF, Diep DB. 2010. The Abi Proteins and Their Involvement in Bacteriocin Self-Immunity. J Bacteriol 192:2068–2076.

178. Gajic O, Buist G, Kojic M, Topisirovic L, Kuipers OP, Kok J. 2003. Novel Mechanism of Bacteriocin Secretion and Immunity Carried Out by Lactococcal Multidrug Resistance Proteins. J Biol Chem 278:34291–34298.

179. Diaz M, Valdivia E, Martínez-Bueno M, Fernández M, Soler-González AS, Ramírez-Rodrigo H, Maqueda M. 2003. Characterization of a New Operon, as-48EFGH, from the as-48 Gene Cluster Involved in Immunity to Enterocin AS-48. Appl Environ Microbiol 69:1229–1236.

180. Nascimento J d. S, Coelho MLV, Ceotto H, Potter A, Fleming LR, Salehian Z, Nes IF, Bastos M d. C d. F. 2012. Genes Involved in Immunity to and Secretion of Aureocin A53, an Atypical Class II Bacteriocin Produced by Staphylococcus aureus A53. J Bacteriol 194:875–883.

181. van Belkum MJ, Martin-Visscher LA, Vederas JC. 2011. Structure and genetics of circular bacteriocins. Trends Microbiol 19:411–418.

182. Fath MJ, Kolter R. 1993. ABC transporters: bacterial exporters. Microbiol Rev 57:995–1017.

183. Ehlert K, Tschierske M, Mori C, Schröder W, Berger-Bächi B. 2000. Site-Specific Serine Incorporation by Lif and Epr into Positions 3 and 5 of the Staphylococcal Peptidoglycan Interpeptide Bridge. J Bacteriol 182:2635–2638.

184. Qiao M, Immonen T, Koponen O, Saris PEJ. 1995. The cellular location and effect on nisin immunity of the NisI protein from Lactococcus lactis N8 expressed in Escherichia coli and L. lactis. FEMS Microbiol Lett 131:75–80.

185. Koponen O, Takala TM, Saarela U, Qiao M, Saris PEJ. 2004. Distribution of the NisI immunity protein and enhancement of nisin activity by the lipid-free NisI. FEMS Microbiol Lett 231:85–90.

186. Aso Y, Okuda K, Nagao J, Kanemasa Y, Thi Bich Phuong N, Koga H, Shioya K, Sashihara T, Nakayama J, Sonomoto K. 2005. A Novel Type of Immunity Protein, NukH, for the Lantibiotic Nukacin ISK-1 Produced by *Staphylococcus warneri* ISK-1. Biosci Biotechnol Biochem 69:1403–1410.

187. Hille M, Kies S, Götz F, Peschel A. 2001. Dual Role of GdmH in Producer Immunity and Secretion of the Staphylococcal Lantibiotics Gallidermin and Epidermin. Appl Environ Microbiol 67:1380–1383.

188. Brown SP, Fredrik Inglis R, Taddei F. 2009. SYNTHESIS: Evolutionary ecology of microbial wars: within-host competition and (incidental) virulence: Microbial warfare. Evol Appl 2:32–39.

189. Vriezen JAC, Valliere M, Riley MA. 2009. The Evolution of Reduced Microbial Killing. Genome Biol Evol 1:400–408.

190. Barnes B, Sidhu H, Gordon DM. 2007. Host gastro-intestinal dynamics and the frequency of colicin production by Escherichia coli. Microbiology 153:2823–2827.

191. Lozupone CA, Stombaugh JI, Gordon JI, Jansson JK, Knight R. 2012. Diversity, stability and resilience of the human gut microbiota. Nature 489:220–230.

192. Chassaing B, Cascales E. 2018. Antibacterial Weapons: Targeted Destruction in the Microbiota. Trends Microbiol 26:329–338.

193. Weiss GA, Hennet T. 2017. Mechanisms and consequences of intestinal dysbiosis. Cell Mol Life Sci 74:2959–2977.

194. Kim S, Covington A, Pamer EG. 2017. The intestinal microbiota: Antibiotics, colonization resistance, and enteric pathogens. Immunol Rev 279:90–105.

195. Wexler AG, Bao Y, Whitney JC, Bobay L-M, Xavier JB, Schofield WB, Barry NA, Russell AB, Tran BQ, Goo YA, Goodlett DR, Ochman H, Mougous JD, Goodman AL. 2016. Human symbionts inject and neutralize antibacterial toxins to persist in the gut. Proc Natl Acad Sci 113:3639–3644.

196. Coyne MJ, Comstock LE. 2019. Type VI Secretion Systems and the Gut Microbiota. Microbiol Spectr 7.

197. Coyne MJ, Roelofs KG, Comstock LE. 2016. Type VI secretion systems of human gut Bacteroidales segregate into three genetic architectures, two of which are contained on mobile genetic elements. BMC Genomics 17:58.

198. Gueguen E, Cascales E. 2013. Promoter Swapping Unveils the Role of the Citrobacter rodentium CTS1 Type VI Secretion System in Interbacterial Competition. Appl Environ Microbiol 79:32–38.

199. MacIntyre DL, Miyata ST, Kitaoka M, Pukatzki S. 2010. The Vibrio cholerae type VI secretion system displays antimicrobial properties. Proc Natl Acad Sci 107:19520–19524.

200. Bernard CS, Brunet YR, Gueguen E, Cascales E. 2010. Nooks and Crannies in Type VI Secretion Regulation. J Bacteriol 192:3850–3860.

201. Bachmann V, Kostiuk B, Unterweger D, Diaz-Satizabal L, Ogg S, Pukatzki S. 2015. Bile Salts Modulate the Mucin-Activated Type VI Secretion System of Pandemic Vibrio cholerae. PLoS Negl Trop Dis 9:e0004031.

202. Brunet YR, Bernard CS, Gavioli M, Lloubès R, Cascales E. 2011. An Epigenetic Switch Involving Overlapping Fur and DNA Methylation Optimizes Expression of a Type VI Secretion Gene Cluster. PLoS Genet 7:e1002205.

203. Gillor O, Giladi I, Riley MA. 2009. Persistence of colicinogenic Escherichia coli in the mouse gastrointestinal tract. BMC Microbiol 9:165.

204. Majeed H, Gillor O, Kerr B, Riley MA. 2011. Competitive interactions in Escherichia coli populations: the role of bacteriocins. ISME J 5:71–81.

205. Sassone-Corsi M, Nuccio S-P, Liu H, Hernandez D, Vu CT, Takahashi AA, Edwards RA, Raffatellu M. 2016. Microcins mediate competition among Enterobacteriaceae in the inflamed gut. Nature 540:280–283.

206. Rea MC, Dobson A, O'Sullivan O, Crispie F, Fouhy F, Cotter PD, Shanahan F, Kiely B, Hill C, Ross RP. 2011. Effect of broad- and narrow-spectrum antimicrobials on Clostridium difficile and microbial diversity in a model of the distal colon. Proc Natl Acad Sci 108:4639–4644.

207. Molohon KJ, Blair PM, Park S, Doroghazi JR, Maxson T, Hershfield JR, Flatt KM, Schroeder NE, Ha T, Mitchell DA. 2016. Plantazolicin Is an Ultranarrow-Spectrum Antibiotic That Targets the Bacillus anthracis Membrane. ACS Infect Dis 2:207–220.

208. Lee SW, Mitchell DA, Markley AL, Hensler ME, Gonzalez D, Wohlrab A, Dorrestein PC, Nizet V, Dixon JE. 2008. Discovery of a widely distributed toxin biosynthetic gene cluster. Proc Natl Acad Sci 105:5879–5884.

209. Molohon KJ, Blair PM, Park S, Doroghazi JR, Maxson T, Hershfield JR, Flatt KM, Schroeder NE, Ha T, Mitchell DA. 2016. Plantazolicin Is an Ultranarrow-Spectrum Antibiotic That Targets the *Bacillus anthracis* Membrane. ACS Infect Dis 2:207–220.

210. Li YM, Milne JC, Madison LL, Kolter R, Walsh CT. 1996. From peptide precursors to oxazole and thiazole-containing peptide antibiotics: microcin B17 synthase. Science 274:1188–1193.

211. Melby JO, Nard NJ, Mitchell DA. 2011. Thiazole/oxazole-modified microcins: complex natural products from ribosomal templates. Curr Opin Chem Biol 15:369–378.

212. Molloy EM, Cotter PD, Hill C, Mitchell DA, Ross RP. 2011. Streptolysin S-like virulence factors: the continuing sagA. Nat Rev Microbiol 9:670–681.

213. Nizet V, Beall B, Bast DJ, Datta V, Kilburn L, Low DE, De Azavedo JC. 2000. Genetic locus for streptolysin S production by group A streptococcus. Infect Immun 68:4245–4254.

214. Haft DH, Basu MK, Mitchell DA. 2010. Expansion of ribosomally produced natural products: a nitrile hydratase- and Nif11-related precursor family. BMC Biol 8:70.

215. Datta V, Myskowski SM, Kwinn LA, Chiem DN, Varki N, Kansal RG, Kotb M, Nizet V. 2005. Mutational analysis of the group A streptococcal operon encoding streptolysin S and its virulence role in invasive infection: SLS operon and invasive GAS infection. Mol Microbiol 56:681–695.

216. Vizán JL, Hernández-Chico C, del Castillo I, Moreno F. 1991. The peptide antibiotic microcin B17 induces double-strand cleavage of DNA mediated by E. coli DNA gyrase. EMBO J 10:467–476.

217. Yorgey P, Lee J, Kordel J, Vivas E, Warner P, Jebaratnam D, Kolter R. 1994. Posttranslational modifications in microcin B17 define an additional class of DNA gyrase inhibitor. Proc Natl Acad Sci 91:4519–4523.

218. Ghilarov D, Stevenson CEM, Travin DY, Piskunova J, Serebryakova M, Maxwell A, Lawson DM, Severinov K. 2019. Architecture of Microcin B17 Synthetase: An Octameric Protein Complex Converting a Ribosomally Synthesized Peptide into a DNA Gyrase Poison. Mol Cell 73:749-762.e5.

219. Yorgey P, Davagnino J, Kolter R. 1993. The maturation pathway of microcin B17, a peptide inhibitor of DNA gyrase. Mol Microbiol 9:897–905.

220. Cunningham MW. 2000. Pathogenesis of Group A Streptococcal Infections. Clin Microbiol Rev 13:470–511.

221. Gonzalez DJ, Lee SW, Hensler ME, Markley AL, Dahesh S, Mitchell DA, Bandeira N, Nizet V, Dixon JE, Dorrestein PC. 2010. Clostridiolysin S, a Post-translationally Modified Biotoxin from *Clostridium botulinum*. J Biol Chem 285:28220–28228.

222. Nizet V. 2002. Streptococcal beta-hemolysins: genetics and role in disease pathogenesis. Trends Microbiol 10:575–580.

223. Ginsburg I. 1999. Is streptolysin S of group A streptococci a virulence factor? APMIS 107:1051–1059.

224. Loridan C, Alouf JE. 1986. Purification of RNA-core Induced Streptolysin S, and Isolation and Haemolytic Characteristics of the Carrier-free Toxin. Microbiology 132:307–315.

225. Keiser H, Weissmann G, Bernheimer AW. 1964. Studies on lysosomes. iv. solubilization of enzymes during mitochondrial swelling and disruption of lysosomes by streptolysin S and other hemolytic agents. J Cell Biol 22:101–113.

226. Hryniewicz W, Pryjma J. 1977. Effect of streptolysin S on human and mouse T and B lymphocytes. Infect Immun 16:730–733.

227. Bernheimer AW, Schwartz LL. 1964. Lysosomal disruption by bacterial toxins. J Bacteriol 87:1100–1104.

228. Bernheimer AW, Schwartz LL. 1965. Effects of staphylococcal and other bacterial toxins on plateletsin vitro. J Pathol Bacteriol 89:209–223.

229. Bernheimer AW. 1966. Disruption of wall-less bacteria by streptococcal and staphylococcal toxins. J Bacteriol 91:1677–1680.

230. Higashi DL, Biais N, Donahue DL, Mayfield JA, Tessier CR, Rodriguez K, Ashfeld BL, Luchetti J, Ploplis VA, Castellino FJ, Lee SW. 2016. Activation of band 3 mediates group A Streptococcus streptolysin S-based beta-haemolysis. Nat Microbiol 1:15004.

231. Humar D, Datta V, Bast DJ, Beall B, De Azavedo JC, Nizet V. 2002. Streptolysin S and necrotising infections produced by group G streptococcus. The Lancet 359:124–129.

232. Miyoshi-Akiyama T, Takamatsu D, Koyanagi M, Zhao J, Imanishi K, Uchiyama T. 2005. Cytocidal Effect of *Streptococcus pyogenes* on Mouse Neutrophils In Vivo and the Critical Role of Streptolysin S. J Infect Dis 192:107–116.

233. Nizet V. 2002. Streptococcal beta-hemolysins: genetics and role in disease pathogenesis. Trends Microbiol 10:575–580.

234. Sumitomo T, Nakata M, Higashino M, Jin Y, Terao Y, Fujinaga Y, Kawabata S. 2011. Streptolysin S Contributes to Group A Streptococcal Translocation across an Epithelial Barrier. J Biol Chem 286:2750–2761.

235. Salim KY, de Azavedo JC, Bast DJ, Cvitkovitch DG. 2007. Role for sagA and siaA in Quorum Sensing and Iron Regulation in Streptococcus pyogenes. Infect Immun 75:5011–5017.

236. Mangold M, Siller M, Roppenser B, Vlaminckx BJM, Penfound TA, Klein R, Novak R, Novick RP, Charpentier E. 2004. Synthesis of group A streptococcal virulence factors is controlled by a regulatory RNA molecule: Control of GAS virulence factors by an RNA molecule. Mol Microbiol 53:1515–1527.

237. Sebaihia M, Peck MW, Minton NP, Thomson NR, Holden MTG, Mitchell WJ, Carter AT, Bentley SD, Mason DR, Crossman L, Paul CJ, Ivens A, Wells-Bennik MHJ, Davis IJ, Cerdeno-Tarraga AM, Churcher C, Quail MA, Chillingworth T, Feltwell T, Fraser A, Goodhead I, Hance Z, Jagels K, Larke N, Maddison M, Moule S, Mungall K, Norbertczak H, Rabbinowitsch E, Sanders M, Simmonds M, White B, Whithead S, Parkhill J. 2007. Genome sequence of a proteolytic (Group I) Clostridium botulinum strain Hall A and comparative analysis of the clostridial genomes. Genome Res 17:1082–1092.

238. Molohon KJ, Melby JO, Lee J, Evans BS, Dunbar KL, Bumpus SB, Kelleher NL, Mitchell DA. 2011. Structure determination and interception of biosynthetic intermediates for the plantazolicin class of highly discriminating antibiotics. ACS Chem Biol 6:1307–1313.

239. Orsi RH, Bakker HC den, Wiedmann M. 2011. *Listeria monocytogenes* lineages: Genomics, evolution, ecology, and phenotypic characteristics. Int J Med Microbiol 301:79–96.

240. Núñez-Montero K, Leclercq A, Moura A, Vales G, Peraza J, Pizarro-Cerdá J, Lecuit M. 2018. Listeria costaricensis sp. nov. Int J Syst Evol Microbiol 68:844–850.

241. Leclercq A, Moura A, Vales G, Tessaud-Rita N, Aguilhon C, Lecuit M. 2019. Listeria thailandensis sp. nov. Int J Syst Evol Microbiol 69:74–81.

242. Cossart P. 2011. Illuminating the landscape of host-pathogen interactions with the bacterium *Listeria monocytogenes*. Proc Natl Acad Sci 108:19484–19491.

243. Radoshevich L, Cossart P. 2017. *Listeria monocytogenes*: towards a complete picture of its physiology and pathogenesis. Nat Rev Microbiol 16:32–46.

244. Rasmussen OF, Beck T, Olsen JE, Dons L, Rossen L. 1991. Listeria monocytogenes isolates can be classified into two major types according to the sequence of the listeriolysin gene. Infect Immun 59:3945–3951.

245. Graves LM, Swaminathan B, Reeves MW, Hunter SB, Weaver RE, Plikaytis BD, Schuchat A. 1994. Comparison of ribotyping and multilocus enzyme electrophoresis for subtyping of Listeria monocytogenes isolates. J Clin Microbiol 32:2936–2943.

246. Brosch R, Chen J, Luchansky JB. 1994. Pulsed-field fingerprinting of listeriae: identification of genomic divisions for Listeria monocytogenes and their correlation with serovar. Appl Environ Microbiol 60:2584–2592.

247. Wiedmann M, Bruce JL, Keating C, Johnson AE, McDonough PL, Batt CA. 1997. Ribotypes and virulence gene polymorphisms suggest three distinct Listeria monocytogenes lineages with differences in pathogenic potential. Infect Immun 65:2707–2716.

248. Doumith M, Cazalet C, Simoes N, Frangeul L, Jacquet C, Kunst F, Martin P, Cossart P, Glaser P, Buchrieser C. 2004. New Aspects Regarding Evolution and Virulence of Listeria monocytogenes Revealed by Comparative Genomics and DNA Arrays. Infect Immun 72:1072–1083.

249. Ragon M, Wirth T, Hollandt F, Lavenir R, Lecuit M, Le Monnier A, Brisse S. 2008. A New Perspective on Listeria monocytogenes Evolution. PLoS Pathog 4:e1000146.

250. Orsi RH, Bakker HC den, Wiedmann M. 2011. Listeria monocytogenes lineages: Genomics, evolution, ecology, and phenotypic characteristics. Int J Med Microbiol 301:79–96.

251. Cotter PD, Draper LA, Lawton EM, Daly KM, Groeger DS, Casey PG, Ross RP, Hill C. 2008. Listeriolysin S, a novel peptide haemolysin associated with a subset of lineage I Listeria monocytogenes. PLoS Pathog 4:e1000144.

252. Maury MM, Tsai Y-H, Charlier C, Touchon M, Chenal-Francisque V, Leclercq A, Criscuolo A, Gaultier C, Roussel S, Brisabois A, Disson O, Rocha EPC, Brisse S, Lecuit M. 2016. Uncovering *Listeria monocytogenes* hypervirulence by harnessing its biodiversity. Nat Genet 48:308–313.

253. Cotter PD, Draper LA, Lawton EM, Daly KM, Groeger DS, Casey PG, Ross RP, Hill C. 2008. Listeriolysin S, a Novel Peptide Haemolysin Associated with a Subset of Lineage I *Listeria monocytogenes*. PLoS Pathog 4:e1000144.

254. Cossart P. 2011. Illuminating the landscape of host-pathogen interactions with the bacterium Listeria monocytogenes. Proc Natl Acad Sci 108:19484–19491.

255. Schlech WF, Lavigne PM, Bortolussi RA, Allen AC, Haldane EV, Wort AJ, Hightower AW, Johnson SE, King SH, Nicholls ES, Broome CV. 1983. Epidemic Listeriosis — Evidence for Transmission by Food. N Engl J Med 308:203–206.

256. McLauchlin J. 1990. Human listeriosis in Britain, 1967–85, a summary of 722 cases: 2. Listeriosis in non-pregnant individuals, a changing pattern of infection and seasonal incidence. Epidemiol Infect 104:191–201.

257. McLauchlin J. 1990. Human listeriosis in Britain, 1967–85, a summary of 722 cases: 1. Listeriosis during pregnancy and in the newborn. Epidemiol Infect 104:181–189.

258. de Noordhout CM, Devleesschauwer B, Angulo FJ, Verbeke G, Haagsma J, Kirk M, Havelaar A, Speybroeck N. 2014. The global burden of listeriosis: a systematic review and meta-analysis. Lancet Infect Dis 14:1073–1082.

259. Nikitas G, Deschamps C, Disson O, Niault T, Cossart P, Lecuit M. 2011. Transcytosis of Listeria monocytogenes across the intestinal barrier upon specific targeting of goblet cell accessible E-cadherin. J Exp Med 208:2263–2277.

260. Bakardjiev AI, Theriot JA, Portnoy DA. 2006. Listeria monocytogenes Traffics from Maternal Organs to the Placenta and Back. PLoS Pathog 2:e66.

261. Pizarro-Cerda J, Kuhbacher A, Cossart P. 2012. Entry of Listeria monocytogenes in Mammalian Epithelial Cells: An Updated View. Cold Spring Harb Perspect Med 2:a010009–a010009.

262. Cossart P, Helenius A. 2014. Endocytosis of Viruses and Bacteria. Cold Spring Harb Perspect Biol 6:a016972–a016972.

263. Jonquières R, Bierne H, Fiedler F, Gounon P, Cossart P. 1999. Interaction between the protein InlB of *Listeria monocytogenes* and lipoteichoic acid: a novel

mechanism of protein association at the surface of gram-positive bacteria. Mol Microbiol 34:902–914.

264. Bierne H, Sabet C, Personnic N, Cossart P. 2007. Internalins: a complex family of leucine-rich repeat-containing proteins in Listeria monocytogenes. Microbes Infect 9:1156–1166.

265. Bierne H, Cossart P. 2002. InlB, a surface protein of Listeria monocytogenes that behaves as an invasin and a growth factor. J Cell Sci 115:3357–3367.

266. Disson O, Grayo S, Huillet E, Nikitas G, Langa-Vives F, Dussurget O, Ragon M, Le Monnier A, Babinet C, Cossart P, Lecuit M. 2008. Conjugated action of two species-specific invasion proteins for fetoplacental listeriosis. Nature 455:1114–1118.

267. Lecuit M. 2001. A Transgenic Model for Listeriosis: Role of Internalin in Crossing the Intestinal Barrier. Science 292:1722–1725.

268. Quereda JJ, Cossart P, Pizarro-Cerdá J. 2016. Role of Listeria monocytogenes Exotoxins in Virulence, p. 1–20. *In* Gopalakrishnakone, P, Stiles, B, Alape-Girón, A, Dubreuil, JD, Mandal, M (eds.), Microbial Toxins. Springer Netherlands, Dordrecht.

269. Seveau S. 2014. Multifaceted Activity of Listeriolysin O, the Cholesterol-Dependent Cytolysin of Listeria monocytogenes, p. 161–195. *In* Anderluh, G, Gilbert, R (eds.), MACPF/CDC Proteins - Agents of Defence, Attack and Invasion. Springer Netherlands, Dordrecht.

270. Peraro MD, van der Goot FG. 2016. Pore-forming toxins: ancient, but never really out of fashion. Nat Rev Microbiol 14:77–92.

271. Ruan Y, Rezelj S, Bedina Zavec A, Anderluh G, Scheuring S. 2016. Listeriolysin O Membrane Damaging Activity Involves Arc Formation and Lineaction -- Implication for Listeria monocytogenes Escape from Phagocytic Vacuole. PLOS Pathog 12:e1005597.

272. Mulvihill E, van Pee K, Mari SA, Müller DJ, Yildiz Ö. 2015. Directly Observing the Lipid-Dependent Self-Assembly and Pore-Forming Mechanism of the Cytolytic Toxin Listeriolysin O. Nano Lett 15:6965–6973.

273. Hamon MA, Ribet D, Stavru F, Cossart P. 2012. Listeriolysin O: the Swiss army knife of Listeria. Trends Microbiol 20:360–368.

274. Schnupf P, Portnoy DA. 2007. Listeriolysin O: a phagosome-specific lysin. Microbes Infect 9:1176–1187.

275. Alberti-Segui C, Goeden KR, Higgins DE. 2007. Differential function of Listeria monocytogenes listeriolysin O and phospholipases C in vacuolar dissolution following cell-to-cell spread. Cell Microbiol 9:179–195.

276. Xayarath B, Alonzo F, Freitag NE. 2015. Identification of a Peptide-Pheromone that Enhances Listeria monocytogenes Escape from Host Cell Vacuoles. PLOS Pathog 11:e1004707.

277. Rabinovich L, Sigal N, Borovok I, Nir-Paz R, Herskovits AA. 2012. Prophage Excision Activates Listeria Competence Genes that Promote Phagosomal Escape and Virulence. Cell 150:792–802.

278. Boujemaa-Paterski R, Gouin E, Hansen G, Samarin S, Le Clainche C, Didry D, Dehoux P, Cossart P, Kocks C, Carlier M-F, Pantaloni D. 2001. *Listeria* Protein ActA Mimics WASP Family Proteins: It Activates Filament Barbed End Branching by Arp2/3 Complex. Biochemistry 40:11390–11404.

279. Rajabian T, Gavicherla B, Heisig M, Müller-Altrock S, Goebel W, Gray-Owen SD, Ireton K. 2009. The bacterial virulence factor InlC perturbs apical cell junctions and promotes cell-to-cell spread of Listeria. Nat Cell Biol 11:1212–1218.

280. Rigano LA, Dowd GC, Wang Y, Ireton K. 2014. *L isteria monocytogenes* antagonizes the human GTPase Cdc42 to promote bacterial spread: Role of host GTPase Cdc42 in *Listeria* spread. Cell Microbiol 16:1068–1079.

281. Czuczman MA, Fattouh R, van Rijn JM, Canadien V, Osborne S, Muise AM, Kuchroo VK, Higgins DE, Brumell JH. 2014. Listeria monocytogenes exploits efferocytosis to promote cell-to-cell spread. Nature 509:230–234.

282. Nguyen BN, Peterson BN, Portnoy DA. 2019. Listeriolysin O: A phagosome-specific cytolysin revisited. Cell Microbiol 21:e12988.

283. Carvalho F, Spier A, Chaze T, Matondo M, Cossart P, Stavru F. 2020. *Listeria monocytogenes* Exploits Mitochondrial Contact Site and Cristae Organizing System Complex Subunit Mic10 To Promote Mitochondrial Fragmentation and Cellular Infection. mBio 11:e03171-19, /mbio/11/1/mBio.03171-19.atom.

284. Stavru F, Palmer AE, Wang C, Youle RJ, Cossart P. 2013. Atypical mitochondrial fission upon bacterial infection. Proc Natl Acad Sci 110:16003–16008.

285. Pillich H, Loose M, Zimmer K-P, Chakraborty T. 2012. Activation of the unfolded protein response by Listeria monocytogenes: Listeria and UPR. Cell Microbiol 14:949–964.

286. Stavru F, Bouillaud F, Sartori A, Ricquier D, Cossart P. 2011. *Listeria monocytogenes* transiently alters mitochondrial dynamics during infection. Proc Natl Acad Sci 108:3612–3617.

287. Samba-Louaka A, Stavru F, Cossart P. 2012. Role for Telomerase in Listeria monocytogenes Infection. Infect Immun 80:4257–4263.

288. Samba-Louaka A, Pereira JM, Nahori M-A, Villiers V, Deriano L, Hamon MA, Cossart P. 2014. Listeria monocytogenes Dampens the DNA Damage Response. PLoS Pathog 10:e1004470.

289. Leitão E, Catarina Costa A, Brito C, Costa L, Pombinho R, Cabanes D, Sousa S. 2014. *Listeria monocytogenes* induces host DNA damage and delays the host cell cycle to promote infection. Cell Cycle 13:928–940.

290. Bierne H, Cossart P. 2012. When bacteria target the nucleus: the emerging family of nucleomodulins: Bacterial hijacking of the nucleus. Cell Microbiol 14:622–633.

291. Lebreton A, Lakisic G, Job V, Fritsch L, Tham TN, Camejo A, Mattei P-J, Regnault B, Nahori M-A, Cabanes D, Gautreau A, Ait-Si-Ali S, Dessen A, Cossart P, Bierne H. 2011. A Bacterial Protein Targets the BAHD1 Chromatin Complex to Stimulate Type III Interferon Response. Science 331:1319–1321.

292. Lebreton A, Job V, Ragon M, Le Monnier A, Dessen A, Cossart P, Bierne H. 2014. Structural Basis for the Inhibition of the Chromatin Repressor BAHD1 by the Bacterial Nucleomodulin LntA. mBio 5:e00775-13.

293. Hamon MA, Batsché E, Régnault B, Tham TN, Seveau S, Muchardt C, Cossart P. 2007. Histone modifications induced by a family of bacterial toxins. Proc Natl Acad Sci U S A 104:13467–13472.

294. Pereira JM, Chevalier C, Chaze T, Gianetto Q, Impens F, Matondo M, Cossart P, Hamon MA. 2018. Infection Reveals a Modification of SIRT2 Critical for Chromatin Association. Cell Rep 23:1124–1137.

295. Eskandarian HA, Impens F, Nahori M-A, Soubigou G, Coppee J-Y, Cossart P, Hamon MA. 2013. A Role for SIRT2-Dependent Histone H3K18 Deacetylation in Bacterial Infection. Science 341:1238858–1238858.

296. Ribet D, Hamon M, Gouin E, Nahori M-A, Impens F, Neyret-Kahn H, Gevaert K, Vandekerckhove J, Dejean A, Cossart P. 2010. Listeria monocytogenes impairs SUMOylation for efficient infection. Nature 464:1192–1195.

297. Impens F, Radoshevich L, Cossart P, Ribet D. 2014. Mapping of SUMO sites and analysis of SUMOylation changes induced by external stimuli. Proc Natl Acad Sci 111:12432–12437.

298. Lebreton A, Cossart P. 2017. RNA- and protein-mediated control of *Listeria monocytogenes* virulence gene expression. RNA Biol 14:460–470.

299. Reniere ML, Whiteley AT, Hamilton KL, John SM, Lauer P, Brennan RG, Portnoy DA. 2015. Glutathione activates virulence gene expression of an intracellular pathogen. Nature 517:170–173.

300. Kazmierczak MJ, Mithoe SC, Boor KJ, Wiedmann M. 2003. Listeria monocytogenes σB Regulates Stress Response and Virulence Functions. J Bacteriol 185:5722–5734.

301. Toledo-Arana A, Dussurget O, Nikitas G, Sesto N, Guet-Revillet H, Balestrino D, Loh E, Gripenland J, Tiensuu T, Vaitkevicius K, Barthelemy M, Vergassola M, Nahori M-A, Soubigou G, Régnault B, Coppée J-Y, Lecuit M, Johansson J,

Cossart P. 2009. The Listeria transcriptional landscape from saprophytism to virulence. Nature 459:950–956.

302. Ollinger J, Bowen B, Wiedmann M, Boor KJ, Bergholz TM. 2009. Listeria monocytogenes σB Modulates PrfA-Mediated Virulence Factor Expression. Infect Immun 77:2113–2124.

303. Nadon CA, Bowen BM, Wiedmann M, Boor KJ. 2002. Sigma B Contributes to PrfA-Mediated Virulence in Listeria monocytogenes. Infect Immun 70:3948–3952.

304. Schubert AM, Sinani H, Schloss PD. 2015. Antibiotic-Induced Alterations of the Murine Gut Microbiota and Subsequent Effects on Colonization Resistance against Clostridium difficile. mBio 6:e00974-15.

305. Buffie CG, Pamer EG. 2013. Microbiota-mediated colonization resistance against intestinal pathogens. Nat Rev Immunol 13:790–801.

306. Archambaud C, Sismeiro O, Toedling J, Soubigou G, Bécavin C, Lechat P, Lebreton A, Ciaudo C, Cossart P. 2013. The Intestinal Microbiota Interferes with the microRNA Response upon Oral Listeria Infection. mBio 4:e00707-13.

307. Becattini S, Littmann ER, Carter RA, Kim SG, Morjaria SM, Ling L, Gyaltshen Y, Fontana E, Taur Y, Leiner IM, Pamer EG. 2017. Commensal microbes provide first line defense against Listeria monocytogenes infection. J Exp Med 214:1973–1989.

308. Quereda JJ, Dussurget O, Nahori M-A, Ghozlane A, Volant S, Dillies M-A, Regnault B, Kennedy S, Mondot S, Villoing B, Cossart P, Pizarro-Cerda J. 2016. Bacteriocin from epidemic Listeria strains alters the host intestinal microbiota to favor infection. Proc Natl Acad Sci 113:5706–5711.

309. Quereda JJ, Meza-Torres J, Cossart P, Pizarro-Cerdá J. 2017. Listeriolysin S: A bacteriocin from epidemic Listeria monocytogenes strains that targets the gut microbiota. Gut Microbes 8:384–391.

310. Ragon M, Wirth T, Hollandt F, Lavenir R, Lecuit M, Le Monnier A, Brisse S. 2008. A New Perspective on Listeria monocytogenes Evolution. PLoS Pathog 4:e1000146.

311. Jeffers GT, Bruce JL, McDonough PL, Scarlett J, Boor KJ, Wiedmann M. 2001. Comparative genetic characterization of Listeria monocytogenes isolates from human and animal listeriosis cases. Microbiology 147:1095–1104.

312. Chakraborty T, Hain T, Domann E. 2000. Genome organization and the evolution of the virulence gene locus in Listeria species. Int J Med Microbiol 290:167–174.

313. Clayton EM, Daly KM, Guinane CM, Hill C, Cotter PD, Ross PR. 2014. Atypical *Listeria innocua* strains possess an intact LIPI-3. BMC Microbiol 14:58.

314. Clayton EM, Hill C, Cotter PD, Ross RP. 2011. Real-Time PCR Assay To Differentiate Listeriolysin S-Positive and -Negative Strains of *Listeria monocytogenes*. Appl Environ Microbiol 77:163–171.

315. Greetham HL, Gibson GR, Giffard C, Hippe H, Merkhoffer B, Steiner U, Falsen E, Collins MD. 2004. Allobaculum stercoricanis gen. nov., sp. nov., isolated from canine feces. Anaerobe 10:301–307.

316. Downes J, Dewhirst FE, Tanner ACR, Wade WG. 2013. Description of Alloprevotella rava gen. nov., sp. nov., isolated from the human oral cavity, and reclassification of Prevotella tannerae Moore et al. 1994 as Alloprevotella tannerae gen. nov., comb. nov. Int J Syst Evol Microbiol 63:1214–1218.

317. Ostling CE, Lindgren SE. 1993. Inhibition of enterobacteria and *Listeria* growth by lactic, acetic and formic acids. J Appl Bacteriol 75:18–24.

318. Sun Y, Wilkinson BJ, Standiford TJ, Akinbi HT, O'Riordan MXD. 2012. Fatty Acids Regulate Stress Resistance and Virulence Factor Production for Listeria monocytogenes. J Bacteriol 194:5274–5284.

319. Quereda JJ, Nahori MA, Meza-Torres J, Sachse M, Titos-Jiménez P, Gomez-Laguna J, Dussurget O, Cossart P, Pizarro-Cerdá J. 2017. Listeriolysin S Is a Streptolysin S-Like Virulence Factor That Targets Exclusively Prokaryotic Cells In Vivo. mBio 8:e00259-17, /mbio/8/2/e00259-17.atom.

320. Cox C, Coburn P, Gilmore M. 2005. Enterococcal Cytolysin: A Novel Two Component Peptide System that Serves as a Bacterial Defense Against Eukaryotic and Prokaryotic Cells. Curr Protein Pept Sci 6:77–84.

321. Wladyka B, Piejko M, Bzowska M, Pieta P, Krzysik M, Mazurek Ł, Guevara-Lora I, Bukowski M, Sabat AJ, Friedrich AW, Bonar E, Międzobrodzki J, Dubin A, Mak P. 2015. A peptide factor secreted by Staphylococcus pseudintermedius exhibits properties of both bacteriocins and virulence factors. Sci Rep 5:14569.

322. Molloy EM, Casjens SR, Cox CL, Maxson T, Ethridge NA, Margos G, Fingerle V, Mitchell DA. 2015. Identification of the minimal cytolytic unit for streptolysin S and an expansion of the toxin family. BMC Microbiol 15:141.

323. Linnan MJ, Mascola L, Lou XD, Goulet V, May S, Salminen C, Hird DW, Yonekura ML, Hayes P, Weaver R, Audurier A, Plikaytis BD, Fannin SL, Kleks A, Broome CV. 1988. Epidemic Listeriosis Associated with Mexican-Style Cheese. N Engl J Med 319:823–828.

324. Wiedemann I, Breukink E, van Kraaij C, Kuipers OP, Bierbaum G, de Kruijff B, Sahl H-G. 2001. Specific Binding of Nisin to the Peptidoglycan Precursor Lipid II Combines Pore Formation and Inhibition of Cell Wall Biosynthesis for Potent Antibiotic Activity. J Biol Chem 276:1772–1779.

325. Spann D, Pross E, Chen Y, Dalbey RE, Kuhn A. 2018. Each protomer of a dimeric YidC functions as a single membrane insertase. Sci Rep 8:589.

326. Troxell B, Hassan HM. 2013. Transcriptional regulation by Ferric Uptake Regulator (Fur) in pathogenic bacteria. Front Cell Infect Microbiol 3.

327. Cox LM, Yamanishi S, Sohn J, Alekseyenko AV, Leung JM, Cho I, Kim SG, Li H, Gao Z, Mahana D, Zárate Rodriguez JG, Rogers AB, Robine N, Loke P, Blaser MJ. 2014. Altering the Intestinal Microbiota during a Critical Developmental Window Has Lasting Metabolic Consequences. Cell 158:705–721.

328. Eckburg PB. 2005. Diversity of the Human Intestinal Microbial Flora. Science 308:1635–1638.

329. Brazas MD, Hancock REW. 2005. Using microarray gene signatures to elucidate mechanisms of antibiotic action and resistance. Drug Discov Today 10:1245–1252.

330. Hutter B, Schaab C, Albrecht S, Borgmann M, Brunner NA, Freiberg C, Ziegelbauer K, Rock CO, Ivanov I, Loferer H. 2004. Prediction of Mechanisms of Action of Antibacterial Compounds by Gene Expression Profiling. Antimicrob Agents Chemother 48:2838–2844.

331. Héchard Y, Sahl H-G. 2002. Mode of action of modified and unmodified bacteriocins from Gram-positive bacteria. Biochimie 84:545–557.

332. Friedrich CL, Rozek A, Patrzykat A, Hancock REW. 2001. Structure and Mechanism of Action of an Indolicidin Peptide Derivative with Improved Activity against Gram-positive Bacteria. J Biol Chem 276:24015–24022.

333. Patrzykat A, Friedrich CL, Zhang L, Mendoza V, Hancock REW. 2002. Sublethal concentrations of pleurocidin-derived antimicrobial peptides inhibit macromolecular synthesis in Escherichia coli. Antimicrob Agents Chemother 46:605–614.

334. Kargatov AM, Boshkova EA, Chirgadze YN. 2018. Novel approach for structural identification of protein family: glyoxalase I. J Biomol Struct Dyn 36:2699–2712.

335. Shaw KJ, Miller N, Liu X, Lerner D, Wan J, Bittner A, Morrow BJ. 2003. Comparison of the Changes in Global Gene Expression of *Escherichia coli* Induced by Four Bactericidal Agents. J Mol Microbiol Biotechnol 5:105–122.

336. Jordan S, Junker A, Helmann JD, Mascher T. 2006. Regulation of LiaRS-Dependent Gene Expression in Bacillus subtilis: Identification of Inhibitor Proteins, Regulator Binding Sites, and Target Genes of a Conserved Cell Envelope Stress-Sensing Two-Component System. J Bacteriol 188:5153–5166.

337. Gravesen A, Sørensen K, Aarestrup FM, Knøchel S. 2001. Spontaneous Nisin-Resistant *Listeria monocytogenes* Mutants with Increased Expression of a Putative Penicillin-Binding Protein and Their Sensitivity to Various Antibiotics. Microb Drug Resist 7:127–135.

338. Gravesen A, Kallipolitis B, HolmstrÃ¯Â¿Â½m K, HÃ¯Â¿Â½iby PE, Ramnath M, KnÃ¯Â¿Â½chel S. 2004. pbp2229-Mediated Nisin Resistance Mechanism in

Listeria monocytogenes Confers Cross-Protection to Class IIa Bacteriocins and Affects Virulence Gene Expression. Appl Environ Microbiol 70:1669–1679.

339. Mandin P, Fsihi H, Dussurget O, Vergassola M, Milohanic E, Toledo-Arana A, Lasa I, Johansson J, Cossart P. 2005. VirR, a response regulator critical for *Listeria monocytogenes* virulence: Novel *Listeria* virulence regulon. Mol Microbiol 57:1367–1380.

340. Li M, Lai Y, Villaruz AE, Cha DJ, Sturdevant DE, Otto M. 2007. Gram-positive three-component antimicrobial peptide-sensing system. Proc Natl Acad Sci 104:9469–9474.

341. Thedieck K, Hain T, Mohamed W, Tindall BJ, Nimtz M, Chakraborty T, Wehland J, Jänsch L. 2006. The MprF protein is required for lysinylation of phospholipids in listerial membranes and confers resistance to cationic antimicrobial peptides (CAMPs) on Listeria monocytogenes. Mol Microbiol 62:1325–1339.

342. Kallipolitis BH, Ingmer H, Gahan CG, Hill C, Søgaard-Andersen L. 2003. CesRK, a Two-Component Signal Transduction System in Listeria monocytogenes, Responds to the Presence of Cell Wall-Acting Antibiotics and Affects β-Lactam Resistance. Antimicrob Agents Chemother 47:3421–3429.

343. Corr SC, Li Y, Riedel CU, O'Toole PW, Hill C, Gahan CGM. 2007. Bacteriocin production as a mechanism for the antiinfective activity of *Lactobacillus salivarius* UCC118. Proc Natl Acad Sci 104:7617–7621.

344. Moore RJ, Lacey JA. 2019. Genomics of the Pathogenic Clostridia. Microbiol Spectr 7.

345. Fiore E, Van Tyne D, Gilmore MS. 2019. Pathogenicity of Enterococci. Microbiol Spectr 7.

346. Turner CE, Bubba L, Efstratiou A. 2019. Pathogenicity Factors in Group C and G Streptococci. Microbiol Spectr 7.

347. Ehling-Schulz M, Lereclus D, Koehler TM. 2019. The Bacillus cereus Group: Bacillus Species with Pathogenic Potential. Microbiol Spectr 7.

348. Pilo P, Frey J. 2018. Pathogenicity, population genetics and dissemination of Bacillus anthracis. Infect Genet Evol 64:115–125.

349. Quereda JJ, Dussurget O, Nahori M-A, Ghozlane A, Volant S, Dillies M-A, Regnault B, Kennedy S, Mondot S, Villoing B, Cossart P, Pizarro-Cerda J. 2016. Bacteriocin from epidemic *Listeria* strains alters the host intestinal microbiota to favor infection. Proc Natl Acad Sci 113:5706–5711.

350. Wieczorek S, Combes F, Lazar C, Giai Gianetto Q, Gatto L, Dorffer A, Hesse A-M, Couté Y, Ferro M, Bruley C, Burger T. 2017. DAPAR & ProStaR: software to perform statistical analyses in quantitative discovery proteomics. Bioinformatics 33:135–136.

351. Giai Gianetto Q, Wieczorek S, Couté Y, Burger T. 2020. A peptide-level multiple imputation strategy accounting for the different natures of missing values in proteomics data. preprint, Bioinformatics.

352. Ritchie ME, Phipson B, Wu D, Hu Y, Law CW, Shi W, Smyth GK. 2015. limma powers differential expression analyses for RNA-sequencing and microarray studies. Nucleic Acids Res 43:e47–e47.

353. Giai Gianetto Q, Combes F, Ramus C, Bruley C, Couté Y, Burger T. 2016. Calibration plot for proteomics: A graphical tool to visually check the assumptions underlying FDR control in quantitative experiments: Calibration Plot for Proteomics (CP4P). PROTEOMICS 16:29–32.

354. Pounds S, Cheng C. 2006. Robust estimation of the false discovery rate. Bioinformatics 22:1979–1987.

355. Lyons NA, Kraigher B, Stefanic P, Mandic-Mulec I, Kolter R. 2016. A Combinatorial Kin Discrimination System in Bacillus subtilis. Curr Biol 26:733–742.

356. Bailey TL, Boden M, Buske FA, Frith M, Grant CE, Clementi L, Ren J, Li WW, Noble WS. 2009. MEME SUITE: tools for motif discovery and searching. Nucleic Acids Res 37:W202–W208.

357. Gupta S, Stamatoyannopoulos JA, Bailey TL, Noble W. 2007. Quantifying similarity between motifs. Genome Biol 8:R24.

358. Titgemeyer F, Hillen W. 2002. Global control of sugar metabolism: a Gram-positive solution. Antonie Van Leeuwenhoek 82:59–71.

359. Warner JB, Lolkema JS. 2003. CcpA-Dependent Carbon Catabolite Repression in Bacteria. Microbiol Mol Biol Rev 67:475–490.

360. Iyer R, Baliga NS, Camilli A. 2005. Catabolite Control Protein A (CcpA) Contributes to Virulence and Regulation of Sugar Metabolism in Streptococcus pneumoniae. J Bacteriol 187:8340–8349.

361. Kinkel TL, McIver KS. 2008. CcpA-Mediated Repression of Streptolysin S Expression and Virulence in the Group A Streptococcus. Infect Immun 76:3451–3463.

362. Mengaud J, Dramsi S, Gouin E, Vazquez-Boland JA, Milon G, Cossart P. 1991. Pleiotropic control of *Listeria monocytogenes* virulence factors by a gene that is autoregulated. Mol Microbiol 5:2273–2283.

363. Mertins S, Joseph B, Goetz M, Ecke R, Seidel G, Sprehe M, Hillen W, Goebel W, Müller-Altrock S. 2007. Interference of Components of the Phosphoenolpyruvate Phosphotransferase System with the Central Virulence Gene Regulator PrfA of Listeria monocytogenes. J Bacteriol 189:473–490.

364. Kreth J, Chen Z, Ferretti J, Malke H. 2011. Counteractive Balancing of Transcriptome Expression Involving CodY and CovRS in Streptococcus pyogenes. J Bacteriol 193:4153–4165.

365. Malke H, Steiner K, McShan WM, Ferretti JJ. 2006. Linking the nutritional status of Streptococcus pyogenes to alteration of transcriptional gene expression: The action of CodY and RelA. Int J Med Microbiol 296:259–275.

366. Vega LA, Malke H, McIver KS. 2016. Virulence-Related Transcriptional Regulators of Streptococcus pyogenes, p. . *In* Ferretti, JJ, Stevens, DL, Fischetti, VA (eds.), Streptococcus pyogenes : Basic Biology to Clinical Manifestations. University of Oklahoma Health Sciences Center, Oklahoma City (OK).

367. Biswas R, Sonenshein AL, Belitsky BR. 2020. Genome-wide identification of *Listeria monocytogenes* CodY-binding sites. Mol Microbiol 113:841–858.

368. Lobel L, Herskovits AA. 2016. Systems Level Analyses Reveal Multiple Regulatory Activities of CodY Controlling Metabolism, Motility and Virulence in Listeria monocytogenes. PLOS Genet 12:e1005870.

369. Brenner M, Lobel L, Borovok I, Sigal N, Herskovits AA. 2018. Controlled branched-chain amino acids auxotrophy in Listeria monocytogenes allows isoleucine to serve as a host signal and virulence effector. PLOS Genet 14:e1007283.

370. Shen A, Higgins DE. 2006. The MogR Transcriptional Repressor Regulates Nonhierarchal Expression of Flagellar Motility Genes and Virulence in Listeria monocytogenes. PLoS Pathog 2:e30.

371. Winkler WC. 2005. Riboswitches and the role of noncoding RNAs in bacterial metabolic control. Curr Opin Chem Biol 9:594–602.

372. Brantl S. 2007. Regulatory mechanisms employed by cis-encoded antisense RNAs. Curr Opin Microbiol 10:102–109.

373. Millman A, Dar D, Shamir M, Sorek R. 2017. Computational prediction of regulatory, premature transcription termination in bacteria. Nucleic Acids Res 45:886–893.

374. Balestrino D, Hamon MA, Dortet L, Nahori MA, Pizarro-Cerda J, Alignani D, Dussurget O, Cossart P, Toledo-Arana A. 2010. Single-Cell Techniques Using Chromosomally Tagged Fluorescent Bacteria To Study *Listeria monocytogenes* Infection Processes. Appl Environ Microbiol 76:3625–3636.

375. Utratna M, Cosgrave E, Baustian C, Ceredig R, O'Byrne C. 2012. Development and optimization of an EGFP-based reporter for measuring the general stress response in *Listeria monocytogenes*. Bioengineered 3:93–103.

376. Kinnunen U, Syrjälä H, Koistinen P, Koskela M. 2009. Idarubicin inhibits the growth of bacteria and yeasts in an automated blood culture system. Eur J Clin Microbiol Infect Dis 28:301–303.

377. Zhao W, Caro F, Robins W, Mekalanos JJ. 2018. Antagonism toward the intestinal microbiota and its effect on *Vibrio cholerae* virulence. Science 359:210–213.

378. Rattanaphan P, Mittraparp-Arthorn P, Srinoun K, Vuddhakul V, Tansila N. 2020. Indole signaling decreases biofilm formation and related virulence of Listeria monocytogenes. FEMS Microbiol Lett 367:fnaa116.

379. Carvalho F, Sousa S, Cabanes D. 2014. How Listeria monocytogenes organizes its surface for virulence. Front Cell Infect Microbiol 4.

380. Kumar A, Sperandio V. 2019. Indole Signaling at the Host-Microbiota-Pathogen Interface. mBio 10:e01031-19, /mbio/10/3/mBio.01031-19.atom.

381. Kohli N, Crisp Z, Riordan R, Li M, Alaniz RC, Jayaraman A. 2018. The microbiota metabolite indole inhibits Salmonella virulence: Involvement of the PhoPQ two-component system. PLOS ONE 13:e0190613.

382. Karlin DA, Mastromarino AJ, Jones RD, Stroehlein JR, Lorentz O. 1985. Fecal skatole and indole and breath methane and hydrogen in patients with large bowel polyps or cancer. J Cancer Res Clin Oncol 109:135–141.

383. Zuccato E, Venturi M, Di Leo G, Colombo L, Bertolo C, Doldi SB, Mussini E. 1993. Role of bile acids and metabolic activity of colonic bacteria in increased risk of colon cancer after cholecystectomy. Dig Dis Sci 38:514–519.

384. Nicholson JK, Holmes E, Kinross J, Burcelin R, Gibson G, Jia W, Pettersson S. 2012. Host-Gut Microbiota Metabolic Interactions. Science 336:1262–1267.

385. Mellin JR, Koutero M, Dar D, Nahori M-A, Sorek R, Cossart P. 2014. Sequestration of a two-component response regulator by a riboswitch-regulated noncoding RNA. Science 345:940–943.

386. Ikeda M. 2003. TMPDB: a database of experimentally-characterized transmembrane topologies. Nucleic Acids Res 31:406–409.

387. Jones P, Binns D, Chang H-Y, Fraser M, Li W, McAnulla C, McWilliam H, Maslen J, Mitchell A, Nuka G, Pesseat S, Quinn AF, Sangrador-Vegas A, Scheremetjew M, Yong S-Y, Lopez R, Hunter S. 2014. InterProScan 5: genome-scale protein function classification. Bioinformatics 30:1236–1240.

388. Sigrist CJA, Cerutti L, de Castro E, Langendijk-Genevaux PS, Bulliard V, Bairoch A, Hulo N. 2010. PROSITE, a protein domain database for functional characterization and annotation. Nucleic Acids Res 38:D161–D166.

389. El-Gebali S, Mistry J, Bateman A, Eddy SR, Luciani A, Potter SC, Qureshi M, Richardson LJ, Salazar GA, Smart A, Sonnhammer ELL, Hirsh L, Paladin L, Piovesan D, Tosatto SCE, Finn RD. 2019. The Pfam protein families database in 2019. Nucleic Acids Res 47:D427–D432.

390. Klein G, Kobylak N, Lindner B, Stupak A, Raina S. 2014. Assembly of Lipopolysaccharide in *Escherichia coli* Requires the Essential LapB Heat Shock Protein. J Biol Chem 289:14829–14853.

391. Ohki R, Giyanto, Tateno K, Masuyama W, Moriya S, Kobayashi K, Ogasawara N. 2003. The BceRS two-component regulatory system induces expression of the bacitracin transporter, BceAB, in Bacillus subtilis: Bacitracin-resistant genes in B. subtilis. Mol Microbiol 49:1135–1144.

392. Lin HT, Bavro VN, Barrera NP, Frankish HM, Velamakanni S, van Veen HW, Robinson CV, Borges-Walmsley MI, Walmsley AR. 2009. MacB ABC Transporter Is a Dimer Whose ATPase Activity and Macrolide-binding Capacity Are Regulated by the Membrane Fusion Protein MacA. J Biol Chem 284:1145–1154.

393. Yu H, Rao X, Zhang K. 2017. Nucleoside diphosphate kinase (Ndk): A pleiotropic effector manipulating bacterial virulence and adaptive responses. Microbiol Res 205:125–134.

394. Cheng C, Wang H, Ma T, Han X, Yang Y, Sun J, Chen Z, Yu H, Hang Y, Liu F, Fang W, Jiang L, Cai C, Song H. 2018. Flagellar Basal Body Structural Proteins FlhB, FliM, and FliY Are Required for Flagellar-Associated Protein Expression in Listeria monocytogenes. Front Microbiol 9:208.

395. Müller M, Reiß S, Schlüter R, Mäder U, Beyer A, Reiß W, Marles-Wright J, Lewis RJ, Pförtner H, Völker U, Riedel K, Hecker M, Engelmann S, Pané-Farré J. 2014. Deletion of membrane-associated Asp23 leads to upregulation of cell wall stress genes in *S taphylococcus aureus*: DUF322 protein Asp23 is membrane localized. Mol Microbiol n/a-n/a.

396. Dolence JM, Steward LE, Dolence EK, Wong DH, Poulter CD. 2000. Studies with Recombinant *Saccharomyces cerevisiae* CaaX Prenyl Protease Rce1p †. Biochemistry 39:4096–4104.

397. Altschul S. 1997. Gapped BLAST and PSI-BLAST: a new generation of protein database search programs. Nucleic Acids Res 25:3389–3402.

398. Vrljic M, Garg J, Bellmann A, Wachi S, Freudl R, Malecki MJ, Sahm H, Kozina VJ, Eggeling L, Saier MH, Eggeling L, Saier MH. 1999. The LysE superfamily: topology of the lysine exporter LysE of Corynebacterium glutamicum, a paradyme for a novel superfamily of transmembrane solute translocators. J Mol Microbiol Biotechnol 1:327–336.

399. Tsu BV, Saier MH. 2015. The LysE Superfamily of Transport Proteins Involved in Cell Physiology and Pathogenesis. PLOS ONE 10:e0137184.

400. Sondén B, Kocíncová D, Deshayes C, Euphrasie D, Rhayat L, Laval F, Frehel C, Daffé M, Etienne G, Reyrat J-M. 2005. Gap, a mycobacterial specific integral membrane protein, is required for glycolipid transport to the cell surface: Glycolipid transport in mycobacteria. Mol Microbiol 58:426–440.

401. Jo G-A, Lee JM, No G, Kang DS, Kim S-H, Ahn S-H, Kong I-S. 2015. Isolation and characterization of a 17-kDa FKBP-type peptidyl-prolyl cis/trans isomerase from Vibrio anguillarum. Protein Expr Purif 110:130–137.

402. Diep DB, Håvarstein LS, Nes IF. 1996. Characterization of the locus responsible for the bacteriocin production in Lactobacillus plantarum C11. J Bacteriol 178:4472–4483.

403. Rojo-Bezares B, Sáenz Y, Navarro L, Jiménez-Díaz R, Zarazaga M, Ruiz-Larrea F, Torres C. 2008. Characterization of a new organization of the plantaricin locus in the inducible bacteriocin-producing Lactobacillus plantarum J23 of grape must origin. Arch Microbiol 189:491–499.

404. Lagos R, Baeza M, Corsini G, Hetz C, Strahsburger E, Castillo JA, Vergara C, Monasterio O. 2008. Structure, organization and characterization of the gene cluster involved in the production of microcin E492, a channel-forming bacteriocin: Genes involved in the production of microcin E492. Mol Microbiol 42:229–243.

405. Saito T, Okano K, Park H-D, Itayama T, Inamori Y, Neilan BA, Burns BP, Sugiura N. 2003. Detection and sequencing of the microcystin LR-degrading gene, *mlrA* , from new bacteria isolated from Japanese lakes. FEMS Microbiol Lett 229:271–276.

406. Lux T, Nuhn M, Hakenbeck R, Reichmann P. 2007. Diversity of Bacteriocins and Activity Spectrum in Streptococcus pneumoniae. J Bacteriol 189:7741–7751.

407. Plummer LJ, Hildebrandt ER, Porter SB, Rogers VA, McCracken J, Schmidt WK. 2006. Mutational Analysis of the Ras Converting Enzyme Reveals a Requirement for Glutamate and Histidine Residues. J Biol Chem 281:4596–4605.

408. Alba BM. 2002. DegS and YaeL participate sequentially in the cleavage of RseA to activate the sigma E-dependent extracytoplasmic stress response. Genes Dev 16:2156–2168.

409. Havarstein LS, Diep DB, Nes IF. 1995. A family of bacteriocin ABC transporters carry out proteolytic processing of their substrates concomitant with export. Mol Microbiol 16:229–240.

410. Arnaud M, Chastanet A, Debarbouille M. 2004. New Vector for Efficient Allelic Replacement in Naturally Nontransformable, Low-GC-Content, Gram-Positive Bacteria. Appl Environ Microbiol 70:6887–6891.

411. Mengaud J, Lecuit M, Lebrun M, Nato F, Mazie JC, Cossart P. 1996. Antibodies to the leucine-rich repeat region of internalin block entry of *Listeria monocytogenes* into cells expressing E-cadherin. Infect Immun 64:5430–5433.

412. Steffen P, Schafer DA, David V, Gouin E, Cooper JA, Cossart P. 2000. *Listeria monocytogenes* ActA protein interacts with phosphatidylinositol 4,5-bisphosphate in vitro. Cell Motil Cytoskeleton 45:58–66.

413. Archambaud C, Gouin E, Pizarro-Cerda J, Cossart P, Dussurget O. 2005. Translation elongation factor EF-Tu is a target for Stp, a serine-threonine phosphatase involved in virulence of *Listeria monocytogenes*: EF-Tu, a target for the Listeria phosphatase Stp. Mol Microbiol 56:383–396.

414. Gouin E, Adib-Conquy M, Balestrino D, Nahori M-A, Villiers V, Colland F, Dramsi S, Dussurget O, Cossart P. 2010. The *Listeria monocytogenes* InlC protein interferes with innate immune responses by targeting the I B kinase subunit IKK. Proc Natl Acad Sci 107:17333–17338.

415. Volokhov DV, Duperrier S, Neverov AA, George J, Buchrieser C, Hitchins AD. 2007. The Presence of the Internalin Gene in Natural Atypically Hemolytic Listeria innocua Strains Suggests Descent from L. monocytogenes. Appl Environ Microbiol 73:1928–1939.

416. Garrido MC, Herrero M, Kolter R, Moreno F. 1988. The export of the DNA replication inhibitor Microcin B17 provides immunity for the host cell. EMBO J 7:1853–1862.

417. Tran JH, Jacoby GA. 2002. Mechanism of plasmid-mediated quinolone resistance. Proc Natl Acad Sci 99:5638–5642.

418. Higashi DL, Biais N, Donahue DL, Mayfield JA, Tessier CR, Rodriguez K, Ashfeld BL, Luchetti J, Ploplis VA, Castellino FJ, Lee SW. 2016. Activation of band 3 mediates group A *Streptococcus* streptolysin S-based beta-haemolysis. Nat Microbiol 1:15004.

419. Enninga J, Mounier J, Sansonetti P, Nhieu GTV. 2005. Secretion of type III effectors into host cells in real time. Nat Methods 2:959–965.

420. Lelek M, Di Nunzio F, Zimmer C. 2014. FlAsH-PALM: Super-resolution Pointillist Imaging with FlAsH-Tetracysteine Labeling, p. 183–193. *In* Ivanov, AI (ed.), Exocytosis and Endocytosis. Springer New York, New York, NY.

421. Lelek M, Di Nunzio F, Henriques R, Charneau P, Arhel N, Zimmer C. 2012. Superresolution imaging of HIV in infected cells with FlAsH-PALM. Proc Natl Acad Sci 109:8564–8569.

422. Spindler EC, Hale JDF, Giddings TH, Hancock REW, Gill RT. 2011. Deciphering the Mode of Action of the Synthetic Antimicrobial Peptide Bac8c. Antimicrob Agents Chemother 55:1706–1716.

423. Ma W, Zhang D, Li G, Liu J, He G, Zhang P, Yang L, Zhu H, Xu N, Liang S. 2017. Antibacterial mechanism of daptomycin antibiotic against Staphylococcus aureus based on a quantitative bacterial proteome analysis. J Proteomics 150:242–251.

424. Gunasekaran P, Rajasekaran G, Han EH, Chung Y-H, Choi Y-J, Yang YJ, Lee JE, Kim HN, Lee K, Kim J-S, Lee H-J, Choi E-J, Kim E-K, Shin SY, Bang JK. 2019. Cationic Amphipathic Triazines with Potent Anti-bacterial, Anti-inflammatory and Anti-atopic Dermatitis Properties. Sci Rep 9:1292.

425. Ghilarov D, Serebryakova M, Stevenson CEM, Hearnshaw SJ, Volkov DS, Maxwell A, Lawson DM, Severinov K. 2017. The Origins of Specificity in the Microcin-Processing Protease TldD/E. Structure 25:1549-1561.e5.

426. Smith TJ, Sondermann H, O'Toole GA. 2018. Type 1 Does the Two-Step: Type 1 Secretion Substrates with a Functional Periplasmic Intermediate. J Bacteriol 200:e00168-18, /jb/200/18/e00168-18.atom.

427. Boyd CD, Chatterjee D, Sondermann H, O'Toole GA. 2012. LapG, Required for Modulating Biofilm Formation by Pseudomonas fluorescens Pf0-1, Is a Calcium-Dependent Protease. J Bacteriol 194:4406–4414.

428. Webb AJ, Karatsa-Dodgson M, Gründling A. 2009. Two-enzyme systems for glycolipid and polyglycerolphosphate lipoteichoic acid synthesis in *Listeria monocytogenes*. Mol Microbiol 74:299–314.

429. Carvalho F, Sousa S, Cabanes D. 2018. Rhamnosylation of wall teichoic acids promotes efficient surface association of *Listeria monocytogenes* virulence factors InlB and Ami through interaction with GW domains: WTA promotes surface association of GW proteins. Environ Microbiol 20:3941–3951.

430. Baumgärtner M, Kärst U, Gerstel B, Loessner M, Wehland J, Jänsch L. 2007. Inactivation of Lgt Allows Systematic Characterization of Lipoproteins from Listeria monocytogenes. J Bacteriol 189:313–324.

431. Markley AL, Jensen ER, Lee SW. 2012. An Escherichia coli-based bioengineering strategy to study streptolysin S biosynthesis. Anal Biochem 420:191–193.

432. Travin DY, Metelev M, Serebryakova M, Komarova ES, Osterman IA, Ghilarov D, Severinov K. 2018. Biosynthesis of Translation Inhibitor Klebsazolicin Proceeds through Heterocyclization and N-Terminal Amidine Formation Catalyzed by a Single YcaO Enzyme. J Am Chem Soc 140:5625–5633.

433. Alouf JE, Loridan C. 1988. Production, purification, and assay of streptolysin S, p. 59–64. *In* Methods in Enzymology. Elsevier.

434. Bishop DK, Hinrichs DJ. 1987. Adoptive transfer of immunity to *Listeria monocytogenes*. The influence of in vitro stimulation on lymphocyte subset requirements. J Immunol Baltim Md 1950 139:2005–2009.

435. de Jong A, van Heel AJ, Kuipers OP. 2011. Genome Exploitation and Bioinformatics Tools, p. 75–80. *In* Drider, D, Rebuffat, S (eds.), Prokaryotic Antimicrobial Peptides. Springer New York, New York, NY.

436. Hammami R, Zouhir A, Ben Hamida J, Fliss I. 2007. BACTIBASE: a new web-accessible database for bacteriocin characterization. BMC Microbiol 7:89.

437. de Jong A, van Heel AJ, Kok J, Kuipers OP. 2010. BAGEL2: mining for bacteriocins in genomic data. Nucleic Acids Res 38:W647–W651.

438. Delcher AL, Bratke KA, Powers EC, Salzberg SL. 2007. Identifying bacterial genes and endosymbiont DNA with Glimmer. Bioinformatics 23:673–679.

ANNEXES

Annex 1: Investigation of the mature post-translationally modified LLS structure

The structure of mature LLS is not known yet. Mature structures of TOMMs have proven difficult to elucidate due to their small size and also abundant post-translational modifications. For example, the structure of SLS is still unknown after more than 100 years of research on this molecule (212). On the other hand, the structures of plantazolicin and microcin B17 have been solved (210, 238). Determination of the LLS structure might be essential to elucidate its mechanism of action. Our aim was to elucidate the LLS mature structure.

1.1 Results

In order to investigate the mature LLS structure, our first goal was to purify the LLS active form. In the first attempt we obtained hemolytic extracts from the LLS producer bacteria as described before (253). Briefly, *L. monocytogenes* F2365 pHELP::*llsA* Δ*hly* (referred to as LLS^+ bacteria) and *L. monocytogenes* F2365 Δ*llsA*Δ*hly* (referred to as LLS^-) bacteria were washed with Induction Buffer (IB) and incubated with an inducer (RNA core) and a stabilizer ammonium acetate buffer (AmmAc). These extracts were hemolytic in blood agar plates (Figure 1). These hemolytic extracts were submitted to mass spectrometry (MS) in collaboration with Sylvie Rebufat (Muséum National d'Histoire Naturelle). Despite their expertise in the study of molecules from the TOMM family (i.e. MccB17), the LLS molecule was not detected by MS (data not shown).

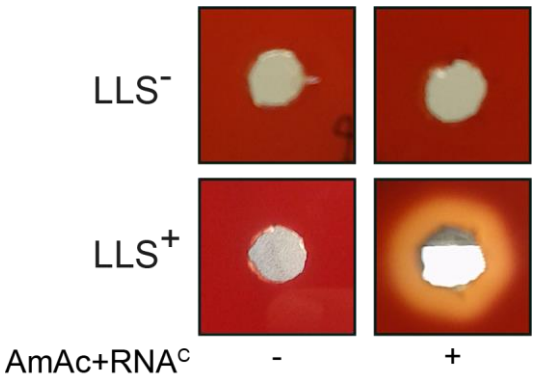

Figure 1. LLS hemolytic extracts. Assessment of hemolytic activity from LLS^+ and LLS^- bacteria free supernatants induced or not with RNA core (RNA^C; inducer) and ammonium acetate (AmAc; stabilizer).

Subsequently, a 6xHis tag was fused to the LLS C-terminus and introduced in a *L. monocytogenes* F2365 pHELP::*llsA* strain (referred as to LLS$^+$-His). This strain kept the bactericidal and hemolytic properties (Figure 2). Bacterial lysates of LLS$^+$-His were used to purify the LLS-His peptide using a Ni Sepharose 6 Fast Flow column. The LLS-His purified fractions were detected in a dot blot though they did not have bactericidal nor hemolytic activity. Unfortunately, by using these fractions the peptide was again not detected by MS (results not shown).

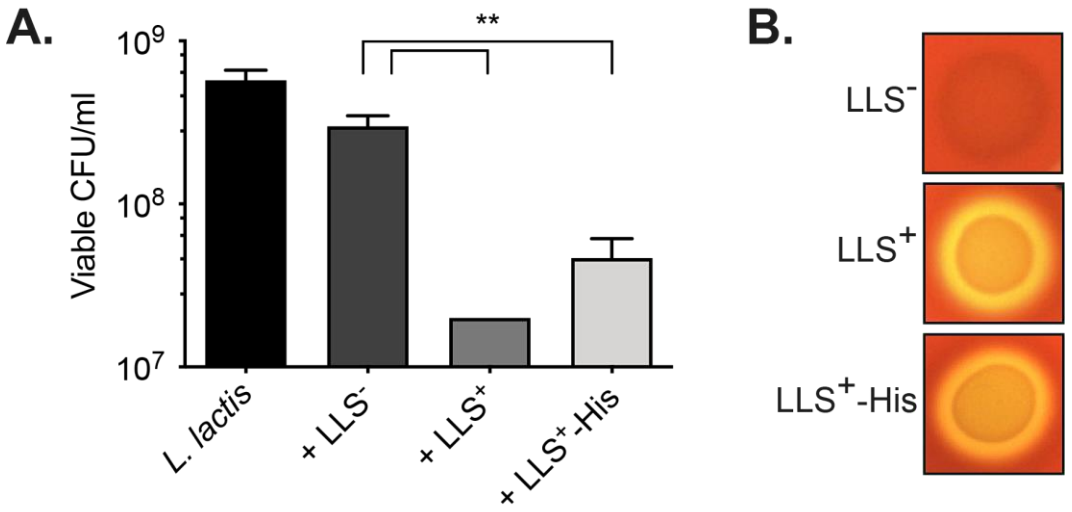

Figure 2. **LLS activity and localization upon addition of His tag.** (A) Target *L. lactis* bacteria were cultivated alone or co-cultivated with LLS mutant bacteria (LLS$^-$), LLS producer bacteria (LLS$^+$) or LLS producer bacteria with a His tag (LLS$^+$-His) during 24 h in BHI. Data from three independent biological experiments are shown. Error bars show SEM. Multiple two-tailed unpaired *t*-test were performed, LLS$^-$ vs LLS$^+$ p= 0.0041, LLS$^-$ vs LLS$^+$-His p= 0.0069 (B) Assessment of hemolytic activity present in LLS$^-$, LLS$^+$, and LLS$^+$-His strains in Columbia agar + 5% sheep blood.

An *E. coli*-based heterologous expression system was constructed as described before for SLS (431). This system allows to study the biosynthesis of bacteriocins *in vitro*. Briefly, two plasmids were generated: the first plasmid that caries the *llsA*, *llsB* (PTM putative enzyme) and *llsX* gene (pCOLA_*llsABX*) and the second plasmid contains two of the putative PTM complex enzymes *llsYD* (pACYC_*llsYD*). One strain will carry only the first plasmid (negative control of PTM modifications) and other strain will carry both plasmids (able to produce LLS mature form). Both plasmids are induced by isopropyl-β-D-thiogalactopyranoside (IPTG). We can detect the induction of the pCOLA_*llsABX* plasmid because we have commercially produced polyclonal

antibodies (Covalab) against LlsX. Several conditions were tested to induce the expression of the LlsX protein (Figure 3A). The induction was higher after 4h at 37°C with IPTG 1 mM (Figure 3A). Interestingly, the LlsX protein was only detected when the two plasmids were present (Figure 3A), suggesting that the proteins LlsYD are important for the LlsX protein stability. After 4h of induction with 1 mM IPTG *E. coli* lysates were prepared by sonication. Later, the lysates were concentrated and incubated with LLS target bacteria in BHI during 24h. Unfortunately, the lysates did not show any bactericidal effect on *L. lactis* or *L. monocytogenes* 10403S (Figure 3B), suggesting that the LLS is not post-translationally modified.

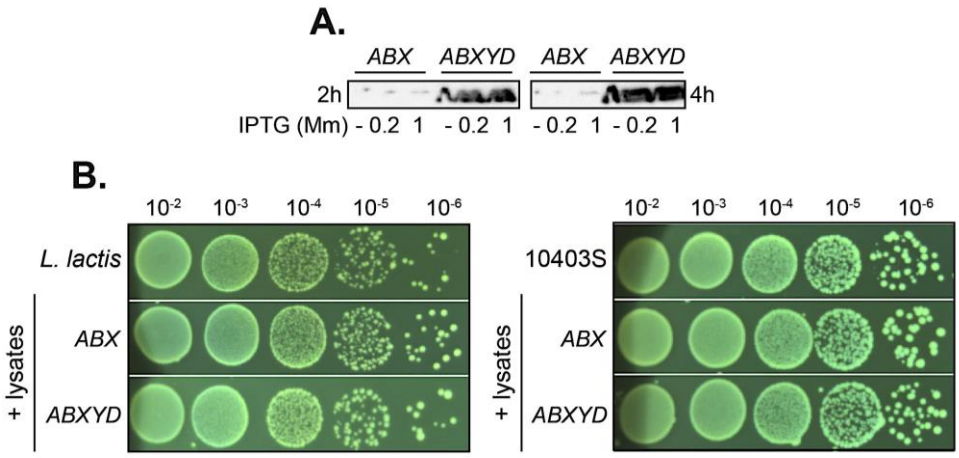

Figure 3. Induction of heterogously expressed genes from the LLS gene cluster and absence of reconstitution of LLS bactericidal activity. A. Induction of the pCOLA_*llsABX* plasmid only in the presence of the second plasmid pACYC_llsYD after addition of different concentrations of IPTG during 2 or 4h at 37°C. B. Absence of reconstitution of LLS bactericidal activity after exposing LLS target bacteria *L. monocytogenes* 10403S and *L. lactis* during 24h to *E. coli* lysates that expressed heterologous the *llsABXYD* genes.

Subsequently, a collaboration with Muriel Delepierre (Institut Pasteur) was established to analyze LLS structure by using NMR. For this, LLS$^+$-FLAG was immunoprecipitated as described previously (Results Part II) using a LLS$^+$ strain without FLAG tag as a negative control. Unfortunately, the spectra from the NMR analyses were identical in both samples (LLS$^+$ and LLS$^+$-FLAG) (results not shown), suggesting that the concentration required to detect LLS$^+$-FLAG was not reached by immunoprecipitating LLS$^+$-FLAG.

More recently, we stablished a collaboration with Olivier Berteau (INRAE), who cloned and expressed the LLS as a Maltose Binding Protein (LLS-MBP) fusion protein in *E. coli*. LLS-MBP was purified and digested with trypsin. The LLS-MBP was reduced, alkylated and successfully analyzed by MS. Since the purification and analysis of LLS-MBP was fulfilled, a second plasmid that contains the *llsBYD* genes was constructed and transformed in the same *E. coli* strain that expresses the LLS-MBP fusion protein. The LLS-MBP was purified, digested, reduced, and alkylated as previously. Afterwards, the LLS peptide was cut and it was analyzed by MS, leading to the identification of 4 modified cysteines in the purified LLS (Cys^{27}, Cys^{28}, Cys^{30}, and Cys^{35}). Interestingly, the first cysteine is the most abundant modification and then the other modified species are present but are less abundant, probably due to their high hydrophobic profile. This is the first evidence that LLS present thiazole heterocycles and represents a major step in the elucidation of the complete LLS mature structure.

1.2 Discussion

The attempts to identify the mature structure of some TOMMs have not been successful. Though is possible to the reconstitute the activity of SLS and CLS *in vitro* the mature structure of these molecules remains unknown (212). The PTMs of SLS and CLS prevented numerous MS methods to identify the structure of the mature toxins (211). Traditional proteomic approaches such as iodoacetamide alkylation, trypsin digestions, dissolution in formic or acetic acid, and capillary LS-MS/MS have failed to recover any of the peptides covering the C-terminal of SLS and CLS (221). The C-terminal of SLS and CLS is very rich in contiguous Cys residues (7 Cys residues and 8 Cys residues, respectively) and is possibly that the modified peptides are highly hydrophobic (221).

Gonzalez and colleagues (2010), identified some PTMs present in SLS and CLS by alkylating the Cys with 2-bromoethylamine (BrEA). The BrEA allowed to improve the water solubility, the ionization by introducing an amine (positively charged) and enables the tryptic digestion after the treatment generating a ladder of peptides. Samples were alkylated with 2-bromoethylamine, then trypsin-digested, and analyzed by nanocapillary LC-MS/MS. By using this approach, they identified two oxazole moieties in SLS (Ser^{46} and Ser^{48}) and three methyl-oxazole moieties in CLS ($Thr1^{1}$,

Thr^{12} and Thr^{46}) (221). For CLS the moieties, these were identified in a protoxin encoding only the C-terminal half of CLS and lacking the other half that is full of Cys residues. Interestingly, the PTM in CLS were identified as a heterogeneous mixture (221). Likewise, the most recent findings regarding LLS structure (see Annex 1) show that some of the 4 PTMs that have been identified so far (Cys^{27}, Cys^{28}, Cys^{30}, and Cys^{35}) were identified as a heterogeneous mixture with some modifications more abundant than others.

In some other TOMMs, the Cys residues are less abundant and discontinuous. In KLB only 3 discontinuous Cys residues are present and the three of them are modified (432). In PZN only two discontinuos Cys residues are present and both of them are modified (238). In the case of MccB17, four Cys residues are present with all of them being modified (58). Altogether these data explain why the mature structures of MccB17, PZN and KLB, where the Cys residues are less abundant, have been already elucidated without major concerns.

Altogether these results suggest that the abundance of Cys residues that could be potentially modified, render the TOMMs more hydrophobic and consequently much harder to elucidate their mature structure. It is tempting to speculate that obtaining the LLS and STS complete mature structure will be harder than CLS and SLS, because the LLS and STS peptides are much richer in continuos Cys residues (8 Cys residues and 9 Cys residues, respectively).

The heterologous expression of TOMMs followed by *in vitro* reconstitution of biological activity to perform MS has been a successful method to study the specific sites of PTMs. However, there are some difficulties to heterologously express all the genes of the TOMMs biosynthetic clusters that rely on: (1) the inability to control the expression of the individual genes into the non-native host, (2) incompatibility between Gram-positive and Gram-negative bacteria, (3) low expression levels or inability to restore the WT levels of activity of these molecules (213, 215, 431). In collaboration with experts in this field we managed to observe some LLS PTMs modifications. We still need to further study whether these PTMs reconstitute completely LLS bactericidal and hemolytic activities *in vitro*.

1.3 Materials and methods

Bacterial strains and growth conditions

Bacterial strains and plasmids used in this study are listed in Table S1 and Table S2 (Annex 3). All the primers used are listed in Table S3 (Annex 3). The *Lm* strains were grown in tubes overnight at 200 rpm and 37°C in BHI broth (Difco). When required, antibiotics were added for *Listeria* chloramphenicol 7 µg/mL and erythromycin 5 µg/mL. *E. coli* was grown overnight at 200 rpm and 37°C in LB medium and Kanamycin (50 µg/mL) and Chloramphenicol (25 µg/mL) were added. A fresh culture of *E. coli* was inoculated with 1 to 100 dilution of the preculture and grown at 37 °C with an OD_{600nm}= 0.7-1. Protein and peptide induction are then triggered by adding 1 mM isopropyl-β-D-thiogalactopyranoside (IPTG) and culture aliquots were recovered after different time points (2 and 4h) to prepare lystes.

Mutant and strains construction

For the strain *Lm* F2365 pHELP: *llsA*-His the His tag was added in the C terminal of the *llsA* gene and the pHELP promoter was fused between two 500-ntd DNA fragments flanking the start codon of *llsA.* These DNA constructions were synthetically produced by gene synthesis (Genecust) and cloned into *Sal*I–*Eco*RI restriction sites of pMAD vector. Mutagenesis was performed by double recombination as described previously (410).

For the heterologous expression of the *llsABXYD* genes in *E. coli,* the method described previously was used (431). Briefly, the *llsABXYD* genes were synthetically produced by gene synthesis. One plasmid (pCOLA) harboring the *llsABX* genes and the second plasmid (pCYC) harboring the genes *llsDY* were constructed. One plasmid or two were transformed in electrocompetent *E. coli* BL21 cells to obtain the expression strain harboring pCOLA_*llsABX* (Kanamycin resistance) + pACYC_*llsDY* (Chloramphenicol resistance) and the control strain harboring only pCOLA_*llsABX*.

Partial purification of LLS hemolytic fractions

Partial purification of LLS was carried out as described before for SLS (433). Briefly, *Lm* F2365 pHELP: *llsA* (LLS^+) and *Lm* F2365 Δ*llsA* (LLS^-) were grown overnight at 37°C in BHI supplemented with maltose (1% w/v) and sodium bicarbonate (2% w/v;

BHI-BM). 20 ml of this culture was inoculated in 1 L of BHI-BM and grown at 37°C for 5 hours. The culture was centrifuged, the cell free supernatant collected for assessment of hemolysis. The cell pellet was washed in 100 mM potassium phosphate buffer pH 7 before resuspension to a final volume of 15 ml in induction buffer (IB; 100 mM KH_2PO_4, 2 mM $MgSO_4$, 30 mM maltose, pH 7). The cell suspension was centrifuged and the cell free supernatant was also collected for assessment. The remaining 14 ml volume of cell suspension was incubated at 37°C for 5 min before being induced through the addition of 0.5 mg yeast RNA core (RNA^C; Sigma)/ml of suspension and immediately centrifuged. The supernatant was collected and supplemented with ammonium acetate (AmAc; 100 mM, pH 7). Hemolytic activity was assessed through the creation of wells (4.6 mm diameter, 200 µl tips diameter) in Columbia blood agar plates (5% sheep's blood) and the introduction of 50 µl to be assessed. Plates were incubated overnight at 37°C.

E. coli bacterial lysates and cultures

After 4h of induction with 1 mM IPTG *E. coli* lysates (from 500 mL) were prepared by washing cells in one volume of HEPES buffer (HEPES 20 mM, NaCl 150 mM), resuspending them in 20 mL HEPES buffer and sonicating them (4 cycles of 30 s, 20% amplitude). Later, 5×10^7 target bacteria from overnight cultures were inoculated into 5 mL of fresh BHI either alone or with 200 µl of *E. coli* lysates. At 24 h after inoculation, cultures were serially diluted and plated on BHI agar plates.

Annex 2: Review LLS Gut Microbes

Gut Microbes

ISSN: 1949-0976 (Print) 1949-0984 (Online) Journal homepage: https://www.tandfonline.com/loi/kgmi20

Listeriolysin S: A bacteriocin from epidemic *Listeria monocytogenes* strains that targets the gut microbiota

Juan J Quereda, Jazmín Meza-Torres, Pascale Cossart & Javier Pizarro-Cerdá

To cite this article: Juan J. Quereda, Jazmín Meza-Torres, Pascale Cossart & Javier Pizarro-Cerdá (2017) Listeriolysin S: A bacteriocin from epidemic *Listeria monocytogenes* strains that targets the gut microbiota, Gut Microbes, 8:4, 384-391, DOI: 10.1080/19490976.2017.1290759

To link to this article: https://doi.org/10.1080/19490976.2017.1290759

Accepted author version posted online: 03 Feb 2017.
Published online: 21 Feb 2017.

GUT MICROBES
2017, VOL. 8, NO. 4, 384–391
https://doi.org/10.1080/19490976.2017.1290759

Taylor & Francis
Taylor & Francis Group

ADDENDUM

Listeriolysin S: A bacteriocin from epidemic *Listeria monocytogenes* strains that targets the gut microbiota

Juan J. Quereda[a,b,c], Jazmín Meza-Torres[a,b,c], Pascale Cossart[a,b,c], and Javier Pizarro-Cerdá[a,b,c]

[a]Institut Pasteur, Unité Des Interactions Bactéries-Cellules, Paris, France; [b]INSERM, U604, Paris, France; [c]INRA, USC2020, Paris, France

ABSTRACT

Listeria monocytogenes is a Gram-positive food-borne pathogen that in humans may traverse the intestinal, placental and blood/brain barriers, causing gastroenteritis, abortions and meningitis. Crossing of these barriers is dependent on the bacterial ability to enter host cells, and several *L. monocytogenes* surface and secreted virulence factors are known to facilitate entry and the intracellular lifecycle. The study of *L. monocytogenes* strains associated to human listeriosis epidemics has revealed the presence of novel virulence factors. One such factor is Listeriolysin S, a thiazole/oxazole modified microcin that displays bactericidal activity and modifies the host microbiota during infection. Our recent results therefore highlight the interaction of *L. monocytogenes* with gut microbes as a crucial step in epidemic listeriosis. In this article, we will discuss novel implications for this family of toxins in the pathogenesis of diverse medically relevant microorganisms.

ARTICLE HISTORY
Received 1 December 2016
Revised 24 January 2017
Accepted 24 January 2017

KEYWORDS
bacteriocin; intestinal barrier; *Listeria monocytogenes*; Listeriolysin S; LLS; microbiota

Introduction bacteriocins

Bacteriocins are ribosomally-synthesized peptides or proteins which have been reported in bacteria and archea, which can kill species closely related to the producer species, and for which the producer often displays an immunity mechanism.[1] Historically, the term 'bacteriocin' coined by François Jacob in 1953[2] referred to colicins produced by *Escherichia coli*[3] and analogous proteins produced by other Gram-negative bacteria including pyocins from *Pseudomonas pyocyanea*,[4] marcenins from *Serratia marcescens*, cloacins produced by *Enterobacter cloacae* or influenzacins by *Haemophilus influenzae*.[5] In Gram-positive bacteria, bacteriocin-like activities were described as early as 1928[6] but the name 'bacteriocin' was used only in later years,[7] in particular as a reference to lantibiotics and other peptides produced mainly by lactic acid bacteria.[8]

Several bacteriocin classification schemes have been proposed, which either include only molecules produced by Gram-positive bacteria[9] or molecules produced by both Gram-positive and Gram-negative bacteria.[10] Nowadays, the term 'bacteriocin' comprises diverse molecules which include circular peptides, non-modified peptides and post-translationally modified peptides, including members of the thiazole/oxazole modified microcins (TOMMs). The prototypic TOMM is Microcin B17 from *Escherichia coli*,[11] a DNA gyrase inhibitor that displays 14 post-translational modifications constituted of thiazole and oxazole rings.[12] Among the TOMMs there are also molecules for which no bacteriocin activity has been reported: for example the *Streptococcus pyogenes* TOMM Streptolysin S (SLS) is a toxin which displays hemolytic activity, and cytotoxic activity against macrophages and neutrophils. SLS is also involved in paracellular invasion of tissues and in soft tissue damage, but has no reported bacteriocin activity.[13]

It has been proposed that 99% of all bacteria may produce at least one bacteriocin.[14] Interestingly, we

CONTACT Javier Pizarro-Cerdá javier.pizarro-cerda@pasteur.fr Unité des Interactions Bactéries-Cellules, Institut Pasteur, 25 rue du Docteur Roux, 75724 Paris Cedex 15, France.

Addendum to: Quereda JJ, Dussurget O, Nahori M-A, Ghozlane A, Volant S, Dillies M-A, Régnault B, Kennedy S, Mondot S, Villoing B, Cossart P, Pizarro-Cerdá J. Bacteriocin from epidemic Listeria strains alters the host intestinal microbiota to favor infection. Proc Nat Acad Sci USA 2016; 113:5706-11.

have recently reported the first bacteriocin produced for the Gram-positive genus *Listeria*.[15]

Listeria monocytogenes: *A food-borne pathogen*

Listeria monocytogenes is a major bacterial model system in diverse research fields including microbiology, immunology and cell biology. This Gram-positive pathogen is responsible for listeriosis, a food-borne disease characterized by potentially fatal septicemia in immunocompromised individuals, severe meningitis in newborns and abortion in pregnant women. Considered for many years as a rare bacterium after its first descriptions in England in 1926[16] and in South Africa in 1927,[17] *L. monocytogenes* has been instrumental in our understanding of cellular immune responses since the pioneering work of George Mackaness in the 1960s,[18] which demonstrated that this bacterium is able to multiply within macrophages and established it as the prototype intracellular parasite. The important listeriosis epidemics in North America and Europe in the 1980s subsequently revealed that *L. monocytogenes* also represents an important public health problem,[19] being responsible for the largest and most deadly food recalls in the United States.[20] In the following years, critical aspects of *L. monocytogenes* virulence mechanisms were discovered due to advances in molecular and cell biology techniques: for example, the pore-forming toxin listeriolysin O (LLO), which allows *L. monocytogenes* escape from phagosomes, became the first bacterial virulence factor to have its gene cloned.[21] Soon afterwards, the intracellular cycle of *L. monocytogenes* was discovered,[22] highlighting that this bacterium manipulates the actin cytoskeleton to spread from cell to cell,[23] allowing its use as a molecular tool to identify the Arp2/3 complex as the first discovered actin nucleator in eukaryotic cells.[24] Since then, *L. monocytogenes* has been studied as a model pathogen,[25] as an exquisite tool to manipulate mammalian cells for the identification of novel cellular functions,[26,27] and as vector to deliver intracellular antigens in anticancer therapies.[28]

The *L. monocytogenes* pathogenicity island I (LIPI-I) and the internalins islet encode for bacterial molecules which modulate host cells functions (reviewed by,[25,29]): these include the surface proteins InlA and InlB which promote bacterial internalization into host cells,[30] the cholesterol-dependent cytotoxin LLO and the phospholipases PlcA and PlcB which disrupt host cell membranes,[21,31] and the surface protein ActA involved in host actin polymerization.[23] Two additional genes in LIPI-I encode for Mpl, a metalloprotease involved in the maturation of PlcB[32] and for PrfA, the major transcription factor which controls the expression of the most important *L. monocytogenes* virulence genes.[33] It is important to note that for decades, *L. monocytogenes* pathogenesis has been mainly studied using a subset of bacterial strains including EGD, EGDe, LO28 and 10403S which belong to the *L. monocytogenes* evolutionary lineage II, an assembly of bacterial clonal groups which are rarely associated to major human listeriosis outbreaks.[34,35] On the other hand, listeriosis epidemics in humans are mostly associated to *L. monocytogenes* clonal groups from the evolutionary lineage I, but these strains have been poorly characterized and the molecular mechanisms that contribute to their higher virulence remained unknown until recent times.[35] In 2008, the *L. monocytogenes* pathogenicity island III (LIPI-III) was discovered in a subset of lineage I strains, suggesting that it could be associated to the higher virulence potential of these bacteria.[36] LIPI-III encodes a biosynthetic cluster involved in the production of Listeriolysin S (LLS), an hemolytic and cytotoxic TOMM shown to be required for *L. monocytogenes* virulence *in vivo* in a mouse intra-peritoneal infection model.[36]

Listeriolysin S: A bacteriocin that modulates the host microbiota

The LLS gene cluster include the gene *llsA* which encodes for the actual LLS toxic peptide, the genes *llsG* and *llsH* which encode for a putative transporter, the genes *llsB, llsY* and *llsD* which encode for putative post-translational modification enzymes involved in the production of thiazole/oxazole/methyloxazole rings, the gene *llsP* which encodes for a putative protease, and the gene *llsX* which encodes for a protein of unknown function specific to the genus *Listeria*.[36,37] Inactivation of the *llsB* gene was sufficient to reduce *L. monocytogenes* numbers in the liver and spleen *in vivo*, suggesting that the post-translational modification of the *llsA* gene product is crucial for its biologic activity.[36]

To better understand the potential contribution of LLS to *L. monocytogenes* virulence, we decided to use a mouse oral infection model, which recapitulates the

normal infection route in humans for this food-borne pathogen. We first compared infection by 2 lineage II strains, EGDe and 10403S, with the lineage I strain F2365 responsible for the 1985 listeriosis California outbreak.[38] Our results indicate that the lineage I strain is more virulent than the 2 lineage II strains after counting colony forming units in the intestinal content, in the intestine and in the spleen 48 hours after infection.[15] To specifically evaluate the role of LLS in this oral infection model, we generated deletions mutants for the *llsA* and *llsB* genes: surprisingly, we observed for these mutants an important reduction in their capacity to invade the intestine and to survive in the intestinal content as early as 6 hours post-infection, suggesting that the LLS could play a role in virulence during the *L. monocytogenes* intestinal stage.[15] To monitor the organs in which LLS is expressed *in vivo*, we fused the promoter region of the LLS gene cluster to the *lux* operon of *Photorhabdus luminescens*: we detected the production of bioluminescence specifically in the intestine of orally-infected mice from 7 hours post-infection (the first post-infection measurement of bioluminescence in our experimental conditions). Upon dissection of animals at 96 hours post-infection, bioluminescence was detected only in the intestine and not in other infected organs including the liver and the spleen (although these organs contained higher bacterial counts), suggesting a major role for LLS in the mouse intestine.[15]

The biosynthetic cluster encoding LLS is homologous to the operon encoding the microcin B17 from environmental *E. coli*, which is a bacteriocin that kills competitor soil bacteria. As *L. monocytogenes* encounters diverse bacterial communities during the intestinal phase of listeriosis, we decided to explore the hypothesis that LLS could behave as a bacteriocin and influence virulence by modulating the host gut microbiota. First, we investigated *in vitro* the capacity of LLS to alter the growth of potential target bacteria by incubating a F2365 lineage I strain constitutively producing LLS with the 10403S and EGD lineage II strains which do not possess the LLS biosynthetic cluster, and which therefore lack the putative immunity gene *llsP*. Our results clearly indicate that the production of LLS is associated with a decrease in the survival of the lineage II strains, suggesting that LLS displays bacteriocin activity. Moreover, a screen of a small library of Gram-positive and Gram-negative bacteria indicate that LLS is only active against other Firmicutes which include *Lactococcus lactis* and *Staphylococcus aureus*.[15] In the light of these results, we decided to monitor changes in the host intestinal microbiota associated to LLS production using high-throughput 16S rDNA analysis. We infected mice with a F2365 wild type strain, with an isogenic deletion mutant of the *llsA* gene or with an isogenic complemented strain, and we examined the microbial community compositions 24 hours after infection. Our results show that LLS production does not promote major changes in the host microbiota at the phylum level: instead, significant changes are detected only at the genus level for representatives of *Alloprevotella, Allobaculum* and *Streptococcus* in mice infected with the wild type and the complemented strains, but not in mice infected with the *llsA* deletion mutant.[15]

In summary, our study reports the first bacteriocin for the *Listeria* genus (Fig. 1). For decades, *L. monocytogenes* had been one of the most studied food-borne bacterial pathogens, from an infection biology perspective. However, investigations focused on lineage II strains have prevented the identification of novel virulence factors exclusively associated to lineage I strains. Our findings pave the way to understand why lineage I *L. monocytogenes* strains are more often associated to human listeriosis outbreaks, and in particular they suggest that modulation of the host microbiota is critical for the infection outcome. Whether bacteriocin production by epidemic entero-pathogenic bacteria is a common strategy to colonize the gastrointestinal tract, or whether it is an exceptional mechanism used only by some *L. monocytogenes* and *Enterococci* strains during their infection processes, remains to be elucidated.[39]

Open questions

Cellular activities

LLS is a member of the TOMM family which has been described previously as an hemolytic and cytotoxic factor.[36] Now, we report LLS behaving also as bacteriocin[15] This dual feature is not specific to LLS as it has been previously observed in a molecule secreted by *Staphylococcus pseudointermedius*: indeed, the peptide BacSp222 displays both features of a cytotoxic factor against eukaryotic cells and a bacteriocin toward Gram-positive bacteria.[40] Our work clearly indicates that the bacteriocin activity of LLS plays a crucial role during infection. Previous results

from Cotter et al. suggest that the cytotoxic activity of LLS also contributes to *L. monocytogenes* virulence.[36] Using our bioluminescent reporter, we were not able to detect the activation of the LLS promoter in other organs besides the intestine.[15] However, we cannot exclude that activation of the LLS operon takes place at levels which are not detected by our reporter system. It remains to be determined which cellular populations are targeted by LLS *in vivo* (Fig. 2): it would be tempting to speculate that LLS may either favor vacuolar escape (in cooperation with LLO, PlcA and PlcB) or that its hemolytic role may favor *L. monocytogenes* survival in the blood.

Bactericidal mechanism

The mechanism by which LLS achieves bacterial killing is unknown. Several lantibiotics use as receptors the lipid II enzyme involved in the translocation of peptidoglycan subunits from the bacterial cytoplasm to the cell wall, and these lantibiotics inhibit therefore cell wall synthesis (reviewed by[13]). Nisin is a particular bacteriocin that binds lipid II and it blocks not only lipid II activity but it can also insert into the bacterial inner membrane inducing the formation of pores and consequently promoting bacterial killing by disrupting ion gradients.[41] On the other hand, the prototypic TOMM microcin B17 uses specific outer membrane and inner membrane transporters to reach the cytoplasm of Gram-negative bacteria, where it inhibits the activity of the DNA gyrase.[12] Whether LLS displays a pore-forming activity, an enzymatic/nuclease activity or both therefore remains to be identified. Determination of the mature structure of LLS may provide clues on its bactericidal mechanism. The mature structures of Gram-negative TOMMs, including the microcin B17, have been identified.[12] Interestingly, the structures of TOMMs from Gram-positive bacteria have proven to be more difficult to solve: despite more than 100 y of investigation on SLS, the structure of its mature form is still unknown.[42] Recent advances in proteomic approaches, coupled to targeted site mutagenesis studies, could allow the identification of key residues in the LLS structure required for its biologic activities.

Microbiota diversity

Our results put forward many crucial implications for the study of listeriosis as a disease. The status of the host microbiota has never been assessed nor taken into account in animal studies upon *L. monocytogenes* infection through the oral route. It is unlikely that *L. monocytogenes* or other enteric pathogens bet on one

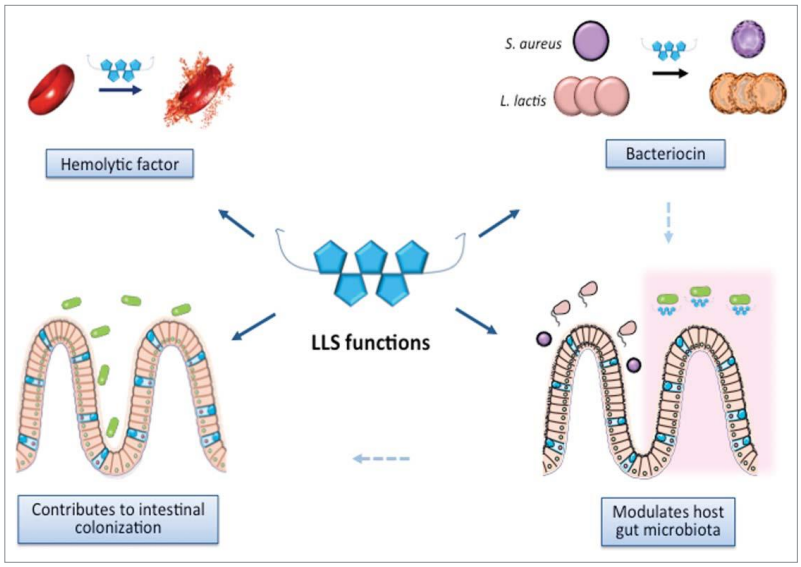

Figure 1. Functional activities of Listeriolysin S. LLS has been initially described as an hemolytic factor (top left) which contributes to the virulence of *L. monocytogenes in vivo*. Our recent work now suggests that LLS is also a bacteriocin which *in vitro* is capable of killing *S. aureus and L. lactis* (top right), and which *in vivo* modulates the host intestinal microbiota (bottom right), allowing *L. monocytogenes* colonization of the intestine (bottom left).

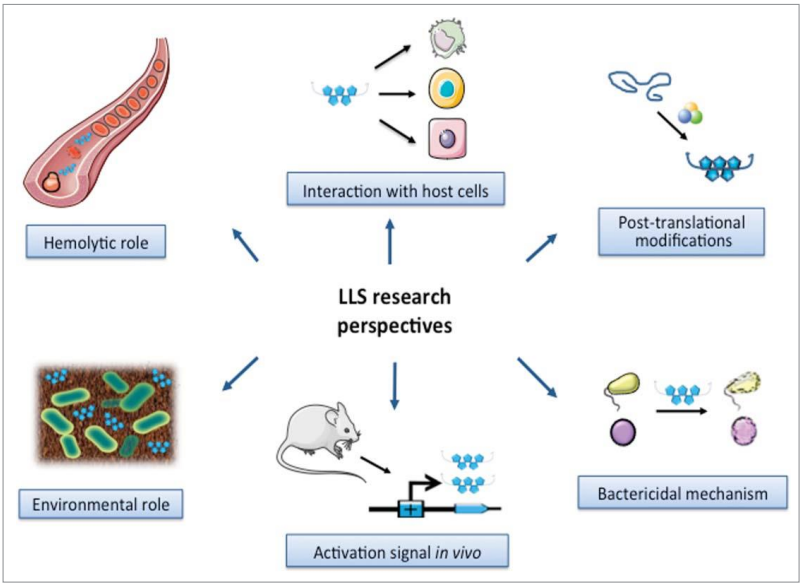

Figure 2. Perspectives on Listeriolysin (S) research. Many functions of LLS remain to be elucidated. LLS has been described as an hemolysin, but it remains to be directly demonstrated whether its hemolytic activity contributes to virulence *in vivo* (top left). Which other cellular populations may be also targeted by LLS *in vivo* has not been determined yet (top center). The structure of the post-translational modifications that characterize the mature LLS are not known (top right), and the bactericidal mechanism on susceptible species needs to be identified (bottom right). The signal that activates the expression of the LLS cluster is unknown at this stage (bottom center), and whether LLS plays a role in the survival of *L. monocytogenes* in the environment remains an open question.

single strategy to fight against intestinal microbiota: this idea makes us think that other bacteriocins or defense systems could be produced by lineage I and by lineage II strains to colonize the intestine and promote infection. We should mention also that intestinal microbiota exhibit diurnal and seasonal oscillations in composition and function.[43] Important variability observed in *in vivo L. monocytogenes* infection experiments could be explained by variations in the host microbiota of individual animals. Previous homogenization of the animal host microbiota now seems to be an important methodological requirement to compare results within animals from a single experiment. The use of controlled microbiotas in animal infection models should allow to better understand the interplay between *L. monocytogenes* and resident bacteria in the intestine.

Target species

In our recent study, we observe a significant decrease in the populations *Alloprevotella* and *Allobaculum* correlating with the production of LLS.[15] These species are producers of acetic and butyric acid, which are small molecules previously shown to either inhibit *L. monocytogenes* growth or transcriptional activity,[44,45] and therefore could be considered as 'protective microbiota species'. Whether these species are the only significant producers of acetic and butyric acid during *L. monocytogenes* infections remains to be elucidated. Interestingly, another study reported that *Allobaculum* is protective during antibiotic-induced disruption of microbiota.[46] Additionally, it is possible that *L. monocytogenes* produces other bactericions besides LLS to target other competing bacteria, expanding its capacity to control the host gut microbiota. It will be important to determine which mechanisms are involved in the reduction of *Alloprevotella* and *Allobaculum* representatives: since *Allobaculum* is a Gram-positive species (Tenericutes), it may be a direct target of LLS. *Alloprevotella* on the other hand is a Gram-negative bacterium (Bacteroidetes) and taking into account the specificity of most bacteriocins, it is highly probable that this species is not a direct target of LLS: the decrease in *Alloprevotella* would therefore be indirect, as a result in the decrease of another species that probably controls *Alloprevotella* growth. Identifying the different interactions between

microbiota species during lineage I *L. monocytogenes* infection will be crucial to understand the contribution of LLS to infection.

Therapeutic uses

We still do not know which bacterial species are controlled by LLS in humans, but our results and data from other teams highlight that protective bacterial species could be used as a strategical treatment to prevent *L. monocytogenes* infection in individuals at risk. The group of Colin Hill and colleagues has elegantly shown that bacteriocin production by *Lactobacillus salivarius* UCC118 allows mice protection against oral *L. monocytogenes* infection.[47] Moreover, they have also shown that thuricin CD, a 2-peptide bacteriocin from *Bacillus thuringiensis*, was found to display antimicrobial activity comparable to the activities of vancomycin and metronidazole in a model of human distal colon infection by *Clostridium difficile*, without changing dramatically the composition of the commensal microbiota (which is observed during vancomycin and metronidazole treatment).[48] In the same line, engineering of LLS may potentially be used to treat infection caused by microorganisms such as *S. aureus* which is already resistant to multiple antibiotics.

Activation signal

We tried to identify specific signals which trigger *in vitro* the expression of LLS, including mucin, gastric fluid, trypsin, pepsin, NaHCO3, bile salts, detergents, succinic acid, propionic acid, valeric acid, ethanolamine, antibiotics, 6% 0_2 or intestinal content added *ex vivo*. However, no signal is able to activate the promoter of the LLS operon.[15] As expression of several bacteriocins is triggered precisely by the presence of other bacteria,[49] we hypothesized that the intestinal microbiota could be precisely the signal recognized by *L. monocytogenes* to induce LLS expression. Nevertheless, experiments in germ-free mice indicate that the LLS promoter may be activated in the absence of microbiota.[15] These results suggest that LLS is probably produced upon exposure to a pleiotropic set of conditions that may combine several parameters. Detection of the LLS activation signals is therefore an important research topic, not only during host infections but also in environmental conditions (see below).

Environmental role

It has been observed that the LLS cluster is present in several isolates of the non-pathogenic species *Listeria innocua*: in some of them, the cluster presents many mutations and it is not functional but in others, the produced LLS is fully hemolytic.[50] The significance of these results is not clear, but may reveal a role for LLS in the environment. Several bacteriocins are produced for niche colonization, and it would not be surprising to discover such a role for *L. innocua* and also for *L. monocytogenes* in the environment. These results also call into attention the evolution of other members of the LLS biosynthetic cluster in *Clostridium botulinum, S. pyogenes* and *S. aureus*, all of them pathogens with different lifestyles. How the regulation and function of this family of TOMM evolved in these bacterial pathogen remains an attractive field for future investigations.

Disclosure of potential conflicts of interest

No potential conflicts of interest were disclosed.

Acknowledgments

We are thankful to members of the Unité des Interactions Bactéries-Cellules and of the C3BI (Pasteur Institute) for helpful discussions. We thank Servier Medical Art (http://www.servier.com/Powerpoint-image-bank) for providing drawings used in Figures 1 and 2.

Funding

This work was supported by the Institut Pasteur, the Institut National de la Santé et de la Recherche Médicale (INSERM Unité 604), the Institut National de la Recherche Agronomique (INRA Unité Sous Contrat 2020), the Institut Pasteur 'Programmes Transversaux de Recherche' (PTR521 to JPC), L'Agence Nationale de la Recherché (ANR-15-CE15–0017 StopBugEntry to JPC), Fondation Le Roch Les Mousquetaires, European Research Council Advanced Grant (670823 BacCellEpi to PC) and Région Ile-de-France (DIM-MALINF to JMT). PC is an International Senior Research Scholar of the Howard Hughes Medical Institute. The authors declare no conflict of interest.

References

[1] Zheng J, Gänzle MG, Lin XB, Ruan L, Sun M. Diversity and dynamics of bacteriocins from human microbiome. Environ Microbiol 2014; 17:2133-43; PMID:25346017; https://doi.org/10.1111/1462-2920.12662

[2] Jacob F, Lwoff A, Siminovitch A, Wollman E. [Definition of some terms relative to lysogeny]. Ann Inst Pasteur (Paris) 1953; 84:222-4; PMID:13031254
[3] Gratia A. Sur un remarquable exemple d'antagonisme entre deux souches de colibacille. Comptes Rendus, Société Biologique (Paris) 1925; 93:1040-2
[4] Gratia A, Fredericq P. Pluralité et complexité des colicines. Bull Soc Chim Biol 1947; 29:354-6; PMID:18900119
[5] Jacob F. [Induced biosynthesis and mode of action of a pyocine, antibiotic produced by Pseudomonas aeruginosa]. Ann Inst Pasteur (Paris) 1954; 86:149-60; PMID:13158940
[6] Fredericq P. [Colicins and Colicinogeny]. Ann Inst Pasteur (Paris) 1964; 107 SUPPL:7-17
[7] Rogers LA, Whittier EO. Limiting factors in the lactic acid fermentation. J Bacteriol 1928; 16:211-29; PMID:16559334
[8] Kellner R, Jung G, Hörner T, Zähner H, Schnell N, Entian KD, Götz F. Gallidermin: a new lanthionine-containing polypeptide antibiotic. Eur J Biochem 1988; 177:53-9; PMID:3181159; https://doi.org/10.1111/j.1432-1033.1988.tb14344.x
[9] Cotter PD, Hill C, Ross RP. Bacteriocins: developing innate immunity for food. Nat Rev Micro 2005; 3:777-88; https://doi.org/10.1038/nrmicro1273
[10] Heng NCK, Tagg JR. What's in a name? Class distinction for bacteriocins. Nat Rev Micro 2006; 4; https://doi.org/10.1038/nrmicro1273-c1
[11] Asensio C, Pérez-Diaz JC, Martinez MC, Baquero F. A new family of low molecular weight antibiotics from enterobacteria. Biochem Biophys Res Commun 1976; 69:7-14; PMID:4071; https://doi.org/10.1016/S0006-291X(76)80264-1
[12] Yorgey P, Lee J, Kördel J, Vivas E, Warner P, Jebaratnam D, Kolter R. Posttranslational modifications in microcin B17 define an additional class of DNA gyrase inhibitor. Proc Natl Acad Sci USA 1994; 91:4519-23; PMID:8183941; https://doi.org/10.1073/pnas.91.10.4519
[13] Molloy EM, Cotter PD, Hill C, Mitchell DA, Ross RP. Streptolysin S-like virulence factors: the continuing sagA. Nat Rev Micro 2011; 9:670-81; https://doi.org/10.1038/nrmicro2624
[14] Klaenhammer TR. Genetics of bacteriocins produced by lactic acid bacteria. FEMS Microbiol Rev 1993; 12:39-85; PMID:8398217; https://doi.org/10.1111/j.1574-6976.1993.tb00012.x
[15] Quereda JJ, Dussurget O, Nahori M-A, Ghozlane A, Volant S, Dillies M-A, Régnault B, Kennedy S, Mondot S, Villoing B, et al. Bacteriocin from epidemic Listeria strains alters the host intestinal microbiota to favor infection. Proc Natl Acad Sci 2016; 113:5706-11:201523899
[16] Murray E, Webb RA, Swan N. A disease of rabbits characterized by leukocytosis caused by *Bacterium monocytogenes*. J Pathol Bacteriol 1926; 29:407-39
[17] Pirie JHH. A new disease of veld rodents, "Tiger River Disease". Pub South Africa Inst Med Res 1927; 62:163-86
[18] Mackaness GB. Cellular resistance to infection. J Exp Med 1962; 116:381-406; PMID:14467923; https://doi.org/10.1084/jem.116.3.381
[19] Schlech WF, Lavigne PM, Bortolussi RA, Allen AC, Haldane EV, Wort AJ, Hightower AW, Johnson SE, King SH, Nicholls ES, et al. Epidemic Listeriosis: evidence for transmission by food. N Eng J Med 1983; 308:203-6
[20] Johnson NB, Hayes LD, Brown K, Hoo EC, Ethier KA. Centers for Disease Control and Prevention (CDC). CDC National Health Report: leading causes of morbidity and mortality and associated behavioral risk and protective factors–United States, 2005–2013. MMWR Surveill Summ 2014; 63 Suppl 4:3-27
[21] Mengaud J, Chenevert J, Geoffroy C, Gaillard JL, Cossart P. Identification of the structural gene encoding the SH-activated hemolysin of Listeria monocytogenes: listeriolysin O is homologous to streptolysin O and pneumolysin. Infect Immun 1987; 55:3225-7; PMID:2824384
[22] Tilney LG, Portnoy DA. Actin filaments and the growth, movement, and spread of the intracellular bacterial parasite, Listeria monocytogenes. J Cell Biol 1989; 109:1597-608; PMID:2507553; https://doi.org/10.1083/jcb.109.4.1597
[23] Kocks C, Gouin E, Tabouret M, Berche P, Ohayon H, Cossart P. L. monocytogenes-induced actin assembly requires the actA gene product, a surface protein. Cell 1992; 68:521-31
[24] Welch MD, Iwamatsu A, Mitchison TJ. Actin polymerization is induced by Arp2/3 protein complex at the surface of Listeria monocytogenes. Nature 1997; 385:265-9; PMID:9000076; https://doi.org/10.1038/385265a0
[25] Pizarro-Cerdá J, Charbit A, Enninga J, Lafont F, Cossart P. Manipulation of host membranes by the bacterial pathogens Listeria, Francisella, Shigella and Yersinia. Semin Cell Dev Biol 2016; 60:155-167
[26] Tham TN, Gouin E, Rubinstein E, Boucheix C, Cossart P, Pizarro-Cerdá J. Tetraspanin CD81 is required for Listeria monocytogenes invasion. Infect Immun 2010; 78:204-9; PMID:19901060; https://doi.org/10.1128/IAI.00661-09
[27] Pizarro-Cerdá J, Chorev DS, Geiger B, Cossart P. The Diverse Family of Arp2/3 Complexes. Trends Cell Biol 2016; 27:93-100
[28] Brockstedt DG, Bahjat KS, Giedlin MA, Liu W, Leong M, Luckett W, Gao Y, Schnupf P, Kapadia D, Castro G, et al. Killed but metabolically active microbes: a new vaccine paradigm for eliciting effector T-cell responses and protective immunity. Nat Med 2005; 11:853-60; PMID:16041382; https://doi.org/10.1038/nm1276
[29] Quereda JJ, Cossart P, Pizarro-Cerdá J. Role of Listeria monocytogenes exotoxins in virulence. Microbial Toxins 2016; 27:93-100
[30] Gaillard JL, Berche P, Frehel C, Gouin E, Cossart P. Entry of L. monocytogenes into cells is mediated by internalin, a repeat protein reminiscent of surface antigens from gram-positive cocci. Cell 1991; 65:1127-

41; PMID:1905979; https://doi.org/10.1016/0092-8674(91)90009-N

[31] Mengaud J, Braun-Breton C, Cossart P. Identification of phosphatidylinositol-specific phospholipase C activity in Listeria monocytogenes: a novel type of virulence factor? Mol Microbiol 1991; 5:367-72; PMID:1645839; https://doi.org/10.1111/j.1365-2958.1991.tb02118.x

[32] Domann E, Leimeister-Wächter M, Goebel W, Chakraborty T. Molecular cloning, sequencing, and identification of a metalloprotease gene from Listeria monocytogenes that is species specific and physically linked to the listeriolysin gene. Infect Immun 1991; 59:65-72; PMID:1898903

[33] Mengaud J, Dramsi S, Gouin E, Vázquez-Boland JA, Milon G, Cossart P. Pleiotropic control of Listeria monocytogenes virulence factors by a gene that is autoregulated. Mol Microbiol 1991; 5:2273-83; PMID:1662763; https://doi.org/10.1111/j.1365-2958.1991.tb02158.x

[34] Becavin C, Bouchier C, Lechat P, Archambaud C, Creno S, Gouin E, Wu Z, Kuhbacher A, Brisse S, Pucciarelli MG, et al. Comparison of Widely Used Listeria monocytogenes Strains EGD, 10403S, and EGD-e Highlights Genomic Variations Underlying Differences in Pathogenicity. mBio 2014; 5:e00969-14; PMID:24667708; https://doi.org/10.1128/mBio.00969-14

[35] Maury MM, Tsai Y-H, Charlier C, Touchon M, Chenal-Francisque V, Leclercq A, Criscuolo A, Gaultier C, Roussel S, Brisabois A, et al. ng.3501. Nature Publishing Group 2016; 48:308-13

[36] Cotter PD, Draper LA, Lawton EM, Daly KM, Groeger DS, Casey PG, Ross RP, Hill C. Listeriolysin S, a novel peptide haemolysin associated with a subset of lineage I Listeria monocytogenes. PLoS Pathog 2008; 4:e1000144; PMID:18787690; https://doi.org/10.1371/journal.ppat.1000144

[37] Clayton EM, Hill C, Cotter PD, Ross RP. Real-Time PCR Assay To Differentiate Listeriolysin S-Positive and -Negative Strains of Listeria monocytogenes. Appl Environ Microbiol 2010; 77:163-71; PMID:21075895; https://doi.org/10.1128/AEM.01673-10

[38] Linnan MJ, Mascola L, Lou XD, Goulet V, May S, Salminen C, Hird DW, Yonekura ML, Hayes P, Weaver R. Epidemic listeriosis associated with Mexican-style cheese. N Engl J Med 1988; 319:823-8; PMID:3137471; https://doi.org/10.1056/NEJM198809293191303

[39] Kommineni S, Bretl DJ, Lam V, Chakraborty R, Hayward M, Simpson P, Cao Y, Bousounis P, Kristich CJ, Salzman NH. Bacteriocin production augments niche competition by enterococci in the mammalian gastrointestinal tract. Nature 2015; 526:719-22; PMID:26479034; https://doi.org/10.1038/nature15524

[40] Wladyka B, Piejko M, Bzowska M, Pieta P, Krzysik M, Mazurek Ł, Guevara-Lora I, Bukowski M, Sabat AJ, Friedrich AW, et al. A peptide factor secreted by Staphylococcus pseudintermedius exhibits properties of both bacteriocins and virulence factors. Sci Rep 2015; 5:14569

[41] Wiedemann I, Benz R, Sahl HG. Lipid II-Mediated Pore Formation by the Peptide Antibiotic Nisin: a Black Lipid Membrane Study. J Bacteriol 2004; 186:3259-61; PMID:15126490; https://doi.org/10.1128/JB.186.10.3259-3261.2004

[42] Gonzalez DJ, Lee SW, Hensler ME, Markley AL, Dahesh S, Mitchell DA, Bandeira N, Nizet V, Dixon JE, Dorrestein PC. Clostridiolysin S, a Post-translationally Modified Biotoxin from Clostridium botulinum. J Biol Chem 2010; 285:28220-8; PMID:20581111; https://doi.org/10.1074/jbc.M110.118554

[43] Sommer F, Ståhlman M, Ilkayeva O, Arnemo JM, Kindberg J, Josefsson J, Newgard CB, Fröbert O, Bäckhed F. The Gut Microbiota Modulates Energy Metabolism in the Hibernating Brown Bear Ursus arctos. CellReports 2016; 14:1655-61

[44] Ostling CE, Lindgren SE. Inhibition of enterobacteria and Listeria growth by lactic, acetic and formic acids. J Appl Bacteriol 1993; 75:18-24; PMID:8365950; https://doi.org/10.1111/j.1365-2672.1993.tb03402.x

[45] Sun Y, Wilkinson BJ, Standiford TJ, Akinbi HT, O'Riordan MXD. Fatty Acids Regulate Stress Resistance and Virulence Factor Production for Listeria monocytogenes. J Bacteriol 2012; 194:5274-84; PMID:22843841; https://doi.org/10.1128/JB.00045-12

[46] Cox LM, Yamanishi S, Sohn J, Alekseyenko AV, Leung JM, Cho I, Kim SG, Li H, Gao Z, Mahana D, et al. Altering the Intestinal Microbiotaduring a Critical Developmental Window Has Lasting Metabolic Consequences. Cell 2014; 158:705-21; PMID:25126780; https://doi.org/10.1016/j.cell.2014.05.052

[47] Corr SC, Li Y, Riedel CU, O'Toole PW, Hill C, Gahan CGM. Bacteriocin production as a mechanism for the anti-infective activity of Lactobacillus salivarius UCC118. Proc Natl Acad Sci USA 2007; 104:7617-21; PMID:17456596; https://doi.org/10.1073/pnas.0700440104

[48] Rea MC, Sit CS, Clayton E, O'Connor PM, Whittal RM, Zheng J, Vederas JC, Ross RP, Hill C. Thuricin CD, a posttranslationally modified bacteriocin with a narrow spectrum of activity against Clostridium difficile. Proc Natl Acad Sci 2010; 107:9352-7; https://doi.org/10.1073/pnas.0913554107

[49] Lyons NA, Kraigher B, Stefanic P, Mandic-Mulec I, Kolter R. Bacillus subtilis. Curr Biol 2016; 26:733-42; PMID:26923784; https://doi.org/10.1016/j.cub.2016.01.032

[50] Clayton EM, Daly KM, Guinane CM, Hill C, Cotter PD, Ross PR. Atypical Listeria innocua strains possess an intact LIPI-3. BMC Microbiol 2014; 14:1-9; https://doi.org/10.1186/1471-2180-14-58

Annex 3: Supplementary information

Table S1. Strains used in this study

Strains	Description	Source	BUG or CIP no.
L. monocytogenes F2365	Strain associated with the California 1985 listeriosis outbreak	(323)	BUG 3012
L. monocytogenes F2365 Δ*llsA*	Deletion of the *llsA* gene	(349)	BUG 3781
L. monocytogenes F2365 pHELP: *llsA*	Strain that expresses the LLS operon constitutively under the control of the pHELP promoter	(349)	BUG 3817
L. monocytogenes F2365 pHELP: *llsA*-FLAG	Strain that expresses the LLS operon constitutively under the control of the pHELP promoter. The FLAG tag was added in the C terminal of the *llsA* gene.	This study	BUG 4177
L. monocytogenes F2365 pHELP: *llsA*-HA	Strain that expresses the LLS operon constitutively under the control of the pHELP promoter. The HA tag was added in the C terminal of the *llsA* gene.	This study	BUG 4179
L. monocytogenes F2365 pHELP: *llsA*-His	Strain that expresses the LLS operon constitutively under the control of the pHELP promoter. The His tag was added in the C terminal of the *llsA* gene.	This study	BUG 4181
L. monocytogenes F2365 pHELP: *llsA* Δ*hly*	Strain *L. monocytogenes* F2365 pHELP: *llsA*- where the *hly* gene was deleted	(319)	BUG 3819
L. monocytogenes F2365 Δ*llsA* Δ*hly*	Deletion of the *llsA* gene and the *hly* gene	(319)	BUG 3828
L. monocytogenes F2365 pHELP: *llsA*-Δ*llsX*	Strain *L. monocytogenes* F2365 pHELP: *llsA*- where the *llsX* gene was deleted	This study	BUG 4318
L. monocytogenes F2365 pHELP: *llsA*-FLAG Δ*llsX*	Strain *L. monocytogenes* F2365 pHELP: *llsA*-*FLAG* where the *llsX* gene was deleted	This study	BUG 4319
L. monocytogenes F2365 pAD::P_{llsA}-GFPmut2	*L. monocytogenes* F2365 with the promoter of the *llsA* gene fused to the cGFPmut2 and inserted into the chromosome using the plasmid pAD.	This study	BUG 4209
L. monocytogenes F2365 pKSV7::$P_{lmo2230}$-eGFP	*L. monocytogenes* F2365 with the promoter of the *lmo2230* gene fused to the eGFP and inserted into the chromosome using the plasmid pKSV7.	This study	BUG 4212
L. monocytogenes F2365 Δ*llsA* pAD-tdTomato	*L. monocytogenes* F2365 Δ*llsA* with tdTomato inserted into the chromosome using the plasmid pAD.	This study	BUG4339
L. monocytogenes F2365 pHELP: *llsA* pAD-tdTomato	*L. monocytogenes* F2365 pHELP: *llsA* with tdTomato inserted into the chromosome using the plasmid pAD.	This study	BUG 4340
L. monocytogenes 10403S	Lineage II strain commonly used in laboratories (it lacks the LLS operon)	(434)	BUG 1361
L. monocytogenes 10403S pAD-*llsP*	*L. monocytogenes* 10403S with the *llsP* gene inserted into the chromosome using the plasmid pAD.	This study	BUG4232
L. monocytogenes 10403S pAD-*llsP* pAT18-cGFP	*L. monocytogenes* 10403S pAD-*llsP* carrying pAT18–Phyper-GFPmut2 (constitutive)	This study	BUG 4248

Table S2. Plasmids used in this study

Plasmids	Description	Source	BUG no.
pMAD	Shuttle vector used for mutagenesis	(410)	BUG 1957
pMAD-llsX	Plasmid used to create the deletion Δ*llsX* mutant	This study	BUG 4308
pMAD-pHELP: llsA	Plasmid used to insert the pHELP promoter into the upstream region of the LLS operon	This study	BUG 3801
pMAD-pHELP: llsA-FLAG	Plasmid used to insert the FLAG tag into the C terminal of the *llsA* gene	This study	BUG 4142
pMAD-pHELP: llsA-HA	Plasmid used to insert the HA tag into the C terminal of the *llsA* gene	This study	BUG 4143
pMAD-pHELP: llsA-His	Plasmid used to insert the His tag into the C terminal of the *llsA* gene	This study	BUG 4144
pPL2	*L. monocytogenes* site-specific phage integration vector	(374)	BUG 2176
pAD-GFPmut2	pPL2-Phyper-GFP (constitutive)	(374)	BUG 2479
pAD-tdTomato	pPL2-Phyper-tdTomato (constitutive)	This study	BUG 4337
pKSV7::Plmo2230-eGFP	pKSV7 carrying the promoter of lmo2230 fused to eGFP	(375)	BUG 4046
pAT18-cGFP	pAT18–Phyper-GFPmut2 (constitutive)	(374)	BUG 2533

Table S3. Primers used in this study

Name	Sequence 5'-3'	Purpose
llsAtag F	gcatattatcaaacggagggata	Verification of the tag insertion
llsAtag R	ctttcaagttcatatttgtgta	Verification of the tag insertion
pmad up	aagcgagaagaatcataatgg	Sequencing of the pMAD inserts
Pmad down v2	cataattattccccctagctaattttcgt	Sequencing of the pMAD inserts
llsX mut Fw	atctggcttggtgaaag	Verification of the *llsX* gene mutation
llsXmut Rv	tcttgtactaaggcca	Verification of the *llsX* gene mutation
pPL2-Fw	ttcgacccggtcgtcggttc	Sequencing insert in pAD-based plasmid
pPL2-Rv	cttagacgtcattaaccctcac	Sequencing insert in pAD-based plasmid
NC16	gtcaaaacatacgctcttatc	Verification of the plasmid integration into the chromosome
PL95	acataatcagtccaaagtagatgc	Verification of the plasmid integration into the chromosome
lmo2229-F	gccttgtcgccatctttg	Verification of the plasmid integration into the chromosome
egfp-R	ggccgtttacatctccatc	Verification of the plasmid integration into the chromosome
gyrA-RT-PCR-F	gcgatgagtgtaattgttg	For quantitative Real-Time PCRs
gyrA-RT-PCR-R	atcagaagtcatacctaagtc	For quantitative Real-Time PCRs
llsA-RT-PCR-F	tcacaatcatcaaatggctaca	For quantitative Real-Time PCRs
llsA-RT-PCR-R	caagaacatgagcaacatcca	For quantitative Real-Time PCRs
llsG-RT-PCR-F	gagagagcgcagtttttacaca	For quantitative Real-Time PCRs
llsG-RT-PCR-R	tcgttgtttttctccaccag	For quantitative Real-Time PCRs
llsH-RT-PCR-F	cccggatattgatgccagta	For quantitative Real-Time PCRs
llsH-RT-PCR-R	ggaagttccgaaaaagatgaaa	For quantitative Real-Time PCRs
llsX-RT-PCR-F	ttcacatgaatgatggcaca	For quantitative Real-Time PCRs
llsX-RT-PCR-R	ttcccaccatctcactacca	For quantitative Real-Time PCRs
llsB-RT-PCR-F	ggcaattcaccaatgctagg	For quantitative Real-Time PCRs
llsB-RT-PCR-R	tccatttctcttgcctcgtt	For quantitative Real-Time PCRs
llsY-RT-PCR-F	acatggagaaactggctgct	For quantitative Real-Time PCRs
llsY-RT-PCR-R	caaacatcaattcagctgtgg	For quantitative Real-Time PCRs
llsD-RT-PCR-F	ggatgcctttgcaatttgtt	For quantitative Real-Time PCRs
llsD-RT-PCR-R	gcagtgcctgttgatacagc	For quantitative Real-Time PCRs
llsP-RT-PCR-F	acagtttgtggtagttttatcgc	For quantitative Real-Time PCRs
llsP-RT-PCR-R	tcacgaatgaaaaggtggct	For quantitative Real-Time PCRs

Annex 4: HTS compounds and libraries

Table S4. List of compounds used for the HTS

Name	Library
Clindamycin·HCl	Enzo FDA Library
Felbamate	Enzo FDA Library
Cyclosporine A	Enzo FDA Library
Lincomycin·HCl	Enzo FDA Library
Mycophenolic Acid	Enzo FDA Library
Sirolimus (Rapamycin)	Enzo FDA Library
Spectinomycin·HCl Pentahydrate	Enzo FDA Library
Tolbutamide	Enzo FDA Library
Glipizide	Enzo FDA Library
Propafenone·HCl	Enzo FDA Library
Phenytoin	Enzo FDA Library
Procainamide·HCl	Enzo FDA Library
Lidocaine·HCl·H2O	Enzo FDA Library
Amantadine·HCl	Enzo FDA Library
Guanabenz Acetate	Enzo FDA Library
Dihydroergotamine Mesylate	Enzo FDA Library
Caffeine	Enzo FDA Library
Salbutamol Hemisulfate	Enzo FDA Library
Pindolol	Enzo FDA Library
Ipratropium·Br	Enzo FDA Library
Pancuronium·2Br	Enzo FDA Library
Ivermectin	Enzo FDA Library
Propofol	Enzo FDA Library
Aminophylline	Enzo FDA Library
Nateglinide	Enzo FDA Library
(±) Isoproterenol·HCl	Enzo FDA Library
Acetylcholine Chloride	Enzo FDA Library
Atropine Sulfate Monohydrate	Enzo FDA Library
Apomorphine·HCl Hemihydrate	Enzo FDA Library
Chlorpromazine·HCl	Enzo FDA Library
Diphenhydramine·HCl	Enzo FDA Library
Promethazine·HCl	Enzo FDA Library
Imipramine·HCl	Enzo FDA Library
Metoclopramide·HCl	Enzo FDA Library
Carbachol (Carbamylcholine) Chloride	Enzo FDA Library
Isoniazid	Enzo FDA Library
Atovaquone	Enzo FDA Library
Cefepime·HCl Hydrate	Enzo FDA Library
Aripiprazole	Enzo FDA Library
Dorzolamide·HCl	Enzo FDA Library
Bleomycin Sulfate	Enzo FDA Library
Gefitinib	Enzo FDA Library
Idarubicin·HCl	**Enzo FDA Library**
Exemestane	Enzo FDA Library
Dinoprostone	Enzo FDA Library
Metformin·HCl	Enzo FDA Library
Erlotinib	Enzo FDA Library
Latanoprost	Enzo FDA Library
Acitretin	Enzo FDA Library
Cromolyn·Na (Disodium Cromoglycate)	Enzo FDA Library
Capsaicin	Enzo FDA Library
Dexamethasone	Enzo FDA Library
Indomethacin	Enzo FDA Library
Bumetanide	Enzo FDA Library
Neomycin Sulfate	*Enzo FDA Library*
Moxifloxacin·HCl	Enzo FDA Library
Terbinafine·HCl	Enzo FDA Library
Sodium Phenylbutyrate	Enzo FDA Library
Goserelin Acetate	Enzo FDA Library
Rifampin (Rifampicin)	Enzo FDA Library
Daunorubicin·HCl	Enzo FDA Library
Doxorubicin·HCl	Enzo FDA Library
Rivastigmine Tartrate	Enzo FDA Library
Ergotamine Tartrate	**Enzo FDA Library**
Valproate·Na	Enzo FDA Library
Glyburide	Enzo FDA Library
Tranexamic Acid	Enzo FDA Library
Clindamycin Palmitate·HCl	Enzo FDA Library
Vorinostat	Enzo FDA Library
Dolasetron	Enzo FDA Library
Fluvastatin·Na	Enzo FDA Library
Gemcitabine·HCl	Enzo FDA Library
Atazanavir	Enzo FDA Library
Ibandronate·Na Monohydrate	Enzo FDA Library
Imipenem	Enzo FDA Library
Meropenem	Enzo FDA Library
Pamidronate Disodium Pentahydrate (Pamidronic Acid)	Enzo FDA Library
Pramipexole Dihydrochloride Monohydrate	Enzo FDA Library
Triptorelin Acetate	Enzo FDA Library
Rocuronium Bromide	Enzo FDA Library
Vinorelbine	Enzo FDA Library

Salmeterol	Enzo FDA Library
Vincristine Sulfate	Enzo FDA Library
Aspirin (Acetylsalicylic Acid)	Enzo FDA Library
Allopurinol	Enzo FDA Library
Altretamine	Enzo FDA Library
Sumatriptan Succinate	Enzo FDA Library
Amifostine	Enzo FDA Library
4-Aminosalicylic Acid	Enzo FDA Library
Mesalamine (5-Aminosalicylic Acid)	Enzo FDA Library
Ampicillin Trihydrate	Enzo FDA Library
(±)-Atenolol	Enzo FDA Library
Vinblastine Sulfate	Enzo FDA Library
Azithromycin	Enzo FDA Library
Aztreonam	Enzo FDA Library
Betamethasone	Enzo FDA Library
Bisacodyl	Enzo FDA Library
Cefotaxime Acid	Enzo FDA Library
Ceftazidime	Enzo FDA Library
Chloramphenicol	Enzo FDA Library
Chlorpheniramine Maleate	Enzo FDA Library
Chloroquine Diphosphate	Enzo FDA Library
Thalidomide	Enzo FDA Library
Ciprofloxacin	Enzo FDA Library
Clarithromycin	Enzo FDA Library
Clomiphene Citrate	Enzo FDA Library
Clobetasol Propionate	Enzo FDA Library
Danazol	Enzo FDA Library
Zalcitabine (2',3'-Dideoxycytidine)	Enzo FDA Library
Estradiol	Enzo FDA Library
Estrone	Enzo FDA Library
Famciclovir	Enzo FDA Library
Finasteride	Enzo FDA Library
Amitriptyline·HCl	Enzo FDA Library
Fluocinolone Acetonide	Enzo FDA Library
Ganciclovir	Enzo FDA Library
Gatifloxacin	Enzo FDA Library
Gentamycin Sulfate	Enzo FDA Library
Gemfibrozil	Enzo FDA Library
Hydrocortisone	Enzo FDA Library
Hydrocortisone Acetate	Enzo FDA Library
Levonorgestrel	Enzo FDA Library
Medroxyprogesterone Acetate	Enzo FDA Library
Mefenamic Acid	Enzo FDA Library
Methyldopa Sesquihydrate (L-?-Methyl-Dopa Sesquihyrate)	Enzo FDA Library
Methylprednisolone	Enzo FDA Library
Minocycline	Enzo FDA Library
Mitoxantrone·HCl	Enzo FDA Library
Nabumetone	Enzo FDA Library
Norethindrone	Enzo FDA Library
Norfloxacin	Enzo FDA Library
Nystatin	Enzo FDA Library
Oxacillin sodium salt monohydrate	Enzo FDA Library
Pantoprazole	Enzo FDA Library
Penicillin V Potassium	Enzo FDA Library
Piperacillin	Enzo FDA Library
Prednisolone	Enzo FDA Library
Progesterone	Enzo FDA Library
Procarbazine·HCl	Enzo FDA Library
Prednisone	Enzo FDA Library
Rimantadine·HCl	Enzo FDA Library
Propranolol·HCl	Enzo FDA Library
Scopolamine·HBr	Enzo FDA Library
Spironolactone	Enzo FDA Library
Streptomycin Sulfate	Enzo FDA Library
Tetracycline	Enzo FDA Library
Tobramycin	Enzo FDA Library
Toremifene Base	Enzo FDA Library
Amoxicillin	Enzo FDA Library
Tramadol·HCl	Enzo FDA Library
Vecuronium Bromide	Enzo FDA Library
Bupivacaine·HCl	Enzo FDA Library
Ondansetron	Enzo FDA Library
Tiotropium Bromide	Enzo FDA Library
Amrinone	**Enzo FDA Library**
Alprostadil	Enzo FDA Library
Misoprostol	Enzo FDA Library
Mifepristone	Enzo FDA Library
Megestrol Acetate	Enzo FDA Library
Efavirenz	Enzo FDA Library
Fulvestrant	Enzo FDA Library
Esmolol	Enzo FDA Library
Succinylcholine Chloride·2H2O	Enzo FDA Library
Abacavir Sulfate	Enzo FDA Library
Acarbose	Enzo FDA Library
Acebutolol·HCl	Enzo FDA Library
Acetaminophen	Enzo FDA Library
Acetylcysteine	Enzo FDA Library
Adefovir Dipivoxil	Enzo FDA Library

Adenosine	Enzo FDA Library
Amcinonide	Enzo FDA Library
Amikacin Disulfate	Enzo FDA Library
Aminocaproic Acid	Enzo FDA Library
Aminohippurate·Na	Enzo FDA Library
Aminolevulinic Acid·HCl	Enzo FDA Library
Amphotericin B	Enzo FDA Library
L-Ascorbic Acid	Enzo FDA Library
Atomoxetine·HCl	Enzo FDA Library
Azacitidine	Enzo FDA Library
Azelaic Acid	Enzo FDA Library
Bacitracin	Enzo FDA Library
Baclofen	Enzo FDA Library
Beclomethasone Dipropionate	Enzo FDA Library
Bendroflumethiazide	Enzo FDA Library
Betaine	Enzo FDA Library
Bethanechol Chloride	Enzo FDA Library
Brompheniramine Maleate	Enzo FDA Library
Budesonide	Enzo FDA Library
Bupropion	Enzo FDA Library
Capreomycin disulfate	*Enzo FDA Library*
Carmustine	Enzo FDA Library
Cefaclor	Enzo FDA Library
Cefadroxil	Enzo FDA Library
Cefazolin·Na	Enzo FDA Library
Cefdinir	Enzo FDA Library
Cefditoren Pivoxil	Enzo FDA Library
Cefixime	Enzo FDA Library
Cefotetan Disodium	Enzo FDA Library
Cefoxitin·Na	Enzo FDA Library
Cefpodoxime Proxetil	Enzo FDA Library
Cefprozil	Enzo FDA Library
Ceftibuten	Enzo FDA Library
Ceftizoxim·Na	Enzo FDA Library
Ceftriaxone·Na	Enzo FDA Library
Cefuroxime Axetil	Enzo FDA Library
Cefuroxime·Na	Enzo FDA Library
Cephalexin Monohydrate	Enzo FDA Library
Chenodiol (Chenodeoxycholic Acid)	Enzo FDA Library
Chlorhexidine Dihydrochloride	Enzo FDA Library
Chlorothiazide	Enzo FDA Library
Ciclesonide	Enzo FDA Library
Cisatracurium Besylate	Enzo FDA Library
Cladribine	Enzo FDA Library

Clavulanate Potassium	Enzo FDA Library
Clotrimazole	Enzo FDA Library
Cloxacillin·Na	Enzo FDA Library
Colistimethate·Na	Enzo FDA Library
Colistin Sulfate	Enzo FDA Library
Cortisone Acetate	Enzo FDA Library
Cyclobenzaprine·HCl	Enzo FDA Library
Cysteamine·HCl	Enzo FDA Library
Dactinomycin (= Actinomycin D)	Enzo FDA Library
Dalfampridine (4-Aminopyridine)	Enzo FDA Library
Daptomycin	Enzo FDA Library
Deferoxamine Mesylate	Enzo FDA Library
Demeclocycline·HCl	Enzo FDA Library
Desogestrel	Enzo FDA Library
Desonide	Enzo FDA Library
Desoximetasone	Enzo FDA Library
Desvenlafaxine Succinate Hydrate	Enzo FDA Library
Dexchlorpheniramine Maleate	Enzo FDA Library
Diatrizoate Meglumine	Enzo FDA Library
Dicloxacillin·Na Salt Monohydrate	Enzo FDA Library
Dienogest	Enzo FDA Library
Difluprednate	Enzo FDA Library
Digoxin	Enzo FDA Library
Dimenhydrinate	Enzo FDA Library
Disopyramide	Enzo FDA Library
Dopamine·HCl	Enzo FDA Library
Doripenem	Enzo FDA Library
Drospirenone	Enzo FDA Library
Duloxetine·HCl	Enzo FDA Library
Dutasteride	Enzo FDA Library
Eflornithine·HCl	Enzo FDA Library
Epirubicin·HCl	Enzo FDA Library
Eplerenone	Enzo FDA Library
Eptifibatide	Enzo FDA Library
Erythromycin	Enzo FDA Library
Estramustine Phosphate·Na	Enzo FDA Library
Estropipate	Enzo FDA Library
Ethambutol Dihydrochloride	Enzo FDA Library
Ethinyl Estradiol	Enzo FDA Library
Ethionamide	Enzo FDA Library
Etodolac	Enzo FDA Library
Etonogestrel	Enzo FDA Library
Everolimus	Enzo FDA Library
Fingolimod	Enzo FDA Library

Flucytosine	Enzo FDA Library
Fludrocortisone Acetate	Enzo FDA Library
Flunisolide	Enzo FDA Library
Fluocinonide	Enzo FDA Library
Fluorometholone	Enzo FDA Library
Flurandrenolide	Enzo FDA Library
Fluticasone Propionate	Enzo FDA Library
Formoterol	Enzo FDA Library
Foscarnet·Na (Sodium Phosphonoformate Tribasic Hexahydrate)	Enzo FDA Library
Fosfomycin Calcium	*Enzo FDA Library*
Gemifloxacin	Enzo FDA Library
Glycopyrrolate Iodide	Enzo FDA Library
Griseofulvin	Enzo FDA Library
Guanidine·HCl	Enzo FDA Library
Halcinonide	Enzo FDA Library
Halobetasol Propionate	Enzo FDA Library
Hydrochlorothiazide	Enzo FDA Library
Hydroflumethiazide	Enzo FDA Library
Hydroxocobalamin·HCl	Enzo FDA Library
Hydroxychloroquine Sulfate	Enzo FDA Library
Hydroxyurea	Enzo FDA Library
Hydroxyzine Dihydrochloride	Enzo FDA Library
Ibutilide Fumarate	Enzo FDA Library
Isotretinoin (13-Cis-Retinoic Acid)	Enzo FDA Library
Kanamycin Sulfate	*Enzo FDA Library*
Ketorolac Tromethamine	Enzo FDA Library
Levobunolol·HCl	Enzo FDA Library
Levocarnitine	Enzo FDA Library
Loteprednol Etabonate	Enzo FDA Library
Mafenide·HCl	Enzo FDA Library
Mechlorethamine·HCl	Enzo FDA Library
Mepenzolate Bromide	Enzo FDA Library
6-Methoxy-1,2,3,4-tetrahydro-9H-pyrido[3,4b] indole	Sigma LOPAC
Acetamide	Sigma LOPAC
Amantadine hydrochloride	Sigma LOPAC
GABA	Sigma LOPAC
Gabaculine hydrochloride	Sigma LOPAC
Ezatiostat	Sigma LOPAC
N-Acetylprocainamide hydrochloride	Sigma LOPAC
N-Phenylanthranilic acid	Sigma LOPAC
GSK-650394	Sigma LOPAC
3'-Azido-3'-deoxythymidine	Sigma LOPAC
(±)-2-Amino-5-phosphonopentanoic acid	Sigma LOPAC

Sodium Taurocholate	Sigma LOPAC
L-azetidine-2-carboxylic acid	Sigma LOPAC
Acetyl-beta-methylcholine chloride	Sigma LOPAC
Amifostine	Sigma LOPAC
Atropine methyl bromide	Sigma LOPAC
5-Aminovaleric acid hydrochloride	Sigma LOPAC
4-Aminopyridine	Sigma LOPAC
Aminopterin	Sigma LOPAC
9-Amino-1,2,3,4-tetrahydroacridine hydrochloride	Sigma LOPAC
Acyclovir	Sigma LOPAC
(±)-Nipecotic acid	Sigma LOPAC
Atropine sulfate	Sigma LOPAC
N-Acetyl-5-hydroxytryptamine	Sigma LOPAC
Azelaic acid	Sigma LOPAC
Atropine methyl nitrate	Sigma LOPAC
Aurintricarboxylic acid	Sigma LOPAC
Acetylthiocholine chloride	Sigma LOPAC
Agmatine sulfate	Sigma LOPAC
Tryptamine hydrochloride	Sigma LOPAC
(±)-2-Amino-4-phosphonobutyric acid	Sigma LOPAC
Apigenin	Sigma LOPAC
UNC0379	Sigma LOPAC
(±)-2-Amino-3-phosphonopropionic acid	Sigma LOPAC
1-Aminocyclopropanecarboxylic acid hydrochloride	Sigma LOPAC
Reserpine	**Sigma LOPAC**
L-Arginine	Sigma LOPAC
2-(2-Aminoethyl)isothiourea dihydrobromide	Sigma LOPAC
3-Aminopropylphosphonic acid	Sigma LOPAC
N-Acetyl-L-Cysteine	Sigma LOPAC
6-Aminohexanoic acid	Sigma LOPAC
L-2-aminoadipic acid	Sigma LOPAC
VU0420373	Sigma LOPAC
SKF-89145	Sigma LOPAC
Allopurinol	Sigma LOPAC
cis-4-Aminocrotonic acid	Sigma LOPAC
Fulvestrant	Sigma LOPAC
1-Amino-1-cyclohexanecarboxylic acid hydrochloride	Sigma LOPAC
N6-2-(4-Aminophenyl)ethyladenosine	Sigma LOPAC
p-Benzoquinone	Sigma LOPAC
(±)-Atenolol	Sigma LOPAC
Adenosine	Sigma LOPAC
L-Aspartic acid	Sigma LOPAC

8-(p-Sulfophenyl)theophylline	Sigma LOPAC
Clemizole	Sigma LOPAC
gamma-Acetylinic GABA	Sigma LOPAC
ATPA	Sigma LOPAC
L-allylglycine	Sigma LOPAC
Amlexanox	Sigma LOPAC
Lercanidipine	Sigma LOPAC
AB-MECA	Sigma LOPAC
ABT-418	Sigma LOPAC
Alprenolol hydrochloride	Sigma LOPAC
S(-)-Atenolol	Sigma LOPAC
AS-252424	Sigma LOPAC
Alloxazine	Sigma LOPAC
Beclomethasone	Sigma LOPAC
Benzamide	Sigma LOPAC
(±)-Baclofen	Sigma LOPAC
Brefeldin A from Penicillium brefeldianum	Sigma LOPAC
CGP-7930	Sigma LOPAC
Betaine hydrochloride	Sigma LOPAC
Budesonide	Sigma LOPAC
CGP-13501	Sigma LOPAC
Choline bromide	Sigma LOPAC
Betaine aldehyde chloride	Sigma LOPAC
8-Bromo-cAMP sodium	Sigma LOPAC
(±)-Butaclamol hydrochloride	Sigma LOPAC
BTO-1	Sigma LOPAC
N-Bromoacetamide	Sigma LOPAC
Benztropine mesylate	Sigma LOPAC
Bromoacetylcholine bromide	Sigma LOPAC
Benzamidine hydrochloride	Sigma LOPAC
Ro 20-1724	Sigma LOPAC
Caffeic Acid	Sigma LOPAC
Benzamil hydrochloride	Sigma LOPAC
Betamethasone	Sigma LOPAC
Bestatin hydrochloride	Sigma LOPAC
Corticosterone	Sigma LOPAC
L-Buthionine-sulfoximine	Sigma LOPAC
Alfuzosin	Sigma LOPAC
Caffeine	Sigma LOPAC
DAPH	Sigma LOPAC
1-(4-Chlorobenzyl)-5-methoxy-2-methylindole-3-acetic acid	Sigma LOPAC
Cortisone	Sigma LOPAC
Cyclosporin A	Sigma LOPAC
Carbachol	Sigma LOPAC

Cephalexin hydrate	Sigma LOPAC
Cantharidin	Sigma LOPAC
D-Cycloserine	Sigma LOPAC
Cefsulodin sodium salt hydrate	Sigma LOPAC
L-Cysteinesulfinic Acid	Sigma LOPAC
Ceftriaxone sodium	Sigma LOPAC
Cefmetazole sodium	Sigma LOPAC
Caffeic acid phenethyl ester	Sigma LOPAC
Lumefantrine	Sigma LOPAC
Cortisone 21-acetate	Sigma LOPAC
Cefazolin sodium	Sigma LOPAC
Cefotaxime sodium	Sigma LOPAC
Imipenem	Sigma LOPAC
Pyrocatechol	Sigma LOPAC
Cephalosporin C zinc salt	Sigma LOPAC
GR 113808	Sigma LOPAC
Cephalothin sodium	Sigma LOPAC
(-)-Cotinine	Sigma LOPAC
Cephradine	Sigma LOPAC
Chloroquine diphosphate	Sigma LOPAC
Cystamine dihydrochloride	Sigma LOPAC
Cyproterone acetate	Sigma LOPAC
Bethanechol chloride	Sigma LOPAC
Clofibrate	Sigma LOPAC
N6-Cyclopentyladenosine	Sigma LOPAC
CNS-1102	Sigma LOPAC
Cantharidic Acid	Sigma LOPAC
N6-Cyclohexyladenosine	Sigma LOPAC
Rosuvastatin calcium	Sigma LOPAC
Dequalinium dichloride	Sigma LOPAC
(S)-(+)-Camptothecin	Sigma LOPAC
Tocainide	Sigma LOPAC
Carvedilol	Sigma LOPAC
Dihydroouabain	Sigma LOPAC
Dihydroergotamine methanesulfonate	Sigma LOPAC
(-)-alpha-Methylnorepinephrine	Sigma LOPAC
Cetirizine	Sigma LOPAC
1,4-Dideoxy-1,4-imino-D-arabinitol	Sigma LOPAC
(±)-CGP-12177A hydrochloride	Sigma LOPAC
8-Cyclopentyl-1,3-dipropylxanthine	Sigma LOPAC
Decamethonium dibromide	Sigma LOPAC
2,3-Butanedione	Sigma LOPAC
Lomeguatrib	Sigma LOPAC
1,7-Dimethylxanthine	Sigma LOPAC

Nepicastat	Sigma LOPAC
8-Cyclopentyl-1,3-dimethylxanthine	Sigma LOPAC
CX 546	Sigma LOPAC
2,3-Dimethoxy-1,4-naphthoquinone	Sigma LOPAC
1,1-Dimethyl-4-phenyl-piperazinium iodide	Sigma LOPAC
Disopyramide	Sigma LOPAC
Doxycycline hydrochloride	Sigma LOPAC
CYM50358	Sigma LOPAC
Anisotropine methyl	Sigma LOPAC
Disopyramide phosphate	Sigma LOPAC
ET-18-OCH3	Sigma LOPAC
Diethylenetriaminepentaacetic acid	Sigma LOPAC
Dicyclomine hydrochloride	Sigma LOPAC
Cytidine 5'-diphosphocholine sodium salt hydrate	Sigma LOPAC
Propofol	Sigma LOPAC
Palonosetron	Sigma LOPAC
1-Deoxynojirimycin hydrochloride	Sigma LOPAC
Nefiracetam	Sigma LOPAC
N,N-Dihexyl-2-(4-fluorophenyl)indole-3-acetamide	Sigma LOPAC
1,10-Diaminodecane	Sigma LOPAC
Vanillic acid diethylamide	Sigma LOPAC
Emetine dihydrochloride hydrate	Sigma LOPAC
Doxofylline	Sigma LOPAC
Donitriptan	Sigma LOPAC
Dipropyldopamine hydrobromide	Sigma LOPAC
(+/-)-Anisodamine	Sigma LOPAC
(±)-2,3-Dichloro-alpha-methylbenzylamine hydrochloride	Sigma LOPAC
Etodolac	Sigma LOPAC
Forskolin	Sigma LOPAC
L-Canavanine	Sigma LOPAC
S-Ethylisothiourea hydrobromide	Sigma LOPAC
N-Ethylmaleimide	Sigma LOPAC
Formoterol	Sigma LOPAC
Glibenclamide	Sigma LOPAC
(-)-Epinephrine bitartrate	Sigma LOPAC
beta-Estradiol	Sigma LOPAC
Edrophonium chloride	Sigma LOPAC
Ethylene glycol-bis(2-aminoethylether)-N,N,N',N'-tetraacetic acid	Sigma LOPAC
Estrone	Sigma LOPAC
Genistein	Sigma LOPAC
Phenserine	Sigma LOPAC

Felbamate	Sigma LOPAC
Fiduxosin hydrochloride	Sigma LOPAC
Flunarizine dihydrochloride	Sigma LOPAC
L-Glutamic acid hydrochloride	Sigma LOPAC
Ethosuximide	Sigma LOPAC
N-Methyl-beta-carboline-3-carboxamide	Sigma LOPAC
Fusidic acid sodium	Sigma LOPAC
5-fluoro-5'-deoxyuridine	Sigma LOPAC
Ganciclovir	Sigma LOPAC
Nitidine chloride	Sigma LOPAC
DPO-1	*Sigma LOPAC*
L-Glutamine	Sigma LOPAC
Gallamine triethiodide	Sigma LOPAC
GW9508	Sigma LOPAC
Emodin	**Sigma LOPAC**
Isoguvacine hydrochloride	Sigma LOPAC
DL-threo-beta-hydroxyaspartic acid	Sigma LOPAC
17alpha-hydroxyprogesterone	Sigma LOPAC
4-Hydroxybenzhydrazide	Sigma LOPAC
Claramine	Sigma LOPAC
Iodoacetamide	Sigma LOPAC
Guvacine hydrochloride	Sigma LOPAC
Hypotaurine	Sigma LOPAC
(±)-8-Hydroxy-DPAT hydrobromide	Sigma LOPAC
Hydroquinone	Sigma LOPAC
Sematilide	Sigma LOPAC
Loxiglumide	Sigma LOPAC
Gabapentin	Sigma LOPAC
L-Dopa ethyl ester	Sigma LOPAC
Dopamine hydrochloride	Sigma LOPAC
Sumanirole maleate	Sigma LOPAC
Ipratropium bromide	Sigma LOPAC
DL-Homatropine hydrobromide	Sigma LOPAC
Hydrocortisone	Sigma LOPAC
Hydroxyurea	Sigma LOPAC
Idarubicin	**Sigma LOPAC**
Harmane	Sigma LOPAC
Serotonin hydrochloride	Sigma LOPAC
JFD00244	Sigma LOPAC
6-Hydroxymelatonin	Sigma LOPAC
Hexamethonium dichloride	Sigma LOPAC
JS-K	Sigma LOPAC
(±)-7-Hydroxy-DPAT hydrobromide	Sigma LOPAC
L-165,041	Sigma LOPAC

Hexamethonium bromide	Sigma LOPAC
Bendamustine	Sigma LOPAC
Retinoic acid p-hydroxyanilide	Sigma LOPAC
SR 142948A	*Sigma LOPAC*
5-Hydroxy-L-tryptophan	Sigma LOPAC
5-hydroxydecanoic acid sodium	Sigma LOPAC
4-Hydroxy-3-methoxyphenylacetic acid	Sigma LOPAC
6-Hydroxy-DL-DOPA	Sigma LOPAC
Hispidin	Sigma LOPAC
5-Hydroxyindolacetic acid	Sigma LOPAC
Hydroxylamine hydrochloride	Sigma LOPAC
R-(+)-8-Hydroxy-DPAT hydrobromide	Sigma LOPAC
R(-)-Isoproterenol (+)-bitartrate	Sigma LOPAC
Iproniazid phosphate	Sigma LOPAC
Agomelatine	Sigma LOPAC
AEG 3482	Sigma LOPAC
Fosmidomycin sodium salt hydrate	Sigma LOPAC
1,5-Isoquinolinediol	Sigma LOPAC
Kainic acid	Sigma LOPAC
Gemifloxacin mesylate	Sigma LOPAC
Capecitabine	Sigma LOPAC
NNC 55-0396	Sigma LOPAC
Ifenprodil tartrate	Sigma LOPAC
Rizatriptan benzoate salt	Sigma LOPAC
BIX	Sigma LOPAC
Alcaftadine	Sigma LOPAC
Molindone hydrochloride	Sigma LOPAC
Perlapine	Sigma LOPAC
Lidocaine hydrochloride	Sigma LOPAC
Isotharine mesylate	Sigma LOPAC
(-)-Isoproterenol hydrochloride	Sigma LOPAC
Ketorolac tris salt	Sigma LOPAC
Lidocaine N-ethyl bromide quaternary salt	Sigma LOPAC
Isoliquiritigenin	Sigma LOPAC
Aurothioglucose	Sigma LOPAC
4-Amidinophenylmethasulfonyl fluoride	Sigma LOPAC
Indomethacin	Sigma LOPAC
Ivermectin	Sigma LOPAC
Iofetamine hydrochloride	Sigma LOPAC
Luliconazole	Sigma LOPAC
LE 300	Sigma LOPAC
JNJ-63533054	Sigma LOPAC
Mifamurtide	Sigma LOPAC
Alclometasone dipropionate	Sigma LOPAC

Isonipecotic acid	Sigma LOPAC
CyPPA	Sigma LOPAC
Isoxanthopterin	Sigma LOPAC
Stevioside	Sigma LOPAC
Thiocolchicine	Sigma LOPAC
Kynurenic acid	Sigma LOPAC
TMPH hydrochloride	Sigma LOPAC
Varespladib	Sigma LOPAC
PF-429242 dihydrochloride	Sigma LOPAC
Metergoline	Sigma LOPAC
(±)-Metoprolol (+)-tartrate	Sigma LOPAC
Linopirdine	Sigma LOPAC
Zoledronic acid monohydrate	Sigma LOPAC
YM-26734	Sigma LOPAC
2-methoxyestradiol	Sigma LOPAC
Lometrexol hydrate	Sigma LOPAC
L-741,626	Sigma LOPAC
N-omega-Methyl-5-hydroxytryptamine oxalate salt	Sigma LOPAC
ML324	Sigma LOPAC
Cysteamine hydrochloride	Sigma LOPAC
NG-Monomethyl-L-arginine acetate	Sigma LOPAC
TFCA	Sigma LOPAC
L-703,606 oxalate	Sigma LOPAC
Buclizine dihydrochloride	Sigma LOPAC
L-DOPS	Sigma LOPAC
BW 723C86	Sigma LOPAC
Metoclopramide hydrochloride	Sigma LOPAC
Psoralidin	Sigma LOPAC
8-Methoxymethyl-3-isobutyl-1-methylxanthine	Sigma LOPAC
MG 624	Sigma LOPAC
(S)-MAP4 hydrochloride	Sigma LOPAC
Methoxamine hydrochloride	Sigma LOPAC
R(-)-Me5	Sigma LOPAC
(2'Z,3'E)-6-Bromoindirubin-3'-oxime	Sigma LOPAC
3-MFA	Sigma LOPAC
N-Methyl-D-aspartic acid	Sigma LOPAC
Mitoxantrone	Sigma LOPAC
Nitisinone	Sigma LOPAC
Dihydrocapsaicin	Sigma LOPAC
Mexiletene hydrochloride	Sigma LOPAC
Melatonin	Sigma LOPAC
Oseltamivir phosphate	Sigma LOPAC
Famciclovir	Sigma LOPAC
Methylergonovine maleate	Sigma LOPAC

Rufinamide	Sigma LOPAC
Eupatorin	Sigma LOPAC
Mifepristone	Sigma LOPAC
(-)-MK-801 hydrogen maleate	Sigma LOPAC
Piperlongumine	Sigma LOPAC
ONO-RS-082	Sigma LOPAC
PD-407824	Sigma LOPAC
L-alpha-Methyl-p-tyrosine	Sigma LOPAC
Perifosine	Sigma LOPAC
Neostigmine bromide	Sigma LOPAC
S-Nitrosoglutathione	Sigma LOPAC
NG-Nitro-L-arginine	Sigma LOPAC
BMS-189453	Sigma LOPAC
Moclobemide	Sigma LOPAC
Naloxone hydrochloride	Sigma LOPAC
Proglumide	Sigma LOPAC
Levetiracetam	Sigma LOPAC
S-(4-Nitrobenzyl)-6-thioinosine	Sigma LOPAC
Nalidixic acid sodium	Sigma LOPAC
3-Nitropropionic acid	Sigma LOPAC
7-Nitroindazole	Sigma LOPAC
Mecamylamine hydrochloride	Sigma LOPAC
NG-Nitro-L-arginine methyl ester hydrochloride	Sigma LOPAC
PMEG hydrate	Sigma LOPAC
L-alpha-Methyl DOPA	Sigma LOPAC
(±)-Normetanephrine hydrochloride	Sigma LOPAC
Memantine hydrochloride	Sigma LOPAC
Methysergide maleate	Sigma LOPAC
CCCI-01	Sigma LOPAC
Nialamide	Sigma LOPAC
Sertraline hydrochloride	Sigma LOPAC
(+)-MK-801 hydrogen maleate	Sigma LOPAC
Ethopropazine	Sigma LOPAC
Nordihydroguaiaretic acid from Larrea divaricata (creosote bush)	Sigma LOPAC
NADPH tetrasodium	Sigma LOPAC
SDZ 220-581 hydrochloride	Sigma LOPAC
Lamotrigine isethionate	Sigma LOPAC
Pancuronium bromide	Sigma LOPAC
Valproic acid sodium	Sigma LOPAC
Oleic Acid	Sigma LOPAC
Progesterone	Sigma LOPAC
(±)-Propranolol hydrochloride	Sigma LOPAC
3-alpha,21-Dihydroxy-5-alpha-pregnan-20-one	Sigma LOPAC

Ofloxacin	Sigma LOPAC
Topotecan hydrochloride hydrate	Sigma LOPAC
Mitiglinide calcium	Sigma LOPAC
Atglistatin	Sigma LOPAC
Sodium Oxamate	Sigma LOPAC
NSC405020	Sigma LOPAC
LP44	Sigma LOPAC
CPCCOEt	Sigma LOPAC
Pemetrexed disodium heptahydrate	Sigma LOPAC
Cycloastragenol	Sigma LOPAC
PNU-282987	Sigma LOPAC
Pentylenetetrazole	Sigma LOPAC
N-Oleoylethanolamine	Sigma LOPAC
Suprafenacine	Sigma LOPAC
Palmitoyl-DL-Carnitine chloride	Sigma LOPAC
Bisoprolol	Sigma LOPAC
Oxolinic acid	Sigma LOPAC
Oxotremorine methiodide	Sigma LOPAC
Pindolol	Sigma LOPAC
Phosphomycin disodium	Sigma LOPAC
(±)-cis-Piperidine-2,3-dicarboxylic acid	Sigma LOPAC
Procaine hydrochloride	Sigma LOPAC
Pregnenolone sulfate sodium	Sigma LOPAC
1-Methylnicotinamide chloride	Sigma LOPAC
Quinacrine dihydrochloride	**Sigma LOPAC**
Phenelzine sulfate	Sigma LOPAC
Putrescine dihydrochloride	Sigma LOPAC
Protoporphyrin IX disodium	Sigma LOPAC
Paromomycin sulfate	Sigma LOPAC
BF-170 hydrochloride	Sigma LOPAC
Pyridostatin trifluoroacetate salt	Sigma LOPAC
Tegaserod maleate	Sigma LOPAC
Pergolide methanesulfonate	Sigma LOPAC
1,10-Phenanthroline monohydrate	Sigma LOPAC
H2L5186303	Sigma LOPAC
Quinolinic acid	Sigma LOPAC
(-)-Quinpirole hydrochloride	Sigma LOPAC
Phosphonoacetic acid	Sigma LOPAC
6(5H)-Phenanthridinone	Sigma LOPAC
Procainamide hydrochloride	Sigma LOPAC
GANT61	Sigma LOPAC
LP 12 hydrochloride hydrate	Sigma LOPAC
(-)-Perillic acid	Sigma LOPAC

5alpha-Pregnan-3alpha-ol-20-one	Sigma LOPAC
Prilocaine hydrochloride	Sigma LOPAC
Pyrazinecarboxamide	Sigma LOPAC
Triflusal	Sigma LOPAC
Cycloastragenol	Sigma LOPAC
Bay 11-7082	Sigma LOPAC
(S)-Propranolol hydrochloride	Sigma LOPAC
Adaphostin	Sigma LOPAC
Phorbol 12-myristate 13-acetate	Sigma LOPAC
Pyridostigmine bromide	Sigma LOPAC
Pinacidil	Sigma LOPAC
Pramipexole dihydrochloride	Sigma LOPAC
Cortexolone	Sigma LOPAC
Auranofin	Sigma LOPAC
Spermidine trihydrochloride	Sigma LOPAC
Stattic	Sigma LOPAC
CRANAD 2	**Sigma LOPAC**
Retinoic acid	Sigma LOPAC
K145 hydrochloride	Sigma LOPAC
Spironolactone	Sigma LOPAC
Steviol	Sigma LOPAC
7,8-Dihydroxyflavone hydrate	Sigma LOPAC
(-)-Scopolamine hydrobromide	Sigma LOPAC
Spermine tetrahydrochloride	Sigma LOPAC
Carmofur	Sigma LOPAC
Succinylcholine chloride	Sigma LOPAC
13-cis-retinoic acid	Sigma LOPAC
(±)-Synephrine	Sigma LOPAC
D-Serine	Sigma LOPAC
IMS2186	Sigma LOPAC
Rutaecarpine	Sigma LOPAC
SB743921 hydrochloride	Sigma LOPAC
Daurisoline	Sigma LOPAC
Ropinirole hydrochloride	Sigma LOPAC
Ibandronate sodium	Sigma LOPAC
(-)-Scopolamine methyl nitrate	Sigma LOPAC
Tirofiban hydrochloride monohydrate	Sigma LOPAC
(-)-Scopolamine,n-Butyl-, bromide	Sigma LOPAC
Resveratrol	Sigma LOPAC
Rotenone	Sigma LOPAC
Auraptene	Sigma LOPAC
Tazarotene	Sigma LOPAC
(-)-Scopolamine methyl bromide	Sigma LOPAC
SU 4312	Sigma LOPAC

Terbutaline hemisulfate	Sigma LOPAC
Estetrol	Sigma LOPAC
Taurine	Sigma LOPAC
4-Hydroxyphenethylamine hydrochloride	Sigma LOPAC
Dolasetron mesylate hydrate	Sigma LOPAC
(E)-4-amino-2-butenoic acid	Sigma LOPAC
KB-R7493	Sigma LOPAC
Tulobuterol hydrochloride	Sigma LOPAC
Tyrphostin 1	Sigma LOPAC
Tetradecylthioacetic acid	Sigma LOPAC
Nedocromil	Sigma LOPAC
Tyrphostin 23	Sigma LOPAC
Abiraterone acetate	Sigma LOPAC
Pseudocantharidin C	Sigma LOPAC
L-Beta-threo-benzyl-aspartate	Sigma LOPAC
Granisetron hydrochloride	Sigma LOPAC
cDPCP	Sigma LOPAC
Triamcinolone	Sigma LOPAC
Danshensu sodium salt	Sigma LOPAC
L-Tryptophan	Sigma LOPAC
Tetraethylammonium chloride	Sigma LOPAC
Entecavir	Sigma LOPAC
(±)-Taxifolin	Sigma LOPAC
Pivmecillinam	Sigma LOPAC
Ara-G hydrate	Sigma LOPAC
4-DAMP	Sigma LOPAC
CCT007093	Sigma LOPAC
SID 3712249	Sigma LOPAC
A-68930 hydrochloride	Sigma LOPAC
Erdosteine	Sigma LOPAC
L-Mimosine from Koa hoale seeds	Sigma LOPAC
TDFA trifluoroacetate salt	Sigma LOPAC
Galloflavin potassium	Sigma LOPAC
Wortmannin from Penicillium funiculosum	Sigma LOPAC
Bropirimine	Sigma LOPAC
3-Tropanyl-indole-3-carboxylate hydrochloride	Sigma LOPAC
Wiskostatin	Sigma LOPAC
Vinpocetine	Sigma LOPAC
SCH 58261	Sigma LOPAC
Caroverine hydrochloride	Sigma LOPAC
Furamidine dihydrochloride	Sigma LOPAC
XCT790	Sigma LOPAC
Vancomycin hydrochloride from Streptomyces orientalis	Sigma LOPAC
Acepromazine maleate	Sigma LOPAC

IPA-3	Sigma LOPAC
Lorcainide	Sigma LOPAC
Tipiracil hydrochloride	Sigma LOPAC
Roslin 2	Sigma LOPAC
Mequinol	Enzo FDA Library
Mercaptopurine Hydrate	Enzo FDA Library
Mestranol	Enzo FDA Library
Metaproterenol Hemisulfate (Orciprenaline)	Enzo FDA Library
Metaraminol Bitartrate	Enzo FDA Library
Methacholine Chloride	Enzo FDA Library
Methazolamide	Enzo FDA Library
Methenamine Hippurate	Enzo FDA Library
Methotrexate	Enzo FDA Library
Methscopolamine Bromide ((?)-Scopolamine Methyl Bromide)	Enzo FDA Library
Methyclothiazide	Enzo FDA Library
Methyl Aminolevulinate·HCl	Enzo FDA Library
Mexiletine·HCl	Enzo FDA Library
Mometasone Furoate	Enzo FDA Library
Mupirocin	Enzo FDA Library
Naftifine·HCl	Enzo FDA Library
Naratriptan·HCl	Enzo FDA Library
Natamycin	Enzo FDA Library
Niacin (Known As Vitamin B3, Nicotinic Acid And Vitamin Pp)	Enzo FDA Library
Nicotine	Enzo FDA Library
Orlistat (Tetrahydrolipstatin)	Enzo FDA Library
Oxtriphylline	Enzo FDA Library
Oxybutynin Chloride	Enzo FDA Library
Oxytetracycline·HCl	Enzo FDA Library
Palonosetron·HCl	Enzo FDA Library
Paromomycin Sulfate	Enzo FDA Library
Penicillamine (D-Penicillamine)	Enzo FDA Library
Penicillin G Potassium (Benzylpenicillin)	Enzo FDA Library
Perindopril Erbumine	Enzo FDA Library
Phenelzine Sulfate	Enzo FDA Library
Phenylephrine	Enzo FDA Library
Phytonadione	Enzo FDA Library
Pralidoxime Chloride	Enzo FDA Library
Pravastatin·Na	Enzo FDA Library
Prilocaine·HCl	Enzo FDA Library
Probenecid	Enzo FDA Library
Proparacaine·HCl	Enzo FDA Library
Propylthiouracil	Enzo FDA Library
Protriptyline·HCl	Enzo FDA Library
Pyrazinamide	Enzo FDA Library
Pyridostigmine Bromide	Enzo FDA Library
Pyrimethamine	Enzo FDA Library
Rifabutin	Enzo FDA Library
Rifapentine	Enzo FDA Library
Rifaximin	Enzo FDA Library
Ritonavir	Enzo FDA Library
Rizatriptan Benzoate	Enzo FDA Library
Selegiline·HCl	Enzo FDA Library
Silver Sulfadiazine	Enzo FDA Library
Sulfacetamide·Na	Enzo FDA Library
Sunitinib Malate	**Enzo FDA Library**
Tacrolimus (Fk506)	Enzo FDA Library
Temsirolimus	Enzo FDA Library
Testosterone Enanthate	Enzo FDA Library
Theophylline	Enzo FDA Library
Thioguanine (6-Thioguanine)	Enzo FDA Library
Thiotepa	Enzo FDA Library
Tigecycline	Enzo FDA Library
Tiludronate Disodium	Enzo FDA Library
Tiopronin	Enzo FDA Library
Tretinoin	Enzo FDA Library
Triamcinolone Acetonide	Enzo FDA Library
Trientine Dihydrochloride	Enzo FDA Library
Trospium Chloride	Enzo FDA Library
Ursodiol	Enzo FDA Library
Vancomycin·HCl	Enzo FDA Library
Eptifibatide acetate	Sigma LOPAC
YM 976	Sigma LOPAC
Rivastigmine tartrate	Sigma LOPAC
Sandoz 58-035	Sigma LOPAC
TNP	Sigma LOPAC
Arbidol hydrochloride	Sigma LOPAC
(+)-Butaclamol hydrochloride	Sigma LOPAC
Kyotorphin acetate salt	Sigma LOPAC
Gardiquimod	Sigma LOPAC
OBAA	Sigma LOPAC
Paroxetine hydrochloride hemihydrate (MW = 374.83)	Sigma LOPAC
HEMADO	Sigma LOPAC
Opipramol dihydrochloride	Sigma LOPAC
TIC10 angular	Sigma LOPAC
WZ4003	Sigma LOPAC
Enclomiphene hydrochloride	Sigma LOPAC
G15	Sigma LOPAC
Gemcitabine hydrochloride	Sigma LOPAC

MK6-83	Sigma LOPAC
PD153035 hydrochloride	Sigma LOPAC
Biperiden hydrochloride	Sigma LOPAC
Clonixin	Sigma LOPAC
Supercinnamaldehyde	Sigma LOPAC
Icaritin	Sigma LOPAC
beta-Estradiol	Sigma LOPAC
Edrophonium chloride	Sigma LOPAC
Ethylene glycol-bis(2-aminoethylether)-N,N,N',N'-tetraacetic acid	Sigma LOPAC
Estrone	Sigma LOPAC
Genistein	Sigma LOPAC
Phenserine	Sigma LOPAC
Felbamate	Sigma LOPAC
Fiduxosin hydrochloride	Sigma LOPAC
Flunarizine dihydrochloride	Sigma LOPAC
L-Glutamic acid hydrochloride	Sigma LOPAC
Ethosuximide	Sigma LOPAC
N-Methyl-beta-carboline-3-carboxamide	Sigma LOPAC
Fusidic acid sodium	Sigma LOPAC
5-fluoro-5'-deoxyuridine	Sigma LOPAC
Ganciclovir	Sigma LOPAC
Nitidine chloride	Sigma LOPAC
DPO-2	*Sigma LOPAC*
L-Glutamine	Sigma LOPAC
Gallamine triethiodide	Sigma LOPAC
GW9509	Sigma LOPAC
Emodin	**Sigma LOPAC**
Isoguvacine hydrochloride	Sigma LOPAC
DL-threo-beta-hydroxyaspartic acid	Sigma LOPAC
17alpha-hydroxyprogesterone	Sigma LOPAC
4-Hydroxybenzhydrazide	Sigma LOPAC
Claramine	Sigma LOPAC

Iodoacetamide	Sigma LOPAC
Guvacine hydrochloride	Sigma LOPAC
Hypotaurine	Sigma LOPAC
(±)-8-Hydroxy-DPAT hydrobromide	Sigma LOPAC
Hydroquinone	Sigma LOPAC
Sematilide	Sigma LOPAC
Loxiglumide	Sigma LOPAC
Gabapentin	Sigma LOPAC
L-Dopa ethyl ester	Sigma LOPAC
Dopamine hydrochloride	Sigma LOPAC
Sumanirole maleate	Sigma LOPAC
Ipratropium bromide	Sigma LOPAC
DL-Homatropine hydrobromide	Sigma LOPAC
Hydrocortisone	Sigma LOPAC
Hydroxyurea	Sigma LOPAC
Idarubicin	**Sigma LOPAC**
Harmane	Sigma LOPAC
Serotonin hydrochloride	Sigma LOPAC
JFD00245	Sigma LOPAC
6-Hydroxymelatonin	Sigma LOPAC
Hexamethonium dichloride	Sigma LOPAC
JS-K	Sigma LOPAC
(±)-7-Hydroxy-DPAT hydrobromide	Sigma LOPAC
L-165,042	Sigma LOPAC
Hexamethonium bromide	Sigma LOPAC
Bendamustine	Sigma LOPAC
Retinoic acid p-hydroxyanilide	Sigma LOPAC
SR 142948A	*Sigma LOPAC*
5-Hydroxy-L-tryptophan	Sigma LOPAC
5-hydroxydecanoic acid sodium	Sigma LOPAC
4-Hydroxy-3-methoxyphenylacetic acid	Sigma LOPAC
6-Hydroxy-DL-DOPA	Sigma LOPAC
Hispidin	Sigma LOPAC

List of compounds present in the GIT used to select HTS compounds based on Nicholson *et al.* (2012) (384)

Short-chain fatty acids: acetate, propionate, butyrate, isobutyrate, 2-methylpropionate, valerate, isovalerate, hexanoate, succinate, octanoid acid
Secondary bile acids deoxycholate and lithocholate.
Bile acids: cholate, hyocholate, deoxycholate, chenodeoxycholate, a-muricholate, b-muricholate, w-muricholate, taurocholate, glycocholate, taurochenoxycholate, glycochenodeoxycholate, taurocholate, tauro-a-muricholate, tauro-b-muricholate, lithocholate, ursodeoxycholate, hyodeoxycholate, glycodeoxylcholate, taurohyocholate, taurodeoxylcholate
Mucins mucin 2, pepsin, trypsin
AMP representatives: defensins, cathelicidins (e.g. LL-37), C-type lectins (such as the regenerating islet-derived protein (REG) family), ribonucleases (RNases RNAse7, Angiogenin4) and S100 proteins (e.g. calprotectin).
GI tract AMP: human β-defensins (hBDs hBD-2 and hBD-3 upregulated during infection), histatins, the cathelicidin LL-37, lactoferrin, lysozyme
Small intestine AMPS: human α-defensins HD5 and HD6, lysozyme, lectin Reg3γ and phospholipase A2 group IIA (sPLA2) less hBD-1, hBD-2, hBD-3, elafin, and LL-37.
Colonic AMPS: LL-37, elafin, as well as another antiprotease, the secretory leukocyte protease inhibitor SLPI, and ß-defensins.
Vitamins: vitamin K, vitamin B12, biotin, folate, thiamine, riboflavin, pyridoxine
Choline metabolites: acetylcholine, methylamine, dimethylamine, trimethylamine, trimethylamine-N-oxide, dimethylglycine, betain.
Phenolic, benzoyl, and phenyl derivatives: phenol, benzoic acid, hippuric acid, 2-hydroxyhippuric acid, 2-hydroxybenzoic acid, 3-hydroxyhippuric acid, 3-hydroxybenzoic acid, 4-hydroxybenzoic acid, 3-hydroxyphenylpropionate, 4-hydroxyphenylpropionate, 3-hydroxycinnamate, 4-ethylphenol, 4-methylphenol, tyrosine, phenylalanine, 4-cresol, 4-cresyl sulfate, 4-cresyl glucuronide, phenylaacetate, 4-cresyl4-hydroxyphenylacetate, 3,4-dihydroxyphenylacetate, phenylacetylglycine, phenylacetylglutamine, phenylacetylglycine, phenylacetate, phenylpropionate, phenylpropionylglycine, cinnamoylglycine.
Indole derivatives: N-acetyltryptophan, indoleacetate, indoleacetylglycine (IAG), indole, indoxyl sulfate, indole-3-propionate, melatonin, melatonin 6-sulfate, serotonin, 5-hydroxyindole, trimethylamine-N-oxide
Polyamines: putrescine, cadaverine, spermidine, spermine
Lipids: conjugated fatty acids, LPS, peptidoglycan, acylglycerols, sphingomyelin, cholesterol, phosphatidylcholines, phosphoethanolamines, triglycerides.
Peptides: glucagon like peptide 1
Hormone: leptin
Antibiotics
lincomicin, Nalidixic acid, streptomycin, nemicin, doxiciclin, vancomycin, rifampicin, erytromicin, nisin, penicillin, trimetroprim, polimixin B, Spectinomicin, ciprofloxacin, levofloxacin,
Sugars: maltose, glucose lactose, sucrose, trehallose, cellobiose, chitobiose, fructose, gucosamine-6-phosphate, inulin
Oligosaccharides: maltodextrins or cellodextrins,
Polysaccharides: such as starch or cellulose.
Detergents: tween 20, triton x-100, igepal, CHAPS,
Coenzymes: Thiamine pyrophosphate, Flavin mononucleotide FMN, Adenosylcobalamin, Tetrahydrofolate, S-Adenosylmethionine.
Nucleobases and related molecules S-Adenosylmethionine/S-adenosylhomocysteine SAM-SAH, S-Adenosylhomocysteine SAH, Molybdenum/tungsten cofactor MoCo/TuCo, Guanine Guanine, Adenine 2-Deoxyguanosine, Cyclic di-GMP, Cyclic AMP-GMP, 7-Aminomethyl-7-deazaguanine
Aminoacids: glycine, lysine, glutamine, 5-Aminoimidazole-4-carboxamide ribonucleotide/5-aminoimidazole-4-carboxamide riboside 5-triphosphate
Ions: Mg2+, Mn2+, F-, Ni2+, Co2+
Others: D-lactate, formate, methanol, ethanol, succinate, lysine, glucose, urea, a-ketoisovalerate, creatine, creatinine, endocannabinoids, 2-arachidonoylglycerol (2-AG), N-arachidonoylethanolamide, LPS, Bicarbonate ions, NaHCO3, Ethanolamine + B12, Cumene, H2O2, taurine, glycine.

Annex 5: Proteomics complete list of proteins

Table S5. Differentially expressed proteins in the target bacteria after co-culture with LLS^+

Name	Description	Peptides	Mol weight (kDa)	log2 (Mean LLS^+/Mean LLS^-)	P value	Adjusted p value
LMRG_00372	Uncharacterized protein	5	12,848	1,0220221	0,00020992	0,00053762
LMRG_00403	Flagellar motor switch protein FliG	10	41,478	1,027109374	0,00120473	0,00141277
LMRG_02128	UPF0356 protein LMRG_02128	7	8,2923	1,032916492	0,00553125	0,00225847
LMRG_01198	Uncharacterized protein	6	20,674	1,05159031	0,0093654	0,00289018
LMRG_01055	MazG domain-containing protein	2	12,733	1,053565993	0,00153074	0,0014959
LMRG_02819	Glutamine amidotransferase	3	27,06	1,063664208	0,00027507	0,00053762
LMRG_02655	50S ribosomal protein L7/L12	15	12,469	1,066557606	0,0031578	0,00185155
LMRG_00685	dITP/XTP pyrophosphatase (EC 3.6.1.66) (Non-canonical purine NTP pyrophosphatase)(NTPase)	4	21,956	1,076549809	0,0029274	0,00185155
LMRG_00682	Uncharacterized protein	9	19,304	1,083038554	0,00616287	0,00225847
LMRG_00927	Protein GrpE (HSP-70 cofactor)	5	21,918	1,106410993	0,00424474	0,00225847
LMRG_00119	Fructose-specific PTS system IIB component	3	11,377	1,110511441	0,03592748	0,00957538
LMRG_00412	Methyl-accepting chemotaxis protein	19	65,85	1,150272195	0,0067502	0,0023282
LMRG_02736	NAD(P)-bd_dom domain-containing protein	5	22,725	1,157521432	0,00205256	0,00171929
LMRG_00820	Probable butyrate kinase (BK) (EC 2.7.2.7) (Branched-chain carboxylic acid kinase)	4	38,969	1,16404296	0,00040588	0,00059497
LMRG_00378	Flagellin	17	30,444	1,182278637	0,02156225	0,00602042
LMRG_01165	Cold shock protein	2	7,298	1,199844808	0,00241199	0,00176782
LMRG_01609	UPF0342 protein LMRG_01609	7	13,502	1,31738505	0,00560299	0,00225847
LMRG_00411	Pyruvate oxidase	5	62,782	1,347889093	2,41E-05	0,00014111
LMRG_01869	Nitroreductase domain-containing protein	9	22,21	1,467458575	0,00609027	0,00225847
LMRG_00814	Cold shock-like protein cspLA	4	7,2658	1,588452339	0,00789272	0,00257103
LMRG_02363	Bacteriophage-type repressor	3	13,191			
LMRG_02403	Uncharacterized protein	5	29,668			
LMRG_02442	Quinol oxidase subunit 2 (EC 1.10.3.-)	4	41,583			
LMRG_02599	Uncharacterized protein	2	30,33			
LMRG_02585	Aminotransferase	2	43,471			
LMRG_00405	Flagellar protein export ATPase FliI	7	48,026			
LMRG_00560	VOC domain-containing protein	4	13,585			
LMRG_02083	Glutathione peroxidase	3	18,008			
LMRG_02108	Uncharacterized protein	4	8,9558			
LMRG_00773	DUF448 domain-containing protein	4	10,611			
LMRG_01688	HTH gntR-type domain-containing protein	3	28,559			
LMRG_01513	Uncharacterized protein	2	20,323			
LMRG_00452	Lipoate--protein ligase (EC 6.3.1.20)	3	37,929			
LMRG_01675	Lactamase_B domain-containing protein	6	71,405			
LMRG_01787	RNA polymerase sigma-54 factor	8	50,854			

LMRG_01569	Peptidase_S9 domain-containing protein	3	28,112			
LMRG_00692	ATP-dependent RNA helicase DbpA (EC 3.6.4.13)	6	52,953			
LMRG_00819	Phosphate butyryltransferase	2	30,774			
LMRG_00831	Membrane protein insertase YidC (Foldase YidC)	2	30,927			
LMRG_01434	Prephenate dehydratase (PDT) (EC 4.2.1.51)	4	31,085			
LMRG_00854	Uncharacterized protein	3	14,679			
LMRG_01405	Transcriptional repressor NrdR	5	17,937			
LMRG_01112	ADP-ribose pyrophosphatase	2	21,305			
LMRG_01170	Transcriptional repressor	3	19,129			
LMRG_00404	Flagellar assembly protein H	5	27,083			
LMRG_00419	DUF4064 domain-containing protein	2	13,423			
LMRG_01103	Fur family transcriptional regulator	6	17,328			
LMRG_00465	Uncharacterized protein	3	14,491			
LMRG_02064	Adenylate cyclase	6	22,763			
LMRG_01705	Release factor glutamine methyltransferase (RF MTase) MTase PrmC	3	32,05			
LMRG_02001	Dihydroxyacetone kinase L subunit	3	21,534			
LMRG_00675	Cell division protein ZapA	3	11,496			
LMRG_01944	ABC transporter	8	66,183			
LMRG_01929	RpiR family phosphosugar-binding transcriptional regulator	3	28,342			
LMRG_01775	Gluconeogenesis factor	4	34,973			
LMRG_02760	Uncharacterized protein	2	42,067			
LMRG_02719	Aspartokinase (EC 2.7.2.4)	4	49,968			
LMRG_01855	Uncharacterized protein	4	78,29			

Table S6. Differentially expressed proteins in the target bacteria after co-culture with LLS^-

Name	Description	Peptides	Mol weight (kDa)	log2 (Mean LLS^- /Mean LLS^+)	P value	Adjusted p value
LMRG_00100	Uncharacterized protein	2	14,984	-1,101390789	0,0100388	0,002943091
LMRG_02704	HD domain-containing protein	8	50,854	-1,008713586	0,0061178	0,002258474
LMRG_00241	Uncharacterized protein	3	35,356			
LMRG_02307	Membrane protein	8	55,766			
LMRG_00788	Uncharacterized protein	2	8,4698			
LMRG_00721	Signal peptidase I (EC 3.4.21.89)	8	20,876			
LMRG_00766	Phosphatidate cytidylyltransferase (EC 2.7.7.41)	2	29,103			
LMRG_00833	Acylphosphatase (EC 3.6.1.7)	3	10,466			
menA LMRG_01290	1,4-dihydroxy-2-naphthoate octaprenyltransferase (DHNA-octaprenyltransferase) (EC 2.5.1.74)	3	34,739			
LMRG_02761	UPF0374 protein LMRG_02761	5	21,134			
LMRG_00936	ComE operon protein 2	2	20,785			
purD LMRG_02507	Phosphoribosylamine--glycine ligase (EC 6.3.4.13) (GARS)	6	45,311			

	(Glycinamide ribonucleotide synthetase) (Phosphoribosylglycinamide synthetase)					
LMRG_01374	NifS/icsS protein	5	41,674			
nth LMRG_01041	Endonuclease III (EC 4.2.99.18) (DNA-(apurinic or apyrimidinic site) lyase)	5	24,756			
LMRG_02524	ABC transporter domain-containing protein	4	28,023			
purM LMRG_02504	Phosphoribosylformylglycinamidine cyclo-ligase (EC 6.3.3.1) (AIR synthase) (AIRS) (Phosphoribosyl-aminoimidazole synthetase)	3	37,425			
LMRG_01757	Hydrolase	6	24,92			
LMRG_02066	GTP pyrophosphokinase	5	26,138			
LMRG_00547	CDP-ribitol:poly(Ribitol phosphate) ribitol phosphotransferase	6	77,394			
LMRG_01897	Oxidoreductase	3	37,914			
LMRG_02556	Rod shape-determining protein MreB	6	34,951			
carB LMRG_00982	Carbamoyl-phosphate synthase large chain (EC 6.3.5.5) (Carbamoyl-phosphate synthetase ammonia chain)	10	117,7			
LMRG_01324	RsbR protein	5	30,427			
LMRG_02314	RsbT antagonist protein rsbS	4	12,597			
LMRG_02008	Uncharacterized protein	4	41,752			
ecfA LMRG_02145	Energy-coupling factor transporter ATP-binding protein EcfA (ECF transporter A component EcfA) (EC 7.-.-.-)	8	32,989			
LMRG_01565	Fumarylacetoacetate hydrolase	3	30,945			
LMRG_01850	Phosphatidylglycerophosphatase A	2	18,319			
LMRG_01431	Glycerol uptake facilitator protein	2	28,866			
LMRG_02132	Morphine 6-dehydrogenase	4	31,469			
LMRG_01306	Radical SAM protein	8	36,463			
LMRG_01618	ABC-2 type transport system permease	5	47,78			
LMRG_01748	Phosphate regulon sensor histidine kinase PhoR	5	66,238			
ecfT LMRG_02143	Energy-coupling factor transporter transmembrane protein EcfT (ECF transporter T component EcfT)	2	30,175			

Table S7. LLS-FLAG co-immunoprecipitated proteins identified by MS.

Fasta headers	Mol weigh t (kDa)	Score	Peptides LLS$^+$-FLAG	Unique peptides LLS$^+$-FLAG	Sequence coverage (%)	iBAQ
>WP_009917805.1 nucleoside-diphosphate kinase	16,449	2,1845	3	3	40,1	3398600
>WP_003730943.1 hypothetical protein LMOf2365_1115	11,629	1,8634	2	2	10,5	2486100
>WP_010958846.1 hypothetical protein LMOf2365_1117	35,321	31,106	3	3	15,1	2220400
>WP_003723533.1 preprotein translocase subunit YajC	11,958	11,789	1	1	20,2	1992600
>WP_010958772.1 DUF4097 domain-containing protein	39,097	6,5367	2	2	13,7	1605100
>WP_003725873.1 dihydroxy-acid dehydratase	59,864	0,77054	1	1	2,7	1125900
>WP_003721799.1 flagellar type III secretion system protein FlhB	39,966	0,83357	1	1	3,7	904340
>WP_003728076.1 class I SAM-dependent methyltransferase	22,59	3,5211	2	2	9,5	890580
>WP_003725828.1 thymidylate synthase	36,177	2,0734	2	2	6,7	805150
>WP_003720130.1 MULTISPECIES: Asp23/Gls24 family envelope stress response protein	13,418	0,96706	1	1	10,7	627970
>WP_003727843.1 beta-ketoacyl-[acyl-carrier-protein] synthase II	44,279	12,42	1	1	7	578460
>WP_003724683.1 ATP-dependent Clp protease proteolytic subunit	21,347	0,79195	1	1	9,5	502010
>WP_003724739.1 ABC transporter ATP-binding protein LMOf2365_1216	29,835	1,0255	1	1	2,6	496880
>WP_003728083.1 2-C-methyl-D-erythritol 2,4-cyclodiphosphate synthase	17,073	1,6593	1	1	13,4	398080
>WP_003724221.1 MULTISPECIES: DNA-binding response regulator	27,286	8,3239	1	1	8	339890
>WP_003727894.1 UDP-N-acetylglucosamine 1-carboxyvinyltransferase	46,006	4,6262	2	2	8,8	332110
>WP_003727892.1 F0F1 ATP synthase subunit alpha	55,077	1,6739	2	2	3,6	327950
>WP_010958692.1 bifunctional tRNA lysidine(34) synthetase TilS/hypoxanthine phosphoribosyltransferase	74,265	2,6774	1	1	2	299180
>WP_010958992.1 cell division protein FtsA	45,953	3,0942	2	2	8,7	279270
>WP_003724960.1 IMP dehydrogenase	55,036	1,62	1	1	4	232420
>WP_003722315.1 ATP-binding cassette domain-containing protein	36,62	2,9456	1	1	7,8	225030
>WP_003726336.1 hypothetical protein [Listeria monocytogenes];>AAT03739.1 conserved hypothetical protein [Listeria monocytogenes serotype 4b str. F2365]	37,182	2,3642	1	1	3,7	217770
>WP_003726833.1 glycerol-3-phosphate dehydrogenase (NAD(P)(+))	36,499	1,9907	1	1	7,4	195050
>WP_003721301.1 universal stress protein	15,411	3,6599	1	1	9,8	163880
>WP_003725406.1 NADPH dehydrogenase	37,049	0,96957	1	1	5,9	161030
>WP_010958990.1 YggS family pyridoxal phosphate-dependent enzyme	25,825	1,2159	1	1	7	112680
>WP_003726017.1 PhoH family protein	35,814	1,3292	1	1	4,7	104370
>WP_003738883.1 DNA repair protein RecN	63,518	2,3707	1	1	2,5	61224
>WP_003728355.1 pyridoxal 5-phosphate synthase lyase subunit PdxS	31,672	1,2693	1	1	4,4	0

Annex 6: Bioinformatic mining tools

The increase in the genomic data available allows the discovery of new bacteriocins by using different genome mining tools. The bacteriocins can be mined based on homology with known bacteriocins, motifs or biosynthetic genes. The bacteriocins can be searched by sequence homology for large bacteriocins and conserved sequence motifs is a good technique for smaller bacteriocins but is limited due to the poor conservation of amino acid sequences between bacteriocins. However, to increase the possibilities of finding bacteriocins is important to include the genomic context which includes the genes that are important for modifications, regulation, transport and immunity proteins (435).

1. Bioinformatic tools

For proteins larger than 200 amino acids an alignment algorithm like BLAST allows to detect if a protein is a bacteriocin or not because the sequences of larger bacteriocins are more conserved, so the standard nr-database at the NCBI BLAST server is enough (435). For smaller proteins (<200 amino acids) there are bacteriocin-specific databases freely available as: BACTIBASE(436), BAGEL2 (437) and PIRSF.

1.1 Mining conserved protein domains

There are online databases suitable for bacteriocins analysis using conserved proteins domains such as PROSITE, PFAM, PRINTS, TIGRFAM, PIRSF and ProDom. Some of them are based on conserved protein domains based on bacteriocin alignments but are limited to 14 protein domains in total (435).

1.2 Screening genomic context

To mine new bacteriocins with low homology to known ones the genomic context of small open reading frames (ORFs) can be screened. The genes that are screened are involved in synthesis, transport, regulation, processing or immunity of bacteriocins. The enzymes involved in modifications are broadly conserved (435). For small ORF that are usually omitted in the annotation process of bacterial genome, the tools Glimmer (438) and Prodigal can be used but the genome context is needed (435).

1.3 Bacteriocin databases

1.3.1 **BAGEL2**

It is a fully automated tool that allows genome mining of bacteriocins. It uses a combined approach of homology search in a bacteriocin database and bacteriocin motif screening together with screening the genome context. The algorithm allows the prediction of a putative bacteriocin based on conserved domains, physical properties and the presence of biosynthesis, transport and immunity genes in their genomic context. There is a Hidden Markov Model (HMM) via simple decision rules for prediction of bacteriocin (sub-)classes (437).

1.3.2 **BACTIBASE**

This database contains calculated or predicted physicochemical properties of 123 bacteriocins produced by Gram-positive and Gram-negative bacteria. It allows the prediction of structure/function and target organisms of these peptides (436).

1.3.3 **PIRSF**

It contains a complete database of proteins and allows a good filtering for the screen of bacteriocins. The cutoff *E*-values are higher than with BLAST without increasing the background. However, novel bacteriocins with low or no homology will not be found (435).